ABSTRACT

WATSON, ATLEE TAYLOR DARR. Aryl Hydrocarbon Receptor-Mediated Inhibition of Osteogenesis in a Teleost Model *In Vivo* and Human Mesenchymal Stromal Cells *In Vitro*. (Under the direction of Dr. Seth W. Kullman, Ph.D.)

Bone formation and homeostasis is a well-orchestrated process governed by multiple developmental pathways integrating endogenous and exogenous stimuli. Perturbations in these pathways are linked to skeletal dysplasias (e.g. osteogenesis imperfecta) and adult degenerative bone diseases (e.g. osteoporosis); however, there is increasing concern that xenobiotic exposure may perturb the regulatory networks that direct osteogenic differentiation from multipotent mesenchymal stem cells. While numerous studies have identified bone as a sensitive target of aryl hydrocarbon receptor (AhR) ligand exposure, we hypothesized that ligand-activated AhR primarily impacts bone formation through inhibition of osteogenic differentiation from mesenchymal stem cell progenitors. To test this hypothesis, we utilized Japanese medaka *in vivo* and human bone-derived mesenchymal stromal cells *in vitro*.

First, we assessed how embryonic exposure to TCDD impacts osteogenesis in Japanese medaka (*Oryzias latipes*). Embryos from inbred wild-type Orange-red Hd-dR and transgenic medaka tg(*twist*:EGFP, *osx/sp7*:mCherry, *col10a1*:nlGFP) were exposed to 0.15 nM and 0.3 nM TCDD and reared until 20 dpf. Exposure to TCDD resulted in an overall attenuation of vertebral ossification, and effects on mineralization were consistent with modifications in cell number and cell localization of transgene-labeled osteoblast and osteoblast progenitor cells. Through a targeted and global gene expression analysis we observe attenuated expression of key osteogenic regulators (*runx2*, *osx/sp7*) and extracellular matrix genes (*opn*/*spp1*, *col1*, *col10a1*, and *bglap/osc*) at 20 dpf following TCDD exposure. Our data revealed enrichment of

several genes within select pathological states including inflammatory disease, connective tissue disorders, and musculoskeletal disorders.

In our next set of experiments, we investigated AhR-mediated osteogenic inhibition in human bone-derived mesenchymal stromal cells (hBMSCs) *in vitro*. Cells from three donors were assessed during early differentiation (3 days post induction, dpi), extracellular matrix synthesis (7 dpi), and apical matrix mineralization (14-17 dpi). In all donors we found a consistent TCDD-mediated attenuation of alkaline phosphatase (ALP) activity, matrix mineralization, and mRNA expression of transcriptional regulators (*DLX5*) and osteogenic markers (*ALP*, *OPN*, *IBSP).* FGFR ligands, *FGF9* and *FGF18*, were upregulated suggesting that TCDD may influence pathways associated with maintaining stemness of hBMSCs. Relative to undifferentiated cells, expression of stemness/potency markers *SOX2*, *OCT4*, *NANOG*, and *SALL4* was reduced in osteogenic controls while expression in TCDD-treated cells remained elevated and comparable to undifferentiated cells. Co-exposure with the AhR antagonist GNF351 partially rescued these effects, suggesting that AhR activation is mechanistically associated with TCDD-mediated inhibition of osteogenesis.

Currently a global RNA-Seq analysis is underway to assess transcriptomic alterations during early (hours), intermediate (days), and apical (two and a half weeks post induction) stages of osteogenesis. Included in this assessment are GM/DMSO- (undifferentiated), ODM/DMSO- (differentiated), and ODM/TCDD-treated hBMSCs, which enables analysis of normal and AhR-inhibited osteogenesis. While this assessment remains in progress, we present preliminary data from three and seven days post induction demonstrating TCDD-mediated alterations in developmental signaling pathways (WNT, FGF, BMP/TGF-β), extracellular matrix genes markers, transcriptional regulators, and lncRNAs. Our assessment has currently

identified numerous candidate epigenetic modulators, most notably *SUV39H1/2*, previously shown to impact post-translational modification of histones, chromatin remodeling, and mRNA transcription or translation. GM/DMSO and ODM/TCDD demonstrate similar patterns in genes associated with stemness phenotypes suggesting that epigenetic modulation may in fact play a significant role in MSC lineage determination.

Our data from Japanese medaka and hBMSCs reveal that TCDD dysregulates bone formation through an overall attenuation of early osteogenic regulators, extracellular matrix genes, and matrix mineralization. We build upon prior studies that suggest a putative role for ligand-activated AhR in influencing skeletal dysplasias and adult bone diseases. Furthermore, we highlight the advantages of two alternative models to investigate xenobiotic-induced skeletal toxicity.

Aryl Hydrocarbon Receptor-Mediated Inhibition of Osteogenesis in a Teleost Model *In Vivo* and Human Mesenchymal Stromal Cells *In Vitro*.

By

AtLee Taylor Darr Watson

A dissertation submitted to the Graduate Faculty of
North Carolina State University
in partial fulfillment of the
requirements for the Degree of
Doctor of Philosophy

Toxicology

Raleigh, North Carolina

2017

APPROVED BY:

Seth W. Kullman, Ph.D Committee Chair	David E. Hinton, Ph.D Inter-Institutional Member
Carolyn J. Mattingly, Ph.D	Antonio J. Planchart, Ph.D

DEDICATION

I dedicate this dissertation to my high school science teachers, Mr. Thomas Buchanan and Mrs. Winnie Ballinger. You made science fun, and played formative roles in my early development as a scientist.

BIOGRAPHY

AtLee T. D. Watson was born April 15, 1987 to John and Charlotte Watson of Oxford, North Carolina, a small rural town of about 9,000 citizens. Small-town life in Oxford was instrumental in AtLee's personal development where he spent his free time playing baseball and soccer, riding bikes, building forts in the woods, and participating in Boy Scouts. To this day, if AtLee hears a whistle blown at dusk he immediately returns home for dinner. At Kerr-Vance Academy, AtLee realized his love for biology and chemistry which stemmed initially from blowing up/lighting stuff on fire in Science Club. From there his teachers Mrs. Winnie Ballinger and Mr. Thomas Buchanan were influential in his early academic career. In 2005 AtLee was awarded the Eagle Scout Award, and later that year, graduated Kerr-Vance Academy as Valedictorian of his class.

The following fall, AtLee attended the University of North Carolina-Chapel Hill where he majored in Biology (B.S.), minored in Chemistry. Aside from the normal college experiences, AtLee pursued a semester study abroad experience in Seville, Spain. There he improved his Spanish language proficiency, and cultivated his sense of wanderlust and spontaneity. Upon his arrival back in the United States, AtLee re-evaluated his initial aspirations to become a physician, and considered careers in environmental law or biomedical research. His dad (an attorney) did all he could to dissuade AtLee from pursuing law, and introduced AtLee to Dr. David Hinton, a professor at Duke University's Nicholas School for the Environment. The following summer, AtLee worked as an undergraduate research assistant in Dr. Hinton's lab where he was introduced to the concept of using small aquarium fish (Japanese medaka) as research models for human development and toxicity.

After graduating UNC-CH in May of 2009, AtLee worked for two years as a Laboratory Technician in the Hinton Lab. While managing daily laboratory tasks, AtLee was tasked with assisting Post-Doctoral researchers in their projects investigating the impact of endocrine disruptors like ethinyl estradiol (e.g. birth control) on male reproductive development. This experience was pivotal in confirming his aspiration to pursue a research career. Moreover, AtLee was especially interested in understanding how chemical stressors in the environment can impact developmental processes in humans.

In the Fall of 2011, AtLee began his postdoctoral education at North Carolina State University and joined Seth Kullman's laboratory. AtLee furthered his experience in teleost models, and optimized *in vitro* methods to investigate the role of dioxin exposure on bone development. While in the Toxicology Program at N.C. State, AtLee met Allison Camp (another Toxicology Ph.D. student), and they were married two weeks before his defense on October 7th, 2017.

ACKNOWLEDGMENTS

I would first like to acknowledge my advisor, Dr. Seth Kullman, and my committee members, Dr. David Hinton, Dr. Carolyn Mattingly, and Dr. Antonio Planchart. Your guidance, resources and insight helped me to develop sound scientific research and challenged me to think more globally about the scope of my research.

I would also like to acknowledge those who provided technical support for the work I have conducted over the six plus years. To the laboratory technicians, Jeanne Burr, Hong Li, and Gwijun Kwon, your assistance was vital during the early stages of this research during methods development. Dr. Christoph Winkler (National University of Singapore), Dr. Anita Buettner (Technische Universität Dresden), Dr. Eva Johannes (North Carolina State University), and Dr. Jeff Tucker (NIH/NIEHS) who were instrumental in helping me develop confocal imaging techniques of medaka. I am grateful to our collaborators in the Loboa Lab, especially Dr. Elizabeth Loboa for supplying the human cells, and Dr. Rachel Nordberg for her assistance in optimizing the cell protocols used in Chapters 3 and 4. I would also like to acknowledge the undergraduates Jason Phillips and Ian Stancil who aided in various aspects of this research and helped me to develop as a mentor.

To the past (Erin Kollitz, Erin Yost, Crystal Lee-Pow, Catherine Wise) and present members (Debabrata Mahaprata and Megan Knuth) of the Kullman Laboratory, it has been a wild ride but you have been excellent team members during my tenure at N.C. State. Thank you for your patience. I want to acknowledge the members of the N.C. State Toxicology community. The students, faculty and staff have made Toxicology a great and supportive place to work. Janet Roe, your assistance with countless payroll, registration, park, and general life questions has been fantastic. And to my second mother, Jeanne Burr, you were the greatest building liaison, part-time

lab technician, front office receptionist, and friend anyone could hope for in a professional setting. Your next employer will have gotten a real gem of person.

I would also like to acknowledge the funding support I received from the NCSU Graduate School Dissertation Completion Grant for my final semester. I am especially grateful to the support staff, Dr. Mike Carter, Dr. George Nichols, and the current and future PhDs of my cohort.

Last, but certainly not least, I would like to acknowledge my family and friends for their patience and support over the past six years. To my wife, Allison, our relationship has truly been the highlight of my graduate school career. I cannot thank you enough for your feedback, reality checks, and our afternoon walks to Cup a Joe.

TABLE OF CONTENTS

LIST OF TABLES

CHAPTER 1:

CHAPTER 2:

CHAPTER 3:

CHAPTER 4:

LIST OF FIGURES

CHAPTER 1:

CHAPTER 2:

CHAPTER 3:

CHAPTER 1: GENERAL INTRODUCTION

1.1 A REVIEW OF OSTEOGENESIS

Bone formation is a well-conserved processs among vertebrates. In humans, long, short, flat, and irregular bones comprise the 213 bones of the adult skeleton and are formed through endochondral and/or intramembranous ossification. The key difference between the two involves the presence of a cartilage template. Endochondral ossification involves the gradually replacement or remodeling of a cartilage anlage and occurs in long (e.g. humerus, tibia), short (e.g. metacarpals, metatarsals), and irregular bones (e.g. vertebrae) while intramembranous ossification occurs in the absence of a cartilaginous template in the flat bones of the craniofacial skeleton. Both forms of ossification rely on commitment of mesenchymal stem cell progenitors to an osteogenic fate, proliferation as pre-osteoblasts, and differentiation to become mature, matrix-secreting osteoblasts. As the primary bone forming cells, osteoblasts secrete extracellular matrix comprised of collagenous (80%) and noncollagenous (20%) proteins on the bone surface, which undergoes subsequent mineralization comprised of hydroxyapatite, a calcium-phosphate mineral [$Ca_5(PO_4)_3(OH)$].

In contrast, small teleosts such as medaka and zebrafish form bone primarily through perichondral and intramembranous ossification . During perichondral ossification bone is formed *around* an existing cartilage anlage, i.e. the perichondrium, via deposition of bone ECM by osteoblasts and ~~undergo~~ subsequent mineralization. Although a cartilage template is present, bone does not *replace* cartilage as with endochondral ossification. Morphologically, perichondral bones resemble a cartilage rod inside a bone tube with a cartilage condyle at both ends as seen in many of the craniofacial/jaw-like elements (as reviewed by Apschner *et al.*,

2011; Witten and Huysseune, 2009). Formation of the vertebrae in medaka and zebrafish best exemplify intramembranous ossification. In the axial skeleton, the formation of the vertebral bodies begins with initial mineralization of the notochordal sheath in a segmented pattern (chordal ossification) (Nordvik *et al.*, 2005; Grotmol *et al.*, 2005; Fleming *et al.*, 2015). Following the mineralization of the notochord, perichordal ossification drives the formation and remodeling of the centrum, neural arches, and hemal arch elements of the vertebral body. This process requires the migration of mesenchymal stem cells from the intervertebral ligament space to the centrum where they undergo commitment and differentiation to become osteoid-secreting osteoblasts. Given the absence of chondrogenic programming, the vertebral bodies in medaka and zebrafish can serve as a developmental model for examining osteogenic differentiation from a mesenchymal progenitor cell population *in vivo*, and as a potential model of human intramembranous ossification of calvarial (cranial) bone.

Despite these distinctions in ossification patterns, the molecular and cellular events driving bone formation remain conserved among vertebrates (Lefebvre and Bhattaram, 2010; Zhang, 2009). MSC differentiation to an osteogenic lineage requires strict temporal and spatial coordination of early gene regulatory networks. These events integrate stimuli from canonical developmental pathways [Wnt, Hedgehog, Notch, Fibroblast growth factor, BMP signaling (Kneissel and Baron, 2013; Marcellini et al., 2012)] and other endocrine and paracrine mediators (Imai et al., 2013) to regulate osteoblast differentiation (for review see Karsenty et al., 2009; Sinha and Zhou, 2013) (Figure 1). Within these conserved gene regulatory networks, the *Runt-related transcription factor 2* (*RUNX2*) and the zinc-finger transcription factor *Osterix* (*OSX*, or *SP7*) are considered the master regulators of osteoblast differentiation. Runx2

drives MSC commitment toward an osteoblast fate via binding of its *runt* DNA-binding domain to gene promoters containing runx consensus sequences (Karsenty *et al.*, 2009; Komori, 2010). In sclerotome-derived MSCs Runx2 activity is inhibited by the basic helix-loop-helix (bHLH) transcription factor Twist1 (Bialek *et al.*, 2004). Osx drives differentiation of pre-osteoblasts into immature osteoblasts, a critical step in the formation of mature osteoblasts (Nakashima *et al.*, 2002). As osteoblast maturation progresses, Runx2 and Osx regulate the expression of extracellular matrix proteins that support adhesion, proliferation, differentiation, and migration of osteoblasts in the bone microenvironment. Matrix molecules consisting of collagenous [e.g., Collagen Type I alpha 1 (COL1A1) and Collagen Type X alpha 1 (COL10A1) (in teleosts)] as well as non-collagenous proteins [e.g. Osteocalcin (OSC/BGLAP), Osteonectin (SPARC), Osteopontin (OPN/SPP1), Integrin-binding bone sialoprotein (IBSP/BSP2)] also serve as structural support and promote mineralization of bone ECM.

Role of Osteoclasts in Bone Remodeling

Although not the focus of this dissertation, it is important to acknowledge the role of osteoclasts in bone remodeling and homeostasis. Osteoclasts are derived from the hematopoietic lineage and function as bone macrophages to aid in the resorption process. Bone remodeling takes place in four phases. First, osteoclasts differentiate from osteoclast progenitors in the bone marrow by the cytokines macrophage stimulating factor (M-CSF), and receptor activator of NF Kappa B ligand (RANKL). Osteoprotegerin (OPG), which is secreted by MSCs and osteoblasts, inhibits this process by functioning as a decoy receptor for RANKL, thus preventing RANK-RANKL binding and osteoclast differentiation (Simonet *et al.*, 1997;

Boyce and Xing, 2007). Second, mature osteoclasts attach to the bone surface and secrete cathepsin K to degrade bone ECM, and acid to dissolve bone mineral content. In the reversal phase osteoblasts attach to bone and begin to secrete the osteoid layer containing COL1A1, OSC, OPN/SPP1, IBSP. In the final phase, the osteoid undergoes mineralization, and osteoblasts become embedded in the mineralized bone matrix as osteocytes (Gallagher and Sai, 2010; Nakashima *et al.*, 2012; Yamashita *et al.*, 2012). Osteocytes comprise approximately 95% of all cells in mammalian bone, and play a key sensory role in bone through their ability to inhibit or promote mineralization based on mechanical strain (Franz-Odendaal *et al.*, 2006; Marotti, 1996). In contrast, teleosts with acellular bone, such as Japanese medaka, do not have embedded osteocytes. Instead osteoblasts secrete osteoid in a continuous, polarized fashion on the periosteal surface of bone (Ekanayake and Hall, 1988, 1987; Witten and Huysseune, 2009).

Teleosts as models of human skeletal development

Since the release of *Toxicity Testing in the 21st Century: A Vision and a Strategy* (National Research Council, 2007), toxicity testing in animals has shifted toward the inclusion of alternative high-throughput *in vivo* systems as predictive models for human developmental toxicity. Currently the Tox21 testing program, a multiagency collaboration comprised of the National Institute of Environmental Health Sciences/National Toxicology Program (NIEHS/NTP, a division of the National Institute of Health (NIH)), the U.S. Food and Drug Administration (FDA, a division of the U.S. Department of Health and Human Services), National Center for Advancing Translational Sciences (NCATS, a division of the NIH), and National Center for Computational Toxicology (NCCT, a division of the U.S. Environmental Protection Agency (EPA)), has expanded its chemical library to include more than 10,000

chemicals, thus necessitating a more rapid and cost-effective alternative to traditional rodent-based toxicity testing methods (Sipes *et al.*, 2011; Padilla *et al.*, 2012; Tox21: Chemical testing in the 21st century, 2017). The primary goal of the Tox21 program is to validate a suite of *in vitro*, assays that can collectively predict human toxicity of a given chemical. While these cell-based assays may provide valuable insight into molecular mechanisms of toxicity, critical challenges remain prior to fully replacing traditional *in vivo* models. One of the most important being *in vitro* to *in vivo* extrapolation (IVIVE) of results. Cell-based systems cannot reproduce the absorption, distribution, metabolism, and elimination (ADME) parameters present *in vivo*, which may significantly alter the observed toxicity of a test substance. As a result, test compounds may demonstrate toxicity *in vitro* where none exists *in vivo* (false positive), or conversely, demonstrate no toxicity when the parent compound may be metabolized into a more toxic, active form *in vivo* (false negative) (Sipes *et al.*, 2011).

Thus, a compromise is needed to balance the demands for rapid, high-throughput capabilities with the need for an *in vivo* vertebrate model with sufficient homology to human biochemical and molecular pathways. Recognizing this need, the Interagency Coordinating Committee on the Validation of Alternative Methods (ICCVAM) and the NTP Interagency Center for the Evaluation of Alternative Toxicological Methods (NICEATM) have begun implementing the use of teleosts as alternative *in vivo* models, like the Japanese medaka (*Oryzias latipes*) and zebrafish (*Danio rerio*), to better understand the interplay between toxic agents and the cells, tissues, and organ and how these agents may contribute to human disease pathologies. Developmental and neurotoxicity assays of ToxCast Phase I and II chemicals conducted in zebrafish (*Danio rerio*) demonstrate sensitivity, robustness, and promise a

complementary chemical screening tool for the Tox21 chemical library (Sipes *et al.*, 2011; Padilla *et al.*, 2012; Truong *et al.*, 2014). Thus, medaka and zebrafish may represent excellent candidate models to aid in prioritization of chemicals for subsequent testing based on their: i) shared homology with human molecular and cellular pathways, ii) a fully sequenced genome, iii) genetic tractability, v) small size, v) adaptability to high-throughput assays, and vi) rapid, oviparous, and transparent embryonic development.

Many of these same advantages apply when considering medaka and zebrafish as models of human skeletal development and disease. Several transgenic models have been developed that express fluorescent reporter proteins (e.g. GFP, RFP, mCherry) driven by bone cell-specific gene promoters. Coupled with whole-mount staining for bone and high-resolution confocal imaging techniques, medaka and zebrafish offer unparalleled ability to visualize alterations in specific cell populations within the context of mineralized bone. Furthermore, rapid skeletogenesis in teleosts permits a serial assessment of bone formation within a shorter window compared to rodents. Therefore, teleosts are excellent models for investigating and identifying putative mechanisms of chemical action that may shed new information on the role of environmental agents impacting skeletal dysplasias. The same logic also supports increased use of teleosts as screening models for candidate drug therapies targeting bone and cartilage degenerative diseases.

1.2 ARYL HYDROCARBON RECEPTOR BIOLOGY AND TOXICITY

The AhR is a basic-helix-loop-helix/Per-Arnt-Sim (bHLH-PAS) transcription factor and functions as a master regulator of xenobiotic metabolism through genomic and non-genomic mechanisms. In the genomic pathway, the AhR binds a ligand, dissociates from a

chaperone protein complex (XAP2, HSP90, p23, c-Src) and translocates to the nucleus where it heterodimerizes with AhR nuclear translocator (ARNT). AhR-ARNT heterodimers bind to dioxin responsive elements (DREs) and activate transcription of AhR target genes involved in Phase I and II xenobiotic metabolism (Wilson and Safe, 1998; Safe, 1995). Through its nongenomic pathways, however, ligand-activated AhR perturbs cell cycle regulation and influence cell proliferation in a cell-specific manner (Puga *et al.*, 2009, 2000), alters nuclear receptor function (Safe *et al.*, 1998; Ohtake *et al.*, 2009), or activates nuclear factor kappa B (NF-kB)- and phospholipase A-mediated inflammatory signaling pathways (Dong and Matsumura, 2008; Sciullo *et al.*, 2009; Tian *et al.*, 2002). Both pathways appear to be conserved across vertebrates as studies in teleosts and mammals report AhR-mediated toxicity in skeletal, cardiac, immune, and gonadal cells and tissues (Abel and Haarmann-Stemmann, 2010; Dong *et al.*, 2010; King-Heiden *et al.*, 2012).

Exogenous AhR ligands are derived from anthropogenic sources including industrial waste byproducts (Pohl *et al.*, 1998), contaminated food (Fernández-González *et al.*, 2015), and cigarette smoke (Narkowicza *et al.*, 2013; Adams *et al.*, 1987). Of the AhR ligands, polycyclic aromatic hydrocarbons (e.g. benzo[a]pyrene (BaP)), polychlorinated biphenyls (PCBs), and polychlorinated dibenzodioxins/dibenzofurans (PCDDs/PCDFs) have received considerable attention based on their high affinity for the AhR and their influence on cell signaling pathways affecting proliferation, differentiation and apoptosis (Abel and Haarmann-Stemmann, 2010; Chopra and Schrenk, 2011). The most potent PCDD congener, 2,3,7,8-tetrachlorodibenzo-*p*-dioxin (TCDD, dioxin), has been used to probe mechanisms underlying AhR-mediated toxicity and its impact on sensitive cells, tissues, and organs.

Skeletal development is particularly sensitive to AhR ligand exposure. Multiple *in vitro* studies demonstrate AhR-mediated inhibition of adipocyte differentiation through repression of adipogenic regulators PPARγ and C/EBPα (Li *et al.*, 2008; Liu *et al.*, 1996; Gadupudi *et al.*, 2015; Podechard *et al.*, 2009). Chondrogenic programming is also inhibited by TCDD and/or AhR ligand exposure *in vitro* (Kung *et al.*, 2011) and in Japanese medaka and zebrafish (H Teraoka *et al.*, 2006; Dong *et al.*, 2012). Numerous studies also report osteogenic toxicity following AhR ligand exposure; however, the precise mechanisms are not fully understood. AhR is present in osteoblasts and its expression increases during *in vitro* osteoblast differentiation (Ryan *et al.*, 2007); and while several endogenous ligands to the AhR are known, their role and the AhR's role in normal bone formation remain poorly understood (Herlin *et al.*, 2013). Yet osteogenesis is sensitive to AhR ligands with multiple studies demonstrating altered bone formation in rodents *in vivo* (Miettinen *et al.*, 2005; Finnilä *et al.*, 2010), teleosts (Dong *et al.*, 2012; Watson *et al.*, 2017; Baker *et al.*, 2013; Burns *et al.*, 2015), and altered osteoblast differentiation and/or function *in vitro* (Herlin *et al.*, 2015; Korkalainen *et al.*, 2009; Naruse *et al.*, 2002). Overall, we hypothesize that the ligand-activated AhR serves as a negative regulator of cellular differentiation, and its inhibitory action in osteogenesis is rooted in its ability to repress an osteogenic mesenchymal stem cell fate.

1.3 BONE DISORDERS IN HUMANS:

Bone provides several key functions including structural support, mobility, protection of vital organs, an environment to support hematopoietic stem cells, and calcium and phosphate mineral homeostasis (Clarke, 2008). Bone formation, or osteogenesis, is precisely regulated in a temporal and spatial manner to achieve the appropriate bone geometry, morphology, and

composition that supports subsequent growth. Once formed, bone undergoes remodeling (4-10% annually) throughout adulthood in response to biomechanical demands, aging and disease (Manolagas, 2000). Given its dynamic metabolic activity under precise regulatory control, human bone-related disorders arise from defects in either bone formation (e.g. skeletal dysplasias) or an imbalance in the bone remodeling process (e.g. degenerative bone disease).

Although rare in incidence (0.6 per 1000 births), there are more than 350 defined human skeletal dysplasias which arise from genetic defects in skeletal patterning, differentiation, and/or growth of the skeleton (Orioli *et al.*, 1986; Krakow and Rimoin, 2010). The etiology of osteochondrodysplasias, or disorders affecting cartilage and/or bone development, have been linked to gain-of-function or loss-of-function mutations in skeletal pathways (Karsenty, 2008; Hermanns and Lee, 2002) including fibroblast growth factor (FGF), bone morphogenetic protein (BMP), Wnt, and Hedgehog signaling pathways, which influence the expression and/or activity of transcriptional regulators and extracellular matrix proteins (**Table 1**, for a full review see Baldridge et al., 2010; Kornak and Mundlos, 2003; Krakow and Rimoin, 2010). Given the overlap of chondrogenic and osteogenic tissues, osteochondrodysplasias often display common phenotypic malformations (e.g. defects in limb development). Individuals with craniosynostosis syndrome, an achondroplasia linked to mutations in the FGF/FGFR signaling, display premature ossification/fusion of cranial sutures with a concomitant loss of cartilage in these regions. Other achondroplasias such as dwarfism associated with FGF mutations result in premature fusion of the growth plates, resulting in shorter long bones with altered bone geometry and biomechanical properties. Osteogenesis imperfecta (OI), or “brittle bone” disease, is a group of congenital osteodysplasias

characterized by skeletal fragility, reduced bone mass, short stature, bowing of long bones, and in some cases, delayed or abnormal tooth eruption (dentinogenesis imperfecta). Diagnosed early in development and ranging in severity, OI is caused by mutations in genes causing defects in collagen structure or post-translational modification, differentiation of osteoblasts (bone-forming cells), or ossification of bone (Forlino and Marini, 2016).

In contrast to osteochondrodysplasias, degenerative bone diseases disproportionately affect elderly individuals. The arthritic diseases rheumatoid arthritis (RA) and osteoarthritis (OA) afflict 0.24% (17 million) 3.7% (268 million) of the global population, respectively, and involve focal erosions of bone (RA) and articular cartilage (OA) around the joint spaces (Briggs *et al.*, 2016; Felson *et al.*, 2000). Osteoporosis is also prevalent (200 million globally, World Health Organization, Technical Report, 2007) with individuals displaying loss of bone mass, bone mineral density, and structural integrity of bone. OA, RA, and osteoporosis collectively present a major healthcare burden in industrialized nations (e.g. United States, Canada, Western Europe, Japan) where aging demographics comprise an increasingly greater proportion of the population. In the United States, for instance, an estimated 20% of the population will be 65 years of age or older by the year 2030, and those with osteopenia, osteoporosis and/or osteoporosis-related fractures could exceed 60 million (Bone health and osteoporosis: a report of the Surgeon General, 2004). An additional concern is the elevated risk of bone fractures in osteoporotic individuals. Global estimates report 8.9 million osteoporotic fractures annually, or one fracture every three seconds (Johnell and Kanis, 2006).

Clinical and epidemiological studies have identified several endogenous factors associated with bone loss in degenerative bone diseases. Sex, age, and menopausal status are

among the most important determinants in osteoporosis. Post-menopausal women are two-fold more likely than men of the same age to develop osteoporosis due to loss of estrogen (Sozen *et al.*, 2017), a steroid hormone with anabolic properties in bone (Imai *et al.*, 2013). Epidemiological and *in vitro* mechanistic studies establish the role of inflammation as another critical mediator of bone loss in osteoporosis (Mundy, 2007; Barbour *et al.*, 2014) and RA (Redlich and Smolen, 2012) as pro-inflammatory cytokines promote differentiation of bone-resorbing osteoclasts (Lam *et al.*, 2000; Kotake *et al.*, 1996; Zhang *et al.*, 1990; Hardy and Cooper, 2009) and inhibit differentiation of osteoblasts (Lacey *et al.*, 2009; Nakase *et al.*, 1997), thus markedly skewing the balance in favor of bone resorption. Collectively, these examples demonstrate the underlying endogenous influences on bone formation and homeostasis.

In terms of exogenous influences, however, two emergent themes are essential. First, skeletal development, including bone formation and maintenance, is particularly sensitive to chemical perturbation. Bone formation is a tightly regulated process that integrates multiple developmental signaling pathways (WNT, BMP, FGF, Hedgehog, PTH/PTHR) to control the regulatory networks governing cellular differentiation and patterning of bone tissue. Individual mediators within each pathway represent a potential target of chemical exposure that may dysregulate key osteogenic regulatory networks and/or extracellular matrix synthesis and deposition. In fact, chemical agents with broad industrial, household, pharmaceutical, and agricultural applications may modulate skeletal development through multiple dissimilar molecular initiating events. Support for this notion comes from mechanistic studies investigating congenital limb defects following *in utero* exposure to various pharmaceutical

and chemical agents. Phenytoin, an anti-epileptic drug, caused craniofacial and distal limb defects through the generation of excess reactive oxygen species (ROS), oxidative stress, and apoptosis during skeletal morphogenesis (as reviewed by Etemad *et al.*, 2012). The well-documented teratogen, thalidomide caused proximal limb defects (phocomelia, amelia) through binding to cereblon and/or tubulin to modulate expression downstream molecular targets including fibroblast growth factor eight (FGF8) signaling (Ito *et al.*, 2010, and as reviewed by Ito *et al.*, 2011). Excessive consumption of alcohol during pregnancy is linked to craniofacial and distal limb defects, collectively referred to as fetal alcohol syndrome (FAS), via several putative mechanisms, including altered expression of Msh homeobox 2 (MSX2) signaling downstream of Wnt, bone morphogenetic protein (BMP), and FGF signaling pathways involved in bone and cartilage development (Chrisman *et al.*, 2004). Studies in rodents have identified several other skeletal teratogens including valproic acid, boric acid, retinoic acid, 2-deoxyazacytidine, bromoxynil, salicylate, ethylene glycol, and methanol, which cause craniofacial malformations and/or delays in ossification of the axial skeleton. (Tyl *et al.*, 2007). Teleosts are alternative vertebrate models of human toxicity and demonstrate skeletal deficits following exposure to various environmental toxicants (Laize *et al.*, 2014) including gasoline additives (ETBE, TAME) (Bonventre *et al.*, 2012), cigarette smoke condensate (Ellis *et al.*, 2014), and dithiocarbamate pesticides (Hiroki Teraoka *et al.*, 2006; Tilton *et al.*, 2006).

A second emerging theme suggests that chemical exposures during key windows of development contribute to adverse health outcomes later in life, i.e. the fetal origins of adult disease. This theme remains understudied with respect to bone formation and the etiology of

degenerative bone diseases like osteoporosis, RA, and OA. Two longitudinal studies, however, may offer insight into the developmental basis of osteoporosis and its precursor osteopenia. Their major findings suggest that peak bone mass achieved in adolescence is a major determinant of bone loss and fracture risk in the elderly (Rizzoli *et al.*, 2010; McCormack *et al.*, 2017). Moreover, based on theoretical modeling, individuals exceeding the mean peak bone mineral density by 10% may offset the development of osteoporosis by 13 years (Hernandez *et al.*, 2003). Thus, given the sensitivity of osteogenic signaling, it is plausible that even low-level exposure to environmental chemicals during early bone patterning and subsequent development when rate of bone mass accrual is highest, could result in an overall attenuation of peak bone mass and predispose individuals to degenerative bone diseases.

1.4 RESEARCH OBJECTIVES AND APPROACH

The approaches outlined below focus on elucidating AhR-mediated bone toxicity using 2,3,7,8-tetrachlorodibenzo-*p*-dioxin (TCDD, dioxin) as a prototypic AhR ligand. The prevailing hypothesis underlying each approach is that AhR ligands inhibit bone formation through repression of mesenchymal stem cell differentiation. Based on the data presented in Chapters 2, 3 and 4 we expand upon the current literature demonstrating AhR-mediated bone toxicity in two alternative toxicological models: Japanese medaka (*Oryzias latipes*), a teleost model of human skeletal development; and human bone-derived mesenchymal stem cells, an *in vitro* multipotent stem cell model capable of adipogenic, chondrogenic and osteogenic differentiation.

TCDD disruption of axial vertebrae development in Japanese medaka (Chapter 2)

Previous work from our laboratory (Dong et al (2012) demonstrated TCDD-mediated inhibition of chondrogenic differentiation in the hypural cartilage of the medaka caudal vertebrae following embryonic exposure. A secondary finding from TCDD-exposed *osx:mCherry* medaka revealed a reduction in differentiating mCherry-positive osteoblasts in the hypural cartilage, neural and hemal arches suggesting that perichondral ossification is also a target of AhR toxicity. The overall aim of Chapter 2 was to further investigate osteogenic dysregulation following embryonic TCDD exposure in medaka. Given the common mesenchymal origins of osteochondral cell lineages, we hypothesize that TCDD may dysregulate osteogenic commitment and/or differentiation of mesenchymal progenitors.

To test this hypothesis, transgenic medaka with GFP/RFP-labeled sclerotome-derived mesenchymal stem cells (*twist*:EGFP), differentiating osteoblasts (*osx*:mCherry), and immature to mature osteoblasts (*col10a1*:nlGFP) were exposed to TCDD during early embryonic development (mid-gastrula stage) and assessed for morphological deficits in vertebral ossification and corresponding modifications in transgene-labeled cell populations in 20 days post fertilization (dpf) larvae. The vertebrae were selected as the unit of study as they are formed through intramembranous ossification in the absence of a cartilage template, thus enabling the isolation and investigation of osteogenic differentiation from a mesenchymal progenitor in the intervertebral ligament space. Parallel experiments in wildype Orange-red (Hd-rR) medaka were conducted to assess and confirm altered expression of osteogenic markers isolated from the axial tissue of 20-dpf larvae. Based on concordant phenotypic-genotypic responses, RNA-Seq was conducted to identify global changes in gene expression

with the overall goal to identify alterations of genes in pathways associated with skeletal dysplasias/diseases in humans

TCDD-mediated inhibition of osteogenesis from human MSCs (Chapter 3)

In Chapter 3 we further investigate TCDD-mediated dysregulation of osteogenic commitment and differentiation using human bone-derived mesenchymal stromal cells (hBMSCs). Some controversy exists over the nomenclature and labeling of "mesenchymal stromal cells" versus "mesenchymal stem cells". The International Society for Cellular Therapy recommends the use of "mesenchymal stromal cells" rather than "mesenchymal stem cells" to describe bone-derived cells that meet the following criteria: 1) adherence to plastic substrates, 2) ability to differentiate into adipogenic, chondrogenic, osteogenic cell lineages, and 3) presence or absence of specific cell surface antigens (Dominici *et al.*, 2006). Mesenchymal stem cells also meet these criteria but refer to a strictly homogenous population of cells. The use of "mesenchymal stromal cell" accounts for possible heterogeneity of mesenchymal stromal cell isolates, which may contain other cell types (e.g. fibroblasts) with similar cell-surface antigen profiles that also provide a supportive environment for the propagation and/or differentiation of hBMSCs (Lindner *et al.*, 2010).

Overall, the aim of Chapter 3 is to assess whether TCDD alters osteogenic differentiation *in vitro* using a human mesenchymal stromal cell model. If so, does TCDD alter early transcriptional regulation governing osteogenic commitment, intermediate stages of ECM synthesis and deposition, or terminal stages of matrix mineralization? A secondary goal of this study was to determine whether TCDD causes MSCs to favor adipogenesis in lieu of osteogenesis, or whether TCDD inhibits differentiation in both osteogenic and adipogenic

media conditions.Here, we hypothesize that TCDD inhibits osteogenic differentiation of hBMSCs, thus maintaining stemness despite osteo-inductive stimuli.

To address these goals, human bone-derived mesenchymal stem cells isolated from three donors were exposed to TCDD in the presence of osteogenic differentiation media for 14 to 17 days (until mineralization was apparent). Various osteogenic assays were conducted corresponding to early, intermediate, and apical stages of differentiation including: i) targeted gene expression of osteogenic regulators, osteogenic extracellular matrix markers, and stemness; ii) alkaline phosphatase enzymatic activity; iii) histological staining for mineralized bone matrix; and iv) calcium and phosphate content. A separate adipogenic assessment was conducted on TCDD-exposed hBMSCs cultured in adipogenic and osteogenic media to confirm the ability of the hBMSCs to differentiate into adipocytes, and more importantly, to assess whether TCDD promoted adipogenic differentiation over osteogenic differentiation.

Global transcriptomic response of TCDD-exposed hMSCs at early and intermediate stages of differentiation (Chapter 4)

Improving upon the targeted gene expression assessment in the previous chapter, we approach Chapter 4 with the overall goal of understanding global changes in gene expression throughout osteogenic differentiation. In our hBMSC model, exposure to TCDD altered expression of a select few osteogenic regulators (*DLX5*, *FGF9*, *FGF18*) at 3 and 7 days post-osteogenic induction; however, we observe an inconsistent response in *OSX* and *RUNX2* expression (the “master” osteogenic regulators) at 3 dpi. Support for this rationale stems from a recent study from van de Peppel et al. (2017), which identified three unique stages of differentiation within the first 72 hours following osteogenic induction in hBMSCs. Coupled

with recent evidence suggesting that epigenetic modifiers play a significant role in early mesenchymal commitment and differentiation (Wu *et al.*, 2017; Montecino *et al.*, 2015), we hypothesize that AhR-mediated events alter the transcriptomic landscape on the scale of hours rather than days after adding osteogenic media. In addition to early transcriptional regulators, we further believe that TCDD alters the expression of epigenetic "readers", "erasers", and "writers" which have the potential to influence MSC fate and lineage determination. Another study from the van Leeuwen group highlights the role of bone ECM in promoting osteogenic differentiation of MSCs (Marta Baroncelli *et al.*, 2017).

To address our hypotheses, RNA-Seq was conducted in Donor 1 hBMSCs cultured in the presence of GM-, ODM- and ODM+TCDD at multiple timepoints. We expand our assessment to include the 3 and 24 hours-post induction (hpi) timepoints in addition to the 3, 7, and 17 dpi timepoints previously assessed using a targeted qPCR approach. This approach permits three significant comparisons. First, in comparing GM vs ODM-treated cells, we can identify changes occurring globally during normal osteogenic differentiation. Second, through comparison of ODM- and ODM-TCDD treated cells, we can address how TCDD-exposed cells are modified relative to cells undergoing normal osteogenic differentiation. Lastly, a comparison of GM vs ODM-TCDD treated cells may help identify common stemness genes which may be upregulated with exposure to TCDD. Based on a recent study showing the osteo-inductive role of bone ECM in MSC differentiation (M Baroncelli *et al.*, 2017), we also include the terminal 17 dpi timepoint with the goal of further describing the transcriptomic landscape underlying TCDD-mediated changes in bone ECM composition and matrix mineralization.

Currently, only data for 3 and 7 dpi have been received and analyzed. Thus, a cursory analysis of 3 and 7 dpi data will be presented in Chapter 4.

TABLES

Table 1. Osteochondral skeletal dysplasias associated with gene mutations in humans. Inheritance patterns are AD= autosomal dominant, AR= autosomal recessive, XLD= X-linked dominant, XLR= X-linked recessive.

Skeletal Disease/Dysplasia	***Gene***	***Inheritance***
3M syndrome	*CUL7*	*AR*
Acheiropodia	*LMBR1*	*AR*
Achondroplasia	*FGFR3*	*AD*
Acrocapitofemoral dysplasia	*IHH*	*AR*
Acromesomelic dysplasia type Maroteaux	*NPR2*	*AR*
Acromesomelic dysplasia with genital anomalies	*BMPR1B*	*AR*
Acromesomelic dysplasia with genital anomalies	*NOG*	*AR*
Al-Awadi Raas-Rothschild limb-pelvis hypoplasia-aplasia	*WNT7A*	*AR*
Angel-shaped phalangoepiphyseal dysplasia	*GDF5*	*AD*
Apert snydrome	*FGFR2*	*AD*
Atelosteogenesis type 1	*FLNB*	*AR*
Atelosteogenesis type 2	*DTDST*	*AR*
Atelosteogenesis type 3	*FLNB*	*AR*
Baller-Gerold syndrome	*RECQL4*	*AR*
Blomstrand dysplasia	*PTHR1*	*AR*
Brachydactyly type B	*NOG*	*AR*
Brachydactyly type A1	*IHH*	*AD*
Brachydactyly type A2	*BMPR1B*	*AD*
Brachydactyly type A2	*GDF5*	*AD*
Brachydactyly type B1	*ROR2*	*AD*
Brachydactyly type C	*GDF5*	*AD*
Brachydactyly type D	*HOXD13*	*AD*
Brachydactyly type E	*HOXD13*	*AD*
Brachyolmia, autosomal dominant type	*TRPV4*	*AD*
Bruck syndrome type 2	*PLOD2*	*AR*
Campomelic dysplasia	*SOX9*	*AD*
Camurati–Engelmann disease	*TGFB1*	*AD*
CATSHL (camptodactyly, tall stature, and hearing-loss syndrome)	*FGFR3*	*AD*
CDP Conradi-Hünermann type (CDPX2)	*EBP*	*XLD*
CDP X-linked recessive, brachytelephalangic type	*ARSE*	*XLD*
Cleidocranial dysplasia	*RUNX2*	*AD*
Congenital contractural arachnodactyly	*FBN2*	*AD*
Cousin syndrome	*TBX15*	*AR*

Table 1 Continued.

Craniometaphyseal dysplasia	*ANKH*	*AD*
Craniosynostosis Beare-Stevenson syndrome	*FGFR2*	*AD*
Craniosynostosis Boston type	*MSX2*	*AD*
Craniosynostosis Muenke type	*FGFR3*	*AD*
Crouzon syndrome	*FGFR2*	*AD*
Crouzon-like craniosynostosis with acanthosis nigricans	*FGFR3*	*AD*
Diastrophic dysplasia (DTD)	*DTDST*	*AR*
Dyggve-Melchior-Clausen dysplasia (DMC)	*DYM*	*AR*
Dyschondrosteosis (Leri-Weill)	*SHOX*	*AD/AR*
Dyssegmental dysplasia, Silverman-Handmaker type	*HSPG2*	*AR*
Ehlers-Danlos, Arthrochalasis type	*COL1A1/2*	*AD*
Ehlers-Danlos, Cardiac valvular type	*COL1A2*	*AR*
Ehlers-Danlos, Classic type	*COL5A1/2*	*AD*
Ehlers-Danlos, Classic-like type	*TNXB*	*AR/AD*
Ehlers-Danlos, Dermatosparaxis type	*ADAMTS2*	*AR*
Ehlers-Danlos, EDS/OI overlap syndrome	*COL1A1/2*	*AD*
Ehlers-Danlos, Hypermobility type	*COL5A1*	*AR*
Ehlers-Danlos, Hypermobility type	*TNXB*	*AR*
Ehlers-Danlos, Kyphoscoliotic type	*PLOD1*	*AR*
Ehlers-Danlos, Vascular type	*COL3A1*	*AR/AD*
Ehlers-Danlos, Vascular-like type	*COL1A1*	*AD*
Eiken dysplasia	*PTHR1*	*AR*
Familial expansile osteolysis	*TNFRSF11A*	*AD*
Familial hypocalciuric hypercalcemia with transient neonatal hyperparathyroidism	*CASR*	*AD*
Fibrodysplasia ossificans progressiva (FOP)	*ACVR1*	*AD*
Fibrous dysplasia, polyostotic form	*GNAS1*	*AD*
Fibular hypoplasia and complex brachydactyly	*ACVR1*	*AD*
Fibular hypoplasia and complex brachydactyly	*GDF5*	*AR*
Fibular hypoplasia and complex brachydactyly (Du Pan)	*GDF5*	*AR*
Fronometaphyseal dysplasia	*FLNA*	*XLD*
Geleophysic dysplasia	*ADAMTSL2*	*AR*
Geroderma osteodysplasticum	*SCYL1BP1*	*AR*
Gnathodiaphyseal dysplasia	*TMEM16E*	*AD*
Grebe type chondrodysplasia	*GDF5*	*AR*
Greenberg dysplasia	*LBR*	*AR*
Greig cephalopolysyndactyly syndrome	*GLI3*	*AD*
Hematodiaphyseal dysplasia	*TBXAS1*	*AR*
High bone mass (HBD)	*LRP5*	*AD*
Holoprosencephaly type 3	*SHH*	*AD*
Holt-Oram syndrome	*TBX5*	*AD*
Hunter–Thompson type acromesomelic dysplasia	*GDF5*	*AR*

Table 1 Continued.

Hypochondrogenesis	*COL2A1*	*AD*
Hypochondroplasia	*FGFR3*	*AD*
Hypophosphatasia, adult form	*ALPL*	*AD*
Hypophosphatasia, recessive form	*ALPL*	*AR*
Hypophosphatemia rickets with calcinuria	*SCLC34A3*	*AR*
Hypophosphatemic rickets	*FGF23*	*AD*
Hypophosphatemic rickets	*PHEX*	*XLR*
Immuno-osseous dysplasia (Schimke)	*SMARCAL1*	*AR*
Ischiopubic patellar dysplasia	*TBX4*	*AD*
Jackson-Weiss syndrome	*FGFR1*	*AD*
Jackson-Weiss syndrome	*FGFR2*	*AD*
Juvenile osteoporosis	*LRP5*	*AD*
Juvenile Paget disease	*TNFRSF11B (OPG)*	*AR*
Kallman syndrome 2	*FGFR1*	*AD*
Kenny-Caffey dysplasia type 1	*TBCE*	*AR*
Keutel SynAdrome	*MGP*	*AR*
Kniest dysplasia	*COL2A1*	*AD*
Lacrimo-auriculo-dento-digital syndrome	*FGF10*	*AD*
Lacrimo-auriculo-dento-digital syndrome	*FGFR2*	*AD*
Lacrimo-auriculo-dento-digital syndrome	*FGFR3*	*AD*
Langer type (homozygous dyschondrosteosis)	*SHOX*	*XLD*
Larsen Syndrome	*FLNB*	*AD*
Loeys–Dietz type 1a syndrome	*TGFBR1*	*AD*
Loeys–Dietz type 1b syndrome	*TGFBR2*	*AD*
Mandibuloacral dysplasia type A	*LMNA*	*AR*
Mandibuloacral dysplasia type B	*ZMPSTE24*	*AR*
Marfan syndrome	*FBN1*	*AR*
Marshall Syndrome	*COL11A1*	*AD*
Melorheostasis with osteopoikilosis	*LEMD3*	*AD*
Metabolic syndrome with osteoporosis	*LRP6*	*AD*
Metaphyseal dysplasia	*MMP13*	*AD*
Metaphyseal dysplasia, Jansen type	*PTHR1*	*AD*
Metaphyseal dysplasia, Schmid type	*COL10A1*	*AD*
Metatropic dysplasia	*TRPV4*	*AD*
Microcephalic osteodysplastic primordial dwarfism type 2	*PCTN2*	*AR*
Multiple cartilage exostoses 1	*EXT1*	*AD*
Multiple cartilage exostoses 2	*EXT2*	*AD*
Multiple epiphyseal dysplasia type 1	*COMP*	*AD*
Multiple epiphyseal dysplasia type 2	*COL9A2*	*AD*
Multiple epiphyseal dysplasia type 3	*COL9A3*	*AD*
Multiple epiphyseal dysplasia type 4	*DTDST*	*AR*

Table 1. Continued.

Multiple epiphyseal dysplasia type 6	*COL9A1*	*AD*
Multiple synostoses syndrome type 1	*NOG*	*AD*
Multiple synostoses syndrome type 2	*GDF5*	*AD*
Multiple synostoses syndrome type 3	*FGF9*	*AD*
Nail-patella syndrome	*LMX1B*	*AD*
Neonatal hyperparathyroidism, severe form	*CASR*	*AR*
Oculodentosseous dysplasia mild type	*GJA1*	*AD*
Okihiro syndrome	*SALL4*	*AD*
Oral-facial-digital syndrome type I (OFD1)	*CXORF5*	*XLD*
Osteodysplasty, Melnick-Needles	*FLNA*	*XLD*
Osteogenesis imperfecta, type 1	*COL1A1/2*	*AD*
Osteogenesis imperfecta, type 2	*COL1A1/2*	*AD*
Osteogenesis imperfecta, type 3	*COL1A1/2*	*AD*
Osteogenesis imperfecta, type 4	*COL1A1/2*	*AD*
Osteogenesis imperfecta, type 5	*IFITM5*	*AD*
Osteogenesis imperfecta, type 6	*SERPHINH1*	*AR*
Osteogenesis imperfecta, type 7	*CRTAP*	*AR*
Osteogenesis imperfecta, type 8	*LEPRE1*	*AR*
Osteogenesis imperfecta, type 9	*PP1B*	*AR*
Osteogenesis imperfecta, type 10	*SERPINF1*	*AR*
Osteogenesis imperfecta, type 11	*FKBP10*	*AR*
Osteogenesis imperfecta, type 12	*BMP1*	*AR*
Osteogenesis imperfecta, type 13	*OSX*	*AR*
Osteogenesis imperfecta, type 14	*TMEM38B*	*AR*
Osteogenesis imperfecta, type 15	*WNT1*	*AR/AD*
Osteogenesis imperfecta, type 16	*CREB3L1*	*AR*
Osteogenesis imperfecta, type 17	*SPARC*	*AR*
Osteogenesis imperfecta, type 18	*MBTPS2*	*XLD*
Osteogenesis imperfecta, unclassified	*PLOD2*	*AR*
Osteoglophonic dysplasia	*FGFR1*	*AD*
Osteopetrosis	*LRP5*	*AD*
Osteopetrosis with ectodermal dysplasia and immune defect (OLEDAID)	*IKBKG*	*XLR*
Osteopetrosis with renal tubular acidosis	*CA2*	*AR*
Osteopetrosis, infantile form, osteoclast-poor	*TNFSF11 (RANKL)*	*AR*
Osteopetrosis, infantile form, with nervous system involvement	*OSTM1*	*AR*
Osteopetrosis, intermediate form	*CLCN7*	*AR*
Osteopetrosis, late-onset form type 1	*LRP5*	*AR*
Osteopetrosis, late-onset form type 2	*CLCN7*	*AD*

Table 1 Continued.

Osteopetrosis, severe neonatal or infantile form, osteoclast- poor	*TNFSF11 (RANKL)*	*AD*
Osteopetrosis, severe neonatal or infantile forms	*TCIRG1*	*AR*
Osteopoikilosis	*LEMD3*	*AD*
Osteoporosis pseudoglioma syndrome	*LRP5*	*AR*
Otopalatodigital syndrome type 1 (OPD1)	*FLNA*	*XLD*
Otopalatodigital syndrome type 2 (OPD2)	*FLNA*	*XLD*
Otospondylomegaepiphyseal dysplasia (OSMED)	*COL11A2*	*AR*
Pallister-Hall syndrome	*GLI3*	*AD*
Parietal foramina	*MSX2*	*AD*
Parietal foramina (isolated)	*ALX4*	*AD*
Pfeiffer syndrome	*FGFR1*	*AD*
Pfeiffer syndrome	*FGFR2*	*AD*
Postaxial polydactyly type A	*GLI3*	*AD*
Postaxial polydactyly type B	*GLI3*	*AD*
Preaxial polydactyly type 1	*SHH*	*AD*
Preaxial polydactyly type 2	*SHH*	*AD*
Preaxial polydactyly type 2/Triphalangeal Thumb	*LMBR1*	*AD*
Preaxial polydactyly type 4	*GLI3*	*AD*
Progressive osseous heteroplasia	*GNAS1*	*AD*
Progressive pseudorheumatoid dysplasia (PPRD)	*WISP3*	*AR*
Proximal symphalangism type 1	*NOG*	*AD*
Proximal symphalangism type 2	*GDF5*	*AD*
Pseudoachondroplasia (PSACH)	*COMP*	*AD*
Pyknodysostosis	*CTSK*	*AR*
Radio-ulnar synostosis with amegakaryocytic thrombocytopenia	*HOXA11*	*AD*
Rhizomelic CDP type 1	*PEX7*	*AR*
Rhizomelic CDP type 2	*DHPAT*	*AR*
Rhizomelic CDP type 3	*AGPS*	*AR*
Roberts syndrome	*ESCO2*	*AR*
Robinow syndrome	*ROR2*	*AR*
SADDAN (severe achondroplasia-developmental delay-acanthosis nigricans)	*FGFR3*	*AD*
Saethre-Chotzen syndrome	*FGFR2*	*AD*
Saethre-Chotzen syndrome	*FGFR3*	*AD*
Saethre-Chotzen syndrome	*TWIST1*	*AD*
Schwartz-Jampel syndrome (myotonic chondrodystrophy)	*HSPG2*	*AR*
Sclerosteosis	*SOST*	*AR*
SED Kimberley type	*ACAN*	*AD*

Table 1 Continued.

SED tarda, X-linked (SED-XL)	*SEDL*	*XLR*
SED Wolcott-Rallison type	*EIF2AK3*	*AR*
SEMD Aggrecan type	*ACAN*	*AR*
SEMD Matrilin type	*MATN3*	*AR*
SEMD Missouri type	*MMP13*	*AD*
SEMD Pakistani type	*PAPSS2*	*AR*
SEMD short limb—abnormal calcification type	*DDR2*	*AR*
Short rib polydacyty type 1/3	*DYNC2H1*	*AR*
Shwachman-Bodian- Diamond syndrome	*SBDS*	*AR*
Spondylo-carpal-tarsal dysplasia	*FLNB*	*AR*
Spondylocostal dysostosis type 1 (SCDO1)	*DLL3*	*AR*
Spondylocostal dysostosis type 2 (SCDO2)	*MESP2*	*AR*
Spondylocostal dysostosis type 3 (SCDO3)	*LFNG*	*AR*
Spondyloepimetaphyseal dysplasia (SEMD) Strudwick type	*COL2A1*	*AD*
Spondyloepiphyseal dysplasia congenita (SEDC)	*COL2A1*	*AD*
Spondylometaphyseal dysplasia Kozlowski type	*TRPV4*	*AD*
Stapes ankylosing syndrome without symphalangism	*NOG*	*AD*
Stickler syndrome type 1	*COL2A1*	*AD*
Stickler syndrome type 2	*COL11A1*	*AD*
Stuve-Wiedemann dysplasia	*LIFR*	*AR*
Syndactyly type 4	*SHH*	*AD*
Tarsal-carpal coalition syndrome	*NOG*	*AD*
Tetra-amelia	*WNT3*	*AR*
Thanatophoric dysplasia (type I and type II)	*FGFR3*	*AD*
Tooth agenesis	*AXIN2*	*AD*
Tooth agenesis	*EDA*	*XLD*
Tooth agenesis	*MSX1*	*AD*
Tooth agenesis	*PAX9*	*AD*
Tooth agenesis	*WNT10A*	*AR/AD*
Torg-Winchester syndrome	*MMP2*	*AR*
Townes-Brocks syndrome	*SALL1*	*AD*
Trichodentoosseous dysplasia	*DLX3*	*AD*
Trichorhinophalangeal dysplasia type 2 (Langer-Giedion)	*TRPS1*	*AD*
Triphalangeal thumb	*SHH*	*AD*
Ulnar-mammary syndrome	*TBX3*	*AD*
Van Buchem disease	*SOST*	*AR*
Weill-Marchesani syndrome	*FBN1*	*AD*
Weill-Marchesani syndrome, dominant type (Marfan syndrome)	*FBN1*	*AD*
Weill-Marchesani syndrome, recessive type	*ADAMTS10*	*AR*
Weyer acrofacial (acrodental) dysostosis	*EVC1/1*	*AD*

FIGURES

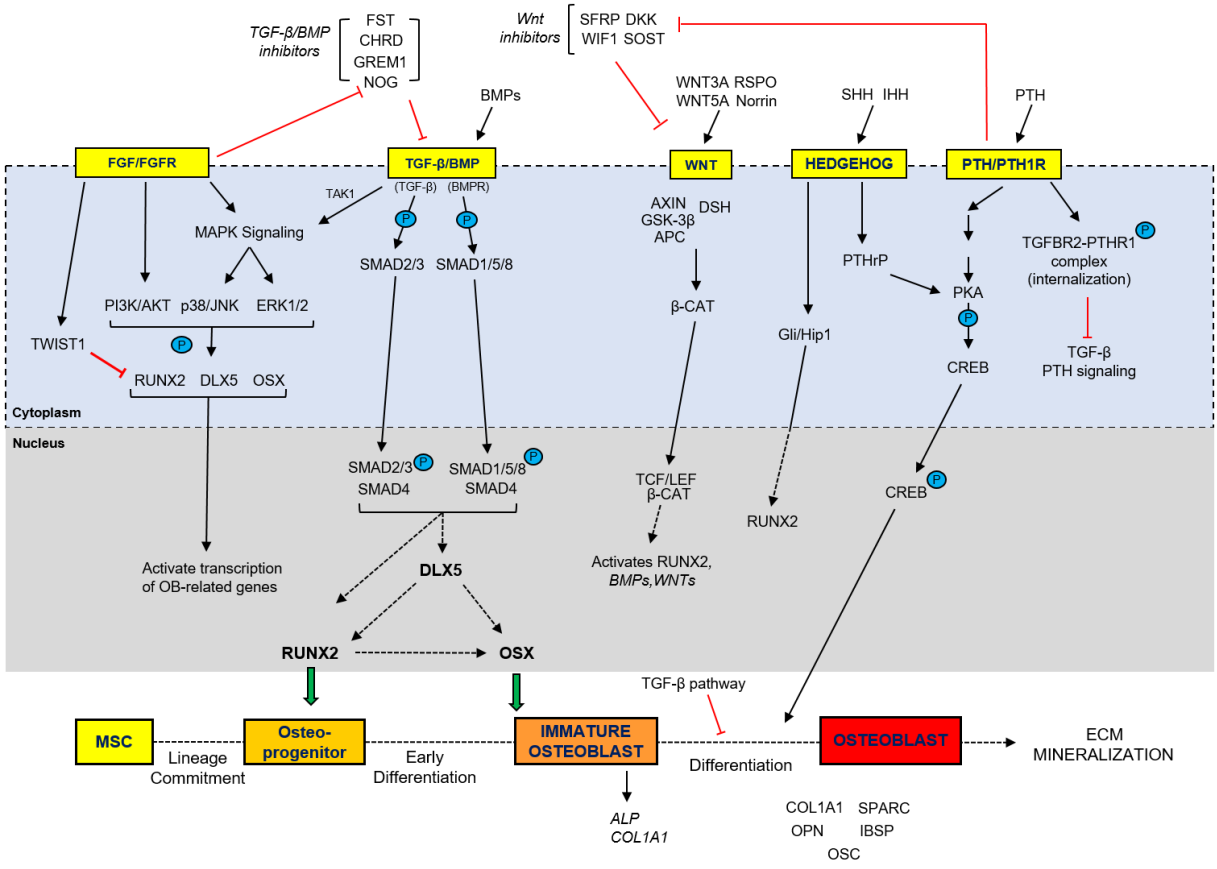

Figure 1. Overview of multiple signaling pathways influencing osteogenic differentiation from mesenchymal stem cells (adapted from Baron and Kneissel, 2013; Chen et al., 2012; Karsenty, 2008; Ornitz and Marie, 2015; Rahman et al., 2015; Wu et al., 2016).

REFERENCES

Abdallah, B.M. and Kassem, M. (2008) Human mesenchymal stem cells: from basic biology to clinical applications. *Gene Ther.*, **15**, 109–116.

Abel, J. and Haarmann-Stemmann, T. (2010) An introduction to the molecular basics of aryl hydrocarbon receptor biology. *Biol. Chem.*, **391**, 1235–1248.

Adams, J.D. *et al.* (1987) Toxic and carcinogenic agents in undiluted mainstream smoke and sidestream smoke of different types of cigarettes. *Carcinogenesis*, **8**, 729–731.

Addison, W.N. *et al.* (2007) Pyrophosphate inhibits mineralization of osteoblast cultures by binding to mineral, up-regulating osteopontin, and inhibiting alkaline phosphatase activity. *J. Biol. Chem.*, **282**, 15872–15883.

Alexander, P.G. *et al.* (2016) Prenatal exposure to environmental factors and congenital limb defects. *Birth Defects Res. Part C - Embryo Today Rev.*, **108**, 243–273.

Apschner, A. *et al.* (2011) Not All Bones are Created Equal – Using Zebrafish and Other Teleost Species in Osteogenesis Research Third Edit. Elsevier Inc.

Avery, S. *et al.* (2017) Analysing the bioactive makeup of demineralised dentine matrix on bone marrow mesenchymal stem cells for enhanced bone repair. *Eur. Cells Mater.*, **34**, 1–14.

Baker, A.H. *et al.* (2015) Tributyltin Engages Multiple Nuclear Receptor Pathways and Suppresses Osteogenesis in Bone Marrow Multipotent Stromal Cells. *Chem. Res. Toxicol.*, **28**, 1156–1166.

Baker, T.R. *et al.* (2014) Adverse effects in adulthood resulting from low-level dioxin exposure in juvenile zebrafish. *Endocr. Disruptors*, **2**, 1–6.

Baker, T.R. *et al.* (2013) Early dioxin exposure causes toxic effects in adult zebrafish. *Toxicol. Sci.*, **135**, 241–250.

Baksh, D. *et al.* (2004) Adult mesenchymal stem cells: characterization, differentiation, and application in cell and gene therapy. *J. Cell. Mol. Med.*, **8**, 301–316.

Baldridge, D. *et al.* (2010) Signaling pathways in human skeletal dysplasias. *Annu Rev Genomics Hum Genet*, **11**, 189–217.

Barbour, K.E. *et al.* (2014) Inflammatory Markers and Risk of Hip Fracture in Older White Women: The Study of Osteoporotic Fractures. *J. Bone Miner. Res.*, **29**, 2057–2064.

Baron, R. and Kneissel, M. (2013) WNT signaling in bone homeostasis and disease: from human mutations to treatments. *Nat. Med.*, **19**, 179–192.

Baroncelli, M. *et al.* (2017) Comparative proteomic profiling of human osteoblast-derived extracellular matrices identifies proteins involved in mesenchymal stromal cell

osteogenic differentiation and mineralization. *J. Cell. Physiol.*, 1–9.

Baroncelli, M. *et al.* (2017) Comparative Proteomic Profiling of Human Osteoblast-Derived Extracellular Matrices Identifies Proteins Involved in Mesenchymal Stromal Cell Osteogenic Differentiation and Mineralization. *J Cell Physiol*.

Benjamini, Y. and Hochberg, Y. (1995) Controlling the False Discovery Rate: A Practical and Powerful Approach to Multiple Testing. *J. R. Stat. Soc. Ser. B*, **57**, 289–300.

Benvenuti, S. *et al.* (2007) Rosiglitazone stimulates adipogenesis and decreases osteoblastogenesis in human mesenchymal stem cells. *J. Endocrinol. Invest.*, **30**, 26–30.

Bialek, P. *et al.* (2004) A Twist Code Determines the Onset of Osteoblast Differentiation. *Dev. Cell*, **6**, 423–435.

Bishop, N. (2016) Bone Material Properties in Osteogenesis Imperfecta. *J. Bone Miner. Res.*, **31**, 699–708.

Bodle, J.C. *et al.* (2014) Age-related effects on the potency of human adipose derived stem cells: Creation and evaluation of superlots and implications for musculoskeletal tissue engineering applications. *Tissue Eng. Part C Methods*, **20**, 1–43.

Bone health and osteoporosis: a report of the Surgeon General (2004) Rockville, Maryland.

Bonventre, J.A. *et al.* (2012) Craniofacial abnormalities and altered wnt and mmp mRNA expression in zebrafish embryos exposed to gasoline oxygenates ETBE and TAME. *Aquat. Toxicol.*, **120**–**121**, 45–53.

Boyce, B.F. and Xing, L. (2007) Biology of RANK, RANKL, and osteoprotegerin. *Arthritis Res. Ther.*, **9 Suppl 1**, S1.

Briggs, A.M. *et al.* (2016) Musculoskeletal Health Conditions Represent a Global Threat to Healthy Aging: A Report for the 2015 World Health Organization World Report on Ageing and Health. *Gerontologist*, **56**, S243–S255.

Burns, F.R. *et al.* (2015) Dioxin disrupts cranial cartilage and dermal bone development in zebrafish larvae. *Aquat. Toxicol.*, **164**, 52–60.

Bustin, S.A. *et al.* (2009) The MIQE Guidelines: Minimum Information for Publication of Quantitative Real-Time PCR Experiments. *Clin. Chem.*, **622**, 611–622.

Carpi, D. *et al.* (2009) Dioxin-sensitive proteins in differentiating osteoblasts: Effects on bone formation in vitro. *Toxicol. Sci.*, **108**, 330–343.

Charoenpanich, A. *et al.* (2014) Cyclic tensile strain enhances osteogenesis and angiogenesis in mesenchymal stem cells from osteoporotic donors. *Tissue Eng. Part A*, **20**, 67–78.

Chen, G. *et al.* (2012) TGF-β and BMP Signaling in Osteoblast Differentiation and Bone Formation. *Int. J. Biol. Sci.*, **8**, 272–288.

Chopra, M. and Schrenk, D. (2011) Dioxin toxicity, aryl hydrocarbon receptor signaling, and apoptosis-persistent pollutants affect programmed cell death. *Crit. Rev. Toxicol.*, **41**, 292–320.

Chrisman, K. *et al.* (2004) Gestational Ethanol Exposure Disrupts the Expression of FGF8 and Sonic hedgehog during Limb Patterning. *Birth Defects Res. Part A - Clin. Mol. Teratol.*, **70**, 163–171.

Christiansen, H.E. *et al.* (2010) Homozygosity for a Missense Mutation in SERPINH1, which Encodes the Collagen Chaperone Protein HSP47, Results in Severe Recessive Osteogenesis Imperfecta. *Am. J. Hum. Genet.*, **86**, 389–398.

Clarke, B. (2008) Normal bone anatomy and physiology. *Clin. J. Am. Soc. Nephrol.*, **3 (Suppl 3**.

Derrien, T. *et al.* (2012) The GENCODE v7 catalogue of human long non-coding RNAs : Analysis of their structure , evolution and expression. *Genome Res.*, **22**, 1775–1789.

Ding, D. *et al.* (2012) Over-expression of Sox2 in C3H10T1/2 cells inhibits osteoblast differentiation through Wnt and MAPK signalling pathways. *Int. Orthop.*, **36**, 1087–1094.

Dobin, A. *et al.* (2013) STAR: Ultrafast universal RNA-seq aligner. *Bioinformatics*, **29**, 15–21.

Dolk, H. *et al.* (2010) The Prevalence of Congenital Anomalies in Europe. In, Paz,M.P. de la and Croft,S.C. (eds), *Rare Diseases Epidemiology*. Springer, New York, New York, pp. 305–334.

Dominici, M. *et al.* (2006) Minimal criteria for defining multipotent mesenchymal stromal cells. The International Society for Cellular Therapy position statement. *Cytotherapy*, **8**, 315–7.

Dong, B. and Matsumura, F. (2008) Roles of cytosolic phospholipase A2 and Src kinase in the early action of 2,3,7,8-tetrachlorodibenzo-p-dioxin through a nongenomic pathway in MCF10A cells. *Mol. Pharmacol.*, **74**, 255–263.

Dong, W. *et al.* (2012) TCDD disrupts hypural skeletogenesis during medaka embryonic development. *Toxicol. Sci.*, **125**, 91–104.

Dong, W. *et al.* (2010) TCDD Induced Pericardial Edema and Relative COX-2 Expression in Medaka (Oryzias Latipes) Embryos. *Toxicol. Sci.*, **118**, 213–223.

Dudakovic, A. *et al.* (2015) Epigenetic Control of Skeletal Development by the Histone Demethylase Ezh2. *J. Biol. Chem.*, **290**, 27604–27617.

Ekanayake, S. and Hall, B.K. (1987) The development of acellularity of the vertebral bone of the Japanese medaka, *Oryzias latipes* (Teleostei; Cyprinidontidae). *J. Morphol.*, **193**, 253–261.

Ekanayake, S. and Hall, B.K. (1988) Ultrastructure of the osteogenesis of acellular vertebral bone in the Japanese medaka, Oryzias latipes (Teleostei, Cyprinidontidae). *Am. J. Anat.*, **182**, 241–249.

Ellis, L.D. *et al.* (2014) Use of the zebrafish larvae as a model to study cigarette smoke condensate toxicity. *PLoS One*, **9**, e115305.

Etemad, L. *et al.* (2012) Epilepsy drugs and effects on fetal development: Potential mechanisms. *J. Res. Med. Sci.*, **17**.

Fakhry, A. *et al.* (2005) Effects of FGF-2/-9 in calvarial bone cell cultures: Differentiation stage-dependent mitogenic effect, inverse regulation of BMP-2 and noggin, and enhancement of osteogenic potential. *Bone*, **36**, 254–266.

Felson, D.T. *et al.* (2000) Osteoarthritis: new insights. Part 1: the disease and its risk factors. *Ann. Intern. Med.*, **133**, 635–646.

Fernández-González, R. *et al.* (2015) A Critical Review about Human Exposure to Polychlorinated Dibenzo-p-Dioxins (PCDDs), Polychlorinated Dibenzofurans (PCDFs) and Polychlorinated Biphenyls (PCBs) through Foods. *Crit. Rev. Food Sci. Nutr.*, **55**, 1590–1617.

Finnilä, M.A.J. *et al.* (2010) Effects of 2,3,7,8-tetrachlorodibenzo-p-dioxin exposure on bone material properties. *J. Biomech.*, **43**, 1097–1103.

Fleming, A. *et al.* (2015) Building the backbone: the development and evolution of vertebral patterning. *Development*, **142**, 1733–44.

Flynn, R.A. and Chang, H.Y. (2014) Long noncoding RNAs in cell-fate programming and reprogramming. *Cell Stem Cell*, **14**, 752–761.

Forlino, A. *et al.* (2011) New perspectives on osteogenesis imperfecta. *Nat. Rev. Endocrinol.*, **7**, 540–557.

Forlino, A. and Marini, J.C. (2016) Osteogenesis imperfecta. *Lancet*, **387**, 1657–1671.

Franz-Odendaal, T.A. *et al.* (2006) Buried alive: How osteoblasts become osteocytes. *Dev. Dyn.*, **235**, 176–190.

Gadupudi, G. *et al.* (2015) PCB126 inhibits adipogenesis of human preadipocytes. *Toxicol. Vitr.*, **29**, 132–141.

Gallagher, J.C. and Sai, a. J. (2010) Molecular biology of bone remodeling: Implications for new therapeutic targets for osteoporosis. *Maturitas*, **65**, 301–307.

Gennari, L. *et al.* (2016) MicroRNAs in bone diseases. *Osteoporos. Int.*, 1–23.

Golub, E.E. and Boesze-Battaglia, K. (2007) The role of alkaline phosphatase in mineralization. *Curr. Opin. Orthop.*, **18**, 444–448.

Gordon, J.A.R. *et al.* (2015) Chromatin modifiers and histone modifications in bone formation, regeneration, and therapeutic intervention for bone-related disease. *Bone*, **81**, 739–745.

Gordon, J.A.R. *et al.* (2014) Epigenetic pathways regulating bone homeostasis: Potential targeting for intervention of skeletal disorders. *Curr. Osteoporos. Rep.*, **12**, 496–506.

Greco, S.J. *et al.* (2007) Functional Similarities Among Genes Regulated by Oct4 in Human Mesenchymal and Embryonic Stem Cells. *Stem Cells*, **25**, 3143–3154.

Grotmol, S. *et al.* (2005) A segmental pattern of alkaline phosphatase activity within the notochord coincides with the initial formation of the vertebral bodies. *J. Anat.*, **206**, 427–436.

Håkelien, A.M. *et al.* (2014) The regulatory landscape of osteogenic differentiation. *Stem Cells*, **32**, 2780–2793.

Hardy, R. and Cooper, M.S. (2009) Bone loss in inflammatory disorders. *J. Endocrinol.*, **201**, 309–320.

Heo, J. *et al.* (2015) Comparison of molecular profiles of human mesenchymal stem cells derived from bone marrow, umbilical cord blood, placenta and adipose tissue. *Int. J. Mol. Med.*, 115–125.

Herlin, M. *et al.* (2015) Inhibitory effects on osteoblast differentiation in vitro by the polychlorinated biphenyl mixture Aroclor 1254 are mainly associated with the dioxin-like constituents. *Toxicol. Vitr.*, **29**, 876–883.

Herlin, M. *et al.* (2013) New insights to the role of aryl hydrocarbon receptor in bone phenotype and in dioxin-induced modulation of bone microarchitecture and material properties. *Toxicol. Appl. Pharmacol.*, **273**, 219–26.

Herlin, M. *et al.* (2010) Quantitative characterization of changes in bone geometry, mineral density and biomechanical properties in two rat strains with different Ah-receptor structures after long-term exposure to 2,3,7,8-tetrachlorodibenzo-p-dioxin. *Toxicology*, **273**, 1–11.

Hermanns, P. and Lee, B. (2002) Transcriptional dysregulation in skeletal malformation syndromes. *Am. J. Med. Genet.*, **106**, 258–271.

Hernandez, C.J. *et al.* (2003) A theoretical analysis of the relative influences of peak BMD, age-related bone loss and menopause on the development of osteoporosis. *Osteoporos. Int.*, **14**, 843–847.

Holz, J.D. *et al.* (2007) Environmental agents affect skeletal growth and development. *Birth Defects Res. Part C - Embryo Today Rev.*, **81**, 41–50.

Huang, J. *et al.* (2010) MicroRNA-204 regulates Runx2 protein expression and mesenchymal progenitor cell differentiation. *Stem Cells*, **28**, 357–364.

Hulsen, T. *et al.* (2008) BioVenn – a web application for the comparison and visualization of biological lists using area-proportional Venn diagrams. *BMC Genomics*, **9**, 488.

Imai, Y. *et al.* (2013) Nuclear Receptors in Bone Physiology and Diseases. *Physiol. Rev.*, **93**, 481–523.

Inose, H. *et al.* (2009) A microRNA regulatory mechanism of osteoblast differentiation. *Proc. Natl. Acad. Sci. U. S. A.*, **106**, 20794–20799.

Ito, T. *et al.* (2010) Identification of a Primary Target of Thalidomide Teratogenicity. *Science (80-.).*, **327**, 1345–1351.

Ito, T. *et al.* (2011) Teratogenic effects of thalidomide: Molecular mechanisms. *Cell. Mol. Life Sci.*, **68**, 1569–1579.

Itoh, T. *et al.* (2009) MicroRNA-141 and -200a Are Involved in Bone Morphogenetic Protein-2-induced Mouse Pre-osteoblast Differentiation by Targeting Distal-less Homeobox 5. *J. Biol. Chem.*, **284**, 19272–19279.

Jämsä, T. *et al.* (2001) Effects of 2,3,7,8-Tetrachlorodibenzo-p-Dioxin on Bone in Two Rat Strains with Different Aryl Hydrocarbon Receptor Structures. *J. Bone Miner. Res.*, **16**, 1812–1820.

Jensen, E.D. *et al.* (2010) Regulation of gene expression in osteoblasts. *Biofactors*, **36**, 25–32.

Jenuwein, T. *et al.* (2001) Translating the Histone Code. *Science (80-.).*, **293**, 1074–1080.

Johnell, O. and Kanis, J.A. (2006) An estimate of the worldwide prevalence and disability associated with osteoporotic fractures. *Osteoporos. Int.*, **17**, 1726–1733.

Joshi-Tope, G. *et al.* (2005) Reactome: A knowledgebase of biological pathways. *Nucleic Acids Res.*, **33**, 428–432.

Kang, H. *et al.* (2017) Osteogenesis imperfecta: new genes reveal novel mechanisms in bone dysplasia. *Transl. Res.*, **181**, 27–48.

Kanis, J. (2007) Assessment of osteoporosis at the primary health care level.

Kanis, J. *et al.* (2005) Smoking and fracture risk: A meta-analysis. *Osteoporos. Int.*, **16**, 155–162.

Karsenty, G. *et al.* (2009) Genetic Control of Bone Formation. *Annu. Rev. Cell Dev. Biol.*, **25**, 629–648.

Karsenty, G. (2008) Transcriptional Control of Skeletogenesis. *Annu. Rev. Genomics Hum. Genet.*, **9**, 183–196.

Kawai, M. *et al.* (2010) The many facets of PPARgamma: novel insights for the skeleton. *Am. J. Physiol. Endocrinol. Metab.*, **299**, E3–E9.

Kimura, H. (2013) Histone modifications for human epigenome analysis. *J. Hum. Genet.*, **58**, 439–445.

King-Heiden, T.C. *et al.* (2012) Reproductive and developmental toxicity of dioxin in fish. *Mol. Cell. Endocrinol.*, **354**, 121–138.

Klareskog, L. *et al.* (2007) Smoking as a trigger for inflammatory rheumatic diseases. *Curr. Opin. Rheumatol.*, **19**, 49–54.

Ko, C.I. *et al.* (2016) Repression of the Aryl Hydrocarbon Receptor Is Required to Maintain Mitotic Progression and Prevent Loss of Pluripotency of Embryonic Stem Cells. *Stem Cells*, **34**, 2825–2839.

Komori, T. (2010) Regulation of bone development and extracellular matrix protein genes by RUNX2. *Cell Tissue Res.*, **339**, 189–195.

Komori, T. *et al.* (1997) Targeted disruption of Cbfa1 results in a complete lack of bone formation owing to maturational arrest of osteoblasts. *Cell*, **89**, 755–64.

Korkalainen, M. *et al.* (2009) Dioxins interfere with differentiation of osteoblasts and osteoclasts. *Bone*, **44**, 1134–1142.

Kornak, U. and Mundlos, S. (2003) Genetic disorders of the skeleton: a developmental approach. *Am. J. Hum. Genet.*, **73**, 447–74.

Kotake, S. *et al.* (1996) Interleukin-6 and Soluble Interleukin-6 Receptors in the Synovial Fluids from Rheumatoid Arthritis Patients Are Responsible for Osteoclast-like Cell Formation. *J. Bone Miner. Res.*, **11**, 88–95.

Krakow, D. and Rimoin, D.L. (2010) The skeletal dysplasias. *Genet. Med.*, **12**, 327–41.

Kung, M.H. *et al.* (2011) Aryl hydrocarbon receptor-mediated impairment of chondrogenesis and fracture healing by cigarette smoke and benzo(α)pyrene. *J. Cell. Physiol.*, **227**, 1062–1070.

Lacey, D.C. *et al.* (2009) Proinflammatory cytokines inhibit osteogenic differentiation from stem cells: implications for bone repair during inflammation. *Osteoarthr. Cartil.*, **17**, 735–742.

Laize, V. *et al.* (2014) Fish : a suitable system to model human bone disorders and discover drugs with osteogenic or osteotoxic activities. *Drug Discov. Today Dis. Model.*, **13**, 29–37.

Lam, J. *et al.* (2000) TNF-α induces osteoclastogenesis by direct stimulation of macrophages exposed to permissive levels of RANK ligand. *J. Clin. Invest.*, **106**, 1481–1488.

Law, M.R. and Hackshaw, a K. (1997) A meta-analysis of cigarette smoking, bone mineral density and risk of hip fracture: recognition of a major effect. *BMJ*, **315**, 841–846.

Lee, J.J. *et al.* (2013) The musculoskeletal effects of cigarette smoking. *J. Bone Jt. Surg.*, **95**,

850–9.

Lee, M.H. *et al.* (2003) BMP-2-induced Osterix expression is mediated by Dlx5 but is independent of Runx2. *Biochem. Biophys. Res. Commun.*, **309**, 689–694.

Lee, M.H. *et al.* (2005) Dlx5 specifically regulates Runx2 type II expression by binding to homeodomain-response elements in the Runx2 distal promoter. *J. Biol. Chem.*, **280**, 35579–35587.

Lefebvre, V. and Bhattaram, P. (2010) Vertebrate Skeletogenesis. In, Koopman,P. (ed), *Current Topics in Developmental Biology: Organogenesis in Development*. Elsevier Inc., San Diego, pp. 291–317.

Li, L. *et al.* (2013) Targeted Disruption of Hotair Leads to Homeotic Transformation and Gene Derepression. *Cell Rep.*, **5**, 3–12.

Li, W. *et al.* (2008) Development of a human adipocyte model derived from human mesenchymal stem cells (hMSC) as a tool for toxicological studies on the action of TCDD. *Biol. Chem.*, **389**, 169–177.

Lian, J.B. *et al.* (2006) Networks and hubs for the transcriptional control of osteoblastogenesis. *Rev. Endocr. Metab. Disord.*, **7**, 1–16.

Lindner, U. *et al.* (2010) Mesenchymal stem or stromal cells: Toward a better understanding of their biology? *Transfus. Med. Hemotherapy*, **37**, 75–83.

Liu, B. *et al.* (2013) Depleting the methyltransferase Suv39h1 improves DNA repair and extends lifespan in a progeria mouse model. *Nat. Commun.*, **4**, 1868.

Liu, P. *et al.* (1996) Alteration by 2,3,7,8-Tetrachlordibenzo-p-dioxin of CCAAT/Enhancer Binding Protein Correlates with Suppression of Adipocyte Differentiation in 3T3-L1 Cells. *Mol. Pharmacol.*, **49**, 989–997.

Livak, K.J. and Schmittgen, T.D. (2001) Analysis of relative gene expression data using real-time quantitative PCR and the 2(-Delta Delta C(T)) Method. *Methods*, **25**, 402–8.

Long, F. (2011) Building strong bones: molecular regulation of the osteoblast lineage. *Nat. Rev. Mol. Cell Biol.*, **13**, 27–38.

Lorentzon, M. *et al.* (2007) Smoking is associated with lower bone mineral density and reduced cortical thickness in young men. *J. Clin. Endocrinol. Metab.*, **92**, 497–503.

Love, M.I. *et al.* (2014) Moderated estimation of fold change and dispersion for RNA-seq data with DESeq2. *Genome Biol.*, **15**, 550.

Lu, J. *et al.* (2015) Effect of fibroblast growth factor 9 on the osteogenic differentiation of bone marrow stromal stem cells and dental pulp stem cells. *Mol. Med. Rep.*, **11**, 1661–1668.

Lu, J. *et al.* (2014) The Effect of Fibroblast Growth Factor 9 on the Osteogenic

Differentiation of Calvaria-Derived Mesenchymal Cells. *J. Craniofac. Surg.*, **25**, 502–505.

Manolagas, S.C. (2000) Birth and death of bone cells: basic regulatory mechanisms and implications for the pathogenesis and treatment of osteoporosis. *Endocr. Rev.*, **21**, 115–137.

Mansukhani, A. *et al.* (2005) Sox2 induction by FGF and FGFR2 activating mutations inhibits Wnt signaling and osteoblast differentiation. *J. Cell Biol.*, **168**, 1065–1076.

Marcellini, S. *et al.* (2012) Control of osteogenesis by the canonical Wnt and BMP pathways in vivo: cooperation and antagonism between the canonical Wnt and BMP pathways as cells differentiate from osteochondroprogenitors to osteoblasts and osteocytes. *BioEssays News Rev. Mol. Cell. Dev. Biol.*, **34**, 953–62.

Marotti, G. (1996) The structure of bone tissues and the cellular control of their deposition. *Ital. J. Anat. Embryol.*, **101**, 25–79.

McCormack, S.E. *et al.* (2017) Association Between Linear Growth and Bone Accrual in a Diverse Cohort of Children and Adolescents. *JAMA Pediatr.*, **19104**, 1–9.

Miettinen, H.M. *et al.* (2005) Effects of in utero and lactational TCDD exposure on bone development in differentially sensitive rat lines. *Toxicol. Sci.*, **85**, 1003–1012.

Mizuno, Y. *et al.* (2008) miR-125b inhibits osteoblastic differentiation by down-regulation of cell proliferation. *Biochem. Biophys. Res. Commun.*, **368**, 267–272.

Montecino, M. *et al.* (2015) Multiple levels of epigenetic control for bone biology and pathology. *Bone*, **81**, 733–738.

Mundy, G.R. (2007) Osteoporosis and Inflammation. *Nutr. Rev.*, **65**.

Murante, F.G. and Gasiewicz, T.A. (2000) Hemopoietic Progenitor Cells Are Sensitive Targets of 2,3,7,8-Tetrachlorodibenzo-p-dioxin in C57BL/6J Mice. *Toxicol. Sci.*, **54**, 374–383.

Nakase, T. *et al.* (1997) Interleukin-1 beta enhances and tumor necrosis factor-alpha inhibits bone morphogenetic protein-2-induced alkaline phosphatase activity in MC3T3-E1 osteoblastic cells. *Bone*, **21**, 17–21.

Nakashima, K. *et al.* (2002) The novel zinc finger-containing transcription factor osterix is required for osteoblast differentiation and bone formation. *Cell*, **108**, 17–29.

Nakashima, T. *et al.* (2012) New insights into osteoclastogenic signaling mechanisms. *Trends Endocrinol. Metab.*, **23**, 582–90.

Narkowicza, S. *et al.* (2013) Environmental Tobacco Smoke: Exposure, Health Effects, and Analysis. *Biocontrol Sci. Technol.*, **43**, 121–161.

Naruse, M. *et al.* (2002) 3-Methylcholanthrene, which binds to the arylhydrocarbon receptor,

inhibits proliferation and differentiation of osteoblasts in vitro and ossification in vivo. *Endocrinology*, **143**, 3575–81.

Nishio, Y. *et al.* (2006) Runx2-mediated regulation of the zinc finger Osterix/Sp7 gene. *Gene*, **372**, 62–70.

Nordvik, K. *et al.* (2005) The salmon vertebral body develops through mineralization of two preformed tissues that are encompassed by two layers of bone. *J. Anat.*, **206**, 103–114.

Ohtake, F. *et al.* (2009) AhR acts as an E3 ubiquitin ligase to modulate steroid receptor functions. *Biochem. Pharmacol.*, **77**, 474–84.

Orioli, I.M. *et al.* (1986) The birth prevalence rates for the skeletal dysplasias. *J. Med. Genet.*, **23**, 328–32.

Ornitz, D.M. and Marie, P.J. (2015) Fibroblast growth factor signaling in skeletal development and disease. *Genes Dev.*, **29**, 1463–1486.

Padilla, S. *et al.* (2012) Zebrafish developmental screening of the ToxCast^{TM} Phase I chemical library. *Reprod. Toxicol.*, **33**, 174–187.

van de Peppel, J. *et al.* (2017) Identification of Three Early Phases of Cell-Fate Determination during Osteogenic and Adipogenic Differentiation by Transcription Factor Dynamics. *Stem Cell Reports*, **172**, 5457–5476.

Pillai, H.K. *et al.* (2014) Ligand Binding and Activation of PPARγ by Firemaster 550: Effects on Adipogenesis and Osteogenesis in Vitro. *Environ. Health Perspect.*, **122**, 1225–1232.

Podechard, N. *et al.* (2009) Inhibition of human mesenchymal stem cell-derived adipogenesis by the environmental contaminant benzo(a)pyrene. *Toxicol. In Vitro*, **23**, 1139–44.

Pohl, H. *et al.* (1998) Toxicological profile for chlorinated dibenzo-p-dioxins.

Puga, A. *et al.* (2000) Aromatic Hydrocarbon Receptor Interaction with the Retinoblastoma Protein Potentiates Repression of E2F-dependent Transcription and Cell Cycle Arrest. *J. Biol. Chem.*, **275**, 2943–2950.

Puga, A. *et al.* (2009) The aryl hydrocarbon receptor cross-talks with multiple signal transduction pathways. *Biochem. Pharmacol.*, **77**, 713–722.

Quiroz, F.G. *et al.* (2010) Housekeeping gene stability influences the quantification of osteogenic markers during stem cell differentiation to the osteogenic lineage. *Cytotechnology*, **62**, 109–120.

Rahman, M.S. *et al.* (2015) TGF-β/BMP signaling and other molecular events: regulation of osteoblastogenesis and bone formation. *Bone Res.*, **3**, 15005.

Redlich, K. and Smolen, J.S. (2012) Inflammatory bone loss: pathogenesis and therapeutic intervention. *Nat. Rev. Drug Discov.*, **11**, 234–250.

Riekstina, U. *et al.* (2009) Embryonic stem cell marker expression pattern in human mesenchymal stem cells derived from bone marrow, adipose tissue, heart and dermis. *Stem Cell Rev. Reports*, **5**, 378–386.

Riss, T.L. *et al.* (2004) Cell Viability Assays Assay Guidance Manual. *Assay Guid. Man.*, 1–23.

Rizzoli, R. *et al.* (2010) Maximizing bone mineral mass gain during growth for the prevention of fractures in the adolescents and the elderly. *Bone*, **46**, 294–305.

Rosano, A. *et al.* (2000) Limb defects associated with major congenital anomalies: Clinical and epidemiological study from the international clearinghouse for birth defects monitoring systems. *Am. J. Med. Genet.*, **93**, 110–116.

Rosen, E.D. and MacDougald, O.A. (2006) Adipocyte differentiation from the inside out. *Nat. Rev. Mol. Cell Biol.*, **7**, 885–896.

Rosset, E.M. and Bradshaw, A.D. (2016) SPARC/osteonectin in mineralized tissue. *Matrix Biol.*, **52**–**54**, 78–87.

Ryan, E.P. *et al.* (2007) Environmental toxicants may modulate osteoblast differentiation by a mechanism involving the aryl hydrocarbon receptor. *J. Bone Miner. Res.*, **22**, 1571–80.

Safe, S. *et al.* (1998) Ah receptor agonists as endocrine disruptors: antiestrogenic activity and mechanisms. *Toxicol. Lett.*, **102**–**103**, 343–7.

Safe, S. (1995) Cellular and molecular biology of aryl hydrocarbon (Ah) receptor-mediated gene expression. *Arch. Toxicol.*, **17**, 99–115.

Sakaguchi, Y. *et al.* (2009) Suspended cells from trabecular bone by collagenase digestion become virtually identical to mesenchymal stem cells obtained from marrow. *Stem Cells*, **104**, 2728–2735.

Sargis, R.M. *et al.* (2009) Environmental Endocrine Disruptors Promote Adipogenesis in the 3T3-L1 Cell Line through Glucocorticoid Receptor Activation. *Obesity*, **18**, 1283–1288.

Schönitzer, V. *et al.* (2014) Sox2 is a potent inhibitor of osteogenic and adipogenic differentiation in human mesenchymal stem cells. *Cell. Reprogram.*, **16**, 355–65.

Schroeder, T.M. *et al.* (2005) Runx2: A master organizer of gene transcription in developing and maturing osteoblasts. *Birth Defects Res. Part C - Embryo Today Rev.*, **75**, 213–225.

Sciullo, E.M. *et al.* (2009) Characterization of the pattern of the nongenomic signaling pathway through which TCDD-induces early inflammatory responses in U937 human macrophages. *Chemosphere*, **74**, 1531–1537.

Scolaro, J.A. *et al.* (2014) Cigarette Smoking Increases Complications Following Fracture. *J. Bone Jt. Surg.*, 674–681.

Seo, E. *et al.* (2011) Distinct Functions of Sox2 Control Self-Renewal and Differentiation in the Osteoblast Lineage. *Mol. Cell. Biol.*, **31**, 4593–4608.

Sheng, G. (2015) The developmental basis of mesenchymal stem/stromal cells (MSCs). *BMC Dev. Biol.*, **15**, 44.

Shimba, S. *et al.* (2001) Aryl hydrocarbon receptor (AhR) is involved in negative regulation of adipose differentiation in 3T3- L1 cells : AhR inhibits adipose differentiation independently of dioxin. *J. Cell Sci.*, **114**, 2809–2817.

Siegel, G. *et al.* (2013) Phenotype, donor age and gender affect function of human bone marrow-derived mesenchymal stromal cells. *BMC Med.*, **11**, 146.

Simonet, W.S. *et al.* (1997) Osteoprotegerin: a novel secreted protein involved in the regulation of bone density. *Cell*, **89**, 309–19.

Singh, K.P. *et al.* (2009) Treatment of mice with the Ah receptor agonist and human carcinogen dioxin results in altered numbers and function of hematopoietic stem cells. *Carcinogenesis*, **30**, 11–19.

Sinha, K.M. and Zhou, X. (2013) Genetic and molecular control of osterix in skeletal formation. *J. Cell. Biochem.*, **114**, 975–84.

Sipes, N.S. *et al.* (2011) Zebrafish-as an integrative model for twenty-first century toxicity testing. *Birth Defects Res. Part C, Embryo Today Rev.*, **93**, 256–267.

Sloan, A. *et al.* (2010) The effects of smoking on fracture healing. *Surg. J. R. Coll. Surg. Edinburgh Irel.*, **8**, 111–6.

Smith, K.J. *et al.* (2011) Identification of a high-affinity ligand that exhibits complete aryl hydrocarbon receptor antagonism. *J. Pharmacol. Exp. Ther.*, **338**, 318–327.

Sozen, T. *et al.* (2017) An overview and management of osteoporosis. *Eur. J. Rheumatol.*, **4**, 46–56.

Spandidos, A. *et al.* (2010) PrimerBank : a resource of human and mouse PCR primer pairs for gene expression detection and quantification. **38**, 792–799.

Staines, K.A. *et al.* (2012) The importance of the SIBLING family of proteins on skeletal mineralisation and bone remodelling. *J. Endocrinol.*, **214**, 241–255.

Su, N. *et al.* (2008) FGF signaling: its role in bone development and human skeletal diseases. *Front. Biosci.*, **13**, 2842–2865.

Teraoka, H. *et al.* (2006) Impairment of lower jaw growth in developing zebrafish exposed to 2,3,7,8-tetrachlorodibenzo-p-dioxin and reduced hedgehog expression. *Aquat. Toxicol.*, **78**, 103–113.

Teraoka, H. *et al.* (2006) Muscular contractions in the zebrafish embryo are necessary to reveal thiuram-induced notochord distortions. *Toxicol. Appl. Pharmacol.*, **212**, 24–34.

The Health Consequences of Smoking - — 50 Years of Progress A Report of the Surgeon General (2014) Rockville, Maryland.

Tian, L. *et al.* (2017) miR-148a-3p regulates adipocyte and osteoblast differentiation by targeting lysine-specific demethylase 6b. *Gene*, **627**, 32–39.

Tian, Y. *et al.* (2002) Ah receptor and NF-kB interactions: Mechanisms and physiological implications. *Chem. Biol. Interact.*, **141**, 97–115.

Tilton, F. *et al.* (2006) Dithiocarbamates have a common toxic effect on zebrafish body axis formation. *Toxicol. Appl. Pharmacol.*, **216**, 55–68.

Tox21: Chemical testing in the 21st century (2017) Research Triangle Park, NC.

Truong, L. *et al.* (2014) Multidimensional in vivo hazard assessment using zebrafish. *Toxicol. Sci.*, **137**, 212–233.

Tye, C.E. *et al.* (2015) Could lncRNAs be the Missing Links in Control of Mesenchymal Stem Cell Differentiation? *J. Cell. Physiol.*, **230**, 526–534.

Tyl, R.W. *et al.* (2007) Altered Axial Skeletal Development. *Birth Defects Res. Part B-Developmental Reprod. Toxicol.*, **472**, 451–472.

Voss, A. *et al.* (2016) Extracellular Matrix of Current Biological Scaffolds Promotes the Differentiation Potential of Mesenchymal Stem Cells. *Arthrosc. - J. Arthrosc. Relat. Surg.*, **32**, 2381–2392.e1.

van de Vyver, M. *et al.* (2014) Thiazolidinedione-induced lipid droplet formation during osteogenic differentiation. *J. Endocrinol.*, **223**, 119–132.

Wade, S.W. *et al.* (2014) Estimating prevalence of osteoporosis: examples from industrialized countries. *Arch. Osteoporos.*, **9**, 182.

Wang, C.-K. *et al.* (2009) Aryl hydrocarbon receptor activation and overexpression upregulated fibroblast growth factor-9 in human lung adenocarcinomas. *Int. J. Cancer*, **125**, 807–815.

Wang, Y. *et al.* (2010) Dioxin Exposure Disrupts the Differentiation of Mouse Embryonic Stem Cells into Cardiomyocytes. **115**, 225–237.

Wang, Z. *et al.* (2012) Distinct lineage specification roles for NANOG, OCT4, and SOX2 in human embryonic stem cells. *Cell Stem Cell*, **10**, 440–454.

Ward, K.D. and Klesges, R.C. (2001) A Meta-Analysis of the Effects of Cigarette Smoking on Bone Mineral Density. *Calcif. Tissue Int.*, **68**, 259–270.

Watson, A.T.D. *et al.* (2017) Embryonic Exposure to TCDD Impacts Osteogenesis of the Axial Skeleton in Japanese medaka, Oryzias latipes. *Toxicol. Sci.*, **155**, 485–496.

Watt, J. and Schlezinger, J.J. (2015) Structurally-diverse, PPARγ-activating environmental

toxicants induce adipogenesis and suppress osteogenesis in bone marrow mesenchymal stromal cells. *Toxicology*, **331**, 66–77.

Wilffert, B. *et al.* (2011) Pharmacogenetics of drug-induced birth defects: what is known so far? *Pharmacogenomics*, **12**, 547–558.

Wilson, C.L. and Safe, S. (1998) Mechanisms of ligand-induced aryl hydrocarbon receptor-mediated biochemical and toxic responses. *Toxicol. Pathol.*, **26**, 657–671.

Witten, P.E. *et al.* (2016) Small teleost fish provide new insights into human skeletal diseases Elsevier Ltd.

Witten, P.E. and Huysseune, A. (2009) A comparative view on mechanisms and functions of skeletal remodelling in teleost fish, with special emphasis on osteoclasts and their function. *Biol. Rev.*, **84**, 315–346.

Wong, P.K.K. *et al.* (2007) The effects of smoking on bone health. *Clin. Sci.*, **113**, 233–41.

Wu, H. *et al.* (2017) Chromatin Dynamics Regulate Mesenchymal Stem Cell Lineage Specification and Differentiation to Osteogenesis. *Biochim. Biophys. Acta - Gene Regul. Mech.*, **1860**, 438–449.

Wu, M. *et al.* (2016) TGF-β and BMP signaling in osteoblast, skeletal development, and bone formation, homeostasis and disease. *Bone Res.*, **4**, 16009.

Yamashita, T. *et al.* (2012) New roles of osteoblasts involved in osteoclast differentiation. *World J. Orthop.*, **3**, 175–81.

Yanbaeva, D.G. *et al.* (2007) Systemic effects of smoking. *Chest*, **131**, 1557–66.

Yang, J.-H. and Lee, H.-G. (2010) 2,3,7,8-Tetrachlorodibenzo-p-dioxin induces apoptosis of articular chondrocytes in culture. *Chemosphere*, **79**, 278–284.

Yoon, V. *et al.* (2012) The effects of smoking on bone metabolism. *Osteoporos. Int.*, **23**, 2081–92.

Zhang, G. (2009) An evo-devo view on the origin of the backbone: evolutionary development of the vertebrae. *Integr. Comp. Biol.*, **49**, 178–186.

Zhang, Y.H. *et al.* (1990) Interleukin-6 induction by tumor necrosis factor and interleukin-1 in human fibroblasts involves activation of a nuclear factor binding to a kappa B-like sequence. *Mol. Cell. Biol.*, **10**, 3818–23.

CHAPTER 2

Embryonic exposure to TCDD impacts osteogenesis of the axial skeleton in Japanese medaka, *Oryzias latipes*

AtLee T. D. Watson*, Antonio Planchart*[†], Carolyn J. Mattingly*[†], Christoph Winkler[‡], David M. Reif[†§¶], Seth W. Kullman*[†]

* Department of Biological Sciences, North Carolina State University, Raleigh, North Carolina 27695

[†] Center for Human Health and the Environment, North Carolina State University, Raleigh, North Carolina 27695

[‡] Department of Biological Sciences, National University of Singapore, Singapore 117543

[§] Department of Statistics, North Carolina State University, Raleigh, North Carolina 27595

[¶] Bioinformatics Research Center, North Carolina State University, Raleigh, North Carolina 27695

Published in Toxicological Sciences (2017) 155: 485-496.

ABSTRACT

Recent studies from mammalian, fish, and *in vitro* models have identified bone and cartilage development as sensitive targets for dioxins and other aryl hydrocarbon receptor ligands. In this study, we assess how embryonic TCDD exposure impacts axial osteogenesis in Japanese medaka (*Oryzias latipes*), a vertebrate model of human bone development. Embryos from inbred wild-type Orange-red Hd-dR and three transgenic medaka lines (*twist*:EGFP, *osx/sp7*:mCherry, *col10a1*:nlGFP) were exposed to 0.15 nM and 0.3 nM TCDD and reared until 20 dpf. Individuals were stained for mineralized bone and imaged using confocal microscopy to assess skeletal alterations in medial vertebrae in combination with qualitative spatial analysis of osteoblast and osteoblast progenitor cell populations. Exposure to TCDD resulted in an overall attenuation of vertebral ossification characterized by truncated centra, and reduced neural and hemal arch lengths. Effects on mineralization were consistent with modifications in cell number and cell localization of transgene-labeled osteoblast and osteoblast progenitor cells. Endogenous expression of osteogenic regulators runt-related transcription factor 2 (*runx2*) and osterix (*osx/sp7*), and extracellular matrix genes osteopontin (*spp1*), collagen type I alpha I (*col1*), collagen type X alpha I (*col10a1*), and osteocalcin (*bglap/osc*) was significantly diminished at 20 dpf following TCDD exposure as compared to controls. Through global transcriptomic analysis more than 590 differentially expressed genes were identified and mapped to select pathological states including inflammatory disease, connective tissue disorders, and skeletal and muscular disorders. Taken together, results from this study suggest that TCDD exposure inhibits axial bone formation through dysregulation of

osteoblast differentiation. This approach highlights the advantages and sensitivity of using small fish models to investigate how xenobiotic exposure may impact skeletal development.

INTRODUCTION

With more than 35 defined disorders, skeletal dysplasias represent a diverse class of congenital defects that occur approximately once in every 5000 human births (Orioli et al., 1986). Affected individuals display a range of functional deficits resulting from defects in early skeletal pattern formation or subsequent defects in growth and development of cartilage and bone (Krakow and Rimoin, 2010). In past decades, clinical and molecular studies have improved our understanding of mechanisms underlying skeletal dysplasias through identification of loss-of-heterozygosity (LOH) mutations in key osteogenic mediators (Hermanns and Lee, 2002).

Normal bone development requires strict temporal and spatial coordination of early gene regulatory networks that govern commitment of mesenchymal stem cells (MSCs) to an osteogenic lineage, and subsequent differentiation to become mature, matrix-secreting osteoblasts (Lefebvre and Bhattaram, 2010). These events integrate stimuli from canonical developmental pathways [Wnt, Hedgehog, Notch, Fibroblast growth factor, Bone morphogenetic protein signaling (Kneissel and Baron, 2013; Marcellini et al., 2012)] and other endocrine and paracrine mediators (Imai et al., 2013) to regulate osteoblast differentiation (for review see Karsenty et al., 2009; Sinha and Zhou, 2013). In mammals and teleosts, mature osteoblasts secrete extracellular bone matrix to form ossified, or mineralized bone comprising the appendicular skeleton and the vertebral bodies and craniofacial elements of the axial skeleton (Apschner et al., 2011). In mammals, vertebrae form via endochondral ossification where cartilage is gradually replaced by bone matrix. To contrast, teleosts undergo perichordal ossification after the initial mineralization and segmental patterning of the notochordal sheath,

a cartilage-like structure (Fleming et al., 2015; Grotmol et al., 2005; Nordvik et al., 2005). Despite these distinctions in how vertebrae are ossified, the molecular events driving bone formation remain conserved among most vertebrates (Lefebvre and Bhattaram, 2010; Zhang, 2009).

Within these conserved gene regulatory networks, the runt-related transcription factor 2 (runx2) and the zinc-finger transcription factor osterix/sp7 (osx/sp7) transcription factors are considered the master regulators of osteoblast differentiation. Runx2 drives MSC commitment toward an osteoblast fate via binding of its runt DNA-binding domain to gene promoters containing runx consensus sequences (Karsenty et al., 2009; Komori, 2010). In sclerotome-derived MSCs Runx2 activity is inhibited by the basic helix-loop-helix (bHLH) transcription factor Twist1 (Bialek et al., 2004). Osx/Sp7 drives differentiation of pre-osteoblasts into immature osteoblasts, a critical step in the formation of mature osteoblasts (Nakashima et al., 2002). As osteoblast maturation progresses, Runx2 and Osx/Sp7 regulate the expression of extracellular matrix proteins that support adhesion, proliferation, differentiation, and migration of osteoblasts in the bone microenvironment. Matrix molecules consisting of collagenous (e.g. Collagen Type X alpha 1, Collagen Type I alpha 1) as well as non-collagenous proteins (e.g. Osteocalcin, Osteonectin, Osteopontin) also serve as structural support for bone (Kirkham and Cartmell, 2007).

There is increasing concern, however, that xenobiotic exposure during embryonic development may perturb the complex transcriptional landscape required for osteoblast differentiation and ossification. Assessments of chemical toxicity in mammalian species (mouse, rat, rabbit) suggest that alterations to skeletal development are a commonly observed

phenotype (Sipes et al., 2011). Over the past decade small aquarium fish such as zebrafish (Danio rerio) and Japanese medaka (Oryzias latipes) have seen increasing use as vertebrate models of human bone development due to their high fecundity, transparent embryonic development, genetic tractability, and ease of creating transgenic models (Hammond and Moro, 2012). By screening 1060 chemicals in a zebrafish developmental assay, Truong et al. identified numerous compounds that elicit craniofacial and axial deficits (2014). Specifically, alterations in axial skeletal development in fish were identified as a sensitive endpoint in screening assays with dissimilar classes of chemical agents (McCollum et al., 2011; Tyl et al., 2007), suggesting that there may be multiple mechanisms associated with chemically induced skeletal deficits.

The toxicity of the environmental contaminant, 2,3,7,8-tetrachlorodibenzo-p-dioxin (TCDD, or dioxin) has been extensively studied as a potent ligand of aryl hydrocarbon receptor (AhR). The AhR is a well characterized transcription factor in medaka and has been identified as early as the neurula stage of development [medaka stage 17, approximately 24 hours post fertilization, hpf (Iwamatsu, 2004)] (Hanno et al., 2010). Conversely, functional assays demonstrate AhR transactivation as early as 6 hpf in tg(*cyp1a*:gfp) medaka (Ng and Gong, 2013), where cyp1a induction serves as a sensitive marker of AhR activation. Numerous studies have reported the teratogenic effects of TCDD in multiple organ systems in medaka and zebrafish following developmental exposure (King-Heiden et al., 2012). Specifically, in terms of skeletal toxicity, TCDD exposure in teleosts disrupts cartilage formation in craniofacial (Burns et al., 2015; Planchart and Mattingly, 2010; Teraoka et al., 2006; Xiong et al., 2008) and axial regions (Tracie R. Baker et al., 2014; Dong et al., 2012). Additionally,

TCDD has been shown to alter dermal bone formation within the craniofacial skeleton (Burns et al., 2015), however the effects of TCDD on axial bone formation remain unknown.

In this study, Japanese medaka were exposed to low concentrations (pico- to nanomolar) of TCDD during early embryonic development to investigate whether TCDD inhibits formation of the vertebral bodies in larvae. We hypothesized that TCDD would inhibit expression of key regulators of osteoblast differentiation, most notably osx/sp7. To address this, we performed high-resolution confocal microscopy of tg(*twist*:EGFP, *osx/sp7*:mCherry, *col10a1*:nlGFP) medaka, and assessed gene expression of osteogenic regulators and ECM genes. Results of this study demonstrate that 0.15-0.3 nM TCDD elicits a teratogenic effect on axial skeletal development likely through attenuation of osx/sp7 expression.

MATERIALS AND METHODS

Medaka Care and Culture

All Japanese medaka (Oryzias latipes) in this study were used in compliance with protocols approved by the North Carolina State University Institutional Animal Care and Use Committee. Brood stocks were housed in an enclosed, recirculating aquaculture system under a 14:10 light:dark cycle. Temperature, pH, and conductivity were monitored daily and maintained at 24 ± 2^0C, 7.2 ± 0.2, and 300 ± 50 µS, respectively. Under these conditions, medaka spawned daily and offspring were reared to adulthood to replace aging cohorts in the breeding colony. For the following experiments, the inbred Orange-red Hd-dR (OR) and the previously described transgenic strains tg(*osx/sp7*:mCherry) (Renn and Winkler, 2009), tg(c*ol10a1*:nlGFP) (Renn et al., 2013), tg(*twist*:EGFP) (Yasutake et al., 2004) were used (Table 1).

TCDD Exposure

Embryos were collected from breeding tanks, cleaned, and staged according to previously established methods (Iwamatsu, 2004). Fertilized embryos were distributed to six-well tissue culture plates containing five mL of 1X embryo rearing medium (ERM) (17.1 mM NaCl, 272 µM CaCl2•2H2O, 402 µM KCl, and 661 µM MgSO4•7H2O, pH 7.4) at a density of 12-15 embryos/well. At approximately four hours post fertilization (hpf), stage 8-9 embryos were exposed for one hour to 0.1% DMSO (Sigma Aldrich, St. Louis, MO) or 2,3,7,8-tetrachlorochlorodibenzo-p-dioxin (TCDD, or dioxin) (Cambridge Isotopes Laboratory, Andover, MA) in DMSO. Each experiment consisted of three or more replicates. Following TCDD exposure, embryos were washed four times with 1X ERM and cultured at 26-27 °C

with static media renewal every other day until hatch or until dechorionation at nine days post fertilization (dpf). Briefly, embryos were dechorionated with 20-mg/ml pronase (EMD Millipore, Darmstadt, Germany) followed by incubation in hatching enzyme (Kinoshita et al., 2009). Hatched individuals were transferred to plastic containers containing 100 mL of 1X ERM, were fed 1-2 mg of ground Otohime B1 larval diet (Reed Mariculture, Campbell, CA) daily, and media was renewed every other day until the termination of the experiment at 20 dpf.

Whole-mount histological staining for bone

Larvae were euthanized at 20 dpf with 0.125% Tricaine methanesulfonate (MS-222) (Sigma Aldrich, St. Louis, MO, USA) and fixed overnight in 4% paraformaldehyde/0.1% PBS-Tween (PBST). Following fixation, larvae were washed three times with PBST and dehydrated with 50% and 70% ethanol prior to staining. A subset of 10-12 individuals was stained for mineralized bone with 0.05% Alizarin Red S (AR-S) (Sigma Aldrich, St Lois, MO, USA) in 70% ethanol overnight. Post staining, individuals were washed with ddH2O, followed by a 60 minute incubation in 2% hydrogen peroxide in 0.5% KOH, and washed twice in 0.25% KOH. Samples were then digested in 0.05% trypsin (Difco™ BD Biosciences, San Jose, CA, USA) dissolved in 30% saturated sodium borate for 20 minutes at room temperature. Following tissue digestion, samples were washed with 0.25% KOH, and cleared in a graded series of 25%, 50%, and 75% glycerol in 0.1% KOH, and stored at 40 C. Representative samples were then imaged under light microscopy (Nikon SMZ1500).

***In vivo* staining for bone mineralization and confocal microscopy**

Tg(*osx/sp7*:mCherry), tg(*twist*:EGFP) and tg(*col10a1*:nlGFP) medaka were stained and imaged at 20 dpf to assess localization of key cell populations during osteoblastogenesis in relation to mineralized bone. Approximately 12 hours prior to imaging, DMSO- and TCDD-treated 20 dpf *col10a1*:nlGFP and *twist*:EGFP medaka were counter-stained with 0.1% alizarin-3-methylimino-diacetic acid (alizarin complexone, or ALC) (Sigma Aldrich, St. Lois, MO, USA) in ERM for two hours. Similarly, *osx/sp7*:mCherry medaka were counter-stained with 0.01% Calcein (Sigma Aldrich, St. Lois, MO, USA) in ERM (pH 9.0) for two hours. For both staining procedures, larvae were briefly washed twice with 1X ERM, and then remained in 1X ERM overnight to allow equilibration of ALC and Calcein stains.

A representative sample (n=4-6) of stained individuals from each treatment were anesthetized in 0.03% (w/v) tricaine in 1X ERM, immobilized in 35 mm glass-bottom petri dishes (MatTek Corporation, Ashland, MA, USA) in 1.3% low-melting agarose (Apex BioResearch Products, Genesee Scientific, San Diego, CA, USA) containing 0.03% tricaine/ERM. Fish were oriented laterally to permit imaging of the axial vertebrae (vertebrae 17-19) and were imaged *in vivo* using a Zeiss LSM laser scanning confocal microscope (Carl Zeiss Microscopy GmbH, Jena, Germany) with ZEN 2009 version 5.5 SP1 Image Acquisition Software (Carl Zeiss). Vertebrae 17-19 were imaged due to the presence of well mineralized centra and neural and hemal arch structures at 20 dpf, and due to the fact that this region of vertebrae are located at a sufficient distance to minimize signal:noise ratio caused by robust ALC/calcein staining in the gastrointestinal tract.

Morphological assessment

Maximum intensity projections of confocal serial z-stack images (20X magnification) of 20 dpf stained medaka [tg(*twist*:EGFP)/ALC, tg(*osx/sp7*:mCherry)/Calcein, and tg(*col10a1*:nlGFP)/ALC)] were generated using ZEN 2009 Imaging Software to enable a 2-dimensional assessment of axial vertebrae morphology. Vertebrae 17-19 from three to four individuals from each treatment were assayed using ImageJ software (NIH) to quantify the following morphological phenotypes: area of mineralized centra ($pixels^2$), area of intervertebral ligament (pixels2), and lengths of mineralized neural and hemal arches (pixels), where mineralized bone matrix was identified via the presence of positive ALC or Calcein staining. For each phenotype, the mean of three measurements for each individual vertebra was obtained, and subsequently pooled to obtain the mean for vertebrae 17-19. DMSO-treated medaka were set to 1, and TCDD-treated medaka were reported as a proportion relative to DMSO controls.

Axial dissection and RNA isolation

Larval medaka were euthanized at 20 dpf in 0.125% tricaine/ERM solution and replicates were pooled to ensure 15-25 individuals per RNA sample. Specimens were transferred to Leibowitz's media (L-15) (Corning, Mediatech, Inc., Manassas, VA, USA) containing 10% Fetal Bovine Serum (Corning, Mediatech). Dechorionated embryos or hatched larvae were passed through a 20-22 gauge hypodermic needle (Becton, Dickinson, and Company, Franklin Lakes, NJ, USA) and 3-ml syringe (Becton, Dickinson, and Company) several times to isolate the axial skeleton from craniofacial and abdominal viscera. Sheared tissue was collected on 105-μm nylon mesh (Component Supply Co., Fort Meade, FL, USA) and transferred to fresh L-15/10% FBS media. Under a dissecting light microscope (Nikon

SMZ1500, Nikon Instruments, Inc., Melville, NY, USA) axial tissue was inspected and trimmed of any remaining craniofacial or abdominal tissue (S.I. Figure 1). Samples were immediately flash frozen in liquid nitrogen. Tissues were homogenized in TRI Reagent® (Ambion®, Life Technologies, Carlsbad, CA, USA) using a handheld BioVortexer (Thomas Scientific, Swedesboro, NJ, USA). Total RNA was isolated according to the TRI Reagent manufacturer's protocol. Finally, total RNA was quantified using Agilent 2100 Bioanalyzer and 2100 Expert Software package (Agilent Technologies, Santa Clara, CA, USA). RNAs with RNA Integrity numbers (RINs) greater than 9 were used for downstream gene expression applications.

qPCR

The following qPCR methods were conducted and reported in accordance with MIQE guidelines (Bustin et al., 2009). cDNA was synthesized from 2 μg of total RNA using High Capacity cDNA Reverse Transcription Kit (Applied Biosystems, Foster City, CA) containing random primers, MultiScribe Reverse Transcriptase, RNase inhibitor, deoxynucleotide triphosphate mix, and 10X reverse transcription buffer in a 20 μl reaction. Medaka-specific real-time PCR primers were designed in Primer3 and PrimerQuest (Integrated DNA Technologies, Coralville, IA, USA) and procured from IDT. Primer sets were tested for target accuracy by blasting sequences to the medaka genome in Ensembl and NCBI. All primer sequences were validated and are specific for intended targets. Primer efficiencies were conducted for each gene-specific primer set across a range of cDNA dilutionsto ensure efficient amplification of the target exon sequence (Table 2). To quantify relative gene expression, cDNA from DMSO- and TCDD-treated samples (n=3-5) were PCR amplified in triplicate on

clear, 96-well PCR plates (Olympus Plastics, Genesee, San Diego, CA, USA) using an Applied Biosystems 7300 Real Time PCR System and normalized to *gapdh*, a previously described reference gene in medaka (Zhang and Hu, 2007). Briefly, the 25 µl qPCR reaction was comprised of 12.5 µl of SYBR® Green Real-Time PCR Master Mix (Life Technologies), 8.5 µl UltraPure Distilled H2O (Life Technologies), 1 µl of 10 µM forward primer, 1 µl of 10 µM reverse primer, and 2 µl of cDNA. The conditions for each reaction were as follows: i) 50ºC for two minutes, ii) 95ºC for ten minutes, iii) 95ºC for 15 seconds (s) followed by 60ºC for 60s, repeated 40x, and iv) 95ºC for 15 s, 60ºC for 60 s, 95ºC for 15 s, and 60ºC for 15 s to derive dissociation or melt curves and ensure specificity for each primer set used. Threshold cycle (Ct) values for each reaction were determined by the ABI 7300 software package and relative gene expression was quantified according to the ΔΔCt method (Livak and Schmittgen, 2001).

RNA-Sequencing

To assess global changes in gene expression, axial tissue from DMSO- and 0.3 nM TCDD-treated (n=3/treatment) samples was dissected, homogenized, and RNA was isolated as previously described. Next, total RNA was quantified and RIN values were determined using the Agilent 2100 Bioanalyzer and manufacturer's instructions therein. Samples with RINs greater than 9.9 were used. Samples used for RNA-Seq were validated through qPCR assessment as described above.

Whole transcriptome libraries were prepared using Ion Total RNA-Seq Kit v2 (Ion Torrent, Life Technologies, Carlsbad, CA) for the Ion PGM sequencing platform as described by the manufacturer. Briefly, polyA mRNA was purified for each sample from 2 µg of

denatured total RNA with oligo(dT)25 Dynabeads®. Following elution from the beads, poly(A) mRNA yield was analyzed using Agilent RNA 6000 Pico Kit. Poly(A) mRNA was then fragmented with RNaseIII and subsequently purified with Nucleic Acid Binding Beads. Next, adaptors from Ion Adaptor Mix v2 were ligated to poly(A) RNA, and each sample was reverse transcribed to form cDNA (at 42°C in a 20 µl reaction containing 4 µl 10X Superscript® III Enzyme Mix, 2 µl of 10X RT Buffer, 2.5 µl of 2.5 mM dNTP Mix, 8 µl Ion RT Primer v2, and 2 µl of nuclease-free water) and stored overnight at -20°C. The following day, the cDNA was purified with Nucleic Acid Binding Beads, and then amplified using Platinum® PCR Supermix High Fidelity, Ion Xpress™ RNA 3' Barcode Primers, and a different Ion Xpress® RNA-Seq BC Primer (BC#11-16) for each sample to form a barcoded library to aid in downstream analysis. The amplified cDNA was purified once more with Nucleic Acid Binding Beads, a 1:20 dilution was made, and the 1:20 cDNA diluent yield and fragment size distribution was assessed using the Agilent High Sensitivity DNA Kit. The library was then pooled with equimolar amounts from each of the 6 barcoded samples, and analyzed once more using the Agilent High Sensitivity DNA Kit. Finally, the pooled library was diluted to 20 ρM for subsequent template preparation.

Amplification of the pooled library was performed on the Ion OneTouch™ 200 using Ion PGM Template OT2 200 Kit. The amplification solution consisting of the 20 ρM pooled library, nuclease-free water, Ion PGM™ OT2 200 Reagent Mix, Ion PGM™ OT2 200 PCR Reagent B, Ion PGM™ OT2 200 Enzyme, and Ion PGM™ OT2 200 Ion Sphere™ Particles (ISPs) was prepared and run overnight according to manufacturer instructions. The following day, the solution containing template-positive ISPs was enriched on the Ion OneTouch™ ES

following the manufacturer's protocol. Next, the Ion PGM™ System was cleaned, initialized, and calibrated for the Ion 318™ chip. Sequencing primers were annealed to the template-positive ISPs, Ion PGM™ Sequencing 200 v2 Polymerase was added to the ISP solution, and incubated at room temperature for 5 minutes. Finally, the template-positive ISPs + Sequencing Polymerase mixture were carefully loaded into the Ion 318™ chip and sequenced overnight on the Ion PGM™ System.

The resulting reads were trimmed to remove adaptor sequences and low quality base-calls, and were aligned to the Oryzias latipes (Medaka) genome (Version 76; www.ensembl.org) using Bowtie 2.2.6. Binary files generated by Bowtie were visualized using the Integrated Genome Viewer. Differentially expressed genes were identified using Cuffdiff2, whereas principal component analysis was performed with DESeq2 in R. Pathway analysis was conducted using Ingenuity Pathway Analysis (IPA; Ingenuity® Systems, www.ingenuity.com). All RNA-Seq data have been deposited in NCBI's Gene Expression Omnibus (Edgar et al., 2002) and are accessible through GEO Series accession number GSE87168.

Statistical Analysis

For morphometry and qPCR data, a one-way ANOVA with a Tukey post hoc test were performed using GraphPad Prism Software (La Jolla, CA). P-values less than 0.05 were deemed significant. For RNA-Seq, genes with corrected p-values (q-values) less than 0.05 were deemed significant and used for downstream analysis in IPA.

RESULTS

TCDD exposure elicits gross skeletal deficits at 20 dpf.

From a preliminary range-finding experiment in Orange-red medaka, we chose concentrations of 0.15 nM and 0.3 nM TCDD due to a high rate of survivorship to 20 dpf (larval stage) of 85 ± 11% and 49 ± 24%, respectively. These concentrations were also chosen due to the low frequency of adverse cardiovascular effects typically associated with dioxin exposure in medaka and other teleost models at higher TCDD concentrations. Despite no cardiovascular defects, medaka exposed to 0.3 nM TCDD demonstrated gross skeletal morphological deficits including dorsalization of the tail, a truncated lower jaw structure, and an overall reduction in total body length (Figure 1A, D). Alizarin Red S (AR-S) staining was performed on fixed 20 dph larvae to investigate whether TCDD affects bone mineralization in the axial skeleton. DMSO-treated individuals displayed positive staining of the craniofacial elements, and axial vertebral bodies (Figure 1B). Neural and hemal arches were well defined and mineralized in DMSO-treated fish (Figure 1C). Individuals exposed to 0.15 nM TCDD also displayed positive staining of the vertebral bodies and hemal arches in the abdominal and medial regions, however staining of caudal fin rays and caudal vertebrae was reduced when compared to DMSO-treated medaka (S.I. Figure 2). The most dramatic effect was observed at 0.3 nM TCDD where a marked attenuation in AR-S staining was observed throughout the axial skeleton (Figure 1E), with positive staining observed only in the vertebrae that comprise the Weberian apparatus and abdominal vertebrae (Figure 1F).

TCDD exposure results in morphological deficits in vertebral bodies by targeting differentiating osteoblasts.

Medaka transgenic lines including tg(*twist*:EGFP), tg(*osx/sp7*:mCherry), and tg(*col10a1*:nlGFP) were utilized to assess how different cell populations within the osteogenic lineage were impacted following TCDD exposure. Each transgene consists of a fluorescent reporter whose expression is coupled to the promoter of cell-specific genes of interest (S.I. Table 2). Prior to confocal imaging, transgenic individuals were stained *in vivo* with alizarin complexone or calcein to further assess osteoprogenitor [tg(*twist*:EGFP)] or osteoblast [tg(*osx/sp7*:mCherry) and tg(*col10a1*:nlGFP)] populations within the context of mineralized osteoid tissue in vertebrae 17 through 19 (V17-19) at 20 dpf (Figure 2A). At this larval stage, centra from DMSO-treated individuals begin to resemble the hourglass-like morphology observed in adult medaka, while the neural and hemal arches can be observed extending from the rostral nodes of the centra in a dorsal and ventral fashion, respectively (Figure 2B). In contrast to the control fish, the centra of TCDD-treated transgenic medaka exhibited reduced growth and mineralization. A morphometric analysis of the centra area revealed a concentration-dependent and significant decrease in centra area of 16% and 35% in response to 0.15 nM and 0.3 nM TCDD (DMSO vs. 0.15 nM TCDD, $p \leq 0.001$; DMSO vs. 0.3 nM TCDD, $p \leq 0.001$; 0.15 nM TCDD vs. 0.3 nM TCDD, $p \leq 0.001$), respectively (Figure 2C), thus providing higher resolution than standard light microscopy to detect deficits in bone formation. Though not significant, the intervertebral ligament (IVL) area appeared qualitatively larger with TCDD treatment (Figure 2D). TCDD treatment also resulted in significant and dose-dependent reductions in neural arch length TCDD (DMSO vs. 0.15 nM TCDD, $p \leq 0.001$; DMSO vs. 0.3 nM TCDD, $p \leq 0.001$; 0.15 nM TCDD vs. 0.3 nM TCDD, $p \leq 0.01$) (Figure 2E) and a complete loss of hemal arch formation in the 0.3 nM TCDD treated fish (DMSO vs. 0.15

nM TCDD, $p \leq 0.001$; DMSO vs. 0.3 nM TCDD, $p \leq 0.001$; 0.15 nM TCDD vs. 0.3 nM TCDD, $p < 0.05$) (Figure 2F).

In control animals, *twist*:EGFP expression is observed within sclerotome-derived MSCs densely localized to the IVL. Moreover, EGFP+ cells appeared confined within the boundary between the IVL and centra, and these observations were consistent among all imaged centra/IVL imaged. With TCDD treatment, EGFP+ cells displayed a more dispersed pattern and appeared less confined to the IVL-centrum border. In fact, a subset of EGFP+ cells appear localized on the mineralized centra, likely in the process of migrating and differentiating into osteoblasts. This effect was more pronounced in the 0.3 nM TCDD-treated fish (Figure 3A-C).

The tg(*col10a1*:nlGFP) transgenic line labels a heterogeneous population of immature to mature osteoblasts. In control fish, nlGFP+ cells were observed in areas of active mineralization and growth along the centra periphery and the elongating neural and hemal arches. Less abundant, though still present, were nlGFP+ cells within the center of centra. Following TCDD exposure, nlGFP+ cells were distributed along the centra periphery and to a lesser extent within primitive neural and hemal arch structures. Qualitatively, however, the TCDD-treated fish demonstrated an overall attenuation in distribution and intensity of nlGFP+ signal (Figure 3D-F), consistent with gene expression data (see below).

Differentiating osteoblasts are labeled with mCherry in tg(*osx/sp7*:mCherry). In DMSO-controls at 20 dpf, mCherry+ cells are localized along the neural and hemal arches, and lining the rostral and caudal centra periphery. Following exposure to 0.15 nM TCDD, 20 dpf larvae exhibited significant attenuation in mCherry+ expression with an apparent

qualitative reduction in number of mCherry+ cell number consistent with a decrease previously described (Dong et al., 2012). At 0.3 nM TCDD *osx/sp7*:mCherry+ expression was nearly absent, consistent with the absence of neural and hemal arches where mCherry+ cells are normally observed (Figure 3G-I). Taken together, despite the presence of *twist*:EGFP+ and *col10a1*:nlGFP+ cells in TCDD-treated animals, the fact that *osx/sp7*:mCherry+ cells were clearly diminished in a concentration-dependent manner suggests that TCDD may alter differentiation following the initial commitment of mesenchymal cells to an osteoblastic fate.

TCDD significantly downregulates transcriptional regulators of osteogenesis and downstream targets.

qPCR was used to anchor observed deficits in bone mineralization to expression changes in selected genes within the osteoblast gene regulatory network within isolated axial tissues of DMSO- and TCDD-treated medaka. To confirm TCDD-mediated AhR activation, *cyp1a* expression, a canonical marker of TCDD exposure was measured. At 20 days post exposure *cyp1a* expression was significantly induced (>50 fold) in both 0.15 nM and 0.3 nM-treated medaka (DMSO vs. 0.15 nM TCDD, $p \leq 0.003$; DMSO vs. 0.3 nM TCDD, $p \leq 0.02$) (Figure 4) compared to DMSO controls. To assess modulation within the osteoblast gene regulatory network, expression of select transcriptional regulators and markers of osteoblast differentiation and maturation was measured. *twist1*, a marker of mesenchymal/osteoprogenitor cells in the intervertebral ligament was not significantly impacted by TCDD exposure (Figure 5A). Expression of *runx2*, an early osteoblastogenic transcription factor, was significantly downregulated with 0.3 nM TCDD ($p \leq 0.04$) compared to DMSO controls (Figure 5B). Downstream of *twist1* and *runx2*, however, osx/sp7 displayed

a significant, concentration-dependent response with expression reduced 2.7 and 4.3 fold in 0.15 nM and 0.3 nM TCDD, respectively, compared to DMSO controls (0.15 nM TCDD, $p \leq 0.02$; 0.3 nM TCDD, $p \leq 0.008$) (Figure 5C). TCDD-mediated reduction in *osx/sp7* suggests that maturation of osteoblasts is impacted. Therefore, expression of markers of terminally differentiated osteoblasts was measured. *Collagen type X alpha 1* (*col10a1*), a marker of osteoblasts and hypertrophic chondrocytes, demonstrated a significant 3.8- and 4.7-fold reduction in 0.15 nM TCDD- and 0.3 nM TCDD-treated medaka (0.15 nM TCDD, $p \leq 0.004$; 0.3 nM TCDD, $p \leq 0.001$), respectively (Figure 6A). The most dramatic effect occurred in expression of *bglap*, encoding an ECM protein, whose expression is regulated downstream of *osx/sp7* and *runx2*. Compared to controls, *bglap* was significantly reduced 9 and 19 fold with 0.15 nM and 0.3 nM TCDD treatment, respectively (0.15 nM TCDD, $p \leq 0.05$; 0.3 nM TCDD, $p \leq 0.04$) (Figure 6B), although the two treatments were not statistically different from each other. Other ECM markers, including spp1 and col1, were attenuated with both TCDD treatments compared to DMSO controls; however, there was no significant difference between 0.15 nM and 0.3 nM TCDD treatment groups (Figure 6C, 6D). A full summary of qPCR results is available in Table 3.

TCDD significantly alters global inflammatory and musculoskeletal disease pathways.

A global RNA-Seq analysis was conducted using RNA isolated from the axial region of DMSO- and 0.3 nM TCDD-exposed medaka to identify additional targets within the osteochondral pathway potentially impacted by TCDD exposure. In total, 597 genes were significantly up- or down-regulated ($q<0.05$) (for a complete list, refer to GEO accession #GSE87168). Within this dataset, AhR-mediated genes were enriched with marked

upregulation of *ahr*, *ahrr* (aryl hydrocarbon receptor repressor), *cyp1a*, and *cyp1b* as markers of AhR transactivation. Interestingly, the inflammatory mediators *il-1β* and *cxcl-14* were also significantly upregulated. Expression of *il-1β* was validated using qPCR and revealed a significant 8- and 10-fold induction with 0.15 nM ($p<0.02$) and 0.3 nM TCDD treatment ($p<0.01$) (Figure 7). RNA-Seq also identified numerous osteochondral genes with significantly reduced expression in the TCDD-exposed samples. Specifically, we observed significant reduction in *osx/sp7* and *dlx3*, transcriptional regulators of osteoblastogenesis, and reduced expression of the chondrogenic regulator *sox9b*. Likewise, downstream ECM genes associated with bone and cartilage development were also significantly downregulated (*col10a1*, *col5a2*, *col1a1*, *col11a1*, *col2a1*, *sparc*/*osteonectin*). Other observations of interest included TCDD-mediated reduction in the Wnt pathway inhibitors, *dkk3* and sfrp2, and induction of the osteoclastogenic inhibitor, *opg*.

Differentially regulated genes were evaluated using Ingenuity Pathway Analysis (IPA) and were enriched among several musculoskeletal disease and developmental pathways. Arthropathy and arthritis were the two most heavily enriched musculoskeletal disorders with 51 and 49 genes, respectively, and were predicted to be increased in the TCDD-exposed group (z-score>2.0). Also enriched were pathways associated with altered bone mineralization and osteoclastogenesis (Table 4). Furthermore, expression of *osx/sp7*, *sox9*, numerous collagen genes, and genes encoding ECM synthesis and transport were also downregulated by TCDD in this dataset. Mutations in several of these genes are associated with human skeletal maladies including osteogenesis imperfecta, Ehlers-Danlos syndrome, and other lethal skeletal dysplasias. (Figure 8). Taken together, the RNA-Seq data displays concordant findings with

the above qPCR data, and provides additional insight into gene dysregulation associated with musculoskeletal disease pathways.

DISCUSSION

In teleosts, TCDD is a potent teratogen known to elicit pericardial edema and other embryolethal phenotypes at concentrations in the nanomolar range (Antkiewicz et al., 2005; Carney et al., 2006; Dong et al., 2010; Teraoka et al., 2002). Of interest, several studies have investigated the effect of sublethal TCDD concentrations on teleost skeletal development as a means to assess the relationships between AhR activation and skeletal dysplasias (Baker et al., 2013; Baker et al., 2014). In the present study, we establish that embryonic exposure to TCDD, a legacy contaminant and potent AhR ligand, results in significant deficits in perichordal ossification of vertebrae during larval development.

Our findings indicate that TCDD exposure attenuates ossification of the centra and neural and hemal arches as evidenced qualitatively by whole-mount AR-S staining and quantitatively from an ImageJ assessment of alizarin complexone- and calcein-stained transgenic medaka. A similar study in zebrafish previously demonstrated that TCDD inhibits perichondral ossification, i.e. ossification around a cartilage template, in the craniofacial skeleton (Burns et al., 2015). Other studies have also established the role of TCDD in disrupting cell-rich hyaline cartilage and extracellular matrix synthesis in craniofacial (Burns et al., 2015; Planchart and Mattingly, 2010; Teraoka et al., 2006; Xiong et al., 2008) and axial structures (Tracie R. Baker et al., 2014; Dong et al., 2012). To contrast, our results demonstrate that TCDD inhibits perichordal ossification in vertebrae lacking a bone fide cartilage scaffold which suggests that multipotent MSCs or osteoblasts undergoing differentiation are potential targets of TCDD toxicity.

In teleosts, notochordal cells direct the initial mineralization and segmentation of the chordacentra along the vertebral column (Grotmol et al., 2005). Confocal imaging of transgenic medaka used in this experiment illustrates positive ALC and calcein staining of centra in a segmented pattern, indicating that early mineralization of the notochordal sheath does not appear to be impacted following TCDD exposure. Given the fact that chordal ossification is present early, we argue that AhR-mediated events affect perichordal ossification driving the lateral growth of the vertebral body in the rostral and caudal orientations. In *twist*:EGFP fish at 20 dpf, sclerotome-derived MSCs appeared highly dispersed within a larger IVL area compared to controls, and, in the highest TCDD treatment, EGFP+ cells were observed in middle of the centra beyond the IVL space. Based on prior evidence, these *twist*:EGFP+ cells are likely in the process of differentiating into perichordal osteoblasts (Renn et al., 2013). Though distribution of *twist*:EGFP+ MSCs appear to impacted by TCDD exposure, mRNA expression of twist1 remains unchanged. This observation suggests several possibilities. First, TCDD may not specifically target osteoprogenitor cells localized to the IVL and impacts more specifically the terminal maturation of osteoblasts. Second, TCDD may impact the ability of *twist*:EGFP+ osteoprogenitor cells to differentiate to osteoblasts without altering their motility across and within the centra from the IVL. Alternatively, it may be possible that both of these processes are impacted by TCDD. Based on evidence from TCDD-exposed tg(*col10a1*:nlGFP) and tg(*osx/sp7*:mCherry) individuals, it is more likely that TCDD targets intermediate to terminal differentiation of osteoblasts. Structures undergoing perichordal ossification at the centrum periphery and along the neural and hemal arches revealed a reduction in nlGFP+ signal intensity in tg(col10a1:nlGFP) individuals and a

concentration-dependent reduction in mCherry+ cells in tg(*osx/sp7*:mCherry) individuals exposed to TCDD. These cellular observations are further supported at the molecular level where we demonstrate reduced expression of *osx/sp7* and *col10a1* in TCDD-treated medaka. Collectively, these data suggest that TCDD inhibits intermediate to terminal stages of osteoblast differentiation with the possibility of also attenuating differentiation of osteoprogenitors to osteoblasts. This may thus provide an explanation for observed TCDD-mediated deficits in vertebral body ossification.

Our findings are consistent with mammalian studies investigating bone development following exposure to TCDD or other AhR ligands. Developmental exposure to TCDD in rats adversely affects the structural and mechanical properties of bone (Miettinen et al., 2005), and numerous *in vitro* studies have confirmed TCDD-mediated inhibition of osteoblast differentiation in murine cell models (Gierthy et al., 1994; Korkalainen et al., 2009; Ryan et al., 2007; Singh et al., 2000; Yu et al., 2014). In humans, elevated exposure to polychlorinated dibenzo-p-dioxins (PCDD) and furans (PCDF) during breastfeeding has been strongly associated with hypomineralization of teeth (Alaluusua et al., 1996). Moreover, children living in the TCDD-contaminated zones in Seveso, Italy display an increased incidence of tooth enamel defects (Alaluusua et al., 2004). Cementoblasts, the osteoblast-like cells responsible for forming of mineralized tissue surrounding the tooth-root surface, are regulated by OSX/SP7 (Cao et al., 2012), suggesting a possible linkage between TCDD exposure and altered dentition and bone formation observed in humans.

To further investigate the observed phenotypes in TCDD-treated medaka larvae, qPCR was conducted on 20-dpf axial tissue for select targets within the osteogenic gene regulatory

network. In addition to diminished expression of *osx/sp7*, we further illustrate that downstream markers of terminally differentiated osteoblasts including *bglap*, *spp1*, *col1*, and *col10a1*, are significantly diminished by TCDD in this experiment. The morphological results we observed associated with diminished osx/sp7 expression following TCDD treatment recapitulate the phenotype observed in osx/sp7 morpholino (MO)-knockdown medaka. Specifically, *osx/sp7* MOs display reduced formation of mineralized vertebra (Renn and Winkler, 2014). Our observations are also consistent with defects in ossification found in Osx/Sp7$^{-/-}$ mice (Nakashima et al., 2002). Similarly, humans haploinsufficient in the OSX/SP7 allele with osteogenesis imperfecta Type VII experience low bone mass and bone fragility associated with an increased risk of bone fracture (Lapunzina et al., 2010). Moreover, a genome-wide association study (GWAS) of more than 1500 children revealed a strong association between reduced bone mineral density and 4 single-nucleotide polymorphisms (SNPs) at the OSX/SP7 gene locus (Timpson et al., 2009). To the authors' knowledge, repression of osx/sp7 and runx2 as transcriptional regulators of osteoblast differentiation is the first mechanism to explain how TCDD inhibits bone formation.

Given the multiple targets of TCDD toxicity, RNA-Seq was conducted on DMSO- and 0.3 nM TCDD-treated medaka to identify additional pathways impacted by dioxin exposure. As expected, numerous AhR-responsive genes involved in xenobiotic metabolism were heavily enriched with TCDD treatment, a finding similar to a gene array analysis of TCDD-treated adult medaka (Volz et al., 2006). In addition to a suite of osteogenic targets *osx/sp7*, *bglap*, *sparc*/*osteonectin*, and *col10a1*, TCDD exposure attenuates expression of *FKBP10* and *SERPINH1*, genes associated with post translational modification and transport of collagens

that comprise bone ECM. In combination with OSX/SP7, mutations in both *FKBP10* and *SERPINH1* are linked to severe osteogenesis imperfecta (Alanay et al., 2010; Christiansen et al., 2010), which offers further support for the bone phenotype we observed in TCDD-treated medaka.

TCDD may also impact osteogenesis through additional mechanisms. Interestingly, *il1b* expression was upregulated more than 8-fold with TCDD exposure, which may offer additional insight into the putative role of inflammatory regulators in osteoblast maturation and bone formation. Inflammation is associated with adult degenerative bone disease outcomes including rheumatoid arthritis and delayed fracture repair, however, its precise role in bone formation is not yet fully understood. Inhibitory effects of *Il-1b* on differentiation of MC3T3-E1 osteoblast-like cells and MSCs derived from mice have been observed *in vitro* (Lacey et al., 2009; Taichman and Hauschka, 1992). Moreover, *IL1B* in human MG-63 osteoblast-like cells is known to induce expression of osteoprotegerin (OPG; TNFRS11B) via the p38 and ERK pathways (Lambert et al., 2007). OPG functions as a decoy receptor that binds RANKL to prevent osteoclast differentiation thereby slowing bone resorption by mature osteoclasts (Simonet et al., 1997). We observed significant upregulation of *opg-a*, the medaka orthologue of human *OPG*, in TCDD-exposed larvae. This finding was unexpected as endogenous osteoclast activity is not present in the axial skeleton of medaka until 3-4 weeks post fertilization (To et al., 2012) under normal conditions. It is possible that upregulation of opg-a may serve as a compensatory mechanism to prevent bone resorption in larvae lacking sufficient bone development, such as when exposed to TCDD.

In addition to TCDD, other AhR ligands present in the environment elicit similar inhibitory effects on osteoblast development. Of these AhR agonists, the polycyclic aromatic hydrocarbons (PAHs) 3-methlycholanthrene and benzo[a]pyrene have received the most attention due to their presence in direct and second-hand cigarette smoke. These ligands, as well as cigarette smoke condensate, all demonstrate inhibitory effects on osteoblast differentiation and function *in vitro* (Gullihorn et al., 2005; Korkalainen et al., 2009; Naruse et al., 2002; Nishimura et al., 2009) and in mice *in vivo* (Herlin et al., 2013; Naruse et al., 2002). Environmental exposure to xenobiotics such as those found in cigarette smoke, are increasingly associated with various skeletal diseases in humans. For example, smoking is known to trigger or exacerbate the pathogenesis of rheumatoid arthritis and osteoporosis (Lee et al., 2013), and an increasing body of evidence points to the role of the AhR as playing a significant role in the manifestation of these disease states (Kobayashi et al., 2008; Lahoti et al., 2014, 2013; Nguyen et al., 2013). However, the interaction between developmental exposure to xenobiotic stressors and congenital skeletal diseases and the onset of adverse skeletal outcomes is less well established. In the present work, TCDD exposure attenuates bone formation in the axial skeleton in medaka during larval stages. The phenotypic analysis we present is anchored to a thorough assessment of differentially expressed markers and regulators of osteogenesis. Based on these data, we further hypothesize that exposure to ubiquitous AhR ligands during critical windows of development may contribute to the onset of developmental and/or adult skeletal dysplasias including rheumatoid arthritis and osteoporosis. Given the fact that skeletal development is highly conserved across vertebrate phyla, we additionally demonstrate that

teleosts are suitable models to improve our mechanistic understanding of environmental exposures and their pathological role in human skeletal diseases.

TABLES

Table 1. Summary of transgenic medaka lines used for confocal microscopy of select osteogenic cell populations and morphological assessment of ossified bone.

Transgenic line	tg(*twist*:EGFP)	tg(*osx/sp7*:mCherry)	tg(*col10a1*:nlGFP)
Regulatory Region (containing promoter)	5 kb	4.1 kb	5.87 kb
Reporter	EGFP	mCherry	nlGFP
Cells labeled (axial skeleton)	Sclerotome derived mesenchymal stem cells	Early differentiating osteoblasts; remains expressed in mature, mineralizing osteoblasts	Immature and mature osteoblasts
Localization in vertebrae (20 dpf)	Intervertebral ligament (IVL)	Anterior and posterior borders of the mineralized centra; mineralized and not yet mineralized neural and hemal arches	Centra, most notably concentrated along, neural and hemal arches and along edges of outwardly growing centra
Reference	Inohaya et al., 2007	Renn and Winkler, 2009	Renn et al., 2013

Table 2. Primers used for qPCR analysis. Gene names, Ensembl and/or NCBI GenBank Accession IDs, amplicon lengths, and primer efficiencies are included for each gene examined. S=sense, A= antisense.

Gene	Database ID[a]	Primer Sequence (5´- 3´)	Amplicon length (bp)	Primer Efficiency[b]
gapdh[c]	ENSORLG00000012224 XM_004077781.2	S: TGTGGAAAAGGCCTCACTTCA A: CAGACACGACCACACGCTGT	56	97.4%
cyp1a	ENSORLG00000014421 NM_001105087.1	S: ACATCGGCCTGAACCGAAATCCTA A:TGCTTCATTGTGAGCCCGTACTCT	454	103.0%
twist1	ENSORLG00000007251 NM_001104707.1	S: AAAACGGGGAGGACTCAGAT A: GAGGGCAAAGTGGGGATAAT	187	98.9%
runx2	ENSORLG00000010169 NM_001104850.1	S: GAGCTTCACGCTGACAATCA A: CTCTCACTCGCATCCTTTCC	182	101.8%
sp7	ENSORLG00000005215 XM_011474867.1 XM_004068679.2	S: GCCTCTGACCTTCAAACAGC A: GGCTTTGGACACGAGAAGAG	228	100.0%
bglap	NM_001201510.1 (Ensembl ID N/A)	S: AAAGAGACCTGGCTGCTGTT A: GCCCTCAGTGTCAGCCATTT	137	105.5%
spp1	ENSORLG00000020900 (NCBI Accession N/A)	S: TGTCCTCCAGCGTATCTCAA A: CCTCCTCCTCTTCCTCCTGT	141	102.0%
col10a1a	ENSORLG00000013436 NM_001201509.1	S: CCCCATTAAGTTCGACCAGA A: GCACATCAAGCAAGAGGACA	239	95.8%
col1	ENSORLG00000017013 NM_001122918.1	S: GCTCTTTGCCAGAGGATGTC A:TCATTGGAACCTTGGAGGAG	160	97.4%
il-1b	XM_011478737.1 (Ensembl ID N/A)	S: GATCTCGCATCATCCTCACTC A: CCTGAAGTCAGTACCCATCAC	106	105.6%

Table 3. Summarized results from all RT-qPCR experiments. Statistical analyses were conducted using a One-way ANOVA with a Tukey's post-hoc test. P-values less than 0.05 were deemed significant. SD, standard deviation, SEM, standard error of the mean.

	DMSO				0.15 nM TCDD				0.3 nM TCDD				One-way ANOVA results (P-value)		
gene	Fold Change	SD	SEM	n	Fold Change	SD	SEM	n	Fold Change	SD	SEM	n	DMSO vs. 0.15 nM	DMSO vs. 0.3 nM	0.15 nM vs. 0.3 nM
twist1	1	0.07	0.04	4	1.05	0.32	0.18	3	0.93	0.18	0.10	3	0.86	0.903	0.655
runx2	1	0.08	0.04	4	0.81	0.01	0.01	3	0.72	0.25	0.17	3	0.282	0.083	0.704
osx/sp7	1	0.30	0.15	4	0.38	0.22	0.15	3	0.23	0.07	0.05	3	0.023	0.008	0.739
col10a1	1	0.34	0.13	6	0.27	0.25	0.11	5	0.21	0.27	0.12	5	0.004	0.001	0.779
spp1	1	0.46	0.17	7	0.82	0.48	0.21	5	0.55	0.54	0.22	6	0.825	0.395	0.791
bglap	1	0.59	0.30	4	0.11	0.10	0.06	3	0.05	0.02	0.01	3	0.049	0.038	0.982
col1	1	0.31	0.15	3	0.84	0.51	0.34	3	0.79	0.14	0.09	3	0.834	0.753	0.987
cyp1a	1	1.12	0.56	4	83.63	24.79	16.52	3	61.48	21.80	14.54	3	0.002	0.012	0.395
il-1b	1	0.26	0.13	4	8.71	4.01	1.79	5	10.68	3.98	1.99	4	0.016	0.006	0.665

Table 4. Ingenuity Pathway Analysis highlighting a subset of affected pathways including osteochondral diseases and/or altered functional osteogenic states. RNA-Seq was performed on RNA isolated from the axial region of 20 dpf larvae exposed to DMSO or 0.3 nM TCDD at 4 hpf. For each Disease/Functional state, activation z-scores < -2.0 were predicted to be "Decreased"; Activation z-scores > 2.0, "Increased"; N.P= not predicted.

Categories	Disease/Function	P-value	Predicted Activation State	Activation Z-score	Number of Genes
Connective Tissue Disorders, Skeletal & Muscular Disorders	*Arthropathy*	4.73E-04	Increased	2.769	51
Connective Tissue Disorders, Inflammatory Disease, Skeletal & Muscular Disorders	*Arthritis*	9.78E-04	Increased	2.769	49
Cell Death and Survival	*Cell Death Of Connective Tissue Cells*	1.77E-06	Decreased	-2.354	41
Skeletal & Muscular Disorders	*Myopathy*	1.48E-07	N.P.	1.093	40
Skeletal & Muscular System Development/Function	*Mineralization Of Bone*	4.93E-04	N.P.	1.091	12
Skeletal & Muscular System Development/Function	*Osteoclastogenesis*	8.95E-05	N.P.	1.061	10

FIGURES

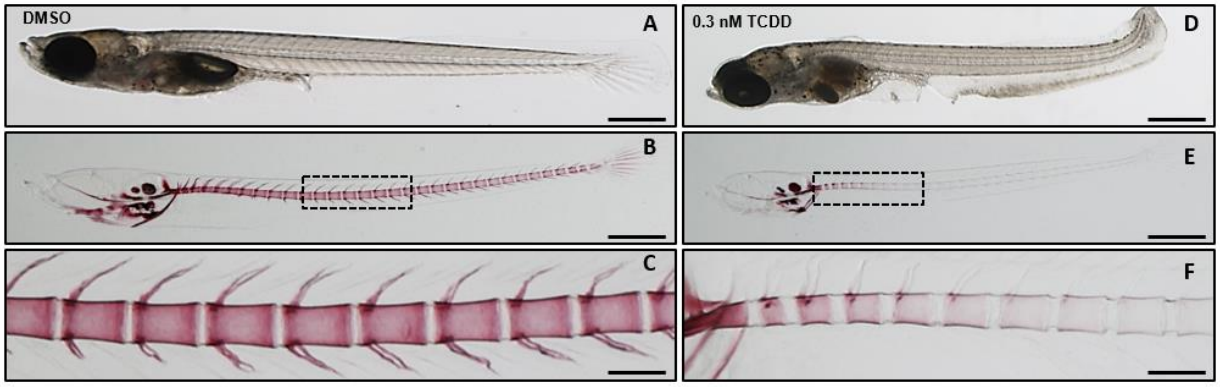

Figure 1. Whole-mount Alizarin Red S staining for mineralized bone in medaka larvae at 20 dpf. Representative individuals from DMSO (A-C) and 0.3 nM TCDD-exposed (D-F) groups are shown. Panels C and F are magnified regions boxed in B and E, respectively. Scale bars represent 500 μm in A, B, D, E, 2X magnification; 100 μm in C and F, 10X magnification.

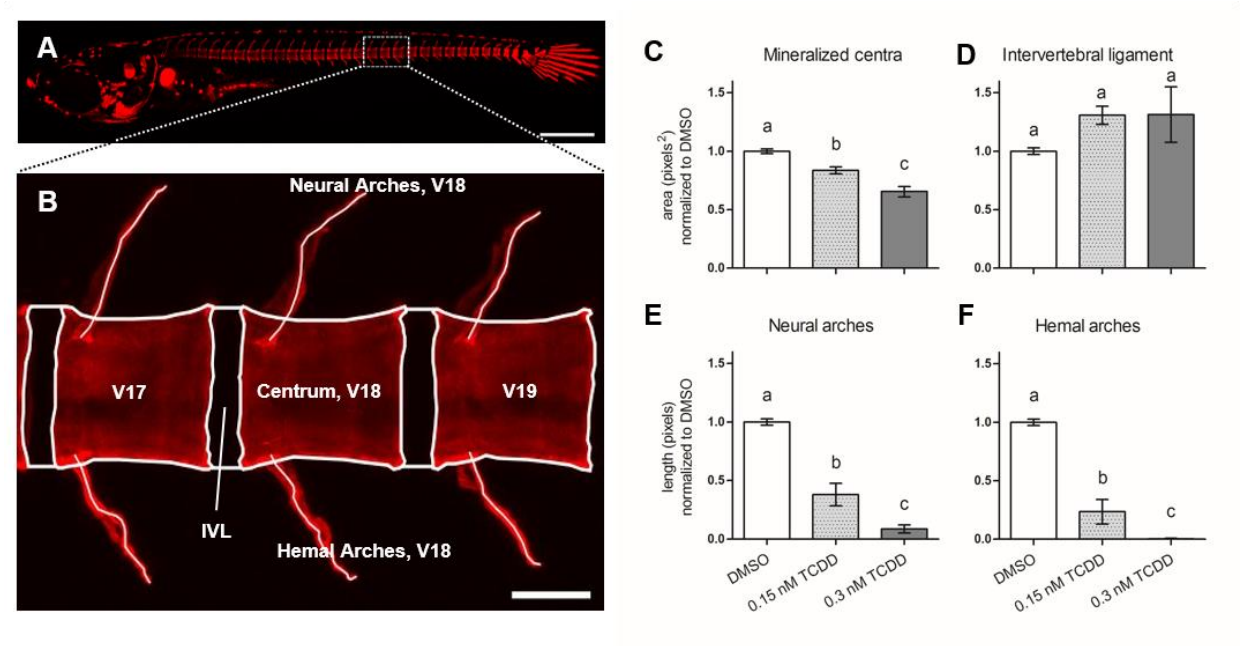

Figure 2. Morphological assessment of axial vertebral elements from vertebrae (V17-19) of DMSO-treated medaka at 20 dpf. Depicted in A) is a representative whole-mount individual stained with alizarin complexone, 6X magnification. Panel B) shows boxed region in A) with morphological atlas labeling V17-19, and centrum, intervertebral ligament (IVL), and hemal and neural arches of vertebra 18 as a representative example, 20X magnification. Centra and intervertebral ligament areas are shown in C) and D), respectively; lengths of neural and hemal arches are shown in E) and F), respectively. Values represent the mean from three separate measurements taken from vertebrae 17-19. Letters denote statistical significance between groups analyzed by One-Way ANOVA with Tukey's post-hoc analysis. Scale bars in A) and B) denote 500 µM and 50 µM, respectively.

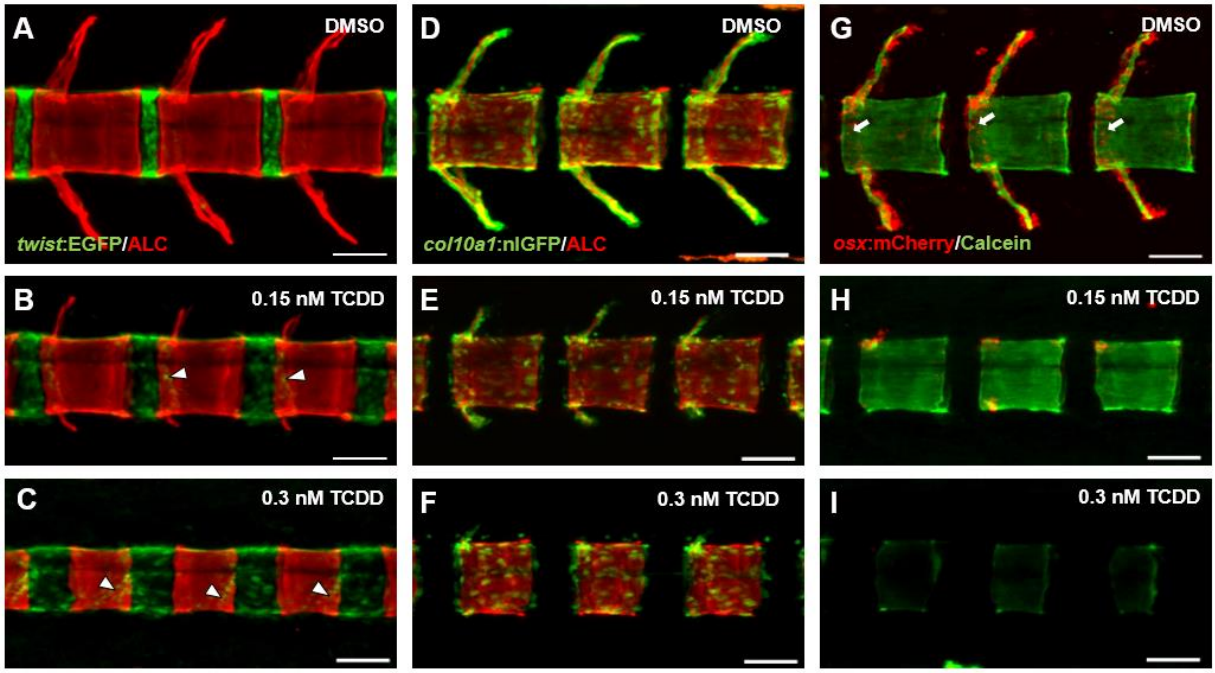

Figure 3. Confocal microscopy of representative DMSO- and TCDD-exposed tg(*twist:*EGFP) (A-C), tg(*col10a1*:nlGFP) (D-F), tg(*osx/sp7:*mCherry) (G-I) medaka at 20 dpf. Individuals were stained with alizarin complexone or calcein to identify mineralized bone matrix within the context of osteoblasts and osteoblast precursors. Arrowheads in B) and C) highlight *twist*:EGFP+ cells on the mineralized chordacentra. Arrows in G) denote *osx/sp7*:mCherry+ cells localized to the periphery of centra undergoing perichordal ossification. Images of vertebrae 17-19 were captured using the Zeiss LSM 710 confocal system, 20X magnification (scale bars= 50 µM).

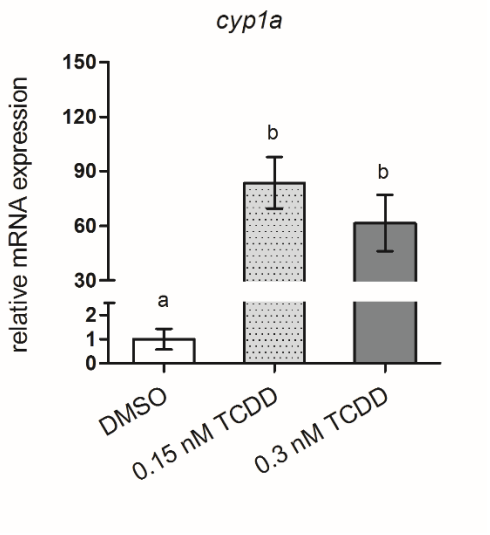

Figure 4. Relative *cyp1a* expression in 20 dpf DMSO- and TCDD-exposed medaka. Statistical assessment was conducted using One-Way ANOVA with a Tukey post-hoc analysis, n=3-4 per treatment, letters indicate significant differences between groups.

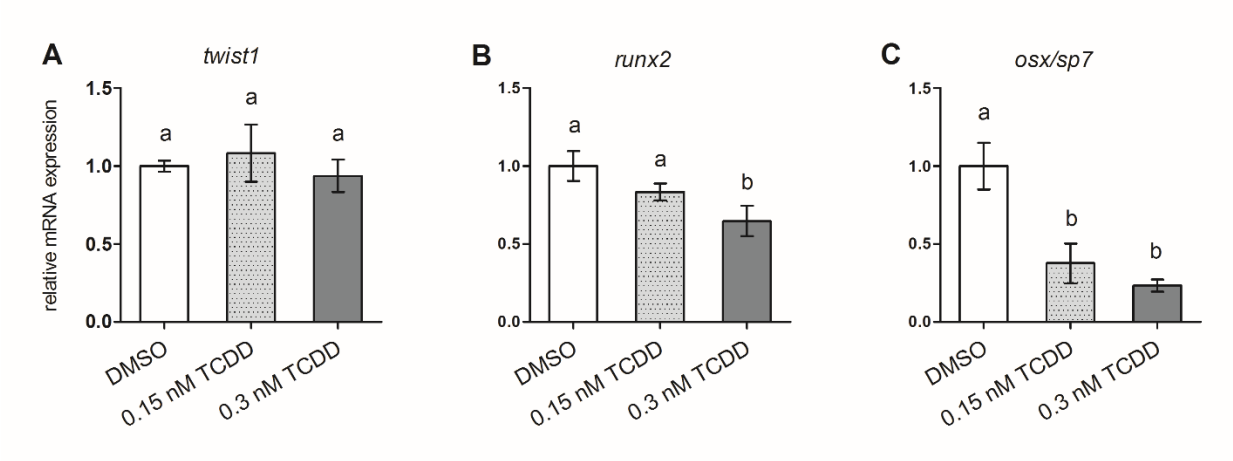

Figure 5. qPCR analysis of select osteogenic transcription factors from axial tissue isolated from Orange-red medaka at 20 dpf. Statistical assessment was conducted using One-Way ANOVA with a Tukey post-hoc analysis, n=3-4 per treatment, letters indicate significant differences between groups ($p<0.05$).

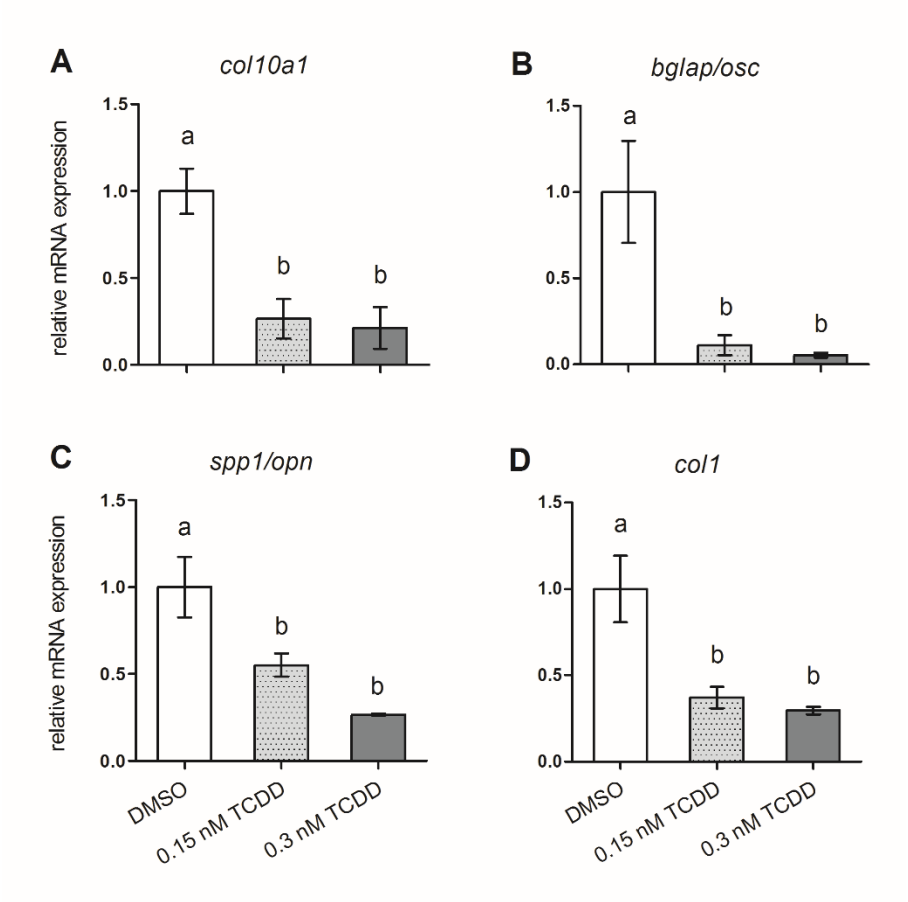

Figure 6. qPCR analysis of select ECM markers from axial tissue isolated from Orange-red medaka at 20 dpf. Statistical assessment was conducted using One-Way ANOVA with a Tukey post-hoc analysis, n=3-5 per treatment, letters denote significant differences between groups ($p<0.05$).

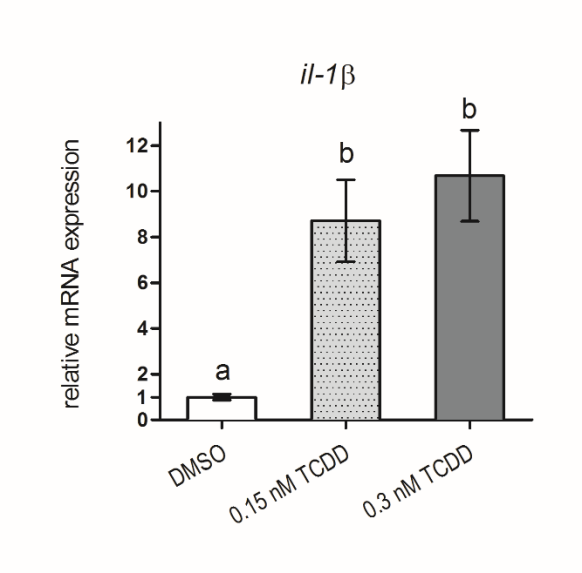

Figure 7. qPCR analysis of *il-1*β from axial tissue isolated from Orange-red medaka at 20 dpf. Letters indicate statistical significance ($p<0.05$) between groups analyzed by One-Way ANOVA with a Tukey post-hoc analysis, n=4-5 per treatment.

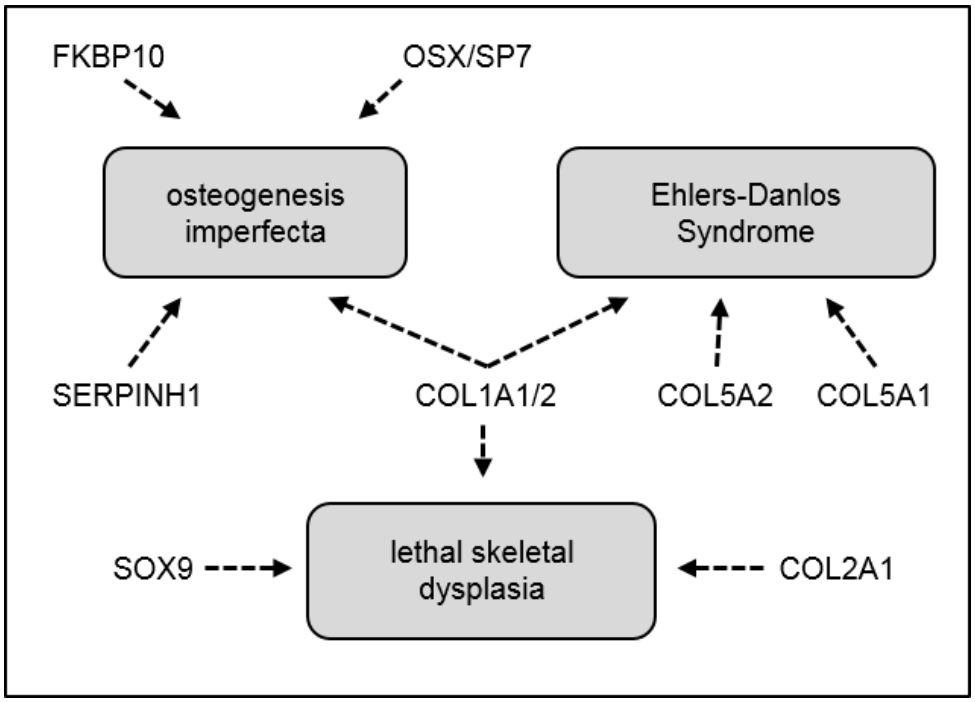

Figure 8. Shared targets of human skeletal anomalies associated with heterozygous/LOF mutations and downregulation of orthologous genes in 0.3 nM TCDD-treated medaka.

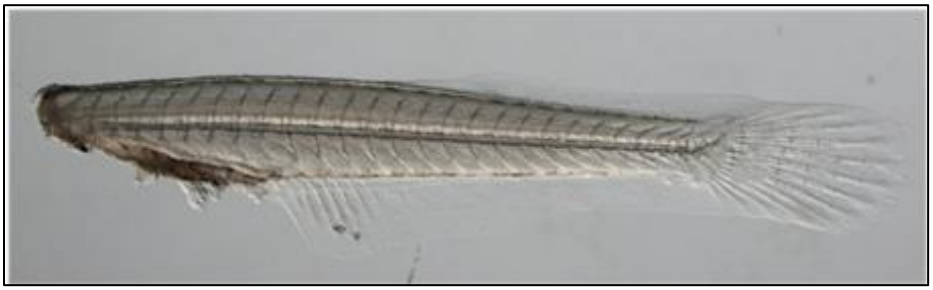

S.I. Figure 1. Representative image of sheared axial tissue from DMSO-treated medaka at 20 dpf. For each sample, axial tissue was inspected and trimmed of any remaining craniofacial or abdominal tissue and immediately flash frozen in liquid nitrogen. Tissues were homogenized in TRI Reagent® and total RNA was isolated according to the TRI Reagent manufacturer's protocol. Total RNA was quantified using Agilent 2100 Bioanalyzer and 2100 Expert Software package and RNAs with RNA Integrity numbers (RINs) greater than 9 were used for downstream RT-qPCR and RNA-Seq. Image depicted was captured on Nikon SMZ1500, 20X magnification.

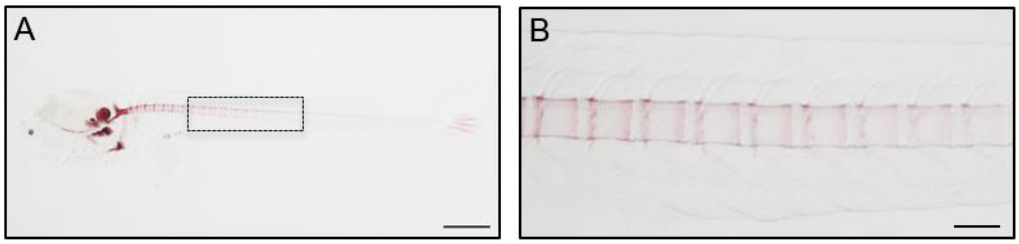

S.I. Figure 2. Representative image from whole-mount Alizarin Red S staining for ossified bone in 0.15 nM TCDD-treated medaka at 20 dpf. A) 2X magnification, scale bar represents 500 μm. B) is 10X magnification of boxed region containing medial vertebrae in A), scale bar represents 100 μm.

REFERENCES

Abdallah, B.M. and Kassem, M. (2008) Human mesenchymal stem cells: from basic biology to clinical applications. *Gene Ther.*, **15**, 109–116.

Abel, J. and Haarmann-Stemmann, T. (2010) An introduction to the molecular basics of aryl hydrocarbon receptor biology. *Biol. Chem.*, **391**, 1235–1248.

Adams, J.D. *et al.* (1987) Toxic and carcinogenic agents in undiluted mainstream smoke and sidestream smoke of different types of cigarettes. *Carcinogenesis*, **8**, 729–731.

Addison, W.N. *et al.* (2007) Pyrophosphate inhibits mineralization of osteoblast cultures by binding to mineral, up-regulating osteopontin, and inhibiting alkaline phosphatase activity. *J. Biol. Chem.*, **282**, 15872–15883.

Alexander, P.G. *et al.* (2016) Prenatal exposure to environmental factors and congenital limb defects. *Birth Defects Res. Part C - Embryo Today Rev.*, **108**, 243–273.

Apschner, A. *et al.* (2011) Not All Bones are Created Equal – Using Zebrafish and Other Teleost Species in Osteogenesis Research Third Edit. Elsevier Inc.

Avery, S. *et al.* (2017) Analysing the bioactive makeup of demineralised dentine matrix on bone marrow mesenchymal stem cells for enhanced bone repair. *Eur. Cells Mater.*, **34**, 1–14.

Baker, A.H. *et al.* (2015) Tributyltin Engages Multiple Nuclear Receptor Pathways and Suppresses Osteogenesis in Bone Marrow Multipotent Stromal Cells. *Chem. Res. Toxicol.*, **28**, 1156–1166.

Baker, T.R. *et al.* (2014) Adverse effects in adulthood resulting from low-level dioxin exposure in juvenile zebrafish. *Endocr. Disruptors*, **2**, 1–6.

Baker, T.R. *et al.* (2013) Early dioxin exposure causes toxic effects in adult zebrafish. *Toxicol. Sci.*, **135**, 241–250.

Baksh, D. *et al.* (2004) Adult mesenchymal stem cells: characterization, differentiation, and application in cell and gene therapy. *J. Cell. Mol. Med.*, **8**, 301–316.

Baldridge, D. *et al.* (2010) Signaling pathways in human skeletal dysplasias. *Annu Rev Genomics Hum Genet*, **11**, 189–217.

Barbour, K.E. *et al.* (2014) Inflammatory Markers and Risk of Hip Fracture in Older White Women: The Study of Osteoporotic Fractures. *J. Bone Miner. Res.*, **29**, 2057–2064.

Baron, R. and Kneissel, M. (2013) WNT signaling in bone homeostasis and disease: from

human mutations to treatments. *Nat. Med.*, **19**, 179–192.

Baroncelli, M. *et al.* (2017) Comparative proteomic profiling of human osteoblast-derived extracellular matrices identifies proteins involved in mesenchymal stromal cell osteogenic differentiation and mineralization. *J. Cell. Physiol.*, 1–9.

Baroncelli, M. *et al.* (2017) Comparative Proteomic Profiling of Human Osteoblast-Derived Extracellular Matrices Identifies Proteins Involved in Mesenchymal Stromal Cell Osteogenic Differentiation and Mineralization. *J Cell Physiol*.

Benjamini, Y. and Hochberg, Y. (1995) Controlling the False Discovery Rate: A Practical and Powerful Approach to Multiple Testing. *J. R. Stat. Soc. Ser. B*, **57**, 289–300.

Benvenuti, S. *et al.* (2007) Rosiglitazone stimulates adipogenesis and decreases osteoblastogenesis in human mesenchymal stem cells. *J. Endocrinol. Invest.*, **30**, 26–30.

Bialek, P. *et al.* (2004) A Twist Code Determines the Onset of Osteoblast Differentiation. *Dev. Cell*, **6**, 423–435.

Bishop, N. (2016) Bone Material Properties in Osteogenesis Imperfecta. *J. Bone Miner. Res.*, **31**, 699–708.

Bodle, J.C. *et al.* (2014) Age-related effects on the potency of human adipose derived stem cells: Creation and evaluation of superlots and implications for musculoskeletal tissue engineering applications. *Tissue Eng. Part C Methods*, **20**, 1–43.

Bone health and osteoporosis: a report of the Surgeon General (2004) Rockville, Maryland.

Bonventre, J.A. *et al.* (2012) Craniofacial abnormalities and altered wnt and mmp mRNA expression in zebrafish embryos exposed to gasoline oxygenates ETBE and TAME. *Aquat. Toxicol.*, **120**–**121**, 45–53.

Boyce, B.F. and Xing, L. (2007) Biology of RANK, RANKL, and osteoprotegerin. *Arthritis Res. Ther.*, **9 Suppl 1**, S1.

Briggs, A.M. *et al.* (2016) Musculoskeletal Health Conditions Represent a Global Threat to Healthy Aging: A Report for the 2015 World Health Organization World Report on Ageing and Health. *Gerontologist*, **56**, S243–S255.

Burns, F.R. *et al.* (2015) Dioxin disrupts cranial cartilage and dermal bone development in zebrafish larvae. *Aquat. Toxicol.*, **164**, 52–60.

Bustin, S.A. *et al.* (2009) The MIQE Guidelines: Minimum Information for Publication of Quantitative Real-Time PCR Experiments. *Clin. Chem.*, **622**, 611–622.

Carpi, D. *et al.* (2009) Dioxin-sensitive proteins in differentiating osteoblasts: Effects on bone formation in vitro. *Toxicol. Sci.*, **108**, 330–343.

Charoenpanich, A. *et al.* (2014) Cyclic tensile strain enhances osteogenesis and angiogenesis in mesenchymal stem cells from osteoporotic donors. *Tissue Eng. Part A*, **20**, 67–78.

Chen, G. *et al.* (2012) TGF-β and BMP Signaling in Osteoblast Differentiation and Bone Formation. *Int. J. Biol. Sci.*, **8**, 272–288.

Chopra, M. and Schrenk, D. (2011) Dioxin toxicity, aryl hydrocarbon receptor signaling, and apoptosis-persistent pollutants affect programmed cell death. *Crit. Rev. Toxicol.*, **41**, 292–320.

Chrisman, K. *et al.* (2004) Gestational Ethanol Exposure Disrupts the Expression of FGF8 and Sonic hedgehog during Limb Patterning. *Birth Defects Res. Part A - Clin. Mol. Teratol.*, **70**, 163–171.

Christiansen, H.E. *et al.* (2010) Homozygosity for a Missense Mutation in SERPINH1, which Encodes the Collagen Chaperone Protein HSP47, Results in Severe Recessive Osteogenesis Imperfecta. *Am. J. Hum. Genet.*, **86**, 389–398.

Clarke, B. (2008) Normal bone anatomy and physiology. *Clin. J. Am. Soc. Nephrol.*, **3 (Suppl 3**.

Derrien, T. *et al.* (2012) The GENCODE v7 catalogue of human long non-coding RNAs : Analysis of their structure , evolution and expression. *Genome Res.*, **22**, 1775–1789.

Ding, D. *et al.* (2012) Over-expression of Sox2 in C3H10T1/2 cells inhibits osteoblast differentiation through Wnt and MAPK signalling pathways. *Int. Orthop.*, **36**, 1087–1094.

Dobin, A. *et al.* (2013) STAR: Ultrafast universal RNA-seq aligner. *Bioinformatics*, **29**, 15–21.

Dolk, H. *et al.* (2010) The Prevalence of Congenital Anomalies in Europe. In, Paz,M.P. de la and Croft,S.C. (eds), *Rare Diseases Epidemiology*. Springer, New York, New York, pp. 305–334.

Dominici, M. *et al.* (2006) Minimal criteria for defining multipotent mesenchymal stromal cells. The International Society for Cellular Therapy position statement. *Cytotherapy*, **8**, 315–7.

Dong, B. and Matsumura, F. (2008) Roles of cytosolic phospholipase A2 and Src kinase in the early action of 2,3,7,8-tetrachlorodibenzo-p-dioxin through a nongenomic pathway in MCF10A cells. *Mol. Pharmacol.*, **74**, 255–263.

Dong, W. *et al.* (2012) TCDD disrupts hypural skeletogenesis during medaka embryonic development. *Toxicol. Sci.*, **125**, 91–104.

Dong, W. *et al.* (2010) TCDD Induced Pericardial Edema and Relative COX-2 Expression in Medaka (Oryzias Latipes) Embryos. *Toxicol. Sci.*, **118**, 213–223.

Dudakovic, A. *et al.* (2015) Epigenetic Control of Skeletal Development by the Histone Demethylase Ezh2. *J. Biol. Chem.*, **290**, 27604–27617.

Ekanayake, S. and Hall, B.K. (1987) The development of acellularity of the vertebral bone of the Japanese medaka, *Oryzias latipes* (Teleostei; Cyprinidontidae). *J. Morphol.*, **193**, 253–261.

Ekanayake, S. and Hall, B.K. (1988) Ultrastructure of the osteogenesis of acellular vertebral bone in the Japanese medaka, Oryzias latipes (Teleostei, Cyprinidontidae). *Am. J. Anat.*, **182**, 241–249.

Ellis, L.D. *et al.* (2014) Use of the zebrafish larvae as a model to study cigarette smoke condensate toxicity. *PLoS One*, **9**, e115305.

Etemad, L. *et al.* (2012) Epilepsy drugs and effects on fetal development: Potential mechanisms. *J. Res. Med. Sci.*, **17**.

Fakhry, A. *et al.* (2005) Effects of FGF-2/-9 in calvarial bone cell cultures: Differentiation stage-dependent mitogenic effect, inverse regulation of BMP-2 and noggin, and enhancement of osteogenic potential. *Bone*, **36**, 254–266.

Felson, D.T. *et al.* (2000) Osteoarthritis: new insights. Part 1: the disease and its risk factors. *Ann. Intern. Med.*, **133**, 635–646.

Fernández-González, R. *et al.* (2015) A Critical Review about Human Exposure to Polychlorinated Dibenzo-p-Dioxins (PCDDs), Polychlorinated Dibenzofurans (PCDFs) and Polychlorinated Biphenyls (PCBs) through Foods. *Crit. Rev. Food Sci. Nutr.*, **55**, 1590–1617.

Finnilä, M.A.J. *et al.* (2010) Effects of 2,3,7,8-tetrachlorodibenzo-p-dioxin exposure on bone material properties. *J. Biomech.*, **43**, 1097–1103.

Fleming, A. *et al.* (2015) Building the backbone: the development and evolution of vertebral patterning. *Development*, **142**, 1733–44.

Flynn, R.A. and Chang, H.Y. (2014) Long noncoding RNAs in cell-fate programming and reprogramming. *Cell Stem Cell*, **14**, 752–761.

Forlino, A. *et al.* (2011) New perspectives on osteogenesis imperfecta. *Nat. Rev. Endocrinol.*,

7, 540–557.

Forlino, A. and Marini, J.C. (2016) Osteogenesis imperfecta. *Lancet*, **387**, 1657–1671.

Franz-Odendaal, T.A. *et al.* (2006) Buried alive: How osteoblasts become osteocytes. *Dev. Dyn.*, **235**, 176–190.

Gadupudi, G. *et al.* (2015) PCB126 inhibits adipogenesis of human preadipocytes. *Toxicol. Vitr.*, **29**, 132–141.

Gallagher, J.C. and Sai, a. J. (2010) Molecular biology of bone remodeling: Implications for new therapeutic targets for osteoporosis. *Maturitas*, **65**, 301–307.

Gennari, L. *et al.* (2016) MicroRNAs in bone diseases. *Osteoporos. Int.*, 1–23.

Golub, E.E. and Boesze-Battaglia, K. (2007) The role of alkaline phosphatase in mineralization. *Curr. Opin. Orthop.*, **18**, 444–448.

Gordon, J.A.R. *et al.* (2015) Chromatin modifiers and histone modifications in bone formation, regeneration, and therapeutic intervention for bone-related disease. *Bone*, **81**, 739–745.

Gordon, J.A.R. *et al.* (2014) Epigenetic pathways regulating bone homeostasis: Potential targeting for intervention of skeletal disorders. *Curr. Osteoporos. Rep.*, **12**, 496–506.

Greco, S.J. *et al.* (2007) Functional Similarities Among Genes Regulated by Oct4 in Human Mesenchymal and Embryonic Stem Cells. *Stem Cells*, **25**, 3143–3154.

Grotmol, S. *et al.* (2005) A segmental pattern of alkaline phosphatase activity within the notochord coincides with the initial formation of the vertebral bodies. *J. Anat.*, **206**, 427–436.

Håkelien, A.M. *et al.* (2014) The regulatory landscape of osteogenic differentiation. *Stem Cells*, **32**, 2780–2793.

Hardy, R. and Cooper, M.S. (2009) Bone loss in inflammatory disorders. *J. Endocrinol.*, **201**, 309–320.

Heo, J. *et al.* (2015) Comparison of molecular profiles of human mesenchymal stem cells derived from bone marrow, umbilical cord blood, placenta and adipose tissue. *Int. J. Mol. Med.*, 115–125.

Herlin, M. *et al.* (2015) Inhibitory effects on osteoblast differentiation in vitro by the polychlorinated biphenyl mixture Aroclor 1254 are mainly associated with the dioxin-like constituents. *Toxicol. Vitr.*, **29**, 876–883.

Herlin, M. *et al.* (2013) New insights to the role of aryl hydrocarbon receptor in bone phenotype and in dioxin-induced modulation of bone microarchitecture and material properties. *Toxicol. Appl. Pharmacol.*, **273**, 219–26.

Herlin, M. *et al.* (2010) Quantitative characterization of changes in bone geometry, mineral density and biomechanical properties in two rat strains with different Ah-receptor structures after long-term exposure to 2,3,7,8-tetrachlorodibenzo-p-dioxin. *Toxicology*, **273**, 1–11.

Hermanns, P. and Lee, B. (2002) Transcriptional dysregulation in skeletal malformation syndromes. *Am. J. Med. Genet.*, **106**, 258–271.

Hernandez, C.J. *et al.* (2003) A theoretical analysis of the relative influences of peak BMD, age-related bone loss and menopause on the development of osteoporosis. *Osteoporos. Int.*, **14**, 843–847.

Holz, J.D. *et al.* (2007) Environmental agents affect skeletal growth and development. *Birth Defects Res. Part C - Embryo Today Rev.*, **81**, 41–50.

Huang, J. *et al.* (2010) MicroRNA-204 regulates Runx2 protein expression and mesenchymal progenitor cell differentiation. *Stem Cells*, **28**, 357–364.

Hulsen, T. *et al.* (2008) BioVenn – a web application for the comparison and visualization of biological lists using area-proportional Venn diagrams. *BMC Genomics*, **9**, 488.

Imai, Y. *et al.* (2013) Nuclear Receptors in Bone Physiology and Diseases. *Physiol. Rev.*, **93**, 481–523.

Inose, H. *et al.* (2009) A microRNA regulatory mechanism of osteoblast differentiation. *Proc. Natl. Acad. Sci. U. S. A.*, **106**, 20794–20799.

Ito, T. *et al.* (2010) Identification of a Primary Target of Thalidomide Teratogenicity. *Science (80-.).*, **327**, 1345–1351.

Ito, T. *et al.* (2011) Teratogenic effects of thalidomide: Molecular mechanisms. *Cell. Mol. Life Sci.*, **68**, 1569–1579.

Itoh, T. *et al.* (2009) MicroRNA-141 and -200a Are Involved in Bone Morphogenetic Protein-2-induced Mouse Pre-osteoblast Differentiation by Targeting Distal-less Homeobox 5. *J. Biol. Chem.*, **284**, 19272–19279.

Jämsä, T. *et al.* (2001) Effects of 2,3,7,8-Tetrachlorodibenzo-p-Dioxin on Bone in Two Rat Strains with Different Aryl Hydrocarbon Receptor Structures. *J. Bone Miner. Res.*, **16**, 1812–1820.

Jensen, E.D. *et al.* (2010) Regulation of gene expression in osteoblasts. *Biofactors*, **36**, 25–32.

Jenuwein, T. *et al.* (2001) Translating the Histone Code. *Science (80-.).*, **293**, 1074–1080.

Johnell, O. and Kanis, J.A. (2006) An estimate of the worldwide prevalence and disability associated with osteoporotic fractures. *Osteoporos. Int.*, **17**, 1726–1733.

Joshi-Tope, G. *et al.* (2005) Reactome: A knowledgebase of biological pathways. *Nucleic Acids Res.*, **33**, 428–432.

Kang, H. *et al.* (2017) Osteogenesis imperfecta: new genes reveal novel mechanisms in bone dysplasia. *Transl. Res.*, **181**, 27–48.

Kanis, J. (2007) Assessment of osteoporosis at the primary health care level.

Kanis, J. *et al.* (2005) Smoking and fracture risk: A meta-analysis. *Osteoporos. Int.*, **16**, 155–162.

Karsenty, G. *et al.* (2009) Genetic Control of Bone Formation. *Annu. Rev. Cell Dev. Biol.*, **25**, 629–648.

Karsenty, G. (2008) Transcriptional Control of Skeletogenesis. *Annu. Rev. Genomics Hum. Genet.*, **9**, 183–196.

Kawai, M. *et al.* (2010) The many facets of PPARgamma: novel insights for the skeleton. *Am. J. Physiol. Endocrinol. Metab.*, **299**, E3–E9.

Kimura, H. (2013) Histone modifications for human epigenome analysis. *J. Hum. Genet.*, **58**, 439–445.

King-Heiden, T.C. *et al.* (2012) Reproductive and developmental toxicity of dioxin in fish. *Mol. Cell. Endocrinol.*, **354**, 121–138.

Klareskog, L. *et al.* (2007) Smoking as a trigger for inflammatory rheumatic diseases. *Curr. Opin. Rheumatol.*, **19**, 49–54.

Ko, C.I. *et al.* (2016) Repression of the Aryl Hydrocarbon Receptor Is Required to Maintain Mitotic Progression and Prevent Loss of Pluripotency of Embryonic Stem Cells. *Stem Cells*, **34**, 2825–2839.

Komori, T. (2010) Regulation of bone development and extracellular matrix protein genes by RUNX2. *Cell Tissue Res.*, **339**, 189–195.

Komori, T. *et al.* (1997) Targeted disruption of Cbfa1 results in a complete lack of bone

formation owing to maturational arrest of osteoblasts. *Cell*, **89**, 755–64.

Korkalainen, M. *et al.* (2009) Dioxins interfere with differentiation of osteoblasts and osteoclasts. *Bone*, **44**, 1134–1142.

Kornak, U. and Mundlos, S. (2003) Genetic disorders of the skeleton: a developmental approach. *Am. J. Hum. Genet.*, **73**, 447–74.

Kotake, S. *et al.* (1996) Interleukin-6 and Soluble Interleukin-6 Receptors in the Synovial Fluids from Rheumatoid Arthritis Patients Are Responsible for Osteoclast-like Cell Formation. *J. Bone Miner. Res.*, **11**, 88–95.

Krakow, D. and Rimoin, D.L. (2010) The skeletal dysplasias. *Genet. Med.*, **12**, 327–41.

Kung, M.H. *et al.* (2011) Aryl hydrocarbon receptor-mediated impairment of chondrogenesis and fracture healing by cigarette smoke and benzo(α)pyrene. *J. Cell. Physiol.*, **227**, 1062–1070.

Lacey, D.C. *et al.* (2009) Proinflammatory cytokines inhibit osteogenic differentiation from stem cells: implications for bone repair during inflammation. *Osteoarthr. Cartil.*, **17**, 735–742.

Laize, V. *et al.* (2014) Fish : a suitable system to model human bone disorders and discover drugs with osteogenic or osteotoxic activities. *Drug Discov. Today Dis. Model.*, **13**, 29–37.

Lam, J. *et al.* (2000) TNF-α induces osteoclastogenesis by direct stimulation of macrophages exposed to permissive levels of RANK ligand. *J. Clin. Invest.*, **106**, 1481–1488.

Law, M.R. and Hackshaw, a K. (1997) A meta-analysis of cigarette smoking, bone mineral density and risk of hip fracture: recognition of a major effect. *BMJ*, **315**, 841–846.

Lee, J.J. *et al.* (2013) The musculoskeletal effects of cigarette smoking. *J. Bone Jt. Surg.*, **95**, 850–9.

Lee, M.H. *et al.* (2003) BMP-2-induced Osterix expression is mediated by Dlx5 but is independent of Runx2. *Biochem. Biophys. Res. Commun.*, **309**, 689–694.

Lee, M.H. *et al.* (2005) Dlx5 specifically regulates Runx2 type II expression by binding to homeodomain-response elements in the Runx2 distal promoter. *J. Biol. Chem.*, **280**, 35579–35587.

Lefebvre, V. and Bhattaram, P. (2010) Vertebrate Skeletogenesis. In, Koopman,P. (ed), *Current Topics in Developmental Biology: Organogenesis in Development*. Elsevier Inc., San Diego, pp. 291–317.

Li, L. *et al.* (2013) Targeted Disruption of Hotair Leads to Homeotic Transformation and Gene Derepression. *Cell Rep.*, **5**, 3–12.

Li, W. *et al.* (2008) Development of a human adipocyte model derived from human mesenchymal stem cells (hMSC) as a tool for toxicological studies on the action of TCDD. *Biol. Chem.*, **389**, 169–177.

Lian, J.B. *et al.* (2006) Networks and hubs for the transcriptional control of osteoblastogenesis. *Rev. Endocr. Metab. Disord.*, **7**, 1–16.

Lindner, U. *et al.* (2010) Mesenchymal stem or stromal cells: Toward a better understanding of their biology? *Transfus. Med. Hemotherapy*, **37**, 75–83.

Liu, B. *et al.* (2013) Depleting the methyltransferase Suv39h1 improves DNA repair and extends lifespan in a progeria mouse model. *Nat. Commun.*, **4**, 1868.

Liu, P. *et al.* (1996) Alteration by 2,3,7,8-Tetrachlordibenzo-p-dioxin of CCAAT/Enhancer Binding Protein Correlates with Suppression of Adipocyte Differentiation in 3T3-L1 Cells. *Mol. Pharmacol.*, **49**, 989–997.

Livak, K.J. and Schmittgen, T.D. (2001) Analysis of relative gene expression data using real-time quantitative PCR and the 2(-Delta Delta C(T)) Method. *Methods*, **25**, 402–8.

Long, F. (2011) Building strong bones: molecular regulation of the osteoblast lineage. *Nat. Rev. Mol. Cell Biol.*, **13**, 27–38.

Lorentzon, M. *et al.* (2007) Smoking is associated with lower bone mineral density and reduced cortical thickness in young men. *J. Clin. Endocrinol. Metab.*, **92**, 497–503.

Love, M.I. *et al.* (2014) Moderated estimation of fold change and dispersion for RNA-seq data with DESeq2. *Genome Biol.*, **15**, 550.

Lu, J. *et al.* (2015) Effect of fibroblast growth factor 9 on the osteogenic differentiation of bone marrow stromal stem cells and dental pulp stem cells. *Mol. Med. Rep.*, **11**, 1661–1668.

Lu, J. *et al.* (2014) The Effect of Fibroblast Growth Factor 9 on the Osteogenic Differentiation of Calvaria-Derived Mesenchymal Cells. *J. Craniofac. Surg.*, **25**, 502–505.

Manolagas, S.C. (2000) Birth and death of bone cells: basic regulatory mechanisms and implications for the pathogenesis and treatment of osteoporosis. *Endocr. Rev.*, **21**, 115–137.

Mansukhani, A. *et al.* (2005) Sox2 induction by FGF and FGFR2 activating mutations

inhibits Wnt signaling and osteoblast differentiation. *J. Cell Biol.*, **168**, 1065–1076.

Marcellini, S. *et al.* (2012) Control of osteogenesis by the canonical Wnt and BMP pathways in vivo: cooperation and antagonism between the canonical Wnt and BMP pathways as cells differentiate from osteochondroprogenitors to osteoblasts and osteocytes. *BioEssays News Rev. Mol. Cell. Dev. Biol.*, **34**, 953–62.

Marotti, G. (1996) The structure of bone tissues and the cellular control of their deposition. *Ital. J. Anat. Embryol.*, **101**, 25–79.

McCormack, S.E. *et al.* (2017) Association Between Linear Growth and Bone Accrual in a Diverse Cohort of Children and Adolescents. *JAMA Pediatr.*, **19104**, 1–9.

Miettinen, H.M. *et al.* (2005) Effects of in utero and lactational TCDD exposure on bone development in differentially sensitive rat lines. *Toxicol. Sci.*, **85**, 1003–1012.

Mizuno, Y. *et al.* (2008) miR-125b inhibits osteoblastic differentiation by down-regulation of cell proliferation. *Biochem. Biophys. Res. Commun.*, **368**, 267–272.

Montecino, M. *et al.* (2015) Multiple levels of epigenetic control for bone biology and pathology. *Bone*, **81**, 733–738.

Mundy, G.R. (2007) Osteoporosis and Inflammation. *Nutr. Rev.*, **65**.

Murante, F.G. and Gasiewicz, T.A. (2000) Hemopoietic Progenitor Cells Are Sensitive Targets of 2,3,7,8-Tetrachlorodibenzo-p-dioxin in C57BL/6J Mice. *Toxicol. Sci.*, **54**, 374–383.

Nakase, T. *et al.* (1997) Interleukin-1 beta enhances and tumor necrosis factor-alpha inhibits bone morphogenetic protein-2-induced alkaline phosphatase activity in MC3T3-E1 osteoblastic cells. *Bone*, **21**, 17–21.

Nakashima, K. *et al.* (2002) The novel zinc finger-containing transcription factor osterix is required for osteoblast differentiation and bone formation. *Cell*, **108**, 17–29.

Nakashima, T. *et al.* (2012) New insights into osteoclastogenic signaling mechanisms. *Trends Endocrinol. Metab.*, **23**, 582–90.

Narkowicza, S. *et al.* (2013) Environmental Tobacco Smoke: Exposure, Health Effects, and Analysis. *Biocontrol Sci. Technol.*, **43**, 121–161.

Naruse, M. *et al.* (2002) 3-Methylcholanthrene, which binds to the arylhydrocarbon receptor, inhibits proliferation and differentiation of osteoblasts in vitro and ossification in vivo. *Endocrinology*, **143**, 3575–81.

Nishio, Y. *et al.* (2006) Runx2-mediated regulation of the zinc finger Osterix/Sp7 gene. *Gene*, **372**, 62–70.

Nordvik, K. *et al.* (2005) The salmon vertebral body develops through mineralization of two preformed tissues that are encompassed by two layers of bone. *J. Anat.*, **206**, 103–114.

Ohtake, F. *et al.* (2009) AhR acts as an E3 ubiquitin ligase to modulate steroid receptor functions. *Biochem. Pharmacol.*, **77**, 474–84.

Orioli, I.M. *et al.* (1986) The birth prevalence rates for the skeletal dysplasias. *J. Med. Genet.*, **23**, 328–32.

Ornitz, D.M. and Marie, P.J. (2015) Fibroblast growth factor signaling in skeletal development and disease. *Genes Dev.*, **29**, 1463–1486.

Padilla, S. *et al.* (2012) Zebrafish developmental screening of the ToxCast^{TM} Phase I chemical library. *Reprod. Toxicol.*, **33**, 174–187.

van de Peppel, J. *et al.* (2017) Identification of Three Early Phases of Cell-Fate Determination during Osteogenic and Adipogenic Differentiation by Transcription Factor Dynamics. *Stem Cell Reports*, **172**, 5457–5476.

Pillai, H.K. *et al.* (2014) Ligand Binding and Activation of PPARγ by Firemaster 550: Effects on Adipogenesis and Osteogenesis in Vitro. *Environ. Health Perspect.*, **122**, 1225–1232.

Podechard, N. *et al.* (2009) Inhibition of human mesenchymal stem cell-derived adipogenesis by the environmental contaminant benzo(a)pyrene. *Toxicol. In Vitro*, **23**, 1139–44.

Pohl, H. *et al.* (1998) Toxicological profile for chlorinated dibenzo-p-dioxins.

Puga, A. *et al.* (2000) Aromatic Hydrocarbon Receptor Interaction with the Retinoblastoma Protein Potentiates Repression of E2F-dependent Transcription and Cell Cycle Arrest. *J. Biol. Chem.*, **275**, 2943–2950.

Puga, A. *et al.* (2009) The aryl hydrocarbon receptor cross-talks with multiple signal transduction pathways. *Biochem. Pharmacol.*, **77**, 713–722.

Quiroz, F.G. *et al.* (2010) Housekeeping gene stability influences the quantification of osteogenic markers during stem cell differentiation to the osteogenic lineage. *Cytotechnology*, **62**, 109–120.

Rahman, M.S. *et al.* (2015) TGF-β/BMP signaling and other molecular events: regulation of osteoblastogenesis and bone formation. *Bone Res.*, **3**, 15005.

Redlich, K. and Smolen, J.S. (2012) Inflammatory bone loss: pathogenesis and therapeutic intervention. *Nat. Rev. Drug Discov.*, **11**, 234–250.

Riekstina, U. *et al.* (2009) Embryonic stem cell marker expression pattern in human mesenchymal stem cells derived from bone marrow, adipose tissue, heart and dermis. *Stem Cell Rev. Reports*, **5**, 378–386.

Riss, T.L. *et al.* (2004) Cell Viability Assays Assay Guidance Manual. *Assay Guid. Man.*, 1–23.

Rizzoli, R. *et al.* (2010) Maximizing bone mineral mass gain during growth for the prevention of fractures in the adolescents and the elderly. *Bone*, **46**, 294–305.

Rosano, A. *et al.* (2000) Limb defects associated with major congenital anomalies: Clinical and epidemiological study from the international clearinghouse for birth defects monitoring systems. *Am. J. Med. Genet.*, **93**, 110–116.

Rosen, E.D. and MacDougald, O.A. (2006) Adipocyte differentiation from the inside out. *Nat. Rev. Mol. Cell Biol.*, **7**, 885–896.

Rosset, E.M. and Bradshaw, A.D. (2016) SPARC/osteonectin in mineralized tissue. *Matrix Biol.*, **52**–**54**, 78–87.

Ryan, E.P. *et al.* (2007) Environmental toxicants may modulate osteoblast differentiation by a mechanism involving the aryl hydrocarbon receptor. *J. Bone Miner. Res.*, **22**, 1571–80.

Safe, S. *et al.* (1998) Ah receptor agonists as endocrine disruptors: antiestrogenic activity and mechanisms. *Toxicol. Lett.*, **102**–**103**, 343–7.

Safe, S. (1995) Cellular and molecular biology of aryl hydrocarbon (Ah) receptor-mediated gene expression. *Arch. Toxicol.*, **17**, 99–115.

Sakaguchi, Y. *et al.* (2009) Suspended cells from trabecular bone by collagenase digestion become virtually identical to mesenchymal stem cells obtained from marrow. *Stem Cells*, **104**, 2728–2735.

Sargis, R.M. *et al.* (2009) Environmental Endocrine Disruptors Promote Adipogenesis in the 3T3-L1 Cell Line through Glucocorticoid Receptor Activation. *Obesity*, **18**, 1283–1288.

Schönitzer, V. *et al.* (2014) Sox2 is a potent inhibitor of osteogenic and adipogenic differentiation in human mesenchymal stem cells. *Cell. Reprogram.*, **16**, 355–65.

Schroeder, T.M. *et al.* (2005) Runx2: A master organizer of gene transcription in developing and maturing osteoblasts. *Birth Defects Res. Part C - Embryo Today Rev.*, **75**, 213–225.

Sciullo, E.M. *et al.* (2009) Characterization of the pattern of the nongenomic signaling pathway through which TCDD-induces early inflammatory responses in U937 human macrophages. *Chemosphere*, **74**, 1531–1537.

Scolaro, J.A. *et al.* (2014) Cigarette Smoking Increases Complications Following Fracture. *J. Bone Jt. Surg.*, 674–681.

Seo, E. *et al.* (2011) Distinct Functions of Sox2 Control Self-Renewal and Differentiation in the Osteoblast Lineage. *Mol. Cell. Biol.*, **31**, 4593–4608.

Sheng, G. (2015) The developmental basis of mesenchymal stem/stromal cells (MSCs). *BMC Dev. Biol.*, **15**, 44.

Shimba, S. *et al.* (2001) Aryl hydrocarbon receptor (AhR) is involved in negative regulation of adipose differentiation in 3T3- L1 cells : AhR inhibits adipose differentiation independently of dioxin. *J. Cell Sci.*, **114**, 2809–2817.

Siegel, G. *et al.* (2013) Phenotype, donor age and gender affect function of human bone marrow-derived mesenchymal stromal cells. *BMC Med.*, **11**, 146.

Simonet, W.S. *et al.* (1997) Osteoprotegerin: a novel secreted protein involved in the regulation of bone density. *Cell*, **89**, 309–19.

Singh, K.P. *et al.* (2009) Treatment of mice with the Ah receptor agonist and human carcinogen dioxin results in altered numbers and function of hematopoietic stem cells. *Carcinogenesis*, **30**, 11–19.

Sinha, K.M. and Zhou, X. (2013) Genetic and molecular control of osterix in skeletal formation. *J. Cell. Biochem.*, **114**, 975–84.

Sipes, N.S. *et al.* (2011) Zebrafish-as an integrative model for twenty-first century toxicity testing. *Birth Defects Res. Part C, Embryo Today Rev.*, **93**, 256–267.

Sloan, A. *et al.* (2010) The effects of smoking on fracture healing. *Surg. J. R. Coll. Surg. Edinburgh Irel.*, **8**, 111–6.

Smith, K.J. *et al.* (2011) Identification of a high-affinity ligand that exhibits complete aryl hydrocarbon receptor antagonism. *J. Pharmacol. Exp. Ther.*, **338**, 318–327.

Sozen, T. *et al.* (2017) An overview and management of osteoporosis. *Eur. J. Rheumatol.*, **4**, 46–56.

Spandidos, A. *et al.* (2010) PrimerBank : a resource of human and mouse PCR primer pairs for gene expression detection and quantification. **38**, 792–799.

Staines, K.A. *et al.* (2012) The importance of the SIBLING family of proteins on skeletal mineralisation and bone remodelling. *J. Endocrinol.*, **214**, 241–255.

Su, N. *et al.* (2008) FGF signaling: its role in bone development and human skeletal diseases. *Front. Biosci.*, **13**, 2842–2865.

Teraoka, H. *et al.* (2006) Impairment of lower jaw growth in developing zebrafish exposed to 2,3,7,8-tetrachlorodibenzo-p-dioxin and reduced hedgehog expression. *Aquat. Toxicol.*, **78**, 103–113.

Teraoka, H. *et al.* (2006) Muscular contractions in the zebrafish embryo are necessary to reveal thiuram-induced notochord distortions. *Toxicol. Appl. Pharmacol.*, **212**, 24–34.

The Health Consequences of Smoking - — 50 Years of Progress A Report of the Surgeon General (2014) Rockville, Maryland.

Tian, L. *et al.* (2017) miR-148a-3p regulates adipocyte and osteoblast differentiation by targeting lysine-specific demethylase 6b. *Gene*, **627**, 32–39.

Tian, Y. *et al.* (2002) Ah receptor and NF-kB interactions: Mechanisms and physiological implications. *Chem. Biol. Interact.*, **141**, 97–115.

Tilton, F. *et al.* (2006) Dithiocarbamates have a common toxic effect on zebrafish body axis formation. *Toxicol. Appl. Pharmacol.*, **216**, 55–68.

Tox21: Chemical testing in the 21st century (2017) Research Triangle Park, NC.

Truong, L. *et al.* (2014) Multidimensional in vivo hazard assessment using zebrafish. *Toxicol. Sci.*, **137**, 212–233.

Tye, C.E. *et al.* (2015) Could lncRNAs be the Missing Links in Control of Mesenchymal Stem Cell Differentiation? *J. Cell. Physiol.*, **230**, 526–534.

Tyl, R.W. *et al.* (2007) Altered Axial Skeletal Development. *Birth Defects Res. Part B-Developmental Reprod. Toxicol.*, **472**, 451–472.

Voss, A. *et al.* (2016) Extracellular Matrix of Current Biological Scaffolds Promotes the Differentiation Potential of Mesenchymal Stem Cells. *Arthrosc. - J. Arthrosc. Relat. Surg.*, **32**, 2381–2392.e1.

van de Vyver, M. *et al.* (2014) Thiazolidinedione-induced lipid droplet formation during osteogenic differentiation. *J. Endocrinol.*, **223**, 119–132.

Wade, S.W. *et al.* (2014) Estimating prevalence of osteoporosis: examples from industrialized countries. *Arch. Osteoporos.*, **9**, 182.

Wang, C.-K. *et al.* (2009) Aryl hydrocarbon receptor activation and overexpression upregulated fibroblast growth factor-9 in human lung adenocarcinomas. *Int. J. Cancer*, **125**, 807–815.

Wang, Y. *et al.* (2010) Dioxin Exposure Disrupts the Differentiation of Mouse Embryonic Stem Cells into Cardiomyocytes. **115**, 225–237.

Wang, Z. *et al.* (2012) Distinct lineage specification roles for NANOG, OCT4, and SOX2 in human embryonic stem cells. *Cell Stem Cell*, **10**, 440–454.

Ward, K.D. and Klesges, R.C. (2001) A Meta-Analysis of the Effects of Cigarette Smoking on Bone Mineral Density. *Calcif. Tissue Int.*, **68**, 259–270.

Watson, A.T.D. *et al.* (2017) Embryonic Exposure to TCDD Impacts Osteogenesis of the Axial Skeleton in Japanese medaka, Oryzias latipes. *Toxicol. Sci.*, **155**, 485–496.

Watt, J. and Schlezinger, J.J. (2015) Structurally-diverse, PPARγ-activating environmental toxicants induce adipogenesis and suppress osteogenesis in bone marrow mesenchymal stromal cells. *Toxicology*, **331**, 66–77.

Wilffert, B. *et al.* (2011) Pharmacogenetics of drug-induced birth defects: what is known so far? *Pharmacogenomics*, **12**, 547–558.

Wilson, C.L. and Safe, S. (1998) Mechanisms of ligand-induced aryl hydrocarbon receptor-mediated biochemical and toxic responses. *Toxicol. Pathol.*, **26**, 657–671.

Witten, P.E. *et al.* (2016) Small teleost fish provide new insights into human skeletal diseases Elsevier Ltd.

Witten, P.E. and Huysseune, A. (2009) A comparative view on mechanisms and functions of skeletal remodelling in teleost fish, with special emphasis on osteoclasts and their function. *Biol. Rev.*, **84**, 315–346.

Wong, P.K.K. *et al.* (2007) The effects of smoking on bone health. *Clin. Sci.*, **113**, 233–41.

Wu, H. *et al.* (2017) Chromatin Dynamics Regulate Mesenchymal Stem Cell Lineage Specification and Differentiation to Osteogenesis. *Biochim. Biophys. Acta - Gene Regul. Mech.*, **1860**, 438–449.

Wu, M. *et al.* (2016) TGF-β and BMP signaling in osteoblast, skeletal development, and bone formation, homeostasis and disease. *Bone Res.*, **4**, 16009.

Yamashita, T. *et al.* (2012) New roles of osteoblasts involved in osteoclast differentiation. *World J. Orthop.*, **3**, 175–81.

Yanbaeva, D.G. *et al.* (2007) Systemic effects of smoking. *Chest*, **131**, 1557–66.

Yang, J.-H. and Lee, H.-G. (2010) 2,3,7,8-Tetrachlorodibenzo-p-dioxin induces apoptosis of articular chondrocytes in culture. *Chemosphere*, **79**, 278–284.

Yoon, V. *et al.* (2012) The effects of smoking on bone metabolism. *Osteoporos. Int.*, **23**, 2081–92.

Zhang, G. (2009) An evo-devo view on the origin of the backbone: evolutionary development of the vertebrae. *Integr. Comp. Biol.*, **49**, 178–186.

Zhang, Y.H. *et al.* (1990) Interleukin-6 induction by tumor necrosis factor and interleukin-1 in human fibroblasts involves activation of a nuclear factor binding to a kappa B-like sequence. *Mol. Cell. Biol.*, **10**, 3818–23.

CHAPTER 3

The Inhibitory Role of AhR Activation on Human Mesenchymal Stromal Cell Differentiation

AtLee T. D. Watson*, Rachel C. Nordberg[#], Elizabeth G. Loboa[#,§], Seth W. Kullman*[†]

* Department of Biological Sciences, North Carolina State University, Raleigh, North Carolina 27695

[#] Joint Department of Biomedical Engineering at University of North Carolina-Chapel Hill and North Carolina State University, Raleigh, North Carolina, 27695

[§] College of Engineering, University of Missouri, Columbia, Missouri, 65211USA

[†] Center for Human Health and the Environment, North Carolina State University, Raleigh, North Carolina 27695

ABSTRACT

Multipotent mesenchymal stem cells maintain the ability to differentiate into adipogenic (fat), chondrogenic (cartilage), or osteogenic (bone) lineages. There is increasing concern, however, that developmental exposure to environmental xenobiotic stressors may perturb the osteogenic pathways responsible for normal bone formation. Aryl hydrocarbon receptor (AhR) ligands are one class of chemicals known to disrupt bone and cartilage formation. Using TCDD as a prototypic AhR agonist, we investigated AhR-mediated osteogenic inhibition in human bone-derived mesenchymal stromal cells (hBMSCs) during phases of early differentiation, extracellular matrix synthesis, and apical matrix mineralization. Across donors we demonstrate a consistent TCDD-mediated attenuation of alkaline phosphatase (ALP) activity and matrix mineralization at terminal stages of differentiation. At the transcriptional level, expression of select transcriptional regulators and osteogenic markers were also attenuated including *DLX5*, *ALP*, *OPN*, and *IBSP*. Members of the FGF family, *FGF9* and *FGF18*, were consistently upregulated suggesting that TCDD may influence pathways associated with maintaining stemness or multipotency in hBMSCs. Relative to undifferentiated cells, expression of stemness/potency markers *SOX2*, *OCT4*, *NANOG*, and *SALL4* showed consistent trends with diminished expression in osteogenic controls, while expression in TCDD-treated cells remained higher and more similar to undifferentiated cells. Co-exposure with GNF351, an AhR antagonist, partially rescued Alizarin Red S staining and expression of select transcriptional regulators and apical markers, thus suggesting that AhR activation is mechanistically associated with TCDD-mediated inhibition of osteogenesis. This study highlights the translational potential of hBMSCs *in vitro* to investigate the osteotoxic and

osteoinductive potential of pharmaceutical mediators and xenobiotics present in the environment.

INTRODUCTION

Bone-related disorders represent a significant health concern among both developing and aging demographics. Skeletal dysplasias, typically diagnosed early in life, arise from mutations in genes responsible for patterning and growth of bone and cartilage structures and result in significant functional deficits during development (Krakow and Rimoin, 2010). Conversely, degenerative bone diseases such as osteopenia and osteoporosis involve a loss of bone mineral density and are more prevalent in elderly individuals (Briggs *et al.*, 2016), especially in industrialized countries where the aging demographic comprises an increasingly larger proportion of the population. Recent epidemiological studies have established that lower peak bone mineral content achieved during development is a contributing factor influencing loss of BMD (bone mineral density) and fracture risk later in life (Rizzoli *et al.*, 2010; McCormack *et al.*, 2017), thus illustrating the critical role of early osteogenesis in determining skeletal health throughout adulthood.

At the cellular level, osteoblasts are the key drivers of bone formation during development and later in maintaining skeletal homeostasis. (Long, 2011; Karsenty, 2008; Lian *et al.*, 2006). Osteoblasts are derived from multipotent mesenchymal stem cells (MSCs), which commit to pre-osteoblasts and differentiate further to form functionally mature osteoblasts. Osteoblast differentiation integrates a milieu of signaling mediators derived from canonical developmental pathways (WNT, FGF, BMP, Notch, and Hedgehog), which converge to influence the expression and/or activity of the "master" transcriptional regulators of osteoblastogenesis, runt-related transcription factor 2 (RUNX2) and osterix (OSX) (for review, see Jensen et al., 2010; Schroeder et al., 2005; Sinha and Zhou, 2013).

Following early differentiation events, osteoblasts secrete osteoid, or unmineralized bone ECM containing collagenous and non-collagenous proteins, which undergoes mineralization to form ossified bone with its characteristic mechanical and structural integrity. Alkaline phosphatase (ALP) plays a critical role during early stages of bone mineralization and is a well-recognized marker of osteogenic activity. ALP hydrolyzes extracellular pyrophosphate (ePP_i), an inhibitor of matrix mineralization, to inorganic phosphate (P_i) which complexes with extracellular calcium ions to form hydroxyapatite (HA) crystals (Golub and Boesze-Battaglia, 2007; Addison *et al.*, 2007). In addition to ALP activity, the composition of the bone ECM also plays an important role in osteoblast differentiation (M Baroncelli *et al.*, 2017). While collagenous proteins such as *collagen type 1 alpha 1* (*COL1A1*) comprise 80-90% of bone ECM, non-collagenous proteins also play a role regulating osteoid mineralization by serving as nucleation sites for HA crystal formation. Among these are o*steocalcin*/*bone gamma-carboxyglutamate protein* (*OSC/BGLAP*), *secreted protein acidic and cysteine rich*/*osteonectin* (*SPARC*), *osteopontin/secreted phosphoprotein 1* (*OPN/SPP1*), and *integrin-binding sialoprotein*/*bone sialoprotein 2* (*IBSP*/*BSP2*) (Komori, 2010; Sinha and Zhou, 2013; Rosset and Bradshaw, 2016; Staines *et al.*, 2012).

While the basic mechanisms underlying osteogenesis are generally well understood, there is increasing concern that exposure to environmental toxicants may alter the transcriptional networks governing osteoblast differentiation and bone growth (Holz *et al.*, 2007; Ryan *et al.*, 2007; Tyl *et al.*, 2007). Furthermore, given the multipotent nature of MSCs and their ability to differentiate into osteogenic, chondrogenic, or adipogenic lineages (Dominici *et al.*, 2006; Sheng, 2015), certain classes of toxicants may shunt MSC

differentiation to favor one lineage over another through disruption of key lineage determining drivers. For instance, the RXR agonist tributyltin (Watt and Schlezinger, 2015; Baker *et al.*, 2015) and the PPARγ agonist triphenyl phosphate (Pillai *et al.*, 2014), both promote adipogenic differentiation of MSCs in lieu of osteogenesis. As a result, deficits in osteoblast number and/or function may pose deleterious effects in developing individuals, or exacerbate loss of bone mineral content in aging individuals. Epidemiological studies also support a clear association between smoking and altered bone homeostasis and repair, evident by reduced BMD (Ward and Klesges, 2001), and increased risk of osteoporotic fractures and delayed fracture repair (Wong *et al.*, 2007; Yoon *et al.*, 2012; Sloan *et al.*, 2010) potentially due to the exposure to aryl hydrocarbon receptor (AhR) agonists present in tobacco.

The AnR is a basic-helix-loop-helix/Per-ARNT-Sim (bHLH-PAS) transcription factor and functions as a master regulator of drug metabolism and cellular pathways including cell proliferation, differentiation and apoptosis (Abel and Haarmann-Stemmann, 2010; Chopra and Schrenk, 2011). Many AhR agonists are highly persistence in the environment and result from anthropogenic sources including industrial waste byproducts (Pohl *et al.*, 1998), contaminated food (Fernández-González *et al.*, 2015), and cigarette smoke (Narkowicza *et al.*, 2013; Adams *et al.*, 1987). Of the AhR ligands, benzo[a]pyrene (BaP), polycyclic biphenyls (PCBs), and polychlorinated dibenzodioxins/dibenzofurans (PCDDs/PCDFs) have received the most attention based on their affinity for the AhR and reported toxicity to pathways involving cell proliferation, and growth and differentiation in multiple organ systems. In terms of skeletal development, the potent PCDD congener, 2,3,7,8-tetrachlorodibenzo-*p*-dioxin (TCDD) has demonstrated inhibition of adipogenic (Li *et al.*, 2008) and chondrogenic (Dong *et al.*, 2012;

Kung *et al.*, 2011) differentiation in both *in vivo* and *in vitro* model systems. However, despite numerous studies investigating TCDD toxicity to bone in rodent and select osteoblast cell models, no study has investigated the impact of TCDD on osteogenic differentiation of primary MSCs isolated from multiple human donors.

In the current study, we investigate the influence of TCDD on osteoblast differentiation in human bone-derived MSCs from three donors. Through assessments of MSC mineralization, gene expression and AhR inhibition, we demonstrate that AhR activation results in significant attenuation of intermediate and terminal stages of osteoblast differentiation. Results are consistent across multiple MSC donors irrespective of age, sex, or osteoporotic status.

MATERIALS AND METHODS

hBMSC Isolation and Characterization

Human bone fragments were obtained during elective procedures from three donors (Table 1) at the University of North Carolina-Chapel Hill hospitals (IRB exemption protocol: 10-0201). Human MSCs were isolated and characterized as described previously (Sakaguchi *et al.*, 2009; Charoenpanich *et al.*, 2014; Bodle *et al.*, 2014). Briefly, the bone fragments were washed in phosphate-buffered saline (PBS) containing 100 U/mL penicillin and 100 µg/mL streptomycin (Corning Inc.). The bone fragments were minced into approximately1 mm^3 cubes using a scalpel and digested in a 3 mg/ml collagenase XI solution (Sigma-Aldrich) on an orbital shaker for three hours at 37°C. The digest solution was filtered through a 100-µm cell strainer, centrifuged at 500 x *g* for five minutes to pellet the cells, and the cells were resuspended in growth medium (GM) comprised of minimal essential medium, α-modification (MEM-α, GE Healthcare) supplemented with 10% fetal bovine serum (FBS, Rocky Mountain Biologicals), 2 mM L-glutamine (Genesee Scientific), 100 U/mL penicillin, and 100 µg/mL streptomycin (Genesee Scientific). The cell suspension was plated and incubated overnight under standard cell culture conditions of 37°C at 5% CO_2 in a humidified incubator, henceforth referred to as "standard culture conditions". After 24 hours, the plates were rinsed with PBS to wash out the nonadherent cells and the media was replaced with fresh GM. Adherent cells were cultured until reaching 80% confluency, at which point they were trypsinized and frozen down at passage 0 (p0).

The proliferation and differentiation characteristics of hBMSC from each donor were assessed. At p0, hBMSCs from each donor were plated in 6-well tissue culture-treated plates

(Genesee Scientific) at a density of $0.6x10^4$ cells/cm^2 in GM. After 24 hours, the media was changed to either GM, adipogenic differentiation medium (ADM) comprised of α-MEM supplemented with 10% FBS, 2 mM L-glutamine, 100 U/mL penicillin and 100 µg/mL streptomycin, 1 µM dexamethasone (Sigma-Aldrich), 5 µg/mL h-insulin (Sigma-Aldrich), 100 µM indomethacin (Sigma-Aldrich), and 500 µM isobutylmethylxanthine (IBMX, Sigma-Aldrich) or osteogenic differentiation medium (ODM) comprised of α-MEM supplemented with 10% FBS, 2 mM L-glutamine, 100 U/mL penicillin, and 100 µg/mL streptomycin, 50 µM ascorbic acid (Sigma-Aldrich), 0.1 µM dexamethasone (Sigma-Aldrich), and 10 mM β-glycerophosphate (Sigma-Aldrich). Media was changed every three to four days for 14 days when cells were assessed for mineralization and lipid accumulation as terminal differentiation markers. Any hBMSC population with aberrant staining patterns (i.e. significant lipid accumulation in ODM, or significant calcium accretion in ADM) was excluded from the study.

TCDD Exposure

Frozen hBMSCs at p0 were revived and cultured in GM under standard culture conditions. hBMSCs between passages 3-6 were seeded into 6- or 12-well tissue culture treated plates (Genesee Scientific) at a density of $1x10^4$ cells/cm^2 in GM. After 24 hours, media was replaced with ODM or ADM to induce differentiation (day 0). For experiments assessing osteogenic differentiation, cells were cultured for up to 17 days in ODM containing one of the following treatments: 0.1% dimethyl sulfoxide (DMSO, vehicle control) (ODM-DMSO), 0.01-10 nM 2,3,7,8-tetrachlorodibenzo-*p*-dioxin (TCDD, Cambridge Isotopes Laboratory), (ODM-TCDD) 100 nM GNF351 (Sigma-Aldrich) (ODM-GNF), or 10 nM TCDD + 100 nM GNF351 (ODM-GNF+TCDD) dissolved in DMSO as a vehicle. For adipogenic assays, ADM-cultured

cells were treated with 0.1% DMSO (ADM-DMSO) or 10 nM TCDD (ADM-TCDD) for 24 days. Negative controls included cells cultured in 0.1% DMSO in GM (GM-DMSO). For all experiments, media was replaced every three to four days and cells were kept under standard culture conditions.

Cell Viability

Cell viability of hBMSCs cultured in GM and ODM dosed with TCDD was assessed using the Resazurin-based assay as previously described (Riss *et al.*, 2004). Positive controls containing 0.1% Triton X-100 were included for both GM and ODM plates. Briefly, cells were seeded into 96-well opaque-walled tissue culture plates at a density of $0.9x10^4$ cells/cm^2 in 100 µl of dosed media. At 24 and 48 hours post seeding, 20 µl of 0.15 mg/ml resazurin (pH 7.4, 0.2-µm filtered) was added to each well and plates were incubated for 2 hours under standard cell culture conditions. Fluorescence was measured in a FLUOstar spectrophotometer using 560nm/590nm excitation/emission parameters and cell viability was reported as a percentage normalized to DMSO-vehicle controls.

Mineralization Assays

Cell monolayers were stained with Alizarin Red S (AR-S) at 14-17 days post induction of differentiation (dpi) to label mineralized extracellular matrix. Briefly, cells were washed twice in PBS, fixed for 20 minutes in 10% neutral buffered formalin, washed twice with ddH2O, and stained for 15 minutes with 40 mM AR-S. Stained monolayers were washed 5 times in ddH_20 and representative wells were imaged using a Nikon SMZ1500 light microscope.

Additional wells run in parallel were used to quantify calcium accretion using the colorimetric-based Calcium (CPC) LiquiColor Assay (EKF Diagnostics-Stanbio Laboratory). After washing with PBS, 250 µL of 0.5 N HCl was added and the contents of each well were harvested by scraping. Samples were shaken at 500 rpm for 24-48 hours at 4^{o}C. Samples were centrifuged at 3000 x *g* for 3 minutes, and the supernatants were dispensed in a clear, flat-bottom 96-well plate. The colorimetric solution was added, and plates were incubated for 45 minutes. Absorbance was measured at 550 nm and total calcium content was derived from a standard curve using linear regression analysis. Calcium content was normalized to total protein concentration quantified using the Pierce BCA Protein Assay Kit (Thermo Scientific) from samples run in parallel. For each sample, absorbance was measured at 560 nm and protein concentrations were derived from a standard curve using linear regression analysis of known concentrations of bovine serum albumin.

Inorganic phosphate concentration was measured from the media at 17 dpi using the QuantiChrom^{TM} Phosphate Assay Kit (BioAssay Systems, Hayward, CA) according to the manufacturer's instructions. Briefly, media aliquots were diluted in ddH_2O, combined with reagent in a 96-well plate, and incubated at room temperature for 30 minutes. Absorbance was measured at 620 nm for all samples and phosphate concentration was derived from a standard curve of known concentrations using linear regression analysis.

Adipogenic Assays Measuring Lipid Accumulation

Cells were stained with Oil Red O and subsequently destained to assess adipogenesis in hBMSCs cultured in ODM and ADM. Cells were washed with PBS, fixed in 10% neutral buffered formalin for 30 min, and washed with ddH_2O twice. Wells were washed with 60%

isopropyl alcohol and then stained for 5 minutes in filtered Oil Red O staining solution composed of three parts 30 mg/ml Oil Red O in 100% isopropyl alcohol to two parts ddH_2O. Wells were washed with ddH_2O and imaged under light microscopy. To quantify lipid accumulation, wells were aspirated, allowed to dry, and de-stained via addition of 60% isopropyl alcohol. Absorbance of destain solution was measured at 500 nm and Oil Red O concentrations were determined from a standard curve measuring known Oil Red O standards.

Alkaline Phosphatase (ALP) Assays

Immunohistochemical staining for ALP was measured at 7 dpi using Blue Color AP Staining Kit. (Systems Biosciences). Cells were washed in PBS, fixed in 10% neutral buffered formalin, and incubated in substrate solution for 30 minutes. Next, cells were washed twice in PBS and imaged under light microscopy (Nikon SMZ1500) at 10X magnification. Alkaline phosphatase activity was measured using the Sensolyte® pNPP Alkaline Phosphatase Assay Kit (Anaspec). Briefly, cells were rinsed in assay buffer, scraped, and incubated under agitation for 10 minutes at 4^oC. Samples were centrifuged at 3000 x *g* for 10 minutes and supernatants were collected. In a 96-well plate format, 30 µl of p-nitrophenyl phosphate was added to each sample or standard in triplicate and incubated for 30 minutes at 37^0C. Absorbance was measured at 405 nm and ALP activity was derived from a standard curve using linear regression analysis from known ALP concentrations. For each sample, ALP activity was normalized to total protein concentration quantified as described above.

qPCR

The following qPCR methods were conducted in accordance with MIQE guidelines (Bustin *et al.*, 2009). hBMSC samples were lysed in TRI Reagent® (Ambion®, Life

Technologies) and total RNA was isolated according to the manufacturer's instructions. Total RNA was quantified using Agilent 2100 Bioanalyzer and 2100 Expert Software package (Agilent Technologies). RNAs with RNA Integrity numbers (RINs) lower than 9 were excluded. Next, cDNA was synthesized from 1 μg of total RNA using High Capacity cDNA Reverse Transcription Kit (Applied Biosystems) containing random primers, MultiScribe Reverse Transcriptase, RNase inhibitor, deoxynucleotide triphosphate mix, and 10X reverse transcription buffer in a 20 μl reaction. Human-specific real-time PCR primer sequences were designed in Primer3 or obtained from PrimerBank (Spandidos *et al.*, 2010) (Table 2) and procured from IDT (Integrated DNA Technologies). Primers sets were first tested to ensure efficient amplification of the target exon sequence. To quantify relative gene expression, cDNA from control and treated samples were PCR amplified in triplicate in 96-well PCR plates (Olympus Plastics, Genesee, San Diego, CA, USA) using an Applied Biosystems 7300 Real Time PCR System. Each 15 μl-reaction was comprised of 7.5 μl of SYBR® Green Real-Time PCR Master Mix (Life Technologies), 5.1 μl UltraPure Distilled H_2O (Life Technologies), 0.6 μl of 10 μM forward primer, 0.6 μl of 10 μM reverse primer, and 1.2 μl of cDNA. The conditions for each reaction were as follows: i) 50°C for two minutes, ii) 95°C for ten minutes, iii) 95°C for 15 seconds (s) followed by 60°C for 60 s, repeated 40x, and iv) 95°C for 15 s, 60°C for 60 s, 95°C for 15 s, and 60°C for 15 s to derive dissociation or melt curves and ensure specificity for each primer set used. Threshold cycle (C_t) values for each reaction were determined by the ABI 7300 software package and each gene was normalized to *RPL13A*, a previously validated reference gene in hBMSCs (Quiroz *et al.*, 2010), and relative gene expression was calculated according to the $\Delta\Delta C_t$ method (Livak and Schmittgen, 2001).

Statistical Analysis

Gene expression analyses comparing ODM-DMSO vs ODM-TCDD were analyzed using an unpaired, two-tailed Student's t-test. Comparisons between two or more conditions were analyzed using a One-Way Analysis of Variance (ANOVA) with a Tukey's posthoc test to determine significant differences between multiple conditions. For all statistical analyses, the threshold for significance was set to $\alpha=0.05$, and means with P-values less than 0.05 were deemed significant.

RESULTS

hBMSCs differentiate into osteoblasts under osteogenic conditions

Cytotoxicity was first assessed in TCDD-exposed hBMSCs cultured in GM and ODM at 24 and 48 hours post seeding. Compared to the 0.1% Triton X positive control, hBMSC cell viability was not impacted following exposure to 1 nM and 10 nM TCDD in GM or ODM assayed (Figure 1). Next, hBMSCs from each of three human donors (Table 1) were assessed to determine their osteogenic potential in the presence of GM-DMSO, ODM-DMSO, and ODM-TCDD. Following 17 days in culture, GM-DMSO cells were negative for Alizarin Red S (AR-S) staining, whereas ODM-DMSO cells demonstrated robust staining of mineralized hydroxyapatite, characteristic of differentiated osteoblasts irrespective of age, sex, or osteoporotic status (Table 1). TCDD-treated cells, despite the presence of ODM, displayed an overall attenuation of AR-S staining relative to cells cultured in ODM-DMSO across each donor (Figure 2A). Based on the composition of hydroxyapatite mineral, calcium, and inorganic phosphate (P_i) content were measured from Donor 1. In both assays, cells cultured in ODM displayed a significant accumulation of both calcium and P_i relative to GM, while TCDD-dosed cells, despite an increase relative to GM, experienced a significant, two-fold reduction relative to ODM-DMSO in each biochemical assay (Figure 2B, 2C).

Alkaline phosphatase was assayed at the transcript, enzymatic, and histochemical levels at 7 days post induction. Relative to GM, Donor 1 hBMSCs in ODM-DMSO demonstrated increased ALP immunohistochemical staining with a concomitant 3.2- and 3.4-fold induction in *ALP* expression and ALP activity, respectively. Treatment with TCDD, however, attenuated ALP staining and resulted in an overall 43% and 30% reduction in *ALP*

expression and ALP activity, respectively, when compared to ODM-DMSO hBMSCs (Figure 3).

Differential expression of a suite of osteogenic genes was next determined to assess the impact of TCDD treatment on hBMSC differentiation. A complete summary of gene expression data from Donors 1-3 at 3, 7, and 17 dpi can be found in Table 3. Of the early transcriptional regulators, *DLX5* expression was significantly attenuated with ODM-TCDD treatment at both early and intermediate (3 dpi and 7 dpi, respectively) stages of differentiation. Despite a reduction in *DLX5*, expression of *RUNX2* was elevated 1.4–2.1 fold at 7 dpi in all donors, and *OSX* remained unchanged in ODM-TCDD except for Donor 1 at 3 dpi (Figure 4A). Based on the role of FGF signaling in MSC differentiation (Baldridge *et al.*, 2010; Su *et al.*, 2008), expression of FGF ligands FGF2/9/18 was assessed at 3 and 7 dpi. TCDD exposure significantly induced expression of FGF9 and FGF18 at 3 and 7 dpi in all three donors with Donor 1 displaying the highest induction (Figure 4B). FGF2 was induced in ODM-TCDD cells at 7 dpi with less consistent expression patterns observed at 3 dpi. (Figure 4A, Table 3).

To assess intermediate and apical stages of differentiation, expression of ECM genes (*COL1A1*, *OSC*, *OPN*, *OGN*, *IBSP*, *SPARC*) was measured at 7 and 17 dpi based on their respective role in matrix mineralization. Across all donors, *OPN and osteoglycin* (*OGN*) demonstrated a two-fold or greater reduction in expression at both 7 and 17 dpi; conversely, *SPARC* was elevated 1.5-3.0 fold. Other genes revealed less consistent responses across both timepoints and donors. In Donor 1, *COL1A1* expression was not altered at 7 dpi in ODM-TCDD-treated hBMSCs, however by 17 dpi expression was significantly increased at 17 dpi when apical assays were conducted. *IBSP* was significantly attenuated at 7 dpi, however, by

17 dpi its expression was significantly higher than hBMSCs in ODM-DMSO (Figure 4C, Table 4).

AhR inhibition rescues TCDD-mediated inhibition of osteogenesis

Next, hBMSCs were examined to assess their responsiveness to AhR transactivation through assessment of select AhR gene markers. At 3 dpi, 10 nM TCDD significantly induced CYP1A1 expression (Figure 5A, Table 5) which was maintained throughout the duration of the experiment (Figure 5B, Table 5). Other AhR-responsive genes including *AHRR* and *TIPARP* displayed elevated expression throughout the experiment when compared to vehicle controls in ODM (Figure 5C, D, Table 5). To confirm that observed effects are mediated through AhR signaling, separate experiments in Donor 1 hBMSCs were repeated with 10 nM TCDD and/or 100 nM GNF351, a specific AhR antagonist (Smith *et al.*, 2011). At apical stages of differentiation, AR-S staining in ODM-TCDD wells was significantly reduced compared to ODM-DMSO controls (Figure 2A, 6A). Conversely, hBMSCs treated with either ODM-GNF alone or ODM-GNF+TCDD demonstrated positive AR-S staining more closely resembling ODM-DMSO controls (Figure 6A). Similarly, calcium content was significantly reduced in ODM-TCDD cells (Figure 6B) and partially rescued in cells with GNF351 co-exposure. At 3, 7, and 14 dpi, *CYP1A1* expression was significantly upregulated in ODM-TCDD cells; however, CYP1A1 expression was significantly lower in ODM-GNF+TCDD. Interestingly, cells treated with GNF351 alone demonstrated markedly lower expression of *CYP1A1*, albeit insignificant, relative to DMSO-treated cells (Figure 6C). To assess the impact of GNF351 on expression of osteogenic regulators, expression of both *DLX5* (3 dpi) and *OPN* (14 dpi), genes with attenuated expression across all three donors was assessed. Similar to CYP1A1 and

calcium deposition, co-incubation of TCDD and GNF351 rescued expression of DLX5 and OPN to near ODM-DMSO levels (Figure 6D, 6E). Taken together, these data suggest critical roles of *DLX5* during early differentiation and *OPN* during extracellular matrix synthesis and mineralization, but more importantly the ability of ligand-activated AhR to inhibit osteogenesis *in vitro.*

TCDD dysregulates adipogenic differentiation.

Based on the ability of TCDD to inhibit osteogenesis, the following experiments were conducted to determine whether TCDD-exposed hBMSCs favored adipogenic differentiation in lieu of osteogenic differentiation. hBMSCs from Donor 1 were exposed to TCDD in ODM and adipogenic differentiation media (ADM) and were stained with Oil Red O to assess lipid formation. By 24 dpi neither the ODM-DMSO nor ODM-TCDD-exposed hBMSCs were positive for lipid vacuole formation, however ADM-DMSO controls displayed positive Oil Red O staining. Although positive for Oil Red O, ADM-TCDD cells demonstrated an overall attenuated lipid accumulation (Figure 7A, B). Additionally, relative mRNA expression of adipogenic markers was measured for all treatments. hBMSCs cultured in ADM displayed significantly higher expression relative to hBMSCs cultured in either GM or ODM. *PPARγ*, a nuclear receptor responsible for promoting adipogenic differentiation (Kawai *et al.*, 2010; Rosen and MacDougald, 2006) was upregulated 6000-fold in ADM-DMSO relative to GM-DMSO. *C/EBPα*, another transcriptional regulator of adipogenesis, as well as the markers of differentiated adipocytes *PLIN1* and *FABP4* also demonstrated marked upregulation in ADM-DMSO controls relative to undifferentiated cells in GM-DMSO (Figure 7C). Despite a

reduction in lipid staining with ADM-TCDD, expression of adipose-related genes was not significantly reduced in ADM-TCDD.

TCDD treatment causes hBMSCs to retain expression of stemness genes

Based on previous experiments demonstrating inhibition of adipogenic and osteogenic programs, we next sought to determine whether TCDD-treated hBMSCs retained expression of markers associated with undifferentiated mesenchymal stromal cells. ODM-DMSO hBMSCs from Donor 1 demonstrate 3- to 8-fold downregulated expression of *NANOG*, *OCT4*, *SOX2*, and *SALL4*, previously validated markers of MSC stemness (Schönitzer *et al.*, 2014) compared to cells in GM at 17 dpi (Figure 8, Table 6). hBMSCs cultured in the presence of both ODM and TCDD, however, demonstrate significantly higher expression of stemness related gene markers that is more similar to hBMSCs cultured in GM (Figure 8, Table 6), suggesting that these cells may remain in an undifferentiated phenotype subsequent to AHR transactivation by TCDD.

DISCUSSION

Osteoblasts and their mesenchymal stem cell progenitors are sensitive targets to exposure to chemical agents in the environment (Holz *et al.*, 2007). In the current study, we demonstrate TCDD-mediated inhibition of osteogenic and adipogenic differentiation of hBMSCs isolated from multiple donors of varying age, sex, and osteoporotic status. With the addition of ODM, hBMSCs were assessed for hallmarks of osteogenesis at early (3 dpi), intermediate (7 dpi), and apical (17 dpi) stages of differentiation. Relative to vehicle controls, TCDD altered the expression of osteogenic regulators (*DLX*, *RUNX2*, *FGF2/9/18*) and ECM markers (*OSC*, *OPN*, *IBSP*, *OSC*, *SPARC*), alkaline phosphatase activity, and the formation of mineralized bone nodules in human mesenchymal cells which together suggest that TCDD is a potent inhibitor of osteoblast differentiation. To the author's knowledge, this is the first study to demonstrate TCDD's inhibitory role in osteogenesis using hBMSCs from multiple donors of varying age, sex, and osteoporotic status.

Mesenchymal stromal cells (MSCs), which contain multipotent stem cells, retain the ability for self-renewal and/or differentiate into a variety of mesenchymal lineages, including osteoblasts (bone cells), chondrocytes (cartilage cells), and adipocytes (fat cells). Both self-renewal and differentiation of MSCs are governed through strict cross-talk between master transcriptional regulators that govern cell differentiation. An emergent theme suggests that exogenous exposures of MSCs to environmental agents may shunt these regulatory networks that coordinate the balance of MSC commitment towards defined mesenchymal lineages. Notable examples include the flame retardant Firemaster® 550 and its organophosphate constituent triphenyl phosphate (Pillai *et al.*, 2014), tributyltin (Baker *et al.*, 2015), and

thiazolinediones (e.g. Rosiglitazone) (van de Vyver *et al.*, 2014; Benvenuti *et al.*, 2007), which promote adipogenic over osteogenic differentiation in MSCs

To address whether TCDD causes hBMSCs to undergo adipogenic in lieu of osteogenic differentiation, we assessed adipogenic differentiation in hBMSCs cultured in ODM and ADM. When assessed at 24 dpi, we observed that neither DMSO- nor TCDD-treated hBMSCs in ODM formed lipid or induced expression of previously established adipose-related genes (*PPARγ*, *C/EBPα, FABP4*, *PLIN1*) (Kawai *et al.*, 2010; Rosen and MacDougald, 2006) to the same degree as hBMSCs in ADM. Noteworthy, however, is the modest induction of *PPARγ* and *C/EBPα* in ODM-treated cells relative to the undifferentiated controls in GM. This induction may reflect the presence of dexamethasone, a glucocorticoid receptor agonist and component of both ODM (0.1 μM) and ADM (1 μM), which has been shown to induce expression of *PPARγ* and *C/EBPα* (Sargis *et al.*, 2009). We additionally cultured MSCs in ADM to illustrate their potential to induce an adipogenic program. At 24 dpi we observed that hBMSCs cultured in ADM-DMSO readily formed lipid and induced expression of adipogenic markers. Conversely, hBMSCs cultured in ADM-TCDD exhibited a significant attenuation in lipid formation, whereas adipose-related genes were unchanged relative to ADM-DMSO cells. These findings are consistent with previous studies that demonstrate the ability of TCDD and other AHR-ligands to inhibit adipogenic differentiation from MSCs (Podechard *et al.*, 2009; Li *et al.*, 2008) and other preadipocyte models (e.g. 3T3-L1) (Shimba *et al.*, 2001; Liu *et al.*, 1996). Together, our data suggests that rather than shunt hBMSC differentiation from osteogenic to adipogenic lineages, TCDD appears to inhibit differentiation of both pathways in our model of hBMSC differentiation.

TCDD and other AHR ligands have previously been shown to target differentiation of multiple cell types of various developmental origins including hematopoietic stem cells (Singh *et al.*, 2009; Murante and Gasiewicz, 2000), cardiomyocytes (Wang *et al.*, 2010), chondrocytes (Dong *et al.*, 2012; Kung *et al.*, 2011; Yang and Lee, 2010), and adipocytes (Li *et al.*, 2008; Liu *et al.*, 1996; Shimba *et al.*, 2001). Our findings of reduced ALP activity and attenuated mineralization confirm results from other studies that demonstrate AHR-mediated inhibition in rat and mouse MSCs or pre-osteoblasts *in vitro* (Ryan *et al.*, 2007; Naruse *et al.*, 2002; Carpi *et al.*, 2009; Korkalainen *et al.*, 2009; Herlin *et al.*, 2015). Consistent with an inhibitory role on osteogenesis, TCDD exposure in rodent models is demonstrated to adversely impact bone size, geometry, and biomechanical strength (Jämsä *et al.*, 2001; Herlin *et al.*, 2010). Specifically, rodents developmentally exposed to TCDD display delayed ossification and attenuated bone mineral density (Miettinen *et al.*, 2005; Finnilä *et al.*, 2010). TCDD has also been shown to disrupt osteogenesis in phylogenetically distant species indicating a conservation in AhR targets. Japanese medaka exposed during embryonic development demonstrate altered vertebral ossification and morphology with concomitant attenuation of OSX and RUNX2 as larvae (Watson *et al.*, 2017). Similarly, embryonic exposure to TCDD results in scoliosis and malformed vertebrae in adult zebrafish (Baker *et al.*, 2014, 2013), thus suggesting a consistent phenotype across evolutionarily divergent mammalian and teleost species.

The precise role of the AHR in normal bone development remains controversial despite its inhibitory role in osteogenesis when activated by exogenous AHR ligands. In the present study, treatment with the AHR antagonist GNF351 demonstrated a partial rescue of TCDD-

mediated osteogenic inhibition, while GNF351 alone appeared to slightly enhance mineralization and induce OPN expression. Our findings suggest that in hBMSCs, TCDD-mediated inhibition is indeed AHR-specific, and that the AHR may play a role as a negative mediator in osteogenesis. AHR may also have a normal role in osteogenesis with a progressive increase in *AHR* expression during osteoblastogenesis *in vitro* (Ryan et al., 2007). *In vivo*, AHR-null mice demonstrate an altered bone phenotype despite an overall phenotypic rescue from the more severe TCDD-mediated effects in wildtype mice (Herlin *et al.*, 2013) also suggesting that the AHR may have a normal role in bone formation.

Apical stages of osteogenic differentiation appear to be particularly susceptible to TCDD exposure. At 17 dpi we demonstrated that TCDD attenuates matrix mineralization based on attenuated AR-S staining, calcium accretion, and inorganic phosphate content. While bone ECM composition is a critical determinant of bone structural integrity, it also can differentially promote osteogenic differentiation of BMSCs *in vitro*. A recent study demonstrated that BMSCs cultured on ECM from differentiated osteoblasts displayed a marked increase in osteogenic differentiation relative to BMSCs cultured on ECM from undifferentiated cells (M Baroncelli *et al.*, 2017). In addition to ECM synthesis and matrix mineralization, our data also suggests that TCDD alters the expression of early osteogenic regulators. *DLX5*, whose expression *in vitro* is associated with osteogenic potential of BMSCs (Heo *et al.*, 2015) was significantly attenuated in TCDD-treated BMSCs from all donors at early and intermediate stages of differentiation. DLX5 is a key upstream regulator of both *OSX* and *RUNX2* within the BMP pathway (Lee *et al.*, 2003, 2005). However, in this study we did not observe a consistent alteration in either *OSX* or *RUNX2* between BMSC donors.

Alternatively, the inconsistency in *OSX* and *RUNX2* expression may reflect the differences in osteogenic potential associated with age, sex, and genotype of each donor (Siegel *et al.*, 2013), e.g. differences in AHR alleles, impacting individual responsiveness as previously demonstrated in rodents (Miettinen *et al.*, 2005; Jämsä *et al.*, 2001; Herlin *et al.*, 2010). Only Donor 1 demonstrated reduced expression of *OSX*, whereas *RUNX2* was induced in TCDD-treated cells from all donors at 7 dpi. One potential explanation for this observation is the attenuated expression of *TWIST1* at 3 dpi in all donors. A reduction of *TWIST1*, an upstream repressor of RUNX2 activity (Bialek *et al.*, 2004), may contribute to elevated expression of *RUNX2*.

In addition to altered DLX5 and RUNX2 expression, TCDD significantly altered the expression of a number of FGF genes which play critical roles in bone and cartilage development (Ornitz and Marie, 2015). TCDD-induced expression of *FGF2*, *FGF9*, and *FGF18* expression at three and seven days post induction followed by inhibition of matrix mineralization markers. Treatment of adenocarcinoma cells with BaP has previously been shown to induce FGF9 expression (Wang *et al.*, 2009), however this study is the first to identify FGF2/9/18 induction by TCDD in human BMSCs. Other studies, however, report similar phenotypic and transcriptional inhibitory responses with FGF9 overexpression in human BMSCs, dental pulp stem cells, and calvaria-derived MSCs (Lu *et al.*, 2014, 2015). This effect may be stage- or time-dependent, however, as FGF2 and FGF9 treatment enhances differentiation of osteoblasts but inhibits differentiation of osteoblast progenitors. (Fakhry *et al.*, 2005). FGF2 signaling has also been demonstrated to inhibit the Wnt pathway through

binding and inhibition of β-catenin activity *in vitro* (Mansukhani *et al.*, 2005), further establishing the potential inhibitory role in osteogenic inhibition.

Given FGFs putative role in maintaining osteoblast progenitors, we further expanded our gene expression analysis to assess whether markers of pluri-/multipotency were affected by TCDD exposure. *SOX2*, *OCT4*, *NANOG*, and *SALL4* demonstrated consistent expression patterns at 17 dpi with untreated cells in ODM-DMSO displaying a significant loss in expression, and ODM-TCDD treated cells displaying expression profiles more closely resembling undifferentiated cells in GM. Together these genes work in concert to control potency in embryonic stem cells (Wang *et al.*, 2010, 2012), yet these factors also play a critical role in maintaining proliferative capacity and self-renewal of mesenchymal stem cells (Riekstina *et al.*, 2009; Siegel *et al.*, 2013; Greco *et al.*, 2007; Schönitzer *et al.*, 2014). Overexpression of SOX2 inhibits osteogenic differentiation of hMSCs *in vitro* through inhibition of the Wnt signaling pathways (Ding *et al.*, 2012; Seo *et al.*, 2011; Greco *et al.*, 2007; Mansukhani *et al.*, 2005). Furthermore, *SOX2* induction is governed in part by FGF-FGFR signaling suggesting a potential link between TCDD-mediated FGF induction and maintenance of stemness markers. Further investigation is required, however, to determine whether these patterns represent the cause of TCDD-mediated repression or simply reflect a less differentiated state in TCDD-treated cells. Alternatively, the observed trends in *SOX2*, *NANOG*, and *OCT4* expression may be due to dysregulation of the epigenetic modifiers responsible for promoting lineage specification in these cells. Recent studies demonstrate an increasingly larger role for histone methylase/demethylases, histone acetylases/deaacetylases, long non-coding RNAs (lncRNAs) and microRNAs (miRs) in affecting expression of essential

osteogenic regulators (Gennari *et al.*, 2016; Wu *et al.*, 2017; Gordon *et al.*, 2015). It is plausible that AhR ligands may repress osteogenic differentiation through modulating gene expression of any number of these epigenetic regulators.

In conclusion, we demonstrate that TCDD alters osteogenic differentiation in hBMSCs from multiple donors. AhR ligands, such as those in tobacco smoke, are ubiquitous in the environment, and exposures are associated with several adverse skeletal outcomes including reduced bone mineral density (Ward and Klesges, 2001; Lorentzon *et al.*, 2007), increased fracture risk and delayed fracture repair (Kanis *et al.*, 2005; Law and Hackshaw, 1997), and increased risk of osteoporosis and rheumatoid arthritis (Klareskog *et al.*, 2007; Lee *et al.*, 2013). It is possible that AhR signaling may alter the differentiation of MSCs into bone-forming osteoblasts, and thus play a mechanistic role in the etiology of degenerative bone diseases. We further highlight the possibility of using mesenchymal stem cells as an *in vitro* tool to screen chemicals suspected of dysregulating or enhancing osteogenic, adipogenic, or chondrogenic differentiation.

TABLES

Table 1. Age, sex, and osteoporotic status of hBMSC donors 1-3 used for osteogenic and adipogenic (only Donor 1) experiments.

Donor	Sex	Age (y)	Osteoporosis
1	Female	25	No
2	Male	64	No
3	Female	95	Yes

Table 2. Primer sequences used for qPCR analysis of AhR-responsive, osteogenic, adipogenic, and mesenchymal and/or stemness markers. S= sense, A= antisense, bp= base pair. Primer efficiencies were conducted for each gene-specific primer using a range of cDNA dilutions from 0.1 to 10 ng/ul. Cycle threshold (C_t) values were plotted against log(cDNA) concentrations, and "Percent Efficiency" was calculated using the following equation,

$$\% \, Efficiency = [[(Dilution \; factor)^{(\frac{1}{-slope})}] - 1] \; \times 100$$

where the dilution factor is 10, and the slope is based on a linear regression trendline. Primers with % efficiencies between 90-110% were used.

Gene	NCBI Accession ID	Primer Sequence (5'→ 3')	Amplicon Length (bp)
RPL13A	NM_012423.3	S: CTATGACCAATAGGAAGAGCAACC	121
		A: GCAGAGTATATGACCAGGTGGAA	
CYP1A1	NM_000499.4	S: CACCATCCCCCACAGCAC	74
		A: ACAAAGACACAACGCCCCTT	
AHRR	NM_020731.4	S: AGAAGTCCAACCCCTCCAAG	93
		A: GATGATGTCAGGCGGGAAC	
TIPARP	NM_001184717.1	S: GGTTCCCACACAAGCTCCTC	131
		A: GGATGAAGTCCTGAGATGGATG	
SOX2	NM_003106.3	S: GCCGAGTGGAAACTTTTGTCG	155
		A: GGCAGCGTGTACTTATCCTTCT	
OCT4	NM_002701.5	S: AGAGGATTTTGAGGCTGCTG	108
		A: GTGAAGTGAGGGCTCCCATA	
NANOG	NM_024865.3	S: TTTGTGGGCCTGAAGAAAACT	116
		A: AGGGCTGTCCTGAATAAGCAG	
SALL4	NM_020436.4	S: CAGGGATGACCCCTTTGTTA	95
		A: AGCGCTAGCAGACGAGAAGT	
FGF9	NM_002010.2	S: CAGGCGGAGGCAGCTATAC	76
		A: CCTGGTTCCCTGGATAGTACC	
FGF18	NM_003862.2	S: ACTTGCCTGTGTTTACACTTCC	180
		A: GACCTGGATGTGTTTCCCACT	
MSX2	NM_002449.4	S: TGCAGAGCGTGCAGAGTTC	144
		A: GGCAGCATAGGTTTTGCAGC	
TWIST1	NM_000474.3	S: CCAGGTACATCGACTTCCTCTA	120
		A: CCATCCTCCAGACCGAGAA	
DLX5	NM_005221.5	S: CGCTAGCTCCTACCACCAGT	83
		A: GGCTCGGTCACTTCTTTCTC	
RUNX2	NM_001024630.3	S: TGGTTACTGTCATGGCGGGTA	101
		A: TCTCAGATCGTTGAACCTTGCTA	

Table 2 Continued.

OSX	NM_001173467.2	S: GCCAGAAGCTGTGAAACCTC	151
		A: TCTCCATAACCATGGCAACA	
ALP	NM_000478.5	S: ATGAAGGAAAAGCCAAGCAG	102
		A: CCACGGTCAGAGTGTCTTCC	
COL1A1	NM_000088.3	S: ACGTCCTGGTGAAGTTGGTC	172
		A: ACCAGGGAAGCCTCTCTCTC	
OSC	NM_199173.5	S: GGCGCTACCTGTATCAATGG	111
		A: GTGGTCAGCCAACTCGTCA	
OPN	NM_001040058.1	S: GGACATCACCTCACACATGG	154
		A: GTGGGTTTCAGCACTCTGGT	
IBSP	NM_004967.3	S: GGGCAGTAGTGACTCATCCG	125
		A: TCAGCCTCAGAGTCTTCATCTTC	
SPARC	NM_004598.3	S: CCCAACCACGGCAATTTCCTA	93
		A: ATCGTCTCGAAAGCGGTTCC	
OGN	NM_033014.3	S: CTACTTGGACCATAATGCCCTG	142
		A: GTCCCGGATGTAACTGGTGTC	
PPARγ	NM_015869.4	S: GATACACTGTCTGCAAACATATCACAA	246
		A: CCACGGAGCTGATCCCAA	
C/EBPα	NM_001287435.1	S: AAGAAGTCGGTGGACAAGAACAG	69
		A: TGCGCACCGCGATGT	
PLIN1	NM_002666	S: TGTGCAATGCCTATGAGAAGG	154
		A: AGGGCGGGGATCTTTTCCT	
FABP4	NM_001442.2	S: TACTGGGCCAGGAATTTGAC	180
		A: GTGGAAGTGACGCCTTTCAT	

Table 3. qPCR assessment of transcriptional regulators of osteoblast differentiation from Donors 1-3 at 3 and 7 days post induction of osteogenic differentiation. Values represent mean ± SEM normalized fold change (n=3-7) relative to DMSO vehicle controls. Bolded values indicate significant induction or inhibition of gene expression with 10 nM TCDD ($p<0.05$, Students T-test).

	3 days post induction					
	Donor 1, 25y/o, F		Donor 2, 64 y/o, M		Donor 3, 95 y/o, F	
Gene	ODM	ODM + TCDD	ODM	ODM + TCDD	ODM	ODM + TCDD
TWIST1	1 ± 0.06	**0.65 ± 0.09**	1 ± 0.05	**0.77 ± 0.05**	1 ± 0.07	**0.73 ± 0.03**
MSX2	1 ± 0.07	1.1 ± 0.07	1 ± 0.05	1.15 ± 0.15	1 ± 0.09	0.81 ± 0.04
DLX5	1 ± 0.07	**0.44 ± 0.08**	1 ± 0.04	**0.74 ± 0.02**	1 ± 0.04	0.55 ± 0.01
RUNX2	1 ± 0.05	**1.31 ± 0.15**	1 ± 0.02	**1.66 ± 0.06**	1 ± 0.09	**1.13 ± 0.02**
OSX	1 ± 0.05	**0.73 ± 0.13**	1 ± 0.07	**0.95 ± 0.07**	1 ± 0.18	**0.99 ± 0.09**
FGF2	1 ± 0.15	1 ± 0.11	1 ± 0.15	**2.3 ± 0.68**	1 ± 0.11	1 ± 0.08
FGF9	1 ± 0.12	**3.11 ± 0.59**	1 ± 0.03	2.67 ± 0.06	1 ± 0.09	1.23 ± 0.07
FGF18	1 ± 0.13	**2.38 ± 0.24**	1 ± 0.04	1.78 ± 0.02	1 ± 0.03	1.36 ± 0.02

	7 days post induction					
	Donor 1, 25y/o, F		Donor 2, 64 y/o, M		Donor 3, 95 y/o, F	
Gene	ODM	ODM + TCDD	ODM	ODM + TCDD	ODM	ODM + TCDD
TWIST1	1 ± 0.03	**0.85 ± 0.1**	1 ± 0.02	**0.77 ± 0.03**	1 ± 0.04	1.07 ± 0.05
MSX2	1 ± 0.02	1.01 ± 0.07	1 ± 0.09	**1.4 ± 0.03**	1 ± 0.06	**1.51 ± 0.09**
DLX5	1 ± 0.05	**0.8 ± 0.02**	1 ± 0.09	**0.67 ± 0.09**	1 ± 0.08	**0.71 ± 0.03**
RUNX2	1 ± 0.03	**1.39 ± 0.13**	1 ± 0.02	**1.92 ± 0.04**	1 ± 0.08	**2.1 ± 0.07**
OSX	1 ± 0.06	**0.74 ± 0.04**	1 ± 0.02	1.02 ± 0.03	1 ± 0.06	**1 ± 0.04**
FGF2	1 ± 0.11	**2.2 ± 0.65**	1 ± 0.07	**1.1 ± 0.09**	1 ± 0.03	**1.1 ± 0.02**
FGF9	1 ± 0.13	**11.02 ± 1.87**	1 ± 0.05	8.73 ± 0.52	1 ± 0.05	1.38 ± 0.08
FGF18	1 ± 0.09	**2.52 ± 0.34**	1 ± 0.03	2.62 ± 0.12	1 ± 0.06	1.56 ± 0.07

Table 4. qPCR assessment of osteoblast-specific ECM markers from Donors 1-3 at 7 and 17 days post induction of osteogenic differentiation. Values represent mean ± SEM normalized fold change (n=3-7) relative to DMSO vehicle controls. Bolded values indicate significant induction or inhibition of gene expression with 10 nM TCDD ($p<0.05$, Students T-test).

	7 days post induction					
	Donor 1, 25y/o, F		Donor 2, 64 y/o, M		Donor 3, 95 y/o, F	
Gene	ODM	ODM + TCDD	ODM	ODM + TCDD	ODM	ODM + TCDD
COL1A1	1 ± 0.02	0.94 ± 0.07	1 ± 0.02	0.92 ± 0.01	1 ± 0.08	0.7 ± 0.04
IBSP	1 ± 0.17	**0.21 ± 0.02**	1 ± 0.05	**0.49 ± 0.07**	1 ± 0.15	**0.72 ± 0.03**
OPN	1 ± 0.06	**0.4 ± 0.06**	1 ± 0.06	**0.65 ± 0.05**	1 ± 0.09	**0.5 ± 0.06**
OSC	1 ± 0.06	1.02 ± 0.07	1 ± 0.04	0.86 ± 0.05	1 ± 0.08	1.1 ± 0.01
OGN	1 ± 0.07	**0.66 ± 0.08**	1 ± 0.11	**0.5 ± 0.07**	1 ± 0.03	0.65 ± 0.08
SPARC	1 ± 0.06	**1.72 ± 0.08**	1 ± 0.03	**1.59 ± 0.01**	1 ± 0.03	**1.4 ± 0.03**

	17 days post induction					
	Donor 1, 25y/o, F		Donor 2, 64 y/o, M		Donor 3, 95 y/o, F	
Gene	ODM	ODM + TCDD	ODM	ODM + TCDD	ODM	ODM + TCDD
COL1A1	1 ± 0.16	**4.7 ± 0.46**	1 ± 0.05	0.93 ± 0.17	1 ± 0.1	0.92 ± 0.05
IBSP	1 ± 0.14	**15.5 ± 0.78**	1 ± 0.08	**0.25 ± 0.05**	1 ± 0.06	**0.37 ± 0.12**
OPN	1 ± 0.05	**0.34 ± 0.05**	1 ± 0.14	**0.35 ± 0.05**	1 ± 0.14	**0.67 ± 0.07**
OSC	1 ± 0.03	**0.41 ± 0.01**	1 ± 0.08	0.72 ± 0.06	1 ± 0.08	**1.34 ± 0.13**
OGN	1 ± 0.07	**1.71 ± 0.16**	1 ± 0.06	0.88 ± 0.16	1 ± 0.18	**0.67 ± 0.03**
SPARC	1 ± 0.06	**3.1 ± 0.3**	1 ± 0.06	**1.99 ± 0.15**	1 ± 0.09	**1.54 ± 0.15**

Table 5. qPCR assessment of AhR target genes from Donors 1-3 at 3, 7, and 17 days post induction of osteogenic differentiation. Values represent mean ± SEM normalized fold change (n=3-7) relative to DMSO vehicle controls. Bolded values indicate significant induction or inhibition of gene expression with 10 nM TCDD ($p<0.05$, Students T-test).

	3 days post induction					
	Donor 1, 25y/o, F		Donor 2, 64 y/o, M		Donor 3, 95 y/o, F	
Gene	ODM	ODM + TCDD	ODM	ODM + TCDD	ODM	ODM + TCDD
CYP1A1	1 ± 0.19	**59.6 ± 2.63**	1 ± 0.03	**237 ± 15.9**	1 ± 0.03	**20.4 ± 0.69**
TIPARP	1 ± 0.12	**3.1 ± 0.17**	1 ± 0.01	**1.9 ± 0.12**	1 ± 0.02	**1.6 ± 0.04**
AHRR	1 ± 0.09	**3.9 ± 0.09**	1 ± 0.05	**2.6 ± 0.28**	1 ± 0.05	**2 ± 0.08**

	7 days post induction					
	Donor 1, 25y/o, F		Donor 2, 64 y/o, M		Donor 3, 95 y/o, F	
Gene	ODM	ODM + TCDD	ODM	ODM + TCDD	ODM	ODM + TCDD
CYP1A1	1 ± 0.11	**141 ± 11.6**	1 ± 0.06	**246 ± 24.9**	1 ± 0.16	**263 ± 0.2**
TIPARP	1 ± 0.11	**2.9 ± 0.06**	1 ± 0.04	**2.9 ± 0.25**	1 ± 0.04	**2.87 ± 0.22**
AHRR	1 ± 0.1	**4.6 ± 0.13**	1 ± 0.1	**3.11 ± 0.16**	1 ± 0.09	**3.17 ± 0.2**

	17 days post induction					
	Donor 1, 25y/o, F		Donor 2, 64 y/o, M		Donor 3, 95 y/o, F	
Gene	ODM	ODM + TCDD	ODM	ODM + TCDD	ODM	ODM + TCDD
CYP1A1	1 ± 0.03	**447 ± 25.3**	1 ± 0.05	**287 ± 26.2**	1 ± 0.25	**65.9 ± 6.56**
TIPARP	1 ± 0.08	**3.8 ± 0.14**	1 ± 0.07	**1.1 ± 0.36**	1 ± 0.12	**3.6 ± 0.69**
AHRR	1 ± 0.05	**3.8 ± 0.05**	1 ± 0.07	**2.9 ± 0.35**	1 ± 0.13	**2.7 ± 0.26**

Table 6. qPCR assessment of MSC and/or stemness-related genes in Donors 1-3 at 17 days post induction of osteogenic differentiation. Values represent the mean ± SEM normalized fold change from 3-8 technical replicates relative to DMSO-treated hMBSCs in GM. Statistical analyses was conducted using One-Way ANOVA with a Tukey post hoc test; *a*, $p<0.05$ when compared to GM, *b*, $p<0.05$ when compared to ODM.

	17 days post induction								
	Donor 1 , 25 y/o, F			Donor 2, 64 y/o, M			Donor 3, 95 y/o, F, OP		
Gene	GM	ODM	ODM + TCDD	GM	ODM	ODM + TCDD	GM	ODM	ODM + TCDD
SOX2	1 ± 0.04	0.23 ± 0.01[a]	0.72 ± 0.02[a,b]	1 ± 0.08	0.39 ± 0.01[a]	0.78 ± 0.11[b]	1 ± 0.16	0.65 ± 0.05[a]	1.13 ± 0.04[b]
OCT4	1 ± 0.03	0.62 ± 0.12[a]	1.02 ± 0.03[b]	1 ± 0.08	1.16 ± 0.14	1.22 ± 0.25	1 ± 0.21	0.63 ± 0.06	0.78 ± 0.08
NANOG	1 ± 0.03	0.49 ± 0.1[a]	0.87 ± 0.08[b]	1 ± 0.15	0.99 ± 0.08	1.17 ± 0.13	1 ± 0.1	0.49 ± 0.08[a]	0.63 ± 0.1[b]
SALL4	1 ± 0.08	0.13 ± 0.02[a]	0.69 ± 0.05[a,b]	1 ± 0.07	0.29 ± 0.03[a]	0.7 ± 0.05[a,b]	1 ± 0.11	0.2 ± 0.04[a]	0.38 ± 0.07[a]

FIGURES

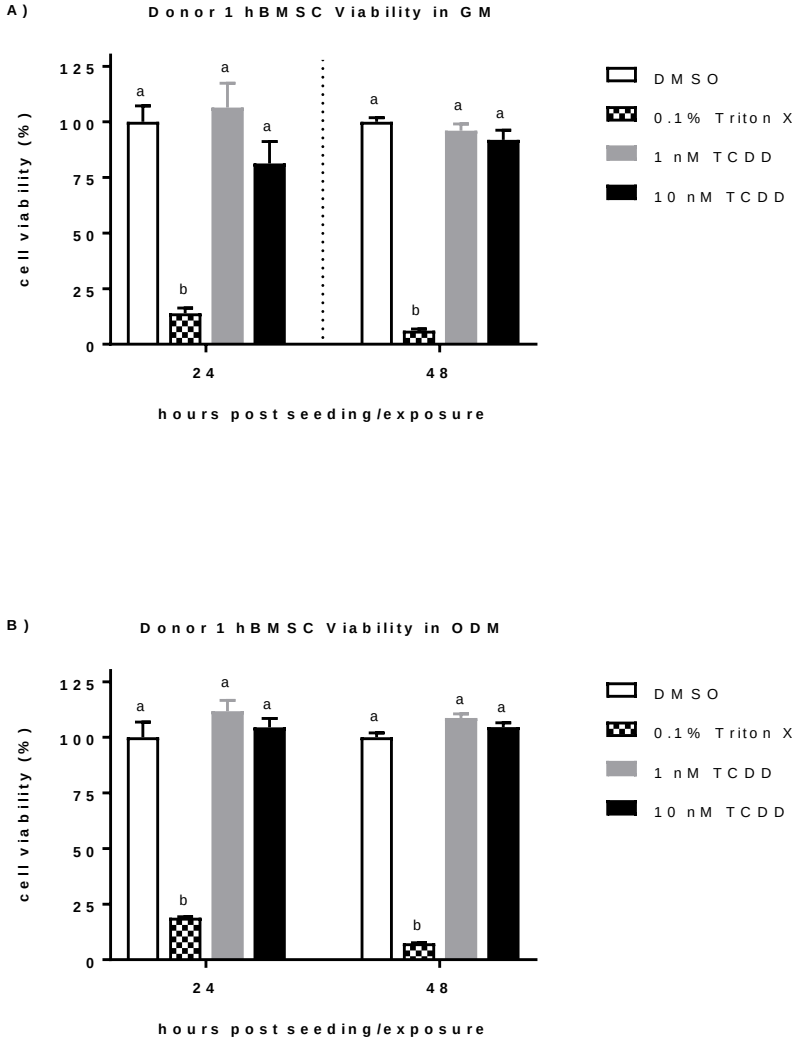

Figure 1. Resazurin cell viability assay in growth media (A) and osteogenic differentiation media (B). For each treatment, percent cell viability is normalized to DMSO-treated controls. Letters denote statistical significance between groups ($p<0.05$, One-Way ANOVA); bars represent the mean ± SEM.

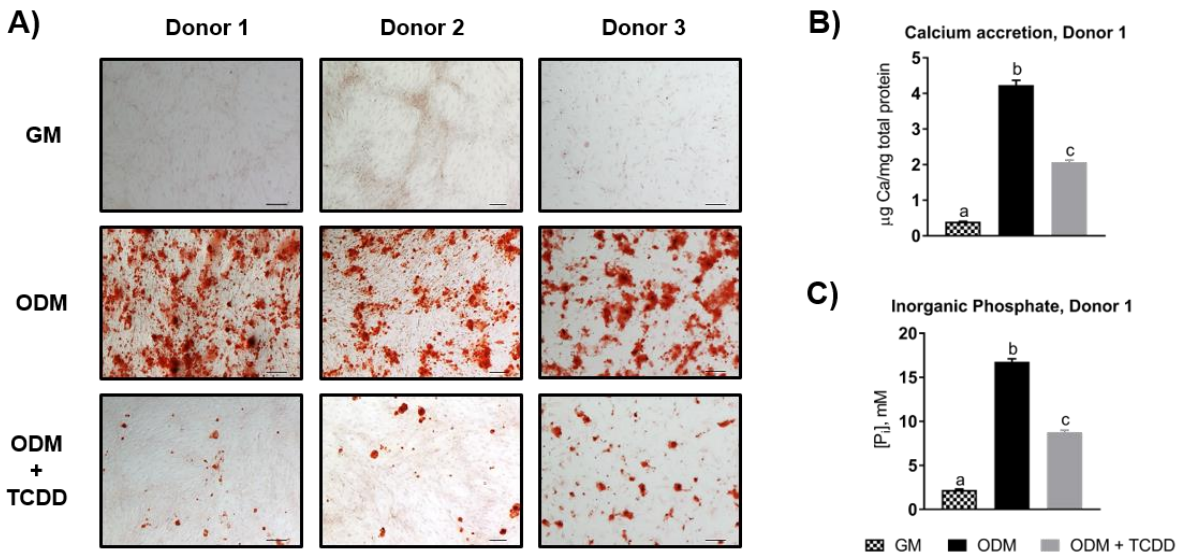

Figure 2. Apical assessment of osteogenic mineralization in hBMSCs. (A) Alizarin Red S staining was conducted at 17 dpi in hBMSCs cultured in GM, ODM, and ODM + TCDD from all three donors assayed. Calcium and inorganic phosphate (P_i) were measured in (B) and (C), respectively, as constituents of hydroxyapatite mineral. Calcium accretion for each sample was normalized to total protein, and inorganic phosphate was from media (n=4/endpoint). Bars in (B) and (C) represent mean ± SEM; letters in denote statistical significance between groups ($p<0.05$, One-Way ANOVA and Tukey's Post hoc test), and scale bars in (A) denote 200 µm.

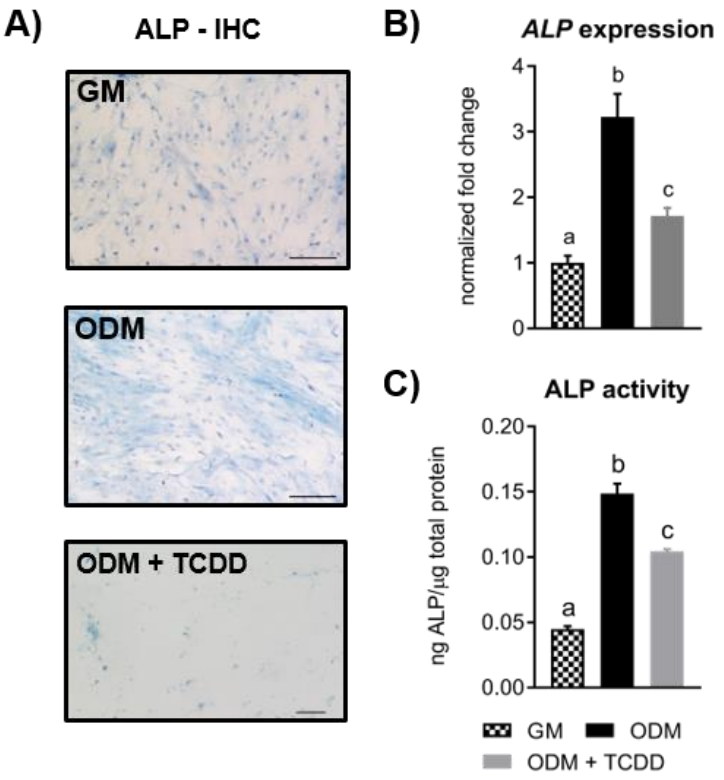

Figure 3. Alkaline phosphatase (ALP) assessment in Donor 1 hBMSCs. Immunohistochemical staining for ALP (A), mRNA expression (B), and ALP enzymatic activity (C) were conducted at 7 dpi. Scale bars in (A) represent 200 µm, images at 5X magnification. Bars in (B) and (C) represent mean ± SEM; letters denote statistical significance between groups as determined by One-Way ANOVA and Tukey's post hoc test ($p<0.05$).

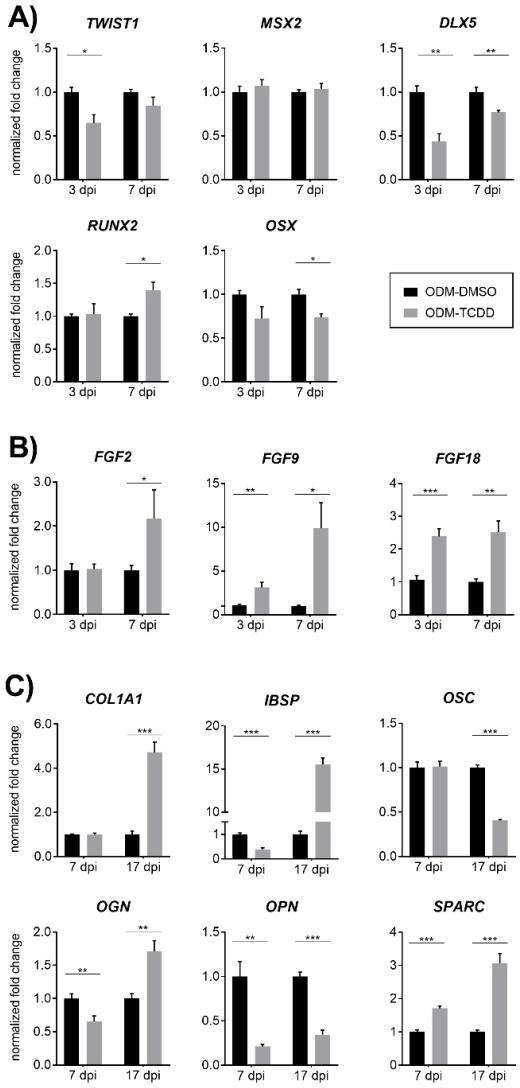

Figure 4. qPCR assessment of Donor 1 hBMSCs cultured in ODM. Osteogenic markers were measured for (A) transcriptional regulators at 3 and 7 dpi, and (B) ECM markers at 7 and 17, and were normalized to DMSO-treated cells in ODM. Bars represent normalized fold change relative to *RPL13A* expression, a previously validated housekeeping gene in hBMSCs (Quiroz *et al.*, 2010); asterisks denote statistical significance between DMSO and 10 nM TCDD groups at each timepoint (*, $p<0.05$; **, $p<0.01$; ***, $p<0.001$; Student's two-tailed t-test).

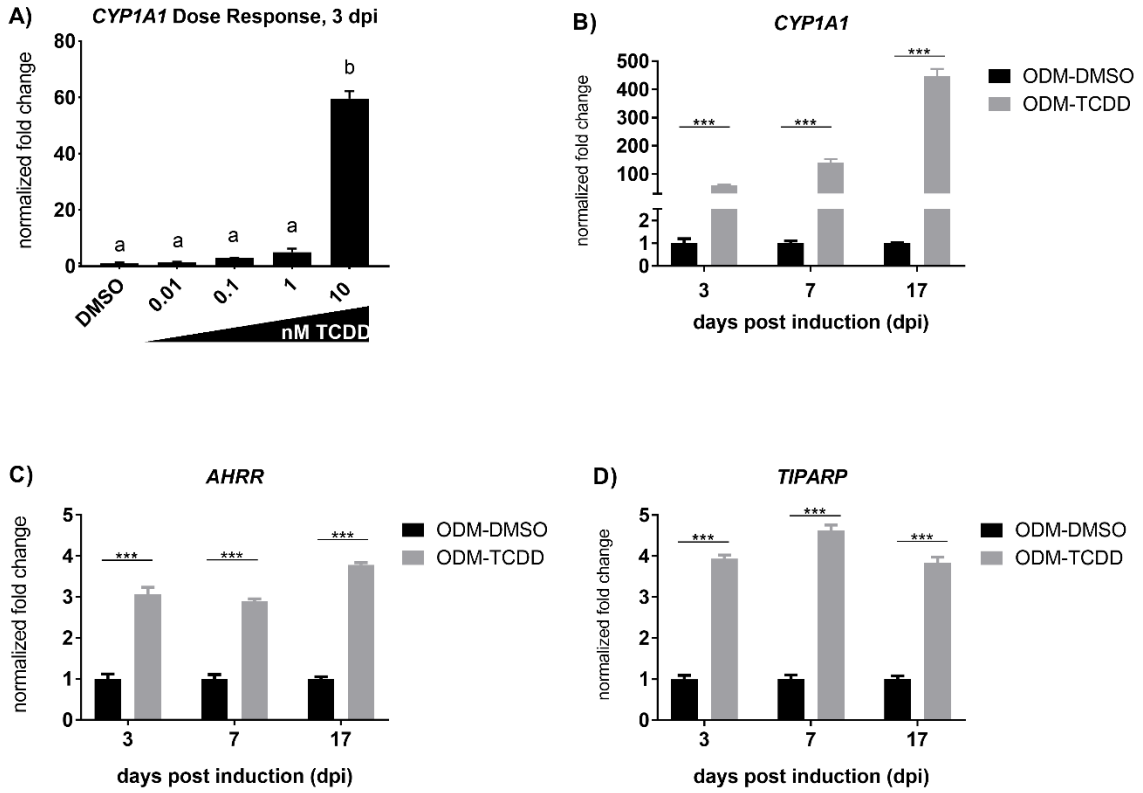

Figure 5. qPCR assessment of AhR-inducible gene targets in Donor 1. A dose response for CYP1A1 expression at 3 dpi is shown in (A). A time-course response is shown for *CYP1A1* (B), *AHRR* (C), and *TIPARP* (D) expression at 3, 7, and 17 dpi. Letters in denote statistical significance between groups in (A) ($p<0.05$, One-Way ANOVA and Tukey's post hoc test); asterisks in B-D indicate statistical significance between DMSO and 10 nM TCDD groups at each timepoint (*, $p<0.05$; **, $p<0.01$; ***, $p<0.001$; Student's two-tailed T-test); bars represent normalized fold change relative to *RPL13A* expression, a previously validated housekeeping gene in hBMSCs (Quiroz *et al.*, 2010) .

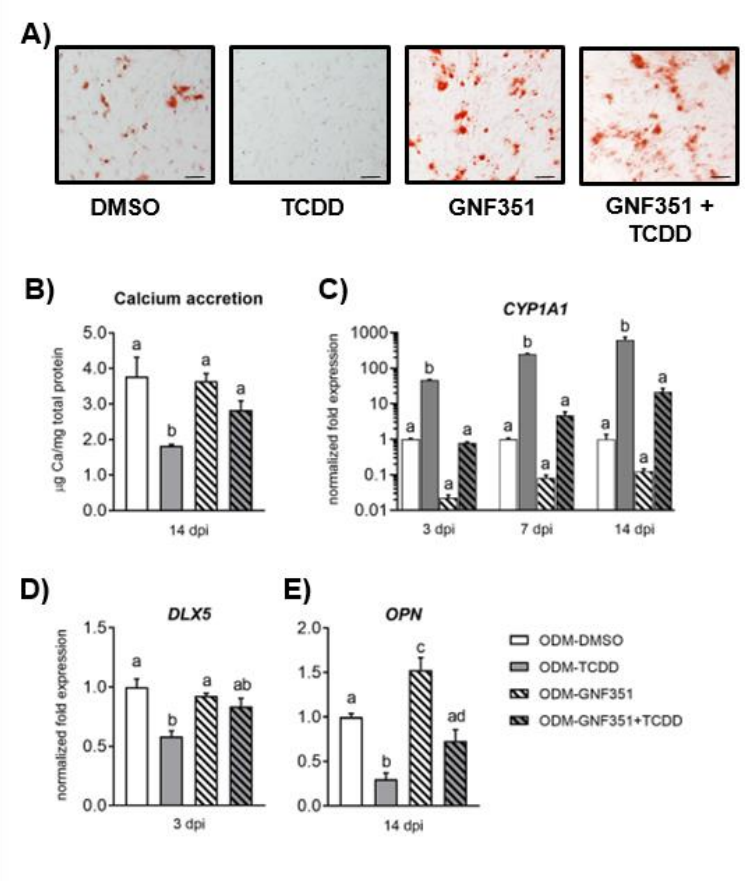

Figure 6. Osteogenic assessment of 10 nM TCDD ± 100 nM GNF351 co-exposure in hBMSCs from Donors 1 and 2 cultured in ODM. Best representative image depicting Alizarin Red S staining in (A) and corresponding calcium accretion in (B) at 14 dpi. GNF351 blocks AhR transactivation evidenced by inhibition of *CYP1A1* expression at 3, 7, and 14 dpi in (C), and partial rescue of osteogenic markers *DLX5* in (D) and SPP1 in (E). Donor 2 shown in (A-B) and Donor 1 shown in (C-E). Scale bars in (A) represent 200 μm, images at 5X magnification. Letters in (B-E) denote statistical significance between groups ($p<0.05$, One-Way ANOVA, Tukeys post hoc test); bars represent mean ± SEM

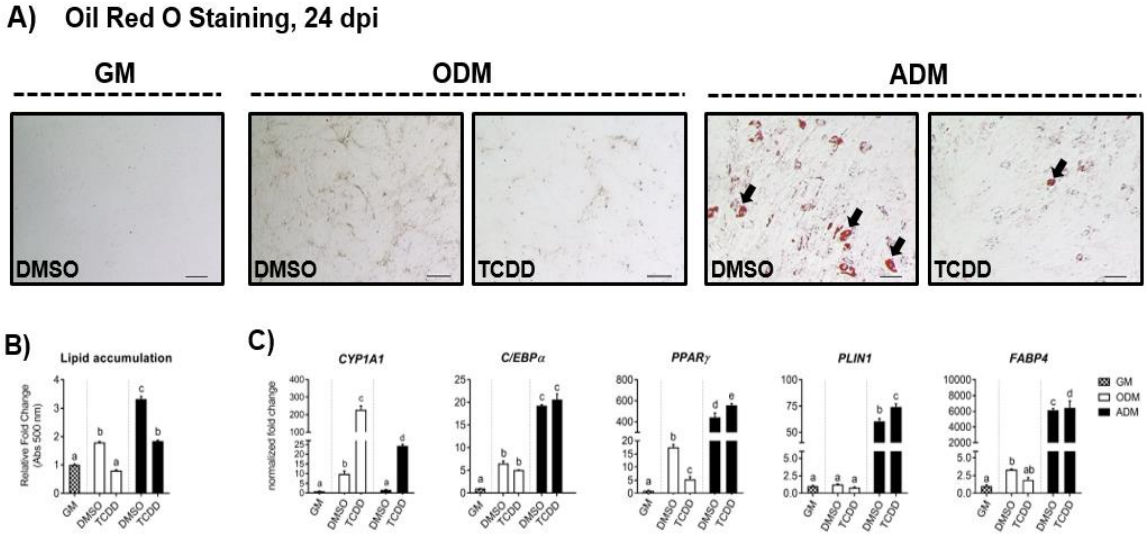

Figure 7. Adipogenic assessment of DMSO- and TCDD-treated hBMSCs in ODM and ADM at 24 dpi. Shown in (A) are representative images of Oil Red O histological staining (A) where scale bars represent 200 µm and black arrows signify Oil Red O-stained lipid vacuoles. Lipid accumulation was quantified in (B) via measuring absorbance at 500 nm of Oil Red O-destaining solution. Relative expression of adipogenic markers *PPARγ*, *C/EBPα*, *PLIN1*, and *FABP4* was assessed via qPCR (C). Bars represent mean ± SEM; letters denote significance between groups ($p<0.05$, One-Way ANOVA, Tukey's Post Hoc Analysis).

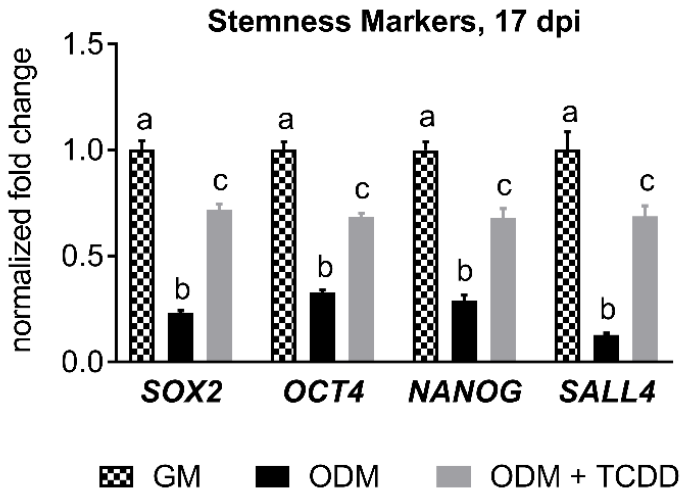

Figure 8. qPCR assessment of MSC stemness markers *SOX2*, *OCT4*, *NANOG*, *SALL4* at 17 days post induction (dpi). Bars represent mean ± SEM; letters denote statistical significance between groups ($p<0.05$, One-Way ANOVA, Tukey's Post Hoc Analysis).

REFERENCES

Abdallah, B.M. and Kassem, M. (2008) Human mesenchymal stem cells: from basic biology to clinical applications. *Gene Ther.*, **15**, 109–116.

Abel, J. and Haarmann-Stemmann, T. (2010) An introduction to the molecular basics of aryl hydrocarbon receptor biology. *Biol. Chem.*, **391**, 1235–1248.

Adams, J.D. *et al.* (1987) Toxic and carcinogenic agents in undiluted mainstream smoke and sidestream smoke of different types of cigarettes. *Carcinogenesis*, **8**, 729–731.

Addison, W.N. *et al.* (2007) Pyrophosphate inhibits mineralization of osteoblast cultures by binding to mineral, up-regulating osteopontin, and inhibiting alkaline phosphatase activity. *J. Biol. Chem.*, **282**, 15872–15883.

Alexander, P.G. *et al.* (2016) Prenatal exposure to environmental factors and congenital limb defects. *Birth Defects Res. Part C - Embryo Today Rev.*, **108**, 243–273.

Apschner, A. *et al.* (2011) Not All Bones are Created Equal – Using Zebrafish and Other Teleost Species in Osteogenesis Research Third Edit. Elsevier Inc.

Avery, S. *et al.* (2017) Analysing the bioactive makeup of demineralised dentine matrix on bone marrow mesenchymal stem cells for enhanced bone repair. *Eur. Cells Mater.*, **34**, 1–14.

Baker, A.H. *et al.* (2015) Tributyltin Engages Multiple Nuclear Receptor Pathways and Suppresses Osteogenesis in Bone Marrow Multipotent Stromal Cells. *Chem. Res. Toxicol.*, **28**, 1156–1166.

Baker, T.R. *et al.* (2014) Adverse effects in adulthood resulting from low-level dioxin exposure in juvenile zebrafish. *Endocr. Disruptors*, **2**, 1–6.

Baker, T.R. *et al.* (2013) Early dioxin exposure causes toxic effects in adult zebrafish. *Toxicol. Sci.*, **135**, 241–250.

Baksh, D. *et al.* (2004) Adult mesenchymal stem cells: characterization, differentiation, and application in cell and gene therapy. *J. Cell. Mol. Med.*, **8**, 301–316.

Baldridge, D. *et al.* (2010) Signaling pathways in human skeletal dysplasias. *Annu Rev Genomics Hum Genet*, **11**, 189–217.

Barbour, K.E. *et al.* (2014) Inflammatory Markers and Risk of Hip Fracture in Older White Women: The Study of Osteoporotic Fractures. *J. Bone Miner. Res.*, **29**, 2057–2064.

Baron, R. and Kneissel, M. (2013) WNT signaling in bone homeostasis and disease: from

human mutations to treatments. *Nat. Med.*, **19**, 179–192.

Baroncelli, M. *et al.* (2017) Comparative proteomic profiling of human osteoblast-derived extracellular matrices identifies proteins involved in mesenchymal stromal cell osteogenic differentiation and mineralization. *J. Cell. Physiol.*, 1–9.

Baroncelli, M. *et al.* (2017) Comparative Proteomic Profiling of Human Osteoblast-Derived Extracellular Matrices Identifies Proteins Involved in Mesenchymal Stromal Cell Osteogenic Differentiation and Mineralization. *J Cell Physiol*.

Benjamini, Y. and Hochberg, Y. (1995) Controlling the False Discovery Rate: A Practical and Powerful Approach to Multiple Testing. *J. R. Stat. Soc. Ser. B*, **57**, 289–300.

Benvenuti, S. *et al.* (2007) Rosiglitazone stimulates adipogenesis and decreases osteoblastogenesis in human mesenchymal stem cells. *J. Endocrinol. Invest.*, **30**, 26–30.

Bialek, P. *et al.* (2004) A Twist Code Determines the Onset of Osteoblast Differentiation. *Dev. Cell*, **6**, 423–435.

Bishop, N. (2016) Bone Material Properties in Osteogenesis Imperfecta. *J. Bone Miner. Res.*, **31**, 699–708.

Bodle, J.C. *et al.* (2014) Age-related effects on the potency of human adipose derived stem cells: Creation and evaluation of superlots and implications for musculoskeletal tissue engineering applications. *Tissue Eng. Part C Methods*, **20**, 1–43.

Bone health and osteoporosis: a report of the Surgeon General (2004) Rockville, Maryland.

Bonventre, J.A. *et al.* (2012) Craniofacial abnormalities and altered wnt and mmp mRNA expression in zebrafish embryos exposed to gasoline oxygenates ETBE and TAME. *Aquat. Toxicol.*, **120**–**121**, 45–53.

Boyce, B.F. and Xing, L. (2007) Biology of RANK, RANKL, and osteoprotegerin. *Arthritis Res. Ther.*, **9 Suppl 1**, S1.

Briggs, A.M. *et al.* (2016) Musculoskeletal Health Conditions Represent a Global Threat to Healthy Aging: A Report for the 2015 World Health Organization World Report on Ageing and Health. *Gerontologist*, **56**, S243–S255.

Burns, F.R. *et al.* (2015) Dioxin disrupts cranial cartilage and dermal bone development in zebrafish larvae. *Aquat. Toxicol.*, **164**, 52–60.

Bustin, S.A. *et al.* (2009) The MIQE Guidelines: Minimum Information for Publication of Quantitative Real-Time PCR Experiments. *Clin. Chem.*, **622**, 611–622.

Carpi, D. *et al.* (2009) Dioxin-sensitive proteins in differentiating osteoblasts: Effects on bone formation in vitro. *Toxicol. Sci.*, **108**, 330–343.

Charoenpanich, A. *et al.* (2014) Cyclic tensile strain enhances osteogenesis and angiogenesis in mesenchymal stem cells from osteoporotic donors. *Tissue Eng. Part A*, **20**, 67–78.

Chen, G. *et al.* (2012) TGF-β and BMP Signaling in Osteoblast Differentiation and Bone Formation. *Int. J. Biol. Sci.*, **8**, 272–288.

Chopra, M. and Schrenk, D. (2011) Dioxin toxicity, aryl hydrocarbon receptor signaling, and apoptosis-persistent pollutants affect programmed cell death. *Crit. Rev. Toxicol.*, **41**, 292–320.

Chrisman, K. *et al.* (2004) Gestational Ethanol Exposure Disrupts the Expression of FGF8 and Sonic hedgehog during Limb Patterning. *Birth Defects Res. Part A - Clin. Mol. Teratol.*, **70**, 163–171.

Christiansen, H.E. *et al.* (2010) Homozygosity for a Missense Mutation in SERPINH1, which Encodes the Collagen Chaperone Protein HSP47, Results in Severe Recessive Osteogenesis Imperfecta. *Am. J. Hum. Genet.*, **86**, 389–398.

Clarke, B. (2008) Normal bone anatomy and physiology. *Clin. J. Am. Soc. Nephrol.*, **3 (Suppl 3**.

Derrien, T. *et al.* (2012) The GENCODE v7 catalogue of human long non-coding RNAs : Analysis of their structure , evolution and expression. *Genome Res.*, **22**, 1775–1789.

Ding, D. *et al.* (2012) Over-expression of Sox2 in C3H10T1/2 cells inhibits osteoblast differentiation through Wnt and MAPK signalling pathways. *Int. Orthop.*, **36**, 1087–1094.

Dobin, A. *et al.* (2013) STAR: Ultrafast universal RNA-seq aligner. *Bioinformatics*, **29**, 15–21.

Dolk, H. *et al.* (2010) The Prevalence of Congenital Anomalies in Europe. In, Paz,M.P. de la and Croft,S.C. (eds), *Rare Diseases Epidemiology*. Springer, New York, New York, pp. 305–334.

Dominici, M. *et al.* (2006) Minimal criteria for defining multipotent mesenchymal stromal cells. The International Society for Cellular Therapy position statement. *Cytotherapy*, **8**, 315–7.

Dong, B. and Matsumura, F. (2008) Roles of cytosolic phospholipase A2 and Src kinase in the early action of 2,3,7,8-tetrachlorodibenzo-p-dioxin through a nongenomic pathway in MCF10A cells. *Mol. Pharmacol.*, **74**, 255–263.

Dong, W. *et al.* (2012) TCDD disrupts hypural skeletogenesis during medaka embryonic development. *Toxicol. Sci.*, **125**, 91–104.

Dong, W. *et al.* (2010) TCDD Induced Pericardial Edema and Relative COX-2 Expression in Medaka (Oryzias Latipes) Embryos. *Toxicol. Sci.*, **118**, 213–223.

Dudakovic, A. *et al.* (2015) Epigenetic Control of Skeletal Development by the Histone Demethylase Ezh2. *J. Biol. Chem.*, **290**, 27604–27617.

Ekanayake, S. and Hall, B.K. (1987) The development of acellularity of the vertebral bone of the Japanese medaka, *Oryzias latipes* (Teleostei; Cyprinidontidae). *J. Morphol.*, **193**, 253–261.

Ekanayake, S. and Hall, B.K. (1988) Ultrastructure of the osteogenesis of acellular vertebral bone in the Japanese medaka, Oryzias latipes (Teleostei, Cyprinidontidae). *Am. J. Anat.*, **182**, 241–249.

Ellis, L.D. *et al.* (2014) Use of the zebrafish larvae as a model to study cigarette smoke condensate toxicity. *PLoS One*, **9**, e115305.

Etemad, L. *et al.* (2012) Epilepsy drugs and effects on fetal development: Potential mechanisms. *J. Res. Med. Sci.*, **17**.

Fakhry, A. *et al.* (2005) Effects of FGF-2/-9 in calvarial bone cell cultures: Differentiation stage-dependent mitogenic effect, inverse regulation of BMP-2 and noggin, and enhancement of osteogenic potential. *Bone*, **36**, 254–266.

Felson, D.T. *et al.* (2000) Osteoarthritis: new insights. Part 1: the disease and its risk factors. *Ann. Intern. Med.*, **133**, 635–646.

Fernández-González, R. *et al.* (2015) A Critical Review about Human Exposure to Polychlorinated Dibenzo-p-Dioxins (PCDDs), Polychlorinated Dibenzofurans (PCDFs) and Polychlorinated Biphenyls (PCBs) through Foods. *Crit. Rev. Food Sci. Nutr.*, **55**, 1590–1617.

Finnilä, M.A.J. *et al.* (2010) Effects of 2,3,7,8-tetrachlorodibenzo-p-dioxin exposure on bone material properties. *J. Biomech.*, **43**, 1097–1103.

Fleming, A. *et al.* (2015) Building the backbone: the development and evolution of vertebral patterning. *Development*, **142**, 1733–44.

Flynn, R.A. and Chang, H.Y. (2014) Long noncoding RNAs in cell-fate programming and reprogramming. *Cell Stem Cell*, **14**, 752–761.

Forlino, A. *et al.* (2011) New perspectives on osteogenesis imperfecta. *Nat. Rev. Endocrinol.*,

7, 540–557.

Forlino, A. and Marini, J.C. (2016) Osteogenesis imperfecta. *Lancet*, **387**, 1657–1671.

Franz-Odendaal, T.A. *et al.* (2006) Buried alive: How osteoblasts become osteocytes. *Dev. Dyn.*, **235**, 176–190.

Gadupudi, G. *et al.* (2015) PCB126 inhibits adipogenesis of human preadipocytes. *Toxicol. Vitr.*, **29**, 132–141.

Gallagher, J.C. and Sai, a. J. (2010) Molecular biology of bone remodeling: Implications for new therapeutic targets for osteoporosis. *Maturitas*, **65**, 301–307.

Gennari, L. *et al.* (2016) MicroRNAs in bone diseases. *Osteoporos. Int.*, 1–23.

Golub, E.E. and Boesze-Battaglia, K. (2007) The role of alkaline phosphatase in mineralization. *Curr. Opin. Orthop.*, **18**, 444–448.

Gordon, J.A.R. *et al.* (2015) Chromatin modifiers and histone modifications in bone formation, regeneration, and therapeutic intervention for bone-related disease. *Bone*, **81**, 739–745.

Gordon, J.A.R. *et al.* (2014) Epigenetic pathways regulating bone homeostasis: Potential targeting for intervention of skeletal disorders. *Curr. Osteoporos. Rep.*, **12**, 496–506.

Greco, S.J. *et al.* (2007) Functional Similarities Among Genes Regulated by Oct4 in Human Mesenchymal and Embryonic Stem Cells. *Stem Cells*, **25**, 3143–3154.

Grotmol, S. *et al.* (2005) A segmental pattern of alkaline phosphatase activity within the notochord coincides with the initial formation of the vertebral bodies. *J. Anat.*, **206**, 427–436.

Håkelien, A.M. *et al.* (2014) The regulatory landscape of osteogenic differentiation. *Stem Cells*, **32**, 2780–2793.

Hardy, R. and Cooper, M.S. (2009) Bone loss in inflammatory disorders. *J. Endocrinol.*, **201**, 309–320.

Heo, J. *et al.* (2015) Comparison of molecular profiles of human mesenchymal stem cells derived from bone marrow, umbilical cord blood, placenta and adipose tissue. *Int. J. Mol. Med.*, 115–125.

Herlin, M. *et al.* (2015) Inhibitory effects on osteoblast differentiation in vitro by the polychlorinated biphenyl mixture Aroclor 1254 are mainly associated with the dioxin-like constituents. *Toxicol. Vitr.*, **29**, 876–883.

Herlin, M. *et al.* (2013) New insights to the role of aryl hydrocarbon receptor in bone phenotype and in dioxin-induced modulation of bone microarchitecture and material properties. *Toxicol. Appl. Pharmacol.*, **273**, 219–26.

Herlin, M. *et al.* (2010) Quantitative characterization of changes in bone geometry, mineral density and biomechanical properties in two rat strains with different Ah-receptor structures after long-term exposure to 2,3,7,8-tetrachlorodibenzo-p-dioxin. *Toxicology*, **273**, 1–11.

Hermanns, P. and Lee, B. (2002) Transcriptional dysregulation in skeletal malformation syndromes. *Am. J. Med. Genet.*, **106**, 258–271.

Hernandez, C.J. *et al.* (2003) A theoretical analysis of the relative influences of peak BMD, age-related bone loss and menopause on the development of osteoporosis. *Osteoporos. Int.*, **14**, 843–847.

Holz, J.D. *et al.* (2007) Environmental agents affect skeletal growth and development. *Birth Defects Res. Part C - Embryo Today Rev.*, **81**, 41–50.

Huang, J. *et al.* (2010) MicroRNA-204 regulates Runx2 protein expression and mesenchymal progenitor cell differentiation. *Stem Cells*, **28**, 357–364.

Hulsen, T. *et al.* (2008) BioVenn – a web application for the comparison and visualization of biological lists using area-proportional Venn diagrams. *BMC Genomics*, **9**, 488.

Imai, Y. *et al.* (2013) Nuclear Receptors in Bone Physiology and Diseases. *Physiol. Rev.*, **93**, 481–523.

Inose, H. *et al.* (2009) A microRNA regulatory mechanism of osteoblast differentiation. *Proc. Natl. Acad. Sci. U. S. A.*, **106**, 20794–20799.

Ito, T. *et al.* (2010) Identification of a Primary Target of Thalidomide Teratogenicity. *Science (80-.).*, **327**, 1345–1351.

Ito, T. *et al.* (2011) Teratogenic effects of thalidomide: Molecular mechanisms. *Cell. Mol. Life Sci.*, **68**, 1569–1579.

Itoh, T. *et al.* (2009) MicroRNA-141 and -200a Are Involved in Bone Morphogenetic Protein-2-induced Mouse Pre-osteoblast Differentiation by Targeting Distal-less Homeobox 5. *J. Biol. Chem.*, **284**, 19272–19279.

Jämsä, T. *et al.* (2001) Effects of 2,3,7,8-Tetrachlorodibenzo-p-Dioxin on Bone in Two Rat Strains with Different Aryl Hydrocarbon Receptor Structures. *J. Bone Miner. Res.*, **16**, 1812–1820.

Jensen, E.D. *et al.* (2010) Regulation of gene expression in osteoblasts. *Biofactors*, **36**, 25–32.

Jenuwein, T. *et al.* (2001) Translating the Histone Code. *Science (80-.).*, **293**, 1074–1080.

Johnell, O. and Kanis, J.A. (2006) An estimate of the worldwide prevalence and disability associated with osteoporotic fractures. *Osteoporos. Int.*, **17**, 1726–1733.

Joshi-Tope, G. *et al.* (2005) Reactome: A knowledgebase of biological pathways. *Nucleic Acids Res.*, **33**, 428–432.

Kang, H. *et al.* (2017) Osteogenesis imperfecta: new genes reveal novel mechanisms in bone dysplasia. *Transl. Res.*, **181**, 27–48.

Kanis, J. (2007) Assessment of osteoporosis at the primary health care level.

Kanis, J. *et al.* (2005) Smoking and fracture risk: A meta-analysis. *Osteoporos. Int.*, **16**, 155–162.

Karsenty, G. *et al.* (2009) Genetic Control of Bone Formation. *Annu. Rev. Cell Dev. Biol.*, **25**, 629–648.

Karsenty, G. (2008) Transcriptional Control of Skeletogenesis. *Annu. Rev. Genomics Hum. Genet.*, **9**, 183–196.

Kawai, M. *et al.* (2010) The many facets of PPARgamma: novel insights for the skeleton. *Am. J. Physiol. Endocrinol. Metab.*, **299**, E3–E9.

Kimura, H. (2013) Histone modifications for human epigenome analysis. *J. Hum. Genet.*, **58**, 439–445.

King-Heiden, T.C. *et al.* (2012) Reproductive and developmental toxicity of dioxin in fish. *Mol. Cell. Endocrinol.*, **354**, 121–138.

Klareskog, L. *et al.* (2007) Smoking as a trigger for inflammatory rheumatic diseases. *Curr. Opin. Rheumatol.*, **19**, 49–54.

Ko, C.I. *et al.* (2016) Repression of the Aryl Hydrocarbon Receptor Is Required to Maintain Mitotic Progression and Prevent Loss of Pluripotency of Embryonic Stem Cells. *Stem Cells*, **34**, 2825–2839.

Komori, T. (2010) Regulation of bone development and extracellular matrix protein genes by RUNX2. *Cell Tissue Res.*, **339**, 189–195.

Komori, T. *et al.* (1997) Targeted disruption of Cbfa1 results in a complete lack of bone

formation owing to maturational arrest of osteoblasts. *Cell*, **89**, 755–64.

Korkalainen, M. *et al.* (2009) Dioxins interfere with differentiation of osteoblasts and osteoclasts. *Bone*, **44**, 1134–1142.

Kornak, U. and Mundlos, S. (2003) Genetic disorders of the skeleton: a developmental approach. *Am. J. Hum. Genet.*, **73**, 447–74.

Kotake, S. *et al.* (1996) Interleukin-6 and Soluble Interleukin-6 Receptors in the Synovial Fluids from Rheumatoid Arthritis Patients Are Responsible for Osteoclast-like Cell Formation. *J. Bone Miner. Res.*, **11**, 88–95.

Krakow, D. and Rimoin, D.L. (2010) The skeletal dysplasias. *Genet. Med.*, **12**, 327–41.

Kung, M.H. *et al.* (2011) Aryl hydrocarbon receptor-mediated impairment of chondrogenesis and fracture healing by cigarette smoke and benzo(α)pyrene. *J. Cell. Physiol.*, **227**, 1062–1070.

Lacey, D.C. *et al.* (2009) Proinflammatory cytokines inhibit osteogenic differentiation from stem cells: implications for bone repair during inflammation. *Osteoarthr. Cartil.*, **17**, 735–742.

Laize, V. *et al.* (2014) Fish : a suitable system to model human bone disorders and discover drugs with osteogenic or osteotoxic activities. *Drug Discov. Today Dis. Model.*, **13**, 29–37.

Lam, J. *et al.* (2000) TNF-α induces osteoclastogenesis by direct stimulation of macrophages exposed to permissive levels of RANK ligand. *J. Clin. Invest.*, **106**, 1481–1488.

Law, M.R. and Hackshaw, a K. (1997) A meta-analysis of cigarette smoking, bone mineral density and risk of hip fracture: recognition of a major effect. *BMJ*, **315**, 841–846.

Lee, J.J. *et al.* (2013) The musculoskeletal effects of cigarette smoking. *J. Bone Jt. Surg.*, **95**, 850–9.

Lee, M.H. *et al.* (2003) BMP-2-induced Osterix expression is mediated by Dlx5 but is independent of Runx2. *Biochem. Biophys. Res. Commun.*, **309**, 689–694.

Lee, M.H. *et al.* (2005) Dlx5 specifically regulates Runx2 type II expression by binding to homeodomain-response elements in the Runx2 distal promoter. *J. Biol. Chem.*, **280**, 35579–35587.

Lefebvre, V. and Bhattaram, P. (2010) Vertebrate Skeletogenesis. In, Koopman,P. (ed), *Current Topics in Developmental Biology: Organogenesis in Development*. Elsevier Inc., San Diego, pp. 291–317.

Li, L. *et al.* (2013) Targeted Disruption of Hotair Leads to Homeotic Transformation and Gene Derepression. *Cell Rep.*, **5**, 3–12.

Li, W. *et al.* (2008) Development of a human adipocyte model derived from human mesenchymal stem cells (hMSC) as a tool for toxicological studies on the action of TCDD. *Biol. Chem.*, **389**, 169–177.

Lian, J.B. *et al.* (2006) Networks and hubs for the transcriptional control of osteoblastogenesis. *Rev. Endocr. Metab. Disord.*, **7**, 1–16.

Lindner, U. *et al.* (2010) Mesenchymal stem or stromal cells: Toward a better understanding of their biology? *Transfus. Med. Hemotherapy*, **37**, 75–83.

Liu, B. *et al.* (2013) Depleting the methyltransferase Suv39h1 improves DNA repair and extends lifespan in a progeria mouse model. *Nat. Commun.*, **4**, 1868.

Liu, P. *et al.* (1996) Alteration by 2,3,7,8-Tetrachlordibenzo-p-dioxin of CCAAT/Enhancer Binding Protein Correlates with Suppression of Adipocyte Differentiation in 3T3-L1 Cells. *Mol. Pharmacol.*, **49**, 989–997.

Livak, K.J. and Schmittgen, T.D. (2001) Analysis of relative gene expression data using real-time quantitative PCR and the 2(-Delta Delta C(T)) Method. *Methods*, **25**, 402–8.

Long, F. (2011) Building strong bones: molecular regulation of the osteoblast lineage. *Nat. Rev. Mol. Cell Biol.*, **13**, 27–38.

Lorentzon, M. *et al.* (2007) Smoking is associated with lower bone mineral density and reduced cortical thickness in young men. *J. Clin. Endocrinol. Metab.*, **92**, 497–503.

Love, M.I. *et al.* (2014) Moderated estimation of fold change and dispersion for RNA-seq data with DESeq2. *Genome Biol.*, **15**, 550.

Lu, J. *et al.* (2015) Effect of fibroblast growth factor 9 on the osteogenic differentiation of bone marrow stromal stem cells and dental pulp stem cells. *Mol. Med. Rep.*, **11**, 1661–1668.

Lu, J. *et al.* (2014) The Effect of Fibroblast Growth Factor 9 on the Osteogenic Differentiation of Calvaria-Derived Mesenchymal Cells. *J. Craniofac. Surg.*, **25**, 502–505.

Manolagas, S.C. (2000) Birth and death of bone cells: basic regulatory mechanisms and implications for the pathogenesis and treatment of osteoporosis. *Endocr. Rev.*, **21**, 115–137.

Mansukhani, A. *et al.* (2005) Sox2 induction by FGF and FGFR2 activating mutations

inhibits Wnt signaling and osteoblast differentiation. *J. Cell Biol.*, **168**, 1065–1076.

Marcellini, S. *et al.* (2012) Control of osteogenesis by the canonical Wnt and BMP pathways in vivo: cooperation and antagonism between the canonical Wnt and BMP pathways as cells differentiate from osteochondroprogenitors to osteoblasts and osteocytes. *BioEssays News Rev. Mol. Cell. Dev. Biol.*, **34**, 953–62.

Marotti, G. (1996) The structure of bone tissues and the cellular control of their deposition. *Ital. J. Anat. Embryol.*, **101**, 25–79.

McCormack, S.E. *et al.* (2017) Association Between Linear Growth and Bone Accrual in a Diverse Cohort of Children and Adolescents. *JAMA Pediatr.*, **19104**, 1–9.

Miettinen, H.M. *et al.* (2005) Effects of in utero and lactational TCDD exposure on bone development in differentially sensitive rat lines. *Toxicol. Sci.*, **85**, 1003–1012.

Mizuno, Y. *et al.* (2008) miR-125b inhibits osteoblastic differentiation by down-regulation of cell proliferation. *Biochem. Biophys. Res. Commun.*, **368**, 267–272.

Montecino, M. *et al.* (2015) Multiple levels of epigenetic control for bone biology and pathology. *Bone*, **81**, 733–738.

Mundy, G.R. (2007) Osteoporosis and Inflammation. *Nutr. Rev.*, **65**.

Murante, F.G. and Gasiewicz, T.A. (2000) Hemopoietic Progenitor Cells Are Sensitive Targets of 2,3,7,8-Tetrachlorodibenzo-p-dioxin in C57BL/6J Mice. *Toxicol. Sci.*, **54**, 374–383.

Nakase, T. *et al.* (1997) Interleukin-1 beta enhances and tumor necrosis factor-alpha inhibits bone morphogenetic protein-2-induced alkaline phosphatase activity in MC3T3-E1 osteoblastic cells. *Bone*, **21**, 17–21.

Nakashima, K. *et al.* (2002) The novel zinc finger-containing transcription factor osterix is required for osteoblast differentiation and bone formation. *Cell*, **108**, 17–29.

Nakashima, T. *et al.* (2012) New insights into osteoclastogenic signaling mechanisms. *Trends Endocrinol. Metab.*, **23**, 582–90.

Narkowicza, S. *et al.* (2013) Environmental Tobacco Smoke: Exposure, Health Effects, and Analysis. *Biocontrol Sci. Technol.*, **43**, 121–161.

Naruse, M. *et al.* (2002) 3-Methylcholanthrene, which binds to the arylhydrocarbon receptor, inhibits proliferation and differentiation of osteoblasts in vitro and ossification in vivo. *Endocrinology*, **143**, 3575–81.

Nishio, Y. *et al.* (2006) Runx2-mediated regulation of the zinc finger Osterix/Sp7 gene. *Gene*, **372**, 62–70.

Nordvik, K. *et al.* (2005) The salmon vertebral body develops through mineralization of two preformed tissues that are encompassed by two layers of bone. *J. Anat.*, **206**, 103–114.

Ohtake, F. *et al.* (2009) AhR acts as an E3 ubiquitin ligase to modulate steroid receptor functions. *Biochem. Pharmacol.*, **77**, 474–84.

Orioli, I.M. *et al.* (1986) The birth prevalence rates for the skeletal dysplasias. *J. Med. Genet.*, **23**, 328–32.

Ornitz, D.M. and Marie, P.J. (2015) Fibroblast growth factor signaling in skeletal development and disease. *Genes Dev.*, **29**, 1463–1486.

Padilla, S. *et al.* (2012) Zebrafish developmental screening of the ToxCast^{TM} Phase I chemical library. *Reprod. Toxicol.*, **33**, 174–187.

van de Peppel, J. *et al.* (2017) Identification of Three Early Phases of Cell-Fate Determination during Osteogenic and Adipogenic Differentiation by Transcription Factor Dynamics. *Stem Cell Reports*, **172**, 5457–5476.

Pillai, H.K. *et al.* (2014) Ligand Binding and Activation of PPARγ by Firemaster 550: Effects on Adipogenesis and Osteogenesis in Vitro. *Environ. Health Perspect.*, **122**, 1225–1232.

Podechard, N. *et al.* (2009) Inhibition of human mesenchymal stem cell-derived adipogenesis by the environmental contaminant benzo(a)pyrene. *Toxicol. In Vitro*, **23**, 1139–44.

Pohl, H. *et al.* (1998) Toxicological profile for chlorinated dibenzo-p-dioxins.

Puga, A. *et al.* (2000) Aromatic Hydrocarbon Receptor Interaction with the Retinoblastoma Protein Potentiates Repression of E2F-dependent Transcription and Cell Cycle Arrest. *J. Biol. Chem.*, **275**, 2943–2950.

Puga, A. *et al.* (2009) The aryl hydrocarbon receptor cross-talks with multiple signal transduction pathways. *Biochem. Pharmacol.*, **77**, 713–722.

Quiroz, F.G. *et al.* (2010) Housekeeping gene stability influences the quantification of osteogenic markers during stem cell differentiation to the osteogenic lineage. *Cytotechnology*, **62**, 109–120.

Rahman, M.S. *et al.* (2015) TGF-β/BMP signaling and other molecular events: regulation of osteoblastogenesis and bone formation. *Bone Res.*, **3**, 15005.

Redlich, K. and Smolen, J.S. (2012) Inflammatory bone loss: pathogenesis and therapeutic intervention. *Nat. Rev. Drug Discov.*, **11**, 234–250.

Riekstina, U. *et al.* (2009) Embryonic stem cell marker expression pattern in human mesenchymal stem cells derived from bone marrow, adipose tissue, heart and dermis. *Stem Cell Rev. Reports*, **5**, 378–386.

Riss, T.L. *et al.* (2004) Cell Viability Assays Assay Guidance Manual. *Assay Guid. Man.*, 1–23.

Rizzoli, R. *et al.* (2010) Maximizing bone mineral mass gain during growth for the prevention of fractures in the adolescents and the elderly. *Bone*, **46**, 294–305.

Rosano, A. *et al.* (2000) Limb defects associated with major congenital anomalies: Clinical and epidemiological study from the international clearinghouse for birth defects monitoring systems. *Am. J. Med. Genet.*, **93**, 110–116.

Rosen, E.D. and MacDougald, O.A. (2006) Adipocyte differentiation from the inside out. *Nat. Rev. Mol. Cell Biol.*, **7**, 885–896.

Rosset, E.M. and Bradshaw, A.D. (2016) SPARC/osteonectin in mineralized tissue. *Matrix Biol.*, **52**–**54**, 78–87.

Ryan, E.P. *et al.* (2007) Environmental toxicants may modulate osteoblast differentiation by a mechanism involving the aryl hydrocarbon receptor. *J. Bone Miner. Res.*, **22**, 1571–80.

Safe, S. *et al.* (1998) Ah receptor agonists as endocrine disruptors: antiestrogenic activity and mechanisms. *Toxicol. Lett.*, **102**–**103**, 343–7.

Safe, S. (1995) Cellular and molecular biology of aryl hydrocarbon (Ah) receptor-mediated gene expression. *Arch. Toxicol.*, **17**, 99–115.

Sakaguchi, Y. *et al.* (2009) Suspended cells from trabecular bone by collagenase digestion become virtually identical to mesenchymal stem cells obtained from marrow. *Stem Cells*, **104**, 2728–2735.

Sargis, R.M. *et al.* (2009) Environmental Endocrine Disruptors Promote Adipogenesis in the 3T3-L1 Cell Line through Glucocorticoid Receptor Activation. *Obesity*, **18**, 1283–1288.

Schönitzer, V. *et al.* (2014) Sox2 is a potent inhibitor of osteogenic and adipogenic differentiation in human mesenchymal stem cells. *Cell. Reprogram.*, **16**, 355–65.

Schroeder, T.M. *et al.* (2005) Runx2: A master organizer of gene transcription in developing and maturing osteoblasts. *Birth Defects Res. Part C - Embryo Today Rev.*, **75**, 213–225.

Sciullo, E.M. *et al.* (2009) Characterization of the pattern of the nongenomic signaling pathway through which TCDD-induces early inflammatory responses in U937 human macrophages. *Chemosphere*, **74**, 1531–1537.

Scolaro, J.A. *et al.* (2014) Cigarette Smoking Increases Complications Following Fracture. *J. Bone Jt. Surg.*, 674–681.

Seo, E. *et al.* (2011) Distinct Functions of Sox2 Control Self-Renewal and Differentiation in the Osteoblast Lineage. *Mol. Cell. Biol.*, **31**, 4593–4608.

Sheng, G. (2015) The developmental basis of mesenchymal stem/stromal cells (MSCs). *BMC Dev. Biol.*, **15**, 44.

Shimba, S. *et al.* (2001) Aryl hydrocarbon receptor (AhR) is involved in negative regulation of adipose differentiation in 3T3- L1 cells : AhR inhibits adipose differentiation independently of dioxin. *J. Cell Sci.*, **114**, 2809–2817.

Siegel, G. *et al.* (2013) Phenotype, donor age and gender affect function of human bone marrow-derived mesenchymal stromal cells. *BMC Med.*, **11**, 146.

Simonet, W.S. *et al.* (1997) Osteoprotegerin: a novel secreted protein involved in the regulation of bone density. *Cell*, **89**, 309–19.

Singh, K.P. *et al.* (2009) Treatment of mice with the Ah receptor agonist and human carcinogen dioxin results in altered numbers and function of hematopoietic stem cells. *Carcinogenesis*, **30**, 11–19.

Sinha, K.M. and Zhou, X. (2013) Genetic and molecular control of osterix in skeletal formation. *J. Cell. Biochem.*, **114**, 975–84.

Sipes, N.S. *et al.* (2011) Zebrafish-as an integrative model for twenty-first century toxicity testing. *Birth Defects Res. Part C, Embryo Today Rev.*, **93**, 256–267.

Sloan, A. *et al.* (2010) The effects of smoking on fracture healing. *Surg. J. R. Coll. Surg. Edinburgh Irel.*, **8**, 111–6.

Smith, K.J. *et al.* (2011) Identification of a high-affinity ligand that exhibits complete aryl hydrocarbon receptor antagonism. *J. Pharmacol. Exp. Ther.*, **338**, 318–327.

Sozen, T. *et al.* (2017) An overview and management of osteoporosis. *Eur. J. Rheumatol.*, **4**, 46–56.

Spandidos, A. *et al.* (2010) PrimerBank : a resource of human and mouse PCR primer pairs for gene expression detection and quantification. **38**, 792–799.

Staines, K.A. *et al.* (2012) The importance of the SIBLING family of proteins on skeletal mineralisation and bone remodelling. *J. Endocrinol.*, **214**, 241–255.

Su, N. *et al.* (2008) FGF signaling: its role in bone development and human skeletal diseases. *Front. Biosci.*, **13**, 2842–2865.

Teraoka, H. *et al.* (2006) Impairment of lower jaw growth in developing zebrafish exposed to 2,3,7,8-tetrachlorodibenzo-p-dioxin and reduced hedgehog expression. *Aquat. Toxicol.*, **78**, 103–113.

Teraoka, H. *et al.* (2006) Muscular contractions in the zebrafish embryo are necessary to reveal thiuram-induced notochord distortions. *Toxicol. Appl. Pharmacol.*, **212**, 24–34.

The Health Consequences of Smoking - — 50 Years of Progress A Report of the Surgeon General (2014) Rockville, Maryland.

Tian, L. *et al.* (2017) miR-148a-3p regulates adipocyte and osteoblast differentiation by targeting lysine-specific demethylase 6b. *Gene*, **627**, 32–39.

Tian, Y. *et al.* (2002) Ah receptor and NF-kB interactions: Mechanisms and physiological implications. *Chem. Biol. Interact.*, **141**, 97–115.

Tilton, F. *et al.* (2006) Dithiocarbamates have a common toxic effect on zebrafish body axis formation. *Toxicol. Appl. Pharmacol.*, **216**, 55–68.

Tox21: Chemical testing in the 21st century (2017) Research Triangle Park, NC.

Truong, L. *et al.* (2014) Multidimensional in vivo hazard assessment using zebrafish. *Toxicol. Sci.*, **137**, 212–233.

Tye, C.E. *et al.* (2015) Could lncRNAs be the Missing Links in Control of Mesenchymal Stem Cell Differentiation? *J. Cell. Physiol.*, **230**, 526–534.

Tyl, R.W. *et al.* (2007) Altered Axial Skeletal Development. *Birth Defects Res. Part B-Developmental Reprod. Toxicol.*, **472**, 451–472.

Voss, A. *et al.* (2016) Extracellular Matrix of Current Biological Scaffolds Promotes the Differentiation Potential of Mesenchymal Stem Cells. *Arthrosc. - J. Arthrosc. Relat. Surg.*, **32**, 2381–2392.e1.

van de Vyver, M. *et al.* (2014) Thiazolidinedione-induced lipid droplet formation during osteogenic differentiation. *J. Endocrinol.*, **223**, 119–132.

Wade, S.W. *et al.* (2014) Estimating prevalence of osteoporosis: examples from industrialized countries. *Arch. Osteoporos.*, **9**, 182.

Wang, C.-K. *et al.* (2009) Aryl hydrocarbon receptor activation and overexpression upregulated fibroblast growth factor-9 in human lung adenocarcinomas. *Int. J. Cancer*, **125**, 807–815.

Wang, Y. *et al.* (2010) Dioxin Exposure Disrupts the Differentiation of Mouse Embryonic Stem Cells into Cardiomyocytes. **115**, 225–237.

Wang, Z. *et al.* (2012) Distinct lineage specification roles for NANOG, OCT4, and SOX2 in human embryonic stem cells. *Cell Stem Cell*, **10**, 440–454.

Ward, K.D. and Klesges, R.C. (2001) A Meta-Analysis of the Effects of Cigarette Smoking on Bone Mineral Density. *Calcif. Tissue Int.*, **68**, 259–270.

Watson, A.T.D. *et al.* (2017) Embryonic Exposure to TCDD Impacts Osteogenesis of the Axial Skeleton in Japanese medaka, Oryzias latipes. *Toxicol. Sci.*, **155**, 485–496.

Watt, J. and Schlezinger, J.J. (2015) Structurally-diverse, PPARγ-activating environmental toxicants induce adipogenesis and suppress osteogenesis in bone marrow mesenchymal stromal cells. *Toxicology*, **331**, 66–77.

Wilffert, B. *et al.* (2011) Pharmacogenetics of drug-induced birth defects: what is known so far? *Pharmacogenomics*, **12**, 547–558.

Wilson, C.L. and Safe, S. (1998) Mechanisms of ligand-induced aryl hydrocarbon receptor-mediated biochemical and toxic responses. *Toxicol. Pathol.*, **26**, 657–671.

Witten, P.E. *et al.* (2016) Small teleost fish provide new insights into human skeletal diseases Elsevier Ltd.

Witten, P.E. and Huysseune, A. (2009) A comparative view on mechanisms and functions of skeletal remodelling in teleost fish, with special emphasis on osteoclasts and their function. *Biol. Rev.*, **84**, 315–346.

Wong, P.K.K. *et al.* (2007) The effects of smoking on bone health. *Clin. Sci.*, **113**, 233–41.

Wu, H. *et al.* (2017) Chromatin Dynamics Regulate Mesenchymal Stem Cell Lineage Specification and Differentiation to Osteogenesis. *Biochim. Biophys. Acta - Gene Regul. Mech.*, **1860**, 438–449.

Wu, M. *et al.* (2016) TGF-β and BMP signaling in osteoblast, skeletal development, and bone formation, homeostasis and disease. *Bone Res.*, **4**, 16009.

Yamashita, T. *et al.* (2012) New roles of osteoblasts involved in osteoclast differentiation. *World J. Orthop.*, **3**, 175–81.

Yanbaeva, D.G. *et al.* (2007) Systemic effects of smoking. *Chest*, **131**, 1557–66.

Yang, J.-H. and Lee, H.-G. (2010) 2,3,7,8-Tetrachlorodibenzo-p-dioxin induces apoptosis of articular chondrocytes in culture. *Chemosphere*, **79**, 278–284.

Yoon, V. *et al.* (2012) The effects of smoking on bone metabolism. *Osteoporos. Int.*, **23**, 2081–92.

Zhang, G. (2009) An evo-devo view on the origin of the backbone: evolutionary development of the vertebrae. *Integr. Comp. Biol.*, **49**, 178–186.

Zhang, Y.H. *et al.* (1990) Interleukin-6 induction by tumor necrosis factor and interleukin-1 in human fibroblasts involves activation of a nuclear factor binding to a kappa B-like sequence. *Mol. Cell. Biol.*, **10**, 3818–23.

CHAPTER 4

A Transcriptomic Assessment of Osteogenesis in TCDD-Exposed Human Bone-Derived Mesenchymal Stromal Cells

AtLee T. D. Watson*, Dereje D. Jima†, Seth W. Kullman*†

* Department of Biological Sciences, North Carolina State University, Raleigh, North Carolina 27695

† Center for Human Health and the Environment, North Carolina State University, Raleigh, North Carolina 27695

ABSTRACT

Bone formation requires strict coordination of transcriptional regulatory pathways to direct commitment and differentiation of mesenchymal stem cells to mature osteoblasts. There is increasing concern, however, that exposure to environmental xenobiotic stressors may perturb the gene regulatory networks and/or modulate the epigenomic landscape promoting lineage specification and differentiation from multipotent mesenchymal stem cells. Previous work indicates that 2,3,7,8-tetrachlorodibenzo-*p*-dioxin (TCDD), an AHR ligand, plays an inhibitory role in osteogenic differentiation in human bone-derived mesenchymal stromal cells (Chapter 3). Here we expand upon our targeted gene expression analysis to assess transcriptomic alterations during early (hours), intermediate (days), and apical (two and a half weeks post induction) stages of osteogenesis. Included in this assessment are GM/DMSO- (undifferentiated), ODM/DMSO- (differentiated), and ODM/TCDD-treated hBMSCs which permits identification of gene expression patterns present under normal and AHR-inhibited osteogenesis. While this assessment remains in progress, we present preliminary data from differentiated MSCs at 3 and 7 days post induction demonstrating TCDD-mediated alterations in extracellular matrix gene markers, transcriptional regulators, miRNA, and lincRNAs with essential roles in osteogenic differentiation. Our assessment has currently identified ~300 candidate epigenetic modulators previously shown to impact post-translational modification of histones, chromatin remodeling, and mRNA transcription or translation. GM/DMSO and ODM/TCDD demonstrate similar patterns in genes associated with stemness phenotypes suggesting that epigenetic modulation may in fact play a significant role in MSC lineage determination.

INTRODUCTION

Given their potential to differentiate into osteogenic, adipogenic, or chondrogenic lineages, mesenchymal stem cells (MSCs) are an attractive cell source for regenerative therapies targeting degenerative bone diseases such as osteoporosis, osteoarthritis, and rheumatoid arthritis (Baksh *et al.*, 2004; Abdallah and Kassem, 2008). At the same time, however, there is increasing concern that exposure to chemical agents in the environment may perturb cellular events governing lineage specification and/or differentiation of multipotent MSCs (Alexander *et al.*, 2016; Tyl *et al.*, 2007).

Bone formation requires strict coordination of cell signaling pathways, transcriptional gene regulatory networks, and epigenetic modifications to promote the transition of multipotent MSCs toward the osteoblast cell lineage (Karsenty *et al.*, 2009; Lian *et al.*, 2006; Montecino *et al.*, 2015; Gordon *et al.*, 2014). Runt-related transcription factor 2 (RUNX2) and osterix (OSX), considered the master regulators of osteogenesis (Nishio *et al.*, 2006; Nakashima *et al.*, 2002; Komori *et al.*, 1997), integrate upstream stimuli from multiple developmental pathways [e.g. WNT, bone morphogenetic protein (BMP), transforming growth factor beta (TGF-β), fibroblast growth factor (FGF), and Hedgehog signaling] to promote osteoblast differentiation (Marcellini *et al.*, 2012; Su *et al.*, 2008; Chen *et al.*, 2012). In doing so, RUNX2 and OSX activate transcription of bone extracellular matrix (ECM) genes encoding collagen type 1 alpha 1 (COL1A1), integrin-binding bone sialoprotein (IBSP), osteopontin (OPN), and osteocalcin (OSC) (Sinha and Zhou, 2013). The composition of bone ECM plays a key role in supporting subsequent osteogenic differentiation of MSCs *in vitro* (Marta

Baroncelli *et al.*, 2017), suggesting multiple levels and temporal stages of control underlying bone formation.

While RUNX2 and OSX are necessary for osteoblast differentiation, additional regulators appear to drive the initial transition from MSC multipotency toward an osteogenic lineage. Under osteogenic conditions *in vitro*, hBMSCs undergo three phases of differentiation during the first four days in culture: initiation (0-3 hours), lineage acquisition (6-24 hours), and early lineage progression (48-96 hours) (van de Peppel *et al.*, 2017). During the initiation phase, cell cycle genes are downregulated, which corresponds with an exit from the proliferative phase. Meanwhile, *distal-less homeobox 5* (*DLX5*), an upstream regulator of *OSX* and *RUNX2*, is upregulated within hours of osteogenic induction. During the second and third phases, expression of lineage specific transcription factors diminishes and by 96 hours hMBSCs have acquired a osteoblastic phenotype characterized by induction of bone ECM genes (van de Peppel *et al.*, 2017).

Epigenetic mechanisms have also been implicated in mesenchymal stem cell fate determination. Thus far, multiple epigenetic mechanisms have been identified (Wu *et al.*, 2017). At the chromatin level, histone modifications and chromatin remodeling can modulate the change between transcriptionally-active euchromatin and transcriptionally-inactive heterochromatin. Structurally, chromatin is packaged into nucleosomes consisting of DNA wrapped around histone octamers consisting of H2A, H2B, H3, H4 (2 of each) subunits with an H1 histone joining adjacent nucleosomes (Jenuwein *et al.*, 2001). At a given gene locus, specific N-terminus residues (lysines, arginines, serines) on H3 and H4 histone tails can undergo post-translational modifications including acetylation, methylation, phosphorylation,

and ubiquitination. These modifications can modulate the recruitment of chromatin remodeling complexes, nucleosome structure, and accessibility of enhancer and promoter elements to specific transcriptional regulators. Under osteogenic conditions, for example, both RUNX2 and ALP promoters demonstrate enrichment of H3K4me3 (trimethylation of lysine 4 on histone 3) (Håkelien *et al.*, 2014), which is typically associated with transcriptionally active gene loci. Conversely, H3K27me3 and H3K9me3 are present in the promoters of transcriptionally-inactive genes. Histone acetylation, on the other hand, alters chromatin structure through recruitment of Polycomb group (PcG) and Trithorax group (TrxG) chromatin remodeling complexes (Kimura, 2013; Gordon *et al.*, 2014).

More recently, long non-coding RNAs (lncRNAs) and microRNAs (miRs) have demonstrated roles in epigenetic regulation of MSC fate and differentiation. Several miRs have essential roles in osteogenic differentiation including *miR-204*, *miR-26*, *miR-206*, *miR-148-3p*, *miR-141*, *miR-200a*, and *miR-125b* (Itoh *et al.*, 2009; Inose *et al.*, 2009; Tian *et al.*, 2017; Huang *et al.*, 2010; Mizuno *et al.*, 2008). In contrast, lncRNAs (>200 nucleotides) modulate gene expression through diverse mechanisms acting as decoys/sponges for miRs, guides to specific promoter/enhancer elements, and scaffold-like structures bridging transcriptional regulators at one locus with another co-regulated locus (Derrien *et al.*, 2012; Flynn and Chang, 2014; Tye *et al.*, 2015). While still an emerging field, several studies in mouse and human MSCs demonstrate repressive roles of *differentiation antagonizing non-protein coding RNA* (*DANCR), Msh homeobox 1 antisense* (*MSX1-as*), *lncRNA associated with liver regeneration 1* (*LALR1*) lncRNAs in repressing osteogenic differentiation (Tye *et al.*, 2015). In mice, loss of the lncRNA *Hotair* results in abnormal skeletal patterning of the vertebral and and distal

limb structures , which suggests a putative role for HOTAIR in human osteogenic differentiation (Li *et al.*, 2013).

In this study we seek to identify how exposure to a prototypic aryl hydrocarbon receptor ligand, 2,3,7,8-tetrachlorodibenzo-*p*-dioxin (TCDD), impacts early regulators of osteogenic specification and differentiation from MSCs. The AhR is a basic-Helix-Loop-Helix/Per-ARNT-Sim (bHLH-PAS) transcription factor and functions as a master regulator of xenobiotic metabolism with reported toxicity to cell specification, differentiation, and proliferation in multiple target tissues (Chopra and Schrenk, 2011; Abel and Haarmann-Stemmann, 2010). Previous work from others demonstrates that differentiation of mesenchymal-derived cells (adipocytes, osteoblasts, chondrocytes) are particularly sensitive targets to AhR-mediated toxicity (Li *et al.*, 2008; Kung *et al.*, 2011; Gadupudi *et al.*, 2015; Naruse *et al.*, 2002; Ryan *et al.*, 2007). Moreover, recent work demonstrates that the AhR plays a role in maintaining pluripotency in embryonic stem cells (Ko *et al.*, 2016). In this study we hypothesize that TCDD inhibits osteogenic differentiation through modification of the epigenomic landscape, thus altering the ability of key lineage-specific regulators to be transcribed and promote the transition to an osteogenic fate. To further guide this hypothesis, we conducted RNA-Seq on GM-, ODM-, and ODM+TCDD-exposed hBMSCs across multiple stages of osteogenic differentiation (3 hours, 24 hours, 3 days, 7 days, and 17 days post osteogenic induction) to identify global changes in gene expression of epigenetic modifiers, which may play a key role in osteogenic differentiation. Here we present the analyzed data from 3 and 7 days post induction (dpi) and will present the remainder of the time points as a peer-reviewed publication at a later date.

METHODS AND MATERIALS

hBMSC Culture and TCDD Exposure

Excess bone fragments were obtained from a single donor (25-year-old, non-osteoporotic female) at the University of North Carolina-Chapel Hill hospitals (IRB exemption protocol: 10-0201). Human MSC cells were isolated and characterized (Sakaguchi *et al.*, 2009; Charoenpanich *et al.*, 2014; Bodle *et al.*, 2014), and multilineage potential was confirmed as described previously in Chapter 3. For subsequent experiments, hBMSCs at passage 2 were revived and expanded in growth media (GM) consisting of α-MEM (GE Healthcare) supplemented with 10% fetal bovine serum (FBS, Rocky Mountain Biologicals), 2 mM L-glutamine (Genesee Scientific), 100 U/ml penicillin, and 100 ug/ml streptomycin (Genesee Scientific) and maintained under standard cell culture conditions (37° C, 5% CO_2, in a sterile humidified chamber).

hBMSCs between passages 5 and 6 were seeded into 12-well tissue culture treated plates (Genesee Scientific) at a density of $1x10^4$ cells/cm^2 in GM. After 24 hours, media was replaced with osteogenic differentiation media (ODM) consisting of α-MEM supplemented with 10% FBS, 2 mM L-glutamine, 100 U/mL penicillin, and 100 μg/mL streptomycin, 50 μM ascorbic acid (Sigma-Aldrich), 0.1 μM dexamethasone (Sigma-Aldrich), and 10 mM β-glycerophosphate (Sigma-Aldrich) to induce differentiation (day 0). Cells were cultured for up to 17 days in ODM containing 0.1% dimethyl sulfoxide (DMSO, vehicle control) (ODM-DMSO) or 10 nM 2,3,7,8-tetrachlorodibenzo-*p*-dioxin (TCDD, Cambridge Isotopes Laboratory) (ODM-TCDD). As a negative control, hBMSCs were cultured in GM with 0.1%

DMSO (GM-DMSO) to provide an undifferentiated reference cell population. Samples from three experiments were used for the experiments described below.

RNA Isolation

Cells were harvested for total RNA at 3 hours, 24 hour, 3 days, 7 days, and 17 days post osteogenic induction (dpi). Briefly, cells were washed twice in PBS and lysed in TRI Reagent® (Ambion®, Life Technologies) and total RNA was isolated according to the manufacturer's instructions. Total RNA was quantified using Agilent 2100 Bioanalyzer and 2100 Expert Software package (Agilent Technologies). RNAs with RNA Integrity numbers (RINs) lower than 9 were excluded for subsequent RNA-Seq and qPCR validation experiments.

RNA-Sequencing

Total RNA samples from GM/DMSO-, ODM/DMSO-, and ODM/10 nM TCDD-treated hBMSCs (n=4/treatment) were submitted to the North Carolina State Genomic Sciences Laboratory (Raleigh, NC, USA) for Illumina RNA library construction and sequencing. Prior to library construction, RNA integrity, purity, and concentration were assessed using an Agilent 2100 Bioanalyzer with an RNA 6000 Nano Chip (Agilent Technologies, USA). Purification of messenger RNA (mRNA) was performed using the oligo-dT beads provided in the NEBNext Poly(A) mRNA Magnetic Isolation Module (New England Biolabs, USA). Complementary DNA (cDNA) libraries for Illumina sequencing were constructed using the NEBNext Ultra Directional RNA Library Prep Kit (NEB) and NEBNext Mulitplex Oligos for Illumina (NEB) using the manufacturer-specified protocol. Briefly, the mRNA was chemically fragmented and primed with random oligos for first strand cDNA

synthesis. Second strand cDNA synthesis was then carried out with dUTPs to preserve strand orientation information. The double-stranded cDNA was then purified, end repaired and "a-tailed" for adaptor ligation. Following ligation, the samples were selected for a final library size (adapters included) of 400-550 bp using sequential AMPure XP bead isolation (Beckman Coulter, USA). Library enrichment was performed and specific indexes for each sample were added during the protocol-specified PCR amplification. The amplified library fragments were purified and checked for quality and final concentration using an Agilent 2200 Tapestation with a High Sensitivity DNA chip (Agilent Technologies, USA) and a Qubit fluorometer (ThermoFisher, USA). The final quantified libraries were pooled in equimolar amounts for clustering and sequencing on an Illumina HiSeq 2500 DNA sequencer, utilizing a 125 bp single end sequencing reagent kit (Illumina, USA). The software package Real Time Analysis (RTA), was used to generate raw bcl, or base call files, which were then de-multiplexed by sample into fastq files for data submission.

Statistical Analysis

Data analysis was performed in consultation with the Bioinformatics Core at North Carolina State University Center for Human Health and the Environment. Approximately ~36 million single-end raw RNAseq reads data were generated for each replicate (n=4/treatment). The quality of sequenced data was assessed using FastQC, and trimmed reads were aligned to the Human reference genome (hg38) using STAR aligner (Dobin *et al.*, 2013). For each replicate, per-gene counts of uniquely mapped reads were calculated using the *htseq-count* script from the HTSEeq python package. Count data were normalized for sequencing depth and distortion, and dispersion was estimated using DESeq2 (Love *et al.*, 2014) Bioconductor

package in the R statistical computing environment. A linear model was fit using the treatment levels, and differentially-expressed genes were identified after applying multiple testing correction using Benjamini-Hochberg procedure (p_{adj}<0.05) (Benjamini and Hochberg, 1995) Downstream analyses were conducted on differentially-expressed genes exhibiting 1.5-fold up- or downregulation (p_{adj}<0.05). BioVenn was used to construct Venn diagrams identifying genes with shared expression patterns between datasets (Hulsen *et al.*, 2008). Pathway analyses were conducted in Reactome (Joshi-Tope *et al.*, 2005) and Ingenuity Pathway Analysis (IPA) to identify functional and disease pathways associated with enriched gene datasets..

RESULTS

In this study hBMSCs were cultured in growth media (GM-DMSO), osteogenic media (ODM-DMSO), and osteogenic media + 10 nM TCDD (ODM-TCDD). In each experiment used for RNA-Seq analysis, a separate plate was cultured until 17 days post inductions (dpi) for Alizarin Red S (AR-S) staining. All experiments demonstrated negative AR-S staining (-) in GM-DMSO cells, robust AR-S positive staining in ODM-DMSO cells (+++), and attenuated AR-S staining (+) in ODM-TCDD cells (data not presented here; see Chapter 3, Figure 2).

Clustering analysis was conducted to compare gene expression profiles in 3 dpi and 7 dpi samples. Hierarchical analysis reveals primary groupings based on media type (GM vs. ODM), with GM-DMSO cells displaying a distinctly different gene expression profile than ODM-DMSO or ODM-TCDD. Secondary clustering reveals differences based on TCDD treatment, and final clustering based on time points (3 dpi vs 7 dpi) (Figure 1A). These data were subjected to a principle component analysis (PCA), which demonstrated that ODM accounts for 84% of the variance in differential gene expression (Figure 1B, x-axis). The effect of TCDD treatment is apparent given the divergence between ODM-DMSO and ODM-TCDD groups which accounts for 10% of the variance between the three groups (Figure 1B, y-axis). Furthermore, the almost overlapping plots of 3 and 7 dpi GM-DMSO samples confirm that their expression profiles are not changing over time in GM, suggesting that they remain in an undifferentiated state. Conversely, the gene expression profiles of 7 dpi ODM-DMSO and ODM-TCDD are more distant from GM-DMSO plots than the same treatments at 3 dpi (Figure 1B).

Next, we compared differentially-expressed genes (DEGs) between ODM-DMSO and GM-DMSO between 3 and 7 dpi. Here the addition of ODM resulted in 3,774 and 4,212 DEGs (≥ 1.5-fold increase or decrease, $p_{adj<}$ 0.05) at 3 dpi and 7 dpi, respectively (Table 1). Next, we compared upregulated genes at both time points to determine overlapping expression profiles. More than two-thirds (n=1,449) of the 2,076 upregulated genes at 3 dpi and 2,106 genes upregulated at 7 dpi demonstrated increased expression. A similar trend was observed with attenuated gene expression where 1,251 genes commonly exhibited a decreased in expression at 3 and 7 dpi. Next, Reactome pathway analysis was performed with combined up and down regulated gene sets to identify functional pathways associated with hMSC osteoinduction. This analysis revealed a prominent signal for WNT, BMP/TGF-β, Hedgehog, and NOTCH signaling, and identified highly enriched pathways involving vesicle-mediated transport, extracellular matrix (ECM) formation, organization, and degradation. Within these pathways we observe increased expression of mediators known to promote osteogenesis (e.g. *DLX5*, *RUNX2*, *NKX3.2*, *RSPO1-3*, *CTNNB1*) and reduced expression of FGF signaling (e.g. *FGF2*, *FGF9*) or other MSC-derived lineage markers (e.g. *SOX9*). We also observed a reduction in expression of FGF signaling mediators associated with MSCs (Figure 2A, B, refer to Tables 2-6).

To investigate the role of ligand-activated AHR on the osteogenic transcriptome, we compared the DEG profiles between ODM-TCDD vs. ODM-DMSO cells. TCDD exposure resulted in 1,247 and 1,941 DEGs (≥ 1.5-fold increase or decrease, $p_{adj<}$ 0.05) at 3 dpi and 7 dpi, respectively (Table 1). Reactome pathway analysis of these DEGs revealed several pathways enriched in genes associated with WNT signaling, vesicle-mediated transport, and

ECM formation, organization, and degradation. When analyzing the shared upregulated genes (n=409) we also observe TCDD-mediated induction of genes associated with xenobiotic metabolism and FGFR signaling/disease pathways (Figure 3A). Common downregulated genes (n=401) between the two timepoints appear to impact pathways associated with interleukin signaling, the unfolded protein response (UPR), and nucleosome and/or chromatin organization (Figure 3B).

To better understand how TCDD impacted osteogenic signaling pathways, an expression analysis was conducted in Ingenuity Pathway Analysis (IPA) using 7 dpi ODM-TCDD vs ODM-DMSO samples. Overall IPA confirmed results obtained from the Reactome pathway analyses and illustrated significant alterations to ligands and receptors within the BMP, FGF, WNT, and TGF-β (Figure 4). In addition, inhibitors to these pathways such as *GREM1* (inhibits BMP) were induced by TCDD exposure. A subsequent analysis investigated shared interactions between genes associated with AHR signaling, differentiation of MSCs, and differentiation of osteoblasts. From this analysis, several genes of interest were identified including the epigenetic modifier *EZH2*, adipogenic regulators PPAR-γ and C/EBPα, angiongenic factor VEGF-A, and extracellular matrix genes FBN2, and VIM (Figure 5).

Next, we attempt to highlight genes that promote osteogenesis whose expression under osteogenic conditions appears to be particularly sensitive to TCDD exposure. Datasets were filtered for DEGs with 1.5-fold induction under osteogenic conditions (ODM-DMSO vs GM-DMSO), but were also repressed 1.5-fold in the presence of TCDD (ODM-TCDD vs ODM-DMSO). Under this criterion we identified consistent expression profiles of a few WNT, FGF, and BMP/TGF-β mediators (*DKK1*, *FGFR3*, *LTBP2*), ECM components/regulators (*ALPL*,

FBN2, *MGP*), and a long intergenic non-coding RNAa (*LINC00707*) and numerous epigenetic modulators (*PRC1*, *METTL7A/B*, *SUSD2*) between 3 dpi and 7 dpi (Figure 6A). Furthermore, *EZH2*, a known epigenetic modulator of MSC differentiation, was also reduced with TCDD exposure despite its increased expression under osteogenic conditions (Figure 6A). Using the reverse criterion (decreased expression ODM-DMSO vs GM-DMSO; increased expression in ODM-TCDD vs ODM-DMSO), we did not observe any overlap between 3 dpi and 7 dpi, however, at 7 dpi we observe several genes associated with either stemness or osteogenic inhibition (e.g. *SALL4*, *FGF9*, *CXCL12*, *INHA*, *IHBB*, *TGFBR1*) Another set of epigenetic modulators, SUV39H1/2 were identified at 7 dpi (Figure 6B).

Given the LINCRNAs identified in Figure 6, we assessed patterns in RNA-seq "transcript abundance" to identify candidate lincRNAs responsive to TCDD exposure. Here we reveal two primary patterns emerging in terms of lincRNA transcript abundance. LINC01616, LINC00900, and LINC01018 demonstrate reduced abundance when cultured in ODM-DMSO, however their abundance more closely resembles that of GM-DMSO when exposed to TCDD (Figure 5, top row). LINC00707 displays the opposite pattern of transcript abundance. That is, its abundance is highest with ODM-DMSO treatment but is reduced with TCDD exposure, more similar to that of GM-DMSO levels. Other abundant lincRNAs (LINC01182, LINC01272) appear responsive to ligand-activated AHR; however, their expression does not return to levels resembling that of GM-DMSO cells (Figure 5).

DISCUSSION

Bone formation is a particularly sensitive target of AhR ligands, including TCDD. Previously, our laboratory demonstrated AhR-mediated inhibition of osteoblast differentiation and bone formation in Japanese medaka following embryonic TCDD exposure (Watson *et al.*, 2017). A follow-up study confirmed the inhibitory role of TCDD in osteogenesis at the cellular level using hBMSCs (Watson *et al*., *in prep*). Using cells from Donor 1, we assessed global changes in gene expression throughout the course of osteogenic differentiation in the presence or absence of TCDD. Although incomplete in its current form (3 hpi, 24 hpi, and 17 dpi are awaiting analysis), our study provides critical insight at two intermediate timepoints at 3 dpi and 7 dpi during osteogenic differentiation. During this window of intermediate differentiation, we note significant differences in the genes comprising ECM pathways and mediators of the WNT, BMP/TGF-β, and FGF pathways. Given that functional pathways are shared between ODM-DMSO/GM-DMSO and ODM-TCDD/ODM-DMSO comparisons, but comprised of different DEGs suggests that TCDD is having a major effect on the osteogenic programming of hMBSCs as early as 3 and 7 dpi.

Expression of several osteogenic markers and regulators were upregulated under osteogenic conditions (ODM-DMSO) within 3 days. *DLX5* and *RUNX2*, were induced and maintained at both timepoints in ODM-DMSO relative to undifferentiated hBMSCs. Exposure to TCDD caused a significant reduction in DLX5 expression at 3 dpi but not 7 dpi; however, *RUNX2* expression was induced 1.44- and 1.47-fold (below the 1.5-fold threshold used in this analysis) above osteogenic controls at 3 dpi and 7 dpi, respectively. This finding confirms a similarly observed upregulation of *RUNX2* from previous experiments (Chapter 3) even though

we observed attenuated matrix mineralization at apical stages (Chapter 3, Watson *et al, in prep*). Though contrary to our hypothesis, this observation suggests that in our hBMSCs model, *RUNX2* induction alone is not sufficient to promote osteogenesis and that DLX5 may play a more prominent role than previously thought.

ALP has been considered a hallmark of immature osteoblasts given its role in converting pyrophosphate to inorganic phosphate in the extracellular environment. During subsequent stages of differentiation, inorganic phosphate and calcium form hydroxyapatite mineral [$Ca_5(PO_4)_3(OH)$] indicative of mineralized ECM (Golub and Boesze-Battaglia, 2007). Our data demonstrates induction of *ALP* in ODM-DMSO relative to undifferentiated controls, which indicates that these cells have acquired an osteogenic phenotype and are progressing through the osteogenic lineage. Under ODM-TCDD conditions, however, *ALP* expression was diminished at 3 dpi through 7 dpi, suggesting that TCDD has inhibited one or more aspects of early specification or differentiation.

The enrichment of functional pathways associated with synthesis, secretion, and organization of extracellular matrix lends additional support suggesting ODM-DMSO treated cells have acquired an osteogenic lineage. Our data demonstrates that TCDD exposure dysregulates genes encoding integrins, laminins, collagens, SERPIN (serine protease inhibitor) family members, ADAMTS (A Disintegrin and Metalloproteinase with Thrombospondin motif) family members, and the non-collagenous proteins IBSP (integrin-binding bone sialoprotein) and MGP (matrix Gla protein). This is important for several reasons. First, the correct balance of ECM proteins not only mediates ECM mineralization during ossification of bone, but it may also provide a supportive environment to promote future MSC differentiation

into osteoblasts during bone remodeling (Marta Baroncelli *et al.*, 2017; Avery *et al.*, 2017; Voss *et al.*, 2016). Second, several osteochondral disease states involve alterations to bone or cartilage ECM. Degenerative diseases such as rheumatoid arthritis (RA) and osteoarthritis (OA) involve focal erosions of bone or cartilage around articular joint spaces. Mutations in genes associated with osteoblast differentiation and collagen formation, synthesis, and processing are attributed to osteogenesis imperfecta (OI), a broad category of osteodysplasias characterized by deficits in ossification (Bishop, 2016; Christiansen *et al.*, 2010; Forlino *et al.*, 2011; Kang *et al.*, 2017). Based on our data from this intermediate window of osteogenesis, TCDD alters gene expression of critical ECM modulators, which may impact the overall composition of the ECM. In doing so, TCDD and other AhR ligands may exacerbate the development of degenerative diseases or mimic the effects of gene mutations in key osteogenic pathways.

Our assessment at 3 dpi and 7 dpi provides insight into early ECM formation events, as well as key insight into various developmental pathways that influence osteogenesis. One of the major goals for this study, however, was to identify epigenetic regulators which may influence TCDD's inhibitory role in osteogenesis. Another gene of interest is the H3K9me3 methyltransferase SUV391H1/2 identified from our ODM-TCDD/ODM-DMSO comparison. At 7 dpi both *SUV39H1* and *SUV39H2* are induced with TCDD, however, both were significantly down in ODM-DMSO. Interestingly, mice with SUV39H1 depletion experienced a greater bone mineral density (Liu *et al.*, 2013), which suggests that SUV39H1 may play a significant role in bone formation and is a sensitive target of AhR activation. Expression of *EZH2*, an important H3K27 methyltransferase and regulator of MSC commitment, was

reduced at 3 dpi with TCDD exposure but upregulated under normal osteogenic conditions. This is an interesting finding in light of a previous study demonstrating that inhibition of EZH2 promotes MSC differentiation to an osteogenic lineage and enhances osteogenic differentiation (Dudakovic *et al.*, 2015). Based on the overall inhibition of osteogenesis following TCDD exposure, one might expect *EZH2* expression to be upregulated thus preventing MSC commitment to an osteogenic lineage. It is worth noting, however, that data from the two early timepoints (3 hpi and 24 hpi) will provide a more accurate assessment of changes in gene expression that may drive the early MSC-osteoblast commitment. The same logic applies for our assessment of genes influencing stem cell potency (*SALL4*, *OCT4*, *NANOG*, and *SOX2*), as *SALL4* was the only gene from that set that was induced (7 dpi) by TCDD and downregulated by ODM-DMSO.

In conclusion, we have provided a cursory assessment corresponding to the intermediate stages of osteogenic differentiation. Here, we demonstrate several osteogenic markers and regulators with critical roles in osteogenesis whose expression is significantly reduced with ODM-TCDD. Furthermore, the identification of altered ECM functional pathways suggests that TCDD may impact the structural scaffolding that enables subsequent differentiation. It is important to note, however, that this may in fact be a "chicken or the egg" scenario. For example, TCDD exposure may inhibit early stages of specification and differentiation, which are thus reflected in an altered ECM environment. Alternatively, does TCDD inhibit or alter later ECM formation, and thus prevent subsequent apical stages of differentiation? As more data become available, we anticipate gaining more insight to address these fundamental questions.

TABLES

Table 1. Summary table describing numbers of differentially-expressed genes (DEGs) at 3 and 7 days post osteogenic induction. Two comparisons were conducted: ODM-DMSO (differentiated) vs. GM-DMSO (undifferentiated) cells, and ODM-TCDD vs. ODM-DMSO cells. Genes 1.5-fold induced or reduced in expression with $p_{adj}<0.05$ were included for subsequent analyses.

ODM-DMSO vs. GM-DMSO			
Timepoint	*Total*	↑ *1.5-fold*	↓ *1.5-fold*
3 dpi	3774	2075	1699
7 dpi	4212	2106	2106
ODM-TCDD vs ODM-DMSO			
Timepoint	*Total*	↑ *1.5-fold*	↓ *1.5-fold*
3 dpi	1247	706	541
7 dpi	1941	1091	850

Table 2. Reactome pathway analysis of induced genes in ODM-DMSO relative to GM-DMSO at 3 days post osteogenic induction. Genes with 1.5-fold increased expression (n=2075, $p_{adj}<0.05$) were identified, and submitted to the Reactome database to identify enrichment within human biological pathways. Among the most highly enriched pathways were generic in classification (e.g. cell cycle, metabolism, gene expression, developmental biology). Specific pathways associated with osteogenic signaling pathways, extracellular matrix synthesis and remodeling, and epigenetic modifications (highlighted in gray) are listed below.

Pathway	# Genes	Enriched Genes
Vesicle-mediated transport	71	*HIP1;ITSN1;HP;CLTB;PRKAG2;ARRB1;KIF11;FNBP1L;ACTB;SLC 2A8;KIF15;TUBA1B;GJA5;KIF13B;KIF1C;POTEF;CTSC;YWHAH;S H3D19;SCARA5;SGIP1;KIF23;KIF22;SPTB;ANK1;TBC1D1;RAB31; MYH3;TBC1D4;COL4A2;COL4A1;DNAJC6;KIFC1;AGTR1;KIF2C; KIF20A;KIF20B;GRIA1;RABGAP1;DCTN1;DENND3;LRP2;ADRB2; ALS2CL;RACGAP1;MYO6;MAN1C1;REPS2;APOE;APOB;DYNC1I1 ;TBC1D16;AP1M1;SORT1;FZD4;HIP1R;RAB27B;HPS5;TRAPPC9; TUBB4B;CENPE;KIF18A;KIF18B;MYO1C;SYNJ1;KIF4B;KIF4A;C OL7A1;SAA1;TRIP10*
Membrane Trafficking	65	*HIP1;ITSN1;CLTB;PRKAG2;ARRB1;KIF11;FNBP1L;ACTB;SLC2A8 ;KIF15;TUBA1B;GJA5;KIF13B;KIF1C;POTEF;CTSC;YWHAH;SH3 D19;SGIP1;KIF23;KIF22;SPTB;ANK1;TBC1D1;RAB31;MYH3;TBC 1D4;DNAJC6;KIFC1;AGTR1;KIF2C;KIF20A;KIF20B;GRIA1;RABG AP1;DCTN1;DENND3;LRP2;ADRB2;ALS2CL;RACGAP1;MYO6;MA N1C1;REPS2;APOB;DYNC1I1;TBC1D16;AP1M1;SORT1;FZD4;HIP 1R;RAB27B;TRAPPC9;TUBB4B;CENPE;KIF18A;KIF18B;MYO1C;S YNJ1;KIF4B;KIF4A;COL7A1;TRIP10*
Interleukin-4 and 13 signaling	54	*LAMA5;CXCL8;MAOA;ITGB2;TWIST1;PIK3R1;FOXO3;PTGS2;FO XO1;ICAM1;SOCS1;CCND1;S1PR1;LBP;JAK2;IL6R;JAK3;JUNB;M CL1;IL18;HPS5;FOS;BATF;POMC;ZEB1;SAA1;FSCN1;BIRC5;BCL 2L1*
Extracellular matrix organization	54	*DDR1;COLGALT2;ITGB5;ELN;ITGB2;ICAM1;COMP;ADAMTS4;M MP24;IBSP;SH3PXD2A;KDR;EMILIN1;ITGB6;ADAMTS9;MMP7;IT GA4;MME;ITGA3;ACTN1;ITGA1;DCN;COL4A2;COL4A1;MMP15; COL4A4;COL4A3;COL8A1;MMP19;ITGA5;MATN3;PLEC;ITGA9;F BN2;LAMA5;COL11A1;FBLN1;LTBP2;FURIN;NID1;NID2;FBLN5; ACAN;SCUBE3;A2M;JAM2;COL28A1;MFAP5;BMP2;COL7A1;ITG A10;COL9A3;COL9A2;FMOD*

Table 2 Continued

Signaling by WNT	32	*WNT2B;HIST1H2BJ;HIST1H2BK;LEF1;ITPR1;CLTB;WNT11;H2AFJ;RSPO2;RSPO3;RSPO1;MIR92B;TLE2;FZD5;FZD4;H2AFX;SOX13;FZD8;AXIN2;GNG11;DKK1;GNAO1;SFRP1;APC;HECW1;GNB4;CTNNB1;HIST1H2BG;PLCB2;LGR5*
Chromosome Maintenance	30	*PCNA;HIST1H2BJ;PRIM1;HIST1H2BK;HJURP;H2AFJ;MIS18BP1;POLD1;OIP5;POLE;CENPU;RFC3;CENPW;LIG1;RFC2;H2AFX;KNL1;POLA2;CENPH;CENPI;POLE2;CENPK;CENPM;CENPN;CENPO;HIST1H2BG;DNA2;CENPP*
MAPK family signaling cascades	30	*CAMK2B;HSPB1;ARRB1;IRS2;RASAL2;FOXO3;FOXO1;ACTB;CCND3;FGF7;POTEF;JAK2;IL6R;JAK3;DUSP4;DUSP5;ANGPT1;DUSP1;NCOA3;ETV4;SPTB;GRIN2D;DUSP7;FGF18;CDK1;IL6ST;FGFR3;VCL*
Cellular Senescence	27	*MAP2K3;CBX6;CXCL8;CDKN2C;HIST1H2BJ;UBE2C;CBX2;H2AFX;HIST1H2BK;FOS;ETS2;LMNB1;CCNA2;MIR24-2;CCNE2;H2AFJ;ID1;CDK2;E2F1;E2F2;HIST1H2BG;MAP2K6;MAP3K5;HIST1H1C*
Organelle biogenesis and maintenance	25	*SHC4;PLK4;C2CD3;DCTN1;NDE1;PLK1;PRKAG2;KIF24;CYS1;TUBB4B;WDR34;KIF17;TUBA1B;ARL13B;PRKAR2B;CENPJ;TCTEX1D1;CNTRL;CDK1;NEK2;PPARGC1A;RAB11FIP3;CEP78*
MAPK1/MAPK3 signaling	24	*DUSP4;CAMK2B;DUSP5;ANGPT1;DUSP1;ARRB1;IRS2;RASAL2;SPTB;ACTB;GRIN2D;DUSP7;FGF7;FGF18;CDK1;POTEF;JAK2;IL6ST;IL6R;JAK3;FGFR3;VCL*
Integrin cell surface interactions	22	*ITGA4;ITGB5;ITGA3;ITGA1;ITGB2;ICAM1;COMP;IBSP;COL4A2;COL4A1;COL4A4;COL7A1;ITGA10;COL4A3;KDR;COL8A1;COL9A3;COL9A2;ITGA5;ITGB6;JAM2;ITGA9*
TCF dependent signaling in response to WNT	22	*TLE2;HIST1H2BJ;FZD5;FZD4;HIST1H2BK;H2AFX;LEF1;SOX13;FZD8;AXIN2;DKK1;SFRP1;APC;H2AFJ;HECW1;RSPO2;RSPO3;CTNNB1;HIST1H2BG;RSPO1;LGR5*
Signalling by NGF	21	*DUSP4;NGFR;PLEKHG2;ARHGEF26;ARHGEF37;MCF2;ARHGEF17;ARHGEF39;PLEKHG5;ITSN1;ARHGEF19;FURIN;IRS2;PIK3R1;PCSK6;DUSP7;NFKBIA;AKAP13;FGD4;PLCG1;ECT2*
Gastrin-CREB signalling pathway via PKC and MAPK	21	*EDN1;OXTR;TRPC6;PRKCH;ITPR1;HPS5;LPAR4;PIK3R1;FPR2;RASGRP2;ADRA1B;GNG11;RGS2;EDNRA;P2RY6;LPAR6;P2RY2;AGTR1;SAA1;GNB4;PLCB2;MGLL*

Table 2 Continued.

PIP3 activates AKT signaling	20	*PHLPP2;USP13;EGR1;HDAC5;CBX6;CBX2;CD80;PIK3CD;IRS2;PIK3R1;FOXO3;FOXO1;MTOR;NR4A1;FGF7;RRAGD;FGF18;PPARG;FGFR3*
Nucleosome assembly	18	*CENPU;CENPW;HIST1H2BJ;HIST1H2BK;H2AFX;HJURP;KNL1;CENPH;CENPI;MIS18BP1;H2AFJ;CENPK;CENPM;OIP5;CENPN;HIST1H2BG;CENPO;CENPP*
Transcriptional regulation by RUNX1	18	*BLK;CBX6;SMARCD2;HIST1H2BJ;CBX2;HIST1H2BK;H2AFX;HIPK2;H19;CCND3;CCND1;H2AFJ;RSPO3;HIST1H2BG;MYL9*
Signaling by VEGF	17	*NRP2;JUP;ROCK1;PXN;ITPR1;HSPB1;CYBA;PIK3R1;MTOR;ACTB;CDH5;KDR;PTK2B;CTNNB1;POTEF;PLCG1;WASF3*
ECM proteoglycans	16	*LAMA5;ITGB5;DCN;COMP;ACAN;IBSP;COL4A2;COL4A1;COL4A4;COL4A3;COL9A3;COL9A2;ITGB6;FMOD;MATN3;ITGA9*
Polo-like kinase mediated events	15	*CCNB2;CCNB1;CENPF;PLK1;MYBL2;LIN9;FOXM1;CDC25C;PKMYT1;CDC25A*
AURKA Activation by TPX2	15	*SHC4;PLK4;DCTN1;NDE1;PLK1;HMMR;TUBB4B;AURKA;TPX2;PRKAR2B;CENPJ;CNTRL;CDK1;NEK2;CEP78*
Transcriptional regulation by RUNX2	15	*DLX5;TWIST1;AR;BMP2;CCNB1;CCND1;CDK1;ITGBL1;HIVEP3;ITGA5;SKP2;PPARGC1A;NKX3-2*
B-cat independent WNT signaling	15	*FZD5;FZD4;LEF1;ITPR1;CLTB;FZD8;AXIN2;GNG11;GNAO1;WNT11;GNB4;CTNNB1;MIR92B;PLCB2*
Transport of inorganic cations/anions and amino acids/oligopeptides	15	*SLC36A1;SLC26A2;SLC24A3;SLC43A2;SLC20A1;SLC43A1;SLC7A2;SLC7A6;SLC7A8;SLC17A5;SLC26A7;SLC17A7;SLC26A6;SLC38A4*
Deubiquitination	25	*BARD1;USP13;HIST1H2BJ;HIST1H2BK;ARRB1;AXIN2;ADRB2;BRCA1;USP18;ACTB;CDC25A;TGFBR2;NFKBIA;CDC20;CCNA2;AR;RNF128;APC;STAMBPL1;CDK1;HIST1H2BG;CLSPN;SKP2;BIRC3*
Regulation of Insulin-like Growth Factor (IGF) transport and uptake by IGF Binding Proteins (IGFBPs)	19	*ITIH2;CSF1;IGFBP4;IGFBP2;IGF2;PCSK9;MSLN;CP;APOA5;FSTL3;C3;ENAM;MGAT4B;MXRA8;APOE;GAS6;APOB;MFGE8;MATN3*
Ub-specific processing proteases	18	*USP13;HIST1H2BJ;HIST1H2BK;ARRB1;AXIN2;ADRB2;USP18;CDC25A;NFKBIA;CDC20;CCNA2;AR;RNF128;HIST1H2BG;CLSPN;SKP2;BIRC3*

Table 2 Continued.

Telomere Maintenance	17	*RFC3;PCNA;HIST1H2BJ;LIG1;RFC2;PRIM1;HIST1H2BK;H2AFX;POLA2;H2AFJ;POLD1;POLE2;HIST1H2BG;DNA2;POLE*
Orc1 removal from chromatin	13	*CCNA2;CDT1;ORC6;ORC1;MCM8;CDK2;MCM3;MCM4;MCM5;MCM6;CDC6;MCM2*
Collagen formation	13	*COL28A1;COLGALT2;MMP7;COL11A1;COL4A2;COL4A1;COL4A4;COL7A1;COL4A3;COL8A1;COL9A3;COL9A2;PLEC*
SUMO E3 ligases SUMOylate target proteins	13	*TOP2A;PIAS3;BLM;PCNA;SP110;CBX2;CDCA8;BRCA1;RANGAP1;AURKB;AURKA;INCENP;BIRC5*
SUMOylation	13	*TOP2A;PIAS3;BLM;PCNA;SP110;CBX2;CDCA8;BRCA1;RANGAP1;AURKB;AURKA;INCENP;BIRC5*
PPARA activates gene expression	13	*FADS2;NCOA3;CYP1A1;ANKRD1;PPARG;ANGPTL4;APOA5;PPARGC1A;SREBF2*
Unwinding of DNA	12	*GINS1;GINS2;CDC45;MCM8;GINS3;GINS4;MCM3;MCM4;MCM5;MCM6;MCM2*
Signaling by TGF-beta family members	12	*ACVRL1;BMP2;RBL1;NOG;PMEPA1;SMAD9;FURIN;BMPR1B;JUNB;FSTL3;TGFBR2*
PI3K/AKT Signaling in Cancer	12	*NR4A1;FGF7;CD80;FGF18;PIK3CD;IRS2;PIK3R1;FOXO3;FGFR3;FOXO1;MTOR*
Assembly of collagen fibrils and other multimeric structures	11	*MMP7;COL4A2;COL4A1;COL4A4;COL7A1;COL11A1;COL4A3;COL8A1;COL9A3;COL9A2;PLEC*
Collagen biosynthesis and modifying enzymes	11	*COL28A1;COLGALT2;COL4A2;COL4A1;COL4A4;COL7A1;COL11A1;COL4A3;COL8A1;COL9A3;COL9A2*
Epigenetic regulation of gene expression	11	*DNMT1;MYO1C;HIST1H2BJ;UHRF1;H2AFJ;SUV39H1;HIST1H2BK;H2AFX;HIST1H2BG;ACTB;PHF19*
Chromatin organization	11	*SMARCD2;CCND1;HIST1H2BJ;H2AFJ;SUV39H1;HIST1H2BK;H2AFX;HIST1H2BG;JADE2;JAK2;ACTB*
Chromatin modifying enzymes	11	*SMARCD2;CCND1;HIST1H2BJ;H2AFJ;SUV39H1;HIST1H2BK;H2AFX;HIST1H2BG;JADE2;JAK2;ACTB*
Laminin interactions	10	*LAMA5;COL4A2;ITGA3;COL4A1;COL4A4;COL7A1;COL4A3;ITGA1;NID1;NID2*
Signaling by NOTCH	10	*HDAC5;NEURL1B;TLE2;CCND1;E2F1;ST3GAL6;ARRB1;FURIN;DTX4*

Table 2 Continued.

TRAF6 mediated induction of NFkB and MAP kinases upon TLR7/8 or 9 activation	9	*MAP2K3;DUSP4;NFKBIA;SAA1;HPS5;FOS;CD14;TLR4;DUSP7;MAP2K6*
Oncogene Induced Senescence	8	*MIR24-2;CDKN2C;ID1;E2F1;E2F2;ETS2*
IGF1R signaling cascade	8	*FGF7;FGF18;IGF2;IRS2;PIK3R1;FGFR3;IGF1R*
Signaling by MET	8	*LAMA5;LIG1;SPINT1;ITGA3;COL11A1;PIK3R1;SPINT2;TNS3*
Unfolded Protein Response (UPR)	8	*EXTL1;CXCL8;TATDN2;DCTN1*
Cell-extracellular matrix interactions	7	*ACTN1;PXN;TESK1;FLNA;POTEF;LIMS2;ACTB*
Regulation of FZD by ubiquitination	7	*FZD5;FZD4;RSPO2;RSPO3;FZD8;RSPO1;LGR5*
Positive epigenetic regulation of rRNA expression	7	*MYO1C;HIST1H2BJ;H2AFJ;HIST1H2BK;H2AFX;HIST1H2BG;ACTB*
Regulation of RUNX2 expression and activity	7	*BMP2;DLX5;TWIST1;HIVEP3;SKP2;PPARGC1A;NKX3-2*
SIRT1 negatively regulates rRNA expression	6	*HIST1H2BJ;H2AFJ;SUV39H1;HIST1H2BK;H2AFX;HIST1H2BG*
Gamma carboxylation, hypusine formation and arylsulfatase activation	6	*F10;PROS1;ARSK;FURIN;GAS6;ARSB*
Hedgehog 'on' state	6	*GPR161;HHIP;PTCH2;GAS1;ARRB1*
Signaling by FGFR	6	*FGF7;FGF18;PLCG1;PIK3R1;FGFR3*
XBP1(S) activates chaperone genes	6	*EXTL1;TATDN2;DCTN1*
IRE1alpha activates chaperones	6	*EXTL1;TATDN2;DCTN1*
Signaling by TGF-beta Receptor Complex	6	*RBL1;PMEPA1;FURIN;JUNB;TGFBR2*
PI Metabolism	6	*SYNJ1;TNFAIP8L1;PLEKHA6;PIK3CD;TNFAIP8L3;PIK3R1*

Table 2 Continued.

Activation of HOX genes during differentiation	6	*HIST1H2BJ;H2AFJ;NCOA3;HIST1H2BK;H2AFX;HIST1H2BG*
Anchoring fibril formation	5	*COL4A2;COL4A1;COL4A4;COL7A1;COL4A3*
Signaling by BMP	5	*ACVRL1;BMP2;NOG;SMAD9;BMPR1B*
Transcriptional regulation of pluripotent stem cells	4	HIF3A;EPHA1;DKK1
AKT phosphorylates targets in the nucleus	3	NR4A1;FOXO3;FOXO1
TNF receptor superfamily (TNFSF) members mediating non-canonical NF-kB pathway	3	TNFSF14;BIRC3
TGF-beta receptor signaling activates SMADs	3	PMEPA1;FURIN;TGFBR2

Table 3. Reactome pathway analysis of genes with reduced expression in ODM-DMSO relative to GM-DMSO at 3 days post osteogenic induction. Genes with 1.5-fold reduced (0.67x) expression (n=1699, p_{adj}<0.05) were identified, and submitted to the Reactome database to identify enrichment within human biological pathways. Among the most highly enriched pathways were generic in classification (e.g. cell cycle, metabolism, gene expression, developmental biology). Specific pathways associated with osteogenic signaling pathways, extracellular matrix synthesis and remodeling, and epigenetic modifications (highlighted in gray) are listed below.

Pathways	**# Genes**	***Genes***
G1/S Transition	25	*CDT1;RRM2;MCM10;CDC6;TYMS;CDC25A;CCNB1;ORC6;CDC45;CCNE2;POLE2;E2F1;CDK1;MCM5;TK1;FBXO5*
G2/M Transition	23	*PLK4;PLK1;HMMR;FOXM1;CDC25C;PKMYT1;CDC25A;AURKA;CCNB2;TUBA1C;CCNB1;TUBA1B;CENPF;CDK1;CEP72;MYBL2;NEK2;GTSE1*
Signaling by Interleukins	20	*KL;DUSP5;DUSP2;IL18;LMNB1;FGF5;IL1RL2;KITLG;CDK1;BIRC5;IL7R;MET;FGFR3;STX1A*
Vesicle-mediated transport	19	*MRPS28;KIF11;TUBA1C;TUBA1B;GJB2;KIF18A;KIF18B;RACGAP1;KIFC1;COL7A1;GJA5;KIF4A;AGTR1;RAC3;KIF2C;KIF20A;AP1S3;KDELR3;KIF20B*
S Phase	18	*GINS1;CDT1;GINS2;LIG1;CDCA5;GINS3;GINS4;CDC6;ESCO2;CDC25A;ORC6;CDC45;CCNE2;POLE2;E2F1;MCM5*
Extracellular matrix organization	18	*FBN2;COLGALT2;PCOLCE2;ITGA3;P3H2;LTBP2;SCUBE3;ADAMTS3;LOX;COL7A1;P4HA3;ADAM12;SDC1;ITGA7;ITGA6;COL9A2;ITGA5;ITGA9*
G2/M Checkpoints	17	*BLM;MCM10;BRCA1;CDC6;CDC25C;PKMYT1;CDC25A;CCNB2;BRIP1;CCNB1;ORC6;CDC45;EXO1;CDK1;MCM5;CLSPN;GTSE1*
Polo-like kinase mediated events	14	*CCNB2;CCNB1;CENPF;PLK1;MYBL2;FOXM1;CDC25C;PKMYT1;CDC25A*
G0 and Early G1	13	*TOP2A;CCNE2;E2F1;CDK1;MYBL2;CDC6;CDC25A*
Chromosome Maintenance	10	*CENPU;CENPW;CENPH;LIG1;CENPI;POLE2;CENPK;CENPM;OIP5;KNL1*
Glycosaminoglycan metabolism	10	*CSGALNACT1;CHST6;CHST7;HYAL1;OGN;SDC1;CHSY3;HMMR*
MAPK1/MAPK3 signaling	10	*FGF5;KL;DUSP5;KITLG;DUSP2;CDK1;FGFR3;MET*

Table 3 Continued.

Collagen formation	9	*COLGALT2;ADAMTS3;PCOLCE2;LOX;COL7A1;P4HA3;P3H2;ITGA6;COL9A2*
Organelle biogenesis and maintenance	9	*PLK4;TUBA1C;TUBA1B;PLK1;CDK1;CEP72;KIF24;NEK2;CYS1*
Nucleosome assembly	8	*CENPU;CENPW;CENPH;CENPI;CENPK;CENPM;OIP5;KNL1*
Cellular Senescence	8	*CCNE2;UBE2C;E2F1;HMGA1;HMGA2;E2F2;LMNB1*
SUMO E3 ligases SUMOylate target proteins	7	*TOP2A;BLM;BIRC5;CDCA8;BRCA1;AURKB;AURKA*
PI3K/AKT Signaling in Cancer	7	*FGF5;KL;KITLG;FGFR3;MET*
SUMOylation	7	*TOP2A;BLM;BIRC5;CDCA8;BRCA1;AURKB;AURKA*
Signaling by FGFR	6	*FGF5;KL;FGFBP3;FGFR3*
Signaling by NOTCH	6	*NEURL1B;NOTCH4;E2F1*
PI3K Cascade	5	*FGF5;KL;FGFR3*
Orc1 removal from chromatin	5	*CDT1;ORC6;MCM5;CDC6*
Laminin interactions	4	*ITGA3;COL7A1;ITGA7;ITGA6*
Assembly of collagen fibrils and other multimeric structures	4	*LOX;COL7A1;ITGA6;COL9A2*
XBP1(S) activates chaperone genes	4	*EXTL1;KDELR3*
IRE1alpha activates chaperones	4	*EXTL1;KDELR3*
Regulation of Insulin-like Growth Factor (IGF) transport and uptake by Insulin-like Growth Factor Binding Proteins (IGFBPs)	4	*ITIH2;PCSK9;IGFBP6;PRSS23*
Interleukin-1 family signaling	4	*IL1RL2;IL18*

Table 3 Continued.

Unfolded Protein Response (UPR)	4	*EXTL1;KDELR3*
Signaling by Hedgehog	4	*TUBA1C;TUBA1B;HHIP*
Signaling by WNT	4	*CAV1;RSPO2;RAC3;DKK1*
Formation of Senescence-Associated Heterochromatin Foci (SAHF)	3	*HMGA1;HMGA2;LMNB1*
ECM proteoglycans	3	*ITGA7;COL9A2;ITGA9*

Table 4. Reactome pathway analysis of induced genes in ODM-DMSO relative to GM-DMSO at 7 days post osteogenic induction. Genes with 1.5-fold increased expression (n=2106, $p_{adj}<0.05$) were identified, and submitted to the Reactome database to identify enrichment within biological pathways. Among the most highly enriched pathways were generic in classification (e.g. cell cycle, metabolism, gene expression, developmental biology). Specific pathways associated with osteogenic signaling pathways, extracellular matrix synthesis and remodeling, and epigenetic modifications (highlighted in gray) are listed below.

Pathway	*# Genes*	Enriched Genes
Vesicle-mediated transport	*72*	*HIP1;ITSN1;HP;CLTB;PRKAG2;KIF11;FNBP1L;ACTB;JCHAIN;SLC2A8;KIF15;TUBA1C;TUBA1B;AP1S2;KIF1C;RAC3;POTEF;CTSC;SH3D19;SCARA5;SGIP1;KIF23;KIF22;TACR1;SPTB;TBC1D1;TBC1D4;DNAJC6;KIFC1;BIN1;AGTR1;RAB38;KIF2C;AMPH;KIF20A;MASP1;KIF20B;GRIA1;DCTN1;DENND3;ADRB2;GJC1;ALS2CL;RACGAP1;CLTCL1;MYO6;MAN1C1;MVB12A;REPS2;APOE;APOB;TBC1D16;AP1M1;ANKRD28;SORT1;GALNT1;HIP1R;RAB27B;HPS5;TUBB4B;CENPE;KIF18A;KIF18B;MYO1C;SYNJ1;KIF4B;KIF4A;COL7A1;SAA1;TRIP10;COPS8*
Interleukin-4 and 13 signaling	*58*	*CXCL8;CEBPD;MAOA;ITGB2;TWIST1;PIK3R1;FOXO3;FOXO1;ICAM1;SOCS3;CCND1;S1PR1;STAT6;LBP;JAK2;JAK3;IL6R;JUNB;MCL1;IL13RA1;IL18;HPS5;FOS;TNFRSF1B;BATF;POMC;ZEB1;BCL6;SAA1;FSCN1;BIRC5;BCL2L1*
Extracellular matrix organization	*51*	*DDR1;COLGALT2;ITGB5;ITGB4;ELN;ITGB2;TNC;CTSS;ICAM1;COMP;ADAMTS4;MMP24;IBSP;CTSK;KDR;EMILIN1;ITGB6;ADAMTS9;CTSB;MMP7;MME;MUSK;PCOLCE;DCN;MMP15;COL4A4;COL4A3;COL8A1;COL6A3;MMP19;ITGA5;MATN3;PLEC;ITGA9;FBN2;LAMA1;COL11A1;FBLN1;LTBP2;FURIN;NID1;NID2;FBLN5;ACAN;SCUBE3;A2M;ELANE;COL28A1;COL7A1;ITGA10;COL9A2*
Glycosaminoglycan metabolism	*29*	*SLC26A1;XYLT1;PRELP;HMMR;ACAN;HYAL1;HAS1;HYAL2;DSEL;GPC3;HAS2;GPC5;ST3GAL6;CHSY3;GPC4;HS3ST3B1;CHST6;CHST7;GLCE;OMD;LYVE1;DCN;CSPG5;CSPG4;HPSE;CHST2*
Cellular Senescence	*29*	*CXCL8;ETS2;LMNB1;H2AFJ;E2F1;E2F2;MAP2K6;MAP3K5;HIST1H1C;APC2;PHC2;CDKN2C;UBE2C;CBX2;H2AFX;HMGA1;HMGA2;FOS;CCNA2;MAPKAPK3;CCNE2;HIST4H4;ID1;CDK2;EZH2*
Signaling by WNT	*29*	*WNT2B;LEF1;CLTB;WNT11;H2AFJ;RSPO2;RAC3;RSPO3;RSPO1;TLE2;FZD2;WNT5B;FZD5;CAV1;H2AFX;FZD6;SOX13;NFATC1;GNG11;DKK1;AES;SFRP1;SFRP2;HIST4H4;HECW1;CTNNB1;TCF4;PLCB2*

Table 4 Continued.

Organelle biogenesis and maintenance	*28*	*PLK4;SHC4;DCTN1;NDE1;PLK1;KIF24;PRKAG2;HAUS5;TUBB4B;TUBG1;WDR34;ATP5O;ATP5G1;TUBA1C;TUBA1B;RXRA;ARL13B;PRKAR2B;TCTEX1D1;CNTRL;CDK1;NEK2;PPARGC1A;RAB11FIP3*
Degradation of the extracellular matrix	*26*	*FBN2;COL11A1;ELN;FURIN;NID1;CTSS;ADAMTS4;ACAN;SCUBE3;MMP24;CTSK;A2M;ADAMTS9;ELANE;CTSB;MMP7;MME;DCN;MMP15;COL4A4;COL7A1;COL4A3;COL8A1;COL6A3;MMP19;COL9A2*
Phospholipid metabolism	*26*	*SLC44A1;ABHD3;CPNE7;PIK3CD;PIK3R1;PLB1;PLD2;LIPH;TNFAIP8L1;TNFAIP8L3;MFSD2A;OSBPL5;PLEKHA2;MBOAT1;PLEKHA6;PLEKHA4;PISD;SYNJ1;PITPNM1;ETNK2;LPCAT3;PITPNM3;PNPLA3;PLBD1;LPIN3;MGLL*
Gastrin-CREB signaling pathway via PKC and MAPK	*23*	*DGKG;PTGFR;CDKL4;EDN1;TRPC6;PRKCH;TRPC3;PRKCD;TACR1;HPS5;PIK3R1;FPR2;RASGRP2;ADRA1B;GNG11;RGS2;EDNRA;P2RY6;LPAR6;P2RY2;AGTR1;SAA1;PLCB2;MGLL*
MAPK1/MAPK3 signaling	*23*	*CAMK2B;DUSP4;DUSP5;CDKL4;ANGPT1;DUSP1;IRS1;IRS2;SPTB;ACTB;GRIN2D;DUSP7;FGF5;FGF7;FGF18;CDK1;POTEF;JAK2;JAK3;IL6R;FGFR3*
G0 and Early G1	*21*	*TOP2A;PCNA;CDC6;LIN9;CDC25A;CDC25B;CCNA2;RBL1;CCNE2;CDK2;E2F1;CDK1;MYBL2*
Regulation of Insulin-like Growth Factor (IGF) transport and uptake by IGF Binding Proteins (IGFBPs)	*21*	*ITIH2;CSF1;IGFBP4;IGFBP2;TNC;IGF2;PCSK9;HSD17B11;CP;APOA5;FSTL3;C3;CST3;LGALS1;MXRA8;GPC3;APOE;IGFBP6;GAS6;APOB;MATN3*
TCF dependent signaling in response to WNT	*20*	*TLE2;FZD2;FZD5;CAV1;H2AFX;FZD6;LEF1;SOX13;DKK1;SFRP1;SFRP2;HIST4H4;H2AFJ;HECW1;RSPO2;RSPO3;CTNNB1;TCF4;RSPO1*
TCF dependent signaling in response to WNT	*20*	*TLE2;FZD2;FZD5;CAV1;H2AFX;FZD6;LEF1;SOX13;DKK1;SFRP1;SFRP2;HIST4H4;H2AFJ;HECW1;RSPO2;RSPO3;CTNNB1;TCF4;RSPO1*
PIP3 activates AKT signaling	*19*	*EGR1;HDAC5;PHC2;IRS1;CBX2;PIK3CD;IRS2;PIK3R1;FOXO3;FOXO1;FGF5;NR4A1;FGF7;FGF18;SNAI1;PPARG;FGFR3;EZH2*
Signaling by VEGF	*17*	*NRP2;CAV1;SPHK1;PRKCD;PXN;HSPB1;CYBA;PIK3R1;PGF;ACTB;CDH5;MAPKAPK3;KDR;PTK2B;CTNNB1;POTEF;WASF3*
Collagen degradation	*15*	*MMP7;MME;COL11A1;FURIN;CTSS;MMP15;COL4A4;COL7A1;CTSK;COL4A3;MMP19;COL8A1;COL6A3;COL9A2;ELANE;CTSB*

Table 4 Continued.

AURKA Activation by TPX2	*15*	*SHC4;PLK4;DCTN1;NDE1;PLK1;HMMR;HAUS5;TUBB4B;TUBG1;AURKA;TPX2;PRKAR2B;CNTRL;CDK1;NEK2*
ECM proteoglycans	*15*	*MUSK;ITGB5;LAMA1;TNC;DCN;COMP;ACAN;IBSP;COL4A4;COL4A3;COL6A3;COL9A2;ITGB6;MATN3;ITGA9*
Collagen formation	*15*	*COL28A1;COLGALT2;MMP7;ITGB4;COL11A1;PCOLCE;CTSS;COL4A4;COL7A1;COL4A3;COL8A1;COL6A3;COL9A2;CTSB;PLEC*
Assembly of collagen fibrils and other multimeric structures	*13*	*MMP7;ITGB4;COL11A1;PCOLCE;CTSS;COL4A4;COL7A1;COL4A3;COL8A1;COL6A3;COL9A2;CTSB;PLEC*
Orc1 removal from chromatin	*13*	*CDT1;MCM7;MCM8;CDC6;CCNA2;ORC6;ORC1;CDK2;MCM3;MCM4;MCM5;MCM6;MCM2*
Signaling by TGF-beta family members	*13*	*ACVRL1;DRAP1;RBL1;ROM1;NOG;PMEPA1;SMAD9;FURIN;BMPR1B;JUNB;FSTL3;TGFBR2*
Signaling by NOTCH	*13*	*HDAC5;NEURL1B;TLE2;CCND1;MDK;DNER;E2F1;ATP2A3;ST3GAL6;FURIN;DTX4;DLL1*
B-cat independent WNT signaling	*13*	*FZD2;WNT5B;FZD5;FZD6;LEF1;CLTB;NFATC1;GNG11;WNT11;RAC3;CTNNB1;TCF4;PLCB2*
Chromatin modifying enzymes	*13*	*SUV39H2;SMARCD2;SUV39H1;H2AFX;JADE2;ACTB;CCND1;HIST4H4;H2AFJ;HIST1H2AG;WHSC1;JAK2;EZH2*
Chromatin organization	*13*	*SUV39H2;SMARCD2;SUV39H1;H2AFX;JADE2;ACTB;CCND1;HIST4H4;H2AFJ;HIST1H2AG;WHSC1;JAK2;EZH2*
PI3K/AKT Signaling in Cancer	*12*	*FGF5;NR4A1;FGF7;IRS1;FGF18;PIK3CD;IRS2;PIK3R1;FOXO3;FGFR3;FOXO1*
Signaling by Hedgehog	*12*	*DISP2;TUBA1C;TUBA1B;PRKAR2B;HHIP;PTCH2;GAS1;ADCY3;GPC5;TUBB4B;ADCY7*
Signaling by FGFR in disease	*11*	*STAT5A;FGF5;CDKL4;FGF7;CNTRL;FGF18;PIK3R1;FGFR3;POLR2L*
Signaling by FGFR	*11*	*FGF5;HNRNPM;CDKL4;FGF7;FGFBP2;FGF18;SPRY2;PIK3R1;FGFR3;POLR2L*
IGF1R signaling cascade	*10*	*FGF5;CDKL4;FGF7;IRS1;FGF18;IGF2;IRS2;PIK3R1;FGFR3*
Signaling by Type 1 Insulin-like Growth Factor 1 Receptor (IGF1R)	*10*	*FGF5;CDKL4;FGF7;IRS1;FGF18;IGF2;IRS2;PIK3R1;FGFR3*

Table 4 Continued.

Collagen biosynthesis and modifying enzymes	*10*	*COL28A1;COLGALT2;COL4A4;COL7A1;COL11A1;COL4A3;COL8A1;COL6A3;PCOLCE;COL9A2*
Signaling by ROBO receptors	*10*	*ROBO2;RPL39L;ENAH;CDKL4;NRP2;TCEB2;RPL22L1;AKAP5*
Formation of the B-cat:TCF transactivating complex	*8*	*TLE2;H2AFJ;HIST4H4;H2AFX;LEF1;CTNNB1;TCF4*
Regulation of RUNX2 expression and activity	*8*	*DLX5;DLX6;TWIST1;PPARGC1A;NKX3-2;RUNX2*
TRAF6 mediated induction of NFkB and MAP kinases upon TLR7/8 or 9 activation	*8*	*DUSP4;NFKBIA;MAPKAPK3;SAA1;HPS5;FOS;TLR4;MAP2K6;DUSP7*
Signaling by TGF-beta Receptor Complex	*7*	*RBL1;ROM1;PMEPA1;FURIN;JUNB;TGFBR2*
Signaling by WNT in cancer	*5*	*FZD5;FZD6;CTNNB1;TCF4;DKK1*
Sialic acid metabolism	*5*	*ST6GAL1;ST6GALNAC2;PRC1;SLC17A5;ST3GAL6*
SUMOylation of DNA damage response and repair proteins	*5*	*PHC2;BLM;SP110;CBX2;BRCA1*
Regulation of Hypoxia-inducible Factor (HIF) by oxygen	*5*	*TCEB2;HIF3A;HIGD1A;WTIP*
RUNX2 regulates genes involved in cell migration	*4*	*ITGA5;RUNX2*
Repression of WNT target genes	*4*	*TLE2;LEF1;TCF4;AES*
Phospholipase C-mediated cascade; FGFR3	*4*	*FGF5;FGF18;FGFR3*
Signaling by BMP	*4*	*ACVRL1;NOG;SMAD9;BMPR1B*
RORA activates gene expression	*4*	*RXRA;PPARGC1A;ARNTL*

Table 4 Continued.

Formation of Senescence-Associated Heterochromatin Foci (SAHF)	*4*	*HMGA1;HMGA2;HIST1H1C;LMNB1*
SIRT1 negatively regulates rRNA expression	*4*	*H2AFJ;HIST4H4;SUV39H1;H2AFX*
Transcriptional regulation by small RNAs	*4*	*H2AFJ;HIST4H4;H2AFX;POLR2L*
Binding of TCF/LEF:CTNNB1 to target gene promoters	*3*	*LEF1;CTNNB1;TCF4*
Interleukin-18 signaling	*3*	*IL18*
AKT phosphorylates targets in the nucleus	*3*	*NR4A1;FOXO3;FOXO1*
Defective EXT2 causes exostoses 2	*3*	*GPC3;GPC5;GPC4*
Defective EXT1 causes exostoses 1, TRPS2 and CHDS	*3*	*GPC3;GPC5;GPC4*
IL-6-type cytokine receptor ligand interactions	*3*	*IL11RA;JAK2;CRLF1*
PKA-mediated phosphorylation of CREB	*3*	*PRKAR2B;ADCY3;ADCY7*
Synthesis, secretion, and deacylation of Ghrelin	*3*	*PCSK1;LEP;SPC25*
WNT ligand biogenesis and trafficking	*3*	*WNT11;WNT2B;WNT5B*
Syndecan interactions	*3*	*ITGB5;ITGB4;TNC*
Regulation of RUNX1 Expression and Activity	*3*	*H19;CCND3;CCND1*
ATF4 activates genes	*3*	*CXCL8;EXOSC9*
RUNX2 regulates osteoblast differentiation	*3*	*AR;RUNX2*

Table 4 Continued.

TGF-beta receptor signaling activates SMADs	*3*	*PMEPA1;FURIN;TGFBR2*
Synthesis of Prostaglandins (PG) and Thromboxanes (TX)	*3*	*TBXAS1;PTGDS;PTGES*

Table 5. Reactome pathway analysis of genes reduced in expression in ODM-DMSO relative to GM-DMSO at 7 day post osteogenic induction. Genes with 1.5-fold reduced expression (n=2106, p_{adj}<0.05) were identified, and submitted to the Reactome database to identify enrichment within human biological pathways. Among the most highly enriched pathways were generic in classification (e.g. cell cycle, metabolism, gene expression, developmental biology). Specific pathways associated with osteogenic signaling pathways, extracellular matrix synthesis and remodeling, and epigenetic modifications (highlighted in gray) are listed.

Pathway	# Genes	*Genes*
Extracellular matrix organization	59	*COL18A1;APP;COL14A1;LOXL4;PLOD2;PLOD1;FGF2;HAPLN1;LOXL2;ADAMTS5;EFEMP1;ADAMTS3;CDH1;ADAMTS1;EMILIN2;ITGB7;MMP2;ITGA2;BGN;CASK;ADAM19;MMP16;ADAM12;COL8A2;ITGA8;PECAM1;COL21A1;ITGA7;ITGA6;DDR2;COL17A1;COL15A1;TNXB;COL11A2;NTN4;FBLN2;ADAMTS16;VTN;ADAMTS14;SPP1;SERPINH1;TGFB2;VCAM1;LAMB3;TGFB3;LUM;COL22A1;FN1;LAMB1;L1CAM;GDF5;MFAP4;P4HA1;P4HA2;COL5A3;ITGA11;SDC1;AGRN;KLKB1;FBN1*
MAPK family signaling cascades	37	*FLG;SPTBN4;SPTBN5;SHC2;SHC3;CSF2RB;FGF1;KALRN;DUSP16;RASGRP1;FGF2;FGF9;ERBB3;JUN;DUSP2;KSR1;EGF;MMP2;HGF;FN1;PPP2R5B;GFRA1;NRG1;DUSP8;IL17RD;EREG;APBB1IP;CNKSR2;BTC;CNKSR1;FGF16;IL6;GDNF;KIT;SOS1*
Interleukin-4 and 13 signaling	36	*CDKN1A;VCAM1;STAT1;MMP2;HGF;FN1;LIF;L1CAM;FGF2;VEGFA;IL1A;IL6;IL1B;PIM1;STAT4;NDN;CCL2;IL12A;CD36;TP53*
MAPK1/MAPK3 signaling	34	*FLG;SPTBN4;SPTBN5;SHC2;SHC3;CSF2RB;FGF1;DUSP16;RASGRP1;FGF2;FGF9;ERBB3;DUSP2;KSR1;EGF;HGF;FN1;PPP2R5B;GFRA1;NRG1;DUSP8;IL17RD;EREG;APBB1IP;CNKSR2;BTC;CNKSR1;FGF16;IL6;GDNF;KIT;SOS1*
PIP3 activates AKT signaling	30	*FLG;CDKN1A;PHLPP1;PTEN;IL1RAP;FGF1;FGF2;PTENP1;FGF9;ERBB3;SALL4;PDK1;IER3;JUN;EGF;HGF;GAB1;PPP2R5B;NRG1;EREG;BTC;FGF16;KIT;MDM2;TRIB3;TP53*
Signaling by WNT	24	*TLE3;TCF7L2;WNT10B;FZD3;SMURF2;FZD7;PPP2R5B;WNT9A;PRICKLE1;PARD6A;DAAM1;HECW2;HIST1H4H;ROR1;SOX9;SOX6;PLCB1;WNT2;SCG2;WNT3;LGR4;PRKG1;DACT1;HIST1H3E*
Collagen formation	20	*COL17A1;COL18A1;COL15A1;LAMB3;COL14A1;COL22A1;COL11A2;LOXL4;PLOD2;PLOD1;LOXL2;ADAMTS14;ADAMTS3;P4HA1;P4HA2;COL5A3;SERPINH1;COL8A2;COL21A1;ITGA6*
Cellular Senescence	20	*KDM6B;CDKN1A;CDKN2B;JUN;IL1A;RPS6KA3;IL6;CDH1;MDM2;HIST1H4H;TNIK;TP53;HIST1H3E*
PI3K/AKT Signaling in Cancer	19	*FLG;CDKN1A;EGF;HGF;GAB1;PTEN;NRG1;FGF1;FGF2;EREG;BTC;FGF16;ERBB3;FGF9;KIT;MDM2;PDK1*

Table 5 Continued.

Transcriptional regulation by RUNX3	19	*LYN;TCF7L2;CDKN1A;JAG1;BCL2L11;SMAD3;SMURF2;MDM2;SPP1;HES1;TP53;RUNX1*
Degradation of the extracellular matrix	19	*COL17A1;COL18A1;COL15A1;LAMB3;COL14A1;MMP2;COL11A2;FN1;LAMB1;ADAMTS16;ADAMTS5;MMP16;CDH1;ADAMTS1;COL5A3;SPP1;COL8A2;KLKB1;FBN1*
Integrin cell surface interactions	18	*COL18A1;VCAM1;LUM;ITGA2;FN1;L1CAM;VTN;CDH1;COL5A3;ITGA11;SPP1;COL8A2;ITGA8;PECAM1;ITGA7;ITGA6;ITGB7;AGRN;FBN1*
Collagen biosynthesis and modifying enzymes	16	*COL17A1;COL18A1;COL15A1;COL14A1;COL22A1;COL11A2;PLOD2;PLOD1;ADAMTS14;ADAMTS3;P4HA1;P4HA2;COL5A3;SERPINH1;COL8A2;COL21A1*
IRE1alpha activates chaperones	16	*ERN1;XBP1;HSPA5;EDEM1;GFPT1;PPP2R5B;DNAJB9;HYOU1;SEC63*
Chromatin organization	16	*KDM6B;KDM3A;KDM4D;JADE1;HIST2H2BF;KANSL3;PRDM16;RBP1;HIST1H4H;PADI2;SMYD3;OGT;PADI1;KDM7A;HIST1H3E*
Chromatin modifying enzymes	16	*KDM6B;KDM3A;KDM4D;JADE1;HIST2H2BF;KANSL3;PRDM16;RBP1;HIST1H4H;PADI2;SMYD3;OGT;PADI1;KDM7A;HIST1H3E*
Organelle biogenesis and maintenance	16	*LYN;HSPA9;SHC2;RAB3IP;HSPA4L;NR1D1;PKD2;LZTFL1;PRKAG3;TUBB2B;KIF3A;HAUS7;DLC1;TTC30A;SDCCAG8*
Defective B3GALTL causes Peters-plus syndrome (PpS)	16	*SEMA5A;SEMA5B;ADAMTS12;THBS2;THSD1;THSD4;ADAMTS16;ADAMTSL1;ADAMTS5;ADAMTS15;ADAMTS14;ADAMTS3;ADAMTS13;ADAMTS1;ADAMTS17;ADAMTS6*
PPARA activates gene expression	16	*LYN;TXNRD1;ME1;G0S2;AHRR;TRIB3;CD36;AHR;NR1D1;TNFRSF21*
ECM proteoglycans	15	*APP;TGFB2;TNXB;TGFB3;LUM;ITGA2;FN1;BGN;LAMB1;HAPLN1;VTN;COL5A3;ITGA8;ITGA7;AGRN*
Signaling by TGF-beta family members	15	*CDKN2B;SMAD3;SMURF2;FST;NEDD4L;INHBB;PRKCZ;ACVR2A;TGFBR1;ACVR1C;PARD6A;PARD3;E2F5;SCG2*
Signaling by NOTCH	15	*JAG2;LFNG;TLE3;JUN;JAG1;HEY1;MFNG;HEY2;SEL1L;HES1;TP53;HDAC9*
Non-integrin membrane-ECM interactions	14	*LAMB3;ITGA2;COL11A2;FN1;NTN4;CASK;LAMB1;FGF2;VTN;COL5A3;SDC1;ITGA6;AGRN;DDR2*
TCF dependent signaling in response to WNT	14	*TLE3;TCF7L2;SMURF2;PPP2R5B;WNT9A;HECW2;HIST1H4H;SOX9;SOX6;SCG2;LGR4;WNT3;DACT1;HIST1H3E*

Table 5 Continued.

Transcriptional regulation by RUNX2	13	*CDKN1A;MSX2;STAT1;PPM1D;NR3C1;RUNX1;MAF;HEY1;HEY2;STAT4;HES1;SOX9;ZNF521*
XBP1(S) activates chaperone genes	12	*XBP1;EDEM1;GFPT1;PPP2R5B;DNAJB9;HYOU1;SEC63*
Signaling by FGFR	12	*FLG;FGF16;FLRT2;FGF9;FLRT3;FLRT1;GAB1;ANOS1;SOS1;FGF1;FGF2*
Signalling by NGF	12	*RPS6KA3;RALA;SHC2;BCL2L11;RPS6KA5;SHC3;ARHGEF3;ARHGEF4;ARHGEF2;SOS1;NGF;KALRN*
Signaling by FGFR1	11	*FLG;FLRT2;FGF9;FLRT3;FLRT1;GAB1;ANOS1;SOS1;FGF1;FGF2*
Signaling by TGF-beta Receptor Complex	11	*CDKN2B;SMAD3;PARD6A;SMURF2;PARD3;NEDD4L;E2F5;SCG2;PRKCZ;TGFBR1*
ATF4 activates genes	10	*EXOSC6;DDIT3;ASNS;CCL2;HERPUD1;ATF4*
Downstream signaling of activated FGFR1	10	*FLG;FLRT2;FGF9;FLRT3;FLRT1;GAB1;SOS1;FGF1;FGF2*
Signaling by VEGF	10	*CYFIP2;AHCYL2;SHC2;NCF2;TRIB3;SHB;PRKCZ;PDK1;VEGFA*
B-cat independent WNT signaling	10	*TCF7L2;FZD3;PARD6A;SMURF2;DAAM1;FZD7;ROR1;PRICKLE1;PLCB1;PRKG1*
Transcriptional regulation by RUNX1	10	*NFE2;OCLN;CCND2;LMO2;HIST1H4H;RUNX1;HIST1H3E*
PI3K Cascade	9	*FLG;FGF16;FGF9;GAB1;TRIB3;FGF1;FGF2;PDK1*
Transcriptional regulation of pluripotent stem cells	9	*EPAS1;SALL4;GATA6;KLF4;FGF2;FOXP1*
Interleukin-1 family signaling	9	*IL1A;APP;IL1B;PELI2;CASP1;PELI1;IL1RAP;S100B;IL18R1*
Signaling by Retinoic Acid	9	*ALDH1A3;CYP26B1;DHRS9;CRABP2;RDH10;AKR1C3;DHRS3;PDK1*
Ub-specific processing proteases	9	*USP25;SMAD3;SMURF2;SIAH2;MDM2;PTEN;HIST2H2BF;TP53;TGFBR1*
Collagen degradation	8	*COL17A1;COL18A1;COL15A1;COL14A1;COL5A3;MMP2;COL11A2;COL8A2*
Signaling by Hedgehog	8	*TUBB2B;HHAT;SMURF2;KIF3A;SEL1L;GLI1;CDON*

Table 5 Continued.

Downregulation of ERBB2 signaling	7	*BTC;ERBB3;EGF;NRG1;RNF41;EREG*
HATs acetylate histones	6	*KANSL3;JADE1;HIST1H4H;HIST2H2BF;OGT;HIST1H3E*
RUNX2 regulates osteoblast differentiation	5	*MAF;HEY1;HEY2;HES1;ZNF521*
SMAD2/SMAD3:SMAD 4 heterotrimer regulates transcription	5	*CDKN2B;SMAD3;E2F5;SCG2*
RUNX2 regulates bone development	5	*MAF;HEY1;HEY2;HES1;ZNF521*
Formation of the B-cat:TCF transactivating complex	5	*TLE3;TCF7L2;HIST1H4H;SCG2;HIST1H3E*
Hedgehog 'on' state	5	*SMURF2;KIF3A;GLI1;CDON*
Gene Silencing by RNA	5	*TDRD9;HIST1H4H;MOV10L1;PLD6;HIST1H3E*
TGF-beta receptor signaling in EMT (epithelial to mesenchymal transition)	4	*PARD6A;PARD3;PRKCZ;TGFBR1*
Downregulation of TGF-beta receptor signaling	4	*SMAD3;SMURF2;NEDD4L;TGFBR1*
WNT ligand biogenesis and trafficking	4	*WNT10B;WNT9A;WNT2;WNT3*
Activation of Matrix Metalloproteinases	4	*COL18A1;MMP16;MMP2;KLKB1*
TGF-beta receptor signaling activates SMADs	4	*SMAD3;SMURF2;NEDD4L;TGFBR1*
AURKA Activation by TPX2	4	*HAUS7;DLC1;HSPA4L;SDCCAG8*

Table 6. Reactome pathway analysis of induced genes in ODM-TCDD relative to ODM-DMSO at 3 days post osteogenic induction. Genes with 1.5-fold increased expression (n=706, $p_{adj}<0.05$) were identified, and submitted to the Reactome database to identify enrichment within human biological pathways. Among the most highly enriched pathways were generic in classification (e.g. cell cycle, metabolism, gene expression, developmental biology). Specific pathways associated with osteogenic signaling pathways, extracellular matrix synthesis and remodeling, and epigenetic modifications (highlighted in gray) are listed below.

Pathway	**# Gene**	***Gene***
Extracellular matrix organization	26	*COL17A1;COL15A1;ELN;LAMA3;COMP;ADAMTS5;SCUBE1;CDH1;KDR;ITGB8;ADAMTS9;JAM2;ELANE;COL28A1;MMP7;COL25A1;TGFB3;GDF5;DCN;GULP1;COL4A4;COL5A3;COL4A3;ITGA11;PECAM1;FMOD*
Degradation of the extracellular matrix	16	*COL17A1;COL15A1;MMP7;COL25A1;ELN;LAMA3;DCN;GULP1;ADAMTS5;SCUBE1;CDH1;COL4A4;COL5A3;COL4A3;ADAMTS9;ELANE*
Diseases of signal transduction	16	*FLG;KSR1;STAT1;LRP5;DKK2;TGFBR1;EREG;HEYL;KIAA1549;HHAT;ERBB3;FGF9;FGF18*
Vesicle-mediated transport	16	*CHRM2;GRIA1;COLEC12;RABGAP1;WNT5A;TRAPPC5;APOA1;ANK3;LRP2;AREG;SYT8;GULP1;SAA1;RAB38;SNX9;APOB*
Phase I - Functionalization of compounds	15	*MAOB;ADH1B;CYP7B1;CYP19A1;PTGS1;CYP39A1;ALDH3A1;ADH4;CYP26B1;ALDH1A1;CYP1A1;AHRR;CYP1B1*
TCF dependent signaling in response to WNT	12	*SFRP2;TLE1;HIST1H2BJ;HECW2;WNT5A;LRP5;HIST1H4H;RSPO3;WNT9A;LGR5;HIST2H2BE;DKK2*
MAPK family signaling cascades	11	*FLG;ERBB3;FGF9;GDNF;KSR1;FGF18;CSF2RB;JAK3;EREG;RASGRP3*
Cellular responses to external stimuli	11	*CXCL8;HIST1H2BJ;CDH1;NOX4;HIST1H4H;SOD2;HIST2H2BE;VEGFA;HIST1H1C*
Collagen formation	10	*COL17A1;COL28A1;COL15A1;MMP7;COL25A1;COL4A4;COL5A3;LAMA3;COL4A3;GULP1*
Collagen degradation	9	*COL17A1;COL15A1;MMP7;COL25A1;COL4A4;COL5A3;COL4A3;ELANE;GULP1*
Diseases associated with O-glycosylation of proteins	9	*SEMA5A;ADAMTS15;ADAMTS5;SEMA5B;MUC1;SPON1;THSD7B;ADAMTS9;MUC5AC*

Table 6 Continued.

ECM proteoglycans	9	*COMP;TGFB3;COL4A4;COL5A3;LAMA3;COL4A3;FMOD;DCN;GULP1*
Assembly of collagen fibrils and other multimeric structures	8	*COL17A1;COL15A1;MMP7;COL4A4;COL5A3;LAMA3;COL4A3;GULP1*
Collagen biosynthesis and modifying enzymes	8	*COL17A1;COL28A1;COL15A1;COL25A1;COL4A4;COL5A3;COL4A3;GULP1*
Negative regulation of the PI3K/AKT network	7	*FLG;ERBB3;FGF9;FGF18;IL1RAP;EREG*
Cytochrome P450 - arranged by substrate type	7	*CYP39A1;CYP26B1;CYP1A1;CYP1B1;CYP7B1;CYP19A1*
Cellular Senescence	7	*CXCL8;HIST1H2BJ;CDH1;HIST1H4H;HIST2H2BE;HIST1H1C*
PIP3 activates AKT signaling	7	*FLG;ERBB3;FGF9;FGF18;IL1RAP;EREG*
Signaling by VEGF	6	*ROCK2;KDR;ITPR1;VEGFD;VEGFA*
Non-integrin membrane-ECM interactions	5	*COL4A4;COL5A3;LAMA3;COL4A3;GULP1*
Signaling by Type 1 Insulin-like Growth Factor 1 Receptor (IGF1R)	5	*FLG;FGF9;FGF18;IGF1*
Signaling by TGF-beta family members	5	*GREM2;INHBB;CHRDL1;ACVR2A;TGFBR1*
Signalling by NGF	5	*MEF2A;FGD4;NTRK2;RPS6KA5;ARHGEF19*
Ub-specific processing proteases	5	*HIST1H2BJ;HIST2H2BE;TGFBR1;BIRC3*
Diseases of metabolism	5	*CYP26B1;CYP1B1;CSF2RB;CYP7B1;CYP19A1*
Deubiquitination	5	*HIST1H2BJ;HIST2H2BE;TGFBR1;BIRC3*
ATF4 activates genes	4	*CXCL8;CCL2*
Gene Silencing by RNA	4	*HIST1H2BJ;HIST1H4H;TDRD6;HIST2H2BE*
Activation of HOX genes during differentiation	4	*MAFB;HIST1H2BJ;HIST1H4H;HIST2H2BE*

Table 6 Continued.

Interleukin-1 family signaling	4	*CASP1;SAA1;IL1RAP;IL18R1*
Epigenetic regulation of gene expression	4	*HIST1H2BJ;HIST1H4H;ERCC6;HIST2H2BE*
TNF receptor superfamily (TNFSF) members mediating non-canonical NF-kB pathway	3	*TNFSF14;BIRC3*
Regulation of FZD by ubiquitination	3	*LRP5;RSPO3;LGR5*
Regulated Necrosis	3	*TNFSF10;BIRC3*
Signaling by BMP	3	*GREM2;CHRDL1;ACVR2A*
Laminin interactions	3	*COL4A4;LAMA3;COL4A3*
DNA methylation	3	*HIST1H2BJ;HIST1H4H;HIST2H2BE*
PRC2 methylates histones and DNA	3	*HIST1H2BJ;HIST1H4H;HIST2H2BE*
SIRT1 negatively regulates rRNA expression	3	*HIST1H2BJ;HIST1H4H;HIST2H2BE*
Activated PKN1 stimulates transcription of AR (androgen receptor) regulated genes KLK2 and KLK3	3	*HIST1H2BJ;HIST1H4H;HIST2H2BE*
Nucleosome assembly	3	*HIST1H2BJ;HIST1H4H;HIST2H2BE*
HDACs deacetylate histones	3	*HIST1H2BJ;HIST1H4H;HIST2H2BE*
Transcriptional regulation by small RNAs	3	*HIST1H2BJ;HIST1H4H;HIST2H2BE*
WNT ligand biogenesis and trafficking	2	*WNT5A;WNT9A*

Table 7. Reactome pathway analysis of genes with reduced expression in ODM-TCDD relative to ODM-DMSO at 3 days post osteogenic induction. Genes with 1.5-fold (0.67x) reduced expression (n=541, $p_{adj}<0.05$) were identified, and submitted to the Reactome database to identify enrichment within human biological pathways. Among the most highly enriched pathways were generic in classification (e.g. cell cycle, metabolism, gene expression, developmental biology). Specific pathways associated with osteogenic signaling pathways, extracellular matrix synthesis and remodeling, and epigenetic modifications (highlighted in gray) are listed below.

Pathway	# Genes	*Genes*
Disease	30	*NOTCH4;THSD1;THSD4;LMNB1;ADAMTSL1;FGF5;NEURL1B;ADAMTS3;HYAL1;ADAMTSL3;AP1S3;KL;CHST6;LIG1;HMGA1;CDC25C;DKK1;CDC25A;KITLG;PC;OGN;SDC1;RPL22L1;MET;FGFR3;STX1A*
Extracellular matrix organization	18	*FBN2;COLGALT2;PCOLCE2;ITGA3;P3H2;LTBP2;SCUBE3;ADAMTS3;LOX;COL7A1;P4HA3;ADAM12;SDC1;ITGA7;ITGA6;COL9A2;ITGA5;ITGA9*
Cellular responses to external stimuli	15	*UBE2C;HMGA1;HMGA2;LMNB1;TUBA1C;MT2A;TUBA1B;CCNE2;E2F1;E2F2;NOX5;CRYAB;MT1E*
Polo-like kinase mediated events	14	*CCNB2;CCNB1;CENPF;PLK1;MYBL2;FOXM1;CDC25C;PKMYT1;CDC25A*
Diseases of signal transduction	10	*FGF5;NEURL1B;KL;KITLG;FGFR3;DKK1;MET*
Collagen formation	9	*COLGALT2;ADAMTS3;PCOLCE2;LOX;COL7A1;P4HA3;P3H2;ITGA6;COL9A2*
Diseases of glycosylation	9	*ADAMTSL1;CHST6;ADAMTS3;NOTCH4;ADAMTSL3;OGN;SDC1;THSD1;THSD4*
Organelle biogenesis and maintenance	9	*PLK4;TUBA1C;TUBA1B;PLK1;CDK1;CEP72;KIF24;NEK2;CYS1*
Nucleosome assembly	8	*CENPU;CENPW;CENPH;CENPI;CENPK;CENPM;OIP5;KNL1*
Deposition of new CENPA-containing nucleosomes at the centromere	8	*CENPU;CENPW;CENPH;CENPI;CENPK;CENPM;OIP5;KNL1*
Cellular Senescence	8	*CCNE2;UBE2C;E2F1;HMGA1;HMGA2;E2F2;LMNB1*

Table 7 Continued.

AURKA Activation by TPX2	7	*PLK4;PLK1;CDK1;CEP72;NEK2;HMMR;AURKA*
Collagen biosynthesis and modifying enzymes	7	*COLGALT2;ADAMTS3;PCOLCE2;COL7A1;P4HA3;P3H2;COL9A2*
SUMO E3 ligases SUMOylate target proteins	7	*TOP2A;BLM;BIRC5;CDCA8;BRCA1;AURKB;AURKA*
Negative regulation of the PI3K/AKT network	7	*FGF5;KL;KITLG;FGFR3;MET*
SUMOylation	7	*TOP2A;BLM;BIRC5;CDCA8;BRCA1;AURKB;AURKA*
Unwinding of DNA	6	*GINS1;GINS2;CDC45;GINS3;GINS4;MCM5*
Removal of licensing factors from origins	6	*CDT1;ORC6;MCM5;MCM10;CDC6*
Signaling by FGFR	6	*FGF5;KL;FGFBP3;FGFR3*
Signaling by NOTCH	6	*NEURL1B;NOTCH4;E2F1*
Deubiquitination	6	*CDC20;USP44;CDK1;BRCA1;CLSPN;CDC25A*
Activation of NIMA Kinases NEK9, NEK6, NEK7	5	*CCNB2;CCNB1;PLK1;NEK7;CDK1*
Condensation of Prometaphase Chromosomes	5	*CCNB2;CCNB1;CDK1;NCAPG;NCAPH*
IGF1R signaling cascade	5	*FGF5;KL;FGFR3*
Orc1 removal from chromatin	5	*CDT1;ORC6;MCM5;CDC6*
Centrosome maturation	5	*PLK4;PLK1;CDK1;CEP72;NEK2*
Transcriptional regulation by RUNX2	5	*CCNB1;DLX6;CDK1;ITGA5*
PPARA activates gene expression	5	*SREBF1;G0S2;RAC3*
Gastrin-CREB signalling pathway via PKC and MAPK	5	*OXTR;P2RY6;PTGER1;AGTR1;MGLL*

Table 7 Continued.

Laminin interactions	4	*ITGA3;COL7A1;ITGA7;ITGA6*
Fanconi Anemia Pathway	4	*EME1;FANCD2;UBE2T;FANCA*
Assembly of collagen fibrils and other multimeric structures	4	*LOX;COL7A1;ITGA6;COL9A2*
Signaling by FGFR in disease	4	*FGF5;FGFR3*
XBP1(S) activates chaperone genes	4	*EXTL1;KDELR3*
IRE1alpha activates chaperones	4	*EXTL1;KDELR3*
Unfolded Protein Response (UPR)	4	*EXTL1;KDELR3*
Signaling by Hedgehog	4	*TUBA1C;TUBA1B;HHIP*
Signaling by WNT	4	*CAV1;RSPO2;RAC3;DKK1*
Neurodegenerative Diseases	3	*CDC25C;CDC25A;LMNB1*
ECM proteoglycans	3	*ITGA7;COL9A2;ITGA9*
Signaling by MET	3	*LIG1;ITGA3;MET*

Table 8. Reactome pathway analysis of induced genes in ODM-TCDD relative to ODM-DMSO at 7 days post osteogenic induction. Genes with 1.5-fold (0.67x) increased expression (n=1091, $p_{adj}<0.05$) were identified, and submitted to the Reactome database to identify enrichment within human biological pathways. Among the most highly enriched pathways were generic in classification (e.g. cell cycle, metabolism, gene expression, developmental biology). Specific pathways associated with osteogenic signaling pathways, extracellular matrix synthesis and remodeling, and epigenetic modifications (highlighted in gray) are listed below.

Pathway	# Genes	*Genes*
Extracellular matrix organization	38	*COL15A1;ELN;LAMA3;ITGB2;NTN4;CTSS;FBLN5;ICAM1;COMP;ADAMTS5;ADAMTS14;SCUBE1;CDH1;ADAMTS1;KDR;ITGB8;ITGB7;ADAMTS9;JAM2;ELANE;MMP7;TGFB3;MMP2;COL23A1;GDF5;DCN;GULP1;BMP4;MMP11;VCAN;BMP2;COL5A3;COL4A3;ITGA11;COL9A3;FMOD;KLKB1*
Diseases of signal transduction	28	*JAG2;FLG;JAG1;FZD5;KSR1;STAT1;CD80;LRP5;IRS2;FGF1;DKK2;TGFBR1;EREG;APBB1IP;BTC;HEYL;KIAA1549;HHAT;FGF9;HEY2;FGF18;STAT4;HES1;ZNF774*
Vesicle-mediated transport	28	*GRIA1;COLEC12;SPTBN5;RABGAP1;SH3KBP1;LRP2;FNBP1L;AREG;PRKAG3;ALS2CL;MVB12B;MAN1C1;SNX9;APOB;CAP2;WNT5A;APOA1;ANK3;SYNJ2;SYT8;KIF6;GULP1;DNM3;MYH3;SAA1;RAB38;RIN3*
Degradation of the extracellular matrix	21	*COL15A1;MMP7;MMP2;ELN;LAMA3;COL23A1;CTSS;DCN;GULP1;ADAMTS5;MMP11;SCUBE1;CDH1;ADAMTS1;COL5A3;COL4A3;COL9A3;ADAMTS9;KLKB1;ELANE*
Interleukin-4 and 13 signaling	21	*MUC1;STAT1;MMP2;ITGB2;SAA1;LIF;STAT4;CCL2;LBP;JAK3;VEGFA;ICAM1*
Cellular responses to external stimuli	20	*NCF2;HIF3A;SOD2;HIST2H2BE;PRKAG3;VEGFA;MAP1LC3C;CDH1;HIST1H4H;AJUBA;HSPA1A;CAP2;HIST1H1C*
MAPK family signaling cascades	19	*FLG;DUSP4;SPTBN5;KSR1;MMP2;CSF2RB;IRS2;DUSP8;FGF1;EREG;APBB1IP;BTC;FGF9;GDNF;FGF18;CDC42EP2;JAK3;ZNF774*
Signaling by WNT	19	*FZD3;TLE1;FZD5;FZD7;WNT5A;ITPR1;LRP5;WNT9A;RUNX3;HIST2H2BE;DKK2;SFRP2;HECW2;HECW1;HIST1H4H;RSPO3;ROR2;LGR5;PRKG1*
MAPK1/MAPK3 signaling	17	*FLG;DUSP4;SPTBN5;KSR1;CSF2RB;IRS2;DUSP8;FGF1;EREG;APBB1IP;BTC;FGF9;GDNF;FGF18;JAK3;ZNF774*

Table 8 Continued.

Phase I - Functionalization of compounds	17	*AOC3;PTGIS;MAOB;ADH1B;CYP7B1;PTGS1;CYP39A1;ALDH3A1;ADH4;CYP26B1;ALDH1A1;CYP1A1;AHRR;CYP1B1*
Regulation of Insulin-like Growth Factor (IGF) transport and uptake by Insulin-like Growth Factor Binding Proteins (IGFBPs)	16	*MMP2;IGFBP3;TMEM132A;IGF2;APOA1;IGF1;CHRDL1;APOA5;C3;BMP4;VCAN;ENAM;PAPPA;STC2;PENK;APOB*
Diseases of glycosylation	16	*SEMA5A;SBSPON;SEMA5B;SPON1;THSD7B;MUC5AC;DCN;ADAMTS5;ADAMTS15;MUC1;VCAN;ADAMTS14;ADAMTS1;FMOD;ADAMTS9;MUC20*
TCF dependent signaling in response to WNT	14	*TLE1;FZD5;WNT5A;LRP5;WNT9A;RUNX3;HIST2H2BE;DKK2;SFRP2;HECW2;HECW1;HIST1H4H;RSPO3;LGR5*
Diseases associated with O-glycosylation of proteins	13	*SEMA5A;SBSPON;SEMA5B;SPON1;THSD7B;MUC5AC;ADAMTS5;ADAMTS15;MUC1;ADAMTS14;ADAMTS1;ADAMTS9;MUC20*
Transcriptional regulation by RUNX1	13	*NFE2;CCND2;GPAM;RSPO3;HIST1H4H;NFATC2;HIST2H2BE;MIR302B;CTSS*
Phospholipid metabolism	12	*CDS1;PCYT1B;GPAM;PLA2G2A;LPCAT2;PNPLA3;PLEKHA6;PLA2G5;SYNJ2;PIK3C2B*
Collagen degradation	11	*MMP11;COL15A1;MMP7;COL5A3;MMP2;COL4A3;COL23A1;COL9A3;ELANE;CTSS;GULP1*
Transport of inorganic cations/anions and amino acids/oligopeptides	11	*SLC7A5;SLC6A6;SLC7A7;SLC9A9;SLC1A3;SLC3A2;SLC7A11;SLC15A3;SLC4A3;SLC12A7;SLC4A4*
PIP3 activates AKT signaling	11	*FLG;BTC;FGF9;CD80;SALL4;FGF18;IRS2;IL1RAP;FGF1;EREG*
Organelle biogenesis and maintenance	11	*LYN;HAUS7;IFT81;TCTEX1D1;SIRT4;DYNLRB2;SOD2;PKD2;PPARGC1A;PRKAG3*
ECM proteoglycans	10	*COMP;VCAN;TGFB3;COL5A3;COL4A3;LAMA3;COL9A3;FMOD;DCN;GULP1*
Collagen formation	10	*COL15A1;ADAMTS14;MMP7;COL5A3;COL4A3;LAMA3;COL23A1;COL9A3;CTSS;GULP1*
Negative regulation of the PI3K/AKT network	10	*FLG;BTC;FGF9;CD80;FGF18;IRS2;IL1RAP;FGF1;EREG*

Table 8 Continued.

Signaling by NOTCH	10	*JAG2;HEYL;JAG1;TLE1;MFNG;HEY2;HES1*
Signalling by NGF	10	*DNM3;DUSP4;MEF2A;NTRK2;FGD4;RPS6KA5;ARHGEF37;IRS2;PCSK6;NGF*
Gastrin-CREB signalling pathway via PKC and MAPK	10	*GPR17;EDNRA;EDN1;DGKE;PRKCH;CCKAR;GPR68;ITPR1;SAA1;BDKRB1*
Signaling by FGFR	9	*FLG;FGFBP2;FLRT2;FGF9;FLRT3;FGF18;ANOS1;FGF1*
Transcriptional regulation of pluripotent stem cells	8	*SALL1;SALL4;GATA6;HIF3A;TDGF1*
Assembly of collagen fibrils and other multimeric structures	8	*COL15A1;MMP7;COL5A3;COL4A3;LAMA3;COL9A3;CTSS;GULP1*
Signaling by MET	8	*SH3KBP1;COL5A3;LAMA3;SPINT2;TNS4;TNS3;MUC20;GULP1*
Transcriptional regulation by RUNX2	8	*BMP2;MAF;STAT1;HEY2;STAT4;TWIST2;HES1;ZNF521;PPARGC1A*
Arachidonic acid metabolism	8	*FAAH;PTGIS;CYP1A1;CYP1B1;DPEP1;ALOX15B;PTGS1*
Elastic fibre formation	7	*BMP4;BMP2;TGFB3;ELN;ITGB8;GDF5;FBLN5*
Collagen biosynthesis and modifying enzymes	7	*COL15A1;ADAMTS14;COL5A3;COL4A3;COL23A1;COL9A3;GULP1*
Signaling by VEGF	7	*ROCK2;NCF2;ITPR1;KDR;VEGFD;VEGFA*
B-cat independent WNT signaling	7	*FZD3;FZD5;FZD7;WNT5A;ITPR1;ROR2;PRKG1*
Activation of Matrix Metalloproteinases	6	*MMP11;MMP7;MMP2;KLKB1;CTSS;ELANE*
Signaling by TGF-beta family members	6	*GREM2;BMP2;INHBB;CHRDL1;ACVR2A;TGFBR1*
Transcriptional regulation by RUNX3	6	*LYN;JAG1;HES1;RUNX3*
Deubiquitination	6	*HIST2H2BE;PARK2;TGFBR1;BIRC3*
Infectious disease	6	*VCAN;CDH1;SH3KBP1;MVB12B;HSPA1A;LTF*

Table 8 Continued.

Negative regulation of TCF-dependent signaling by WNT ligand antagonists	5	*SFRP2;WNT5A;LRP5;WNT9A;DKK2*
RUNX3 regulates NOTCH signaling	5	*JAG1;HES1;RUNX3*
POU5F1 (OCT4), SOX2, NANOG activate genes related to proliferation	5	*SALL1;SALL4;TDGF1*
Non-integrin membrane-ECM interactions	5	*COL5A3;COL4A3;LAMA3;NTN4;GULP1*
Formation of the B-cat:TCF transactivating complex	5	*TLE1;HIST1H4H;RUNX3;HIST2H2BE*
Activation of HOX genes during differentiation	5	*MAFB;HIST1H4H;AJUBA;HIST2H2BE*
Activation of anterior HOX genes in hindbrain development during early embryogenesis	5	*MAFB;HIST1H4H;AJUBA;HIST2H2BE*
Epigenetic regulation of gene expression	5	*HIST1H4H;ERCC6;JARID2;HIST2H2BE*
Cellular Senescence	5	*CDH1;HIST1H4H;HIST2H2BE;HIST1H1C*
Signaling by BMP	4	*GREM2;BMP2;CHRDL1;ACVR2A*
RUNX2 regulates osteoblast differentiation	4	*MAF;HEY2;HES1;ZNF521*
RUNX2 regulates bone development	4	*MAF;HEY2;HES1;ZNF521*
PRC2 methylates histones and DNA	4	*HIST1H4H;JARID2;HIST2H2BE*
ERCC6 (CSB) and EHMT2 (G9a) positively regulate rRNA expression	4	*HIST1H4H;ERCC6;HIST2H2BE*

Table 8 Continued.

Chromatin organization	4	*PRDM16;HIST1H4H;HIST2H2BE*
Chromatin modifying enzymes	4	*PRDM16;HIST1H4H;HIST2H2BE*
WNT5A-dependent internalization of FZD2, FZD5 and ROR2	3	*FZD5;WNT5A;ROR2*
TNF receptor superfamily (TNFSF) members mediating non-canonical NF-kB pathway	3	*TNFSF14;BIRC3*

Table 9. Reactome pathway analysis of genes with reduced expression in ODM-TCDD relative to ODM-DMSO at 7 days post osteogenic induction. Genes with 1.5-fold (0.67x) reduced expression (n=850, p_{adj}<0.05) were identified, and submitted to the Reactome database to identify enrichment within human biological pathways. Among the most highly enriched pathways were generic in classification (e.g. cell cycle, metabolism, gene expression, developmental biology). Specific pathways associated with osteogenic signaling pathways, extracellular matrix synthesis and remodeling, and epigenetic modifications (highlighted in gray) are listed below.

Pathways	# Genes	*Genes*
Cytokine Signaling in Immune system	52	*CSF1R;LAMA5;CXCL3;IFIT1;LMNB1;FGF5;MT2A;MYC;IL12A;IL13RA2;NDC1;KL;DUSP5;DUSP2;TGFB1;CD70;HGF;IL18;IL31RA;NRG1;IL17RE;TNFRSF1B;PRLR;IL17RC;DUSP6;CNKSR2;FGF16;KITLG;MAPKAPK3;OAS1;TNFSF4;CDK1;BIRC5;TRIM14;VIM;IL7R;MAP3K14;MET;STX1A*
Signaling by Interleukins	43	*CSF1R;LAMA5;CXCL3;LMNB1;FGF5;MYC;IL12A;IL13RA2;KL;DUSP5;DUSP2;TGFB1;HGF;IL31RA;IL18;NRG1;IL17RE;TNFRSF1B;IL17RC;DUSP6;CNKSR2;FGF16;KITLG;MAPKAPK3;CDK1;BIRC5;VIM;IL7R;MET;STX1A*
Vesicle-mediated transport	34	*ARPC1A;KIF11;JCHAIN;KIF15;TUBA1C;TUBA1B;RACGAP1;GJA5;RAC3;APOE;AP1S3;SEC16B;SYT1;TUBB;RAB27B;KIF23;KIF22;CENPE;GJB2;KIF18A;KIF18B;TBC1D4;KIFC1;KIF4B;COL7A1;KIF4A;AGTR1;KIF2C;AMPH;KDELR3;KIF20A;MNS1;KIF20B;PAFAH1B3*
Extracellular matrix organization	29	*FBN2;LAMA5;COLGALT2;PCOLCE2;LAMA1;LTBP2;PLOD2;NID1;LTBP1;NID2;ADAMTS4;SCUBE3;IBSP;SPP1;TGFB1;LAMB3;MME;ITGA3;P3H2;COL7A1;P4HA3;ADAM12;COL4A6;COL6A3;ITGA7;SDC1;ITGA6;ITGA5;ITGA9*
Chromosome Maintenance	22	*CENPU;RFC3;CENPW;LIG1;RFC2;H2AFZ;PRIM1;HJURP;KNL1;CENPA;POLA2;CENPH;CENPI;POLE2;CENPK;POLD2;CENPM;OIP5;CENPN;CENPO*
Cellular responses to stress	21	*NDC1;H2AFZ;UBE2C;TUBB;HMGA1;HMGA2;LMNB1;CCNA2;TUBA1C;AR;TUBA1B;MAPKAPK3;CCNE2;E2F1;COL4A6;E2F2;EZH2;MAP4K4*
Interleukin-4 and 13 signaling	19	*LAMA5;TGFB1;MYC;HGF;IL18;BIRC5;IL12A;VIM;IL13RA2;TNFRSF1B*
MAPK family signaling cascades	18	*KL;DUSP5;DUSP2;HGF;NRG1;ETV4;DUSP6;CNKSR2;FGF5;FGF16;KITLG;MYC;CDK1;RAC3;MET*

Table 9 Continued.

Diseases of signal transduction	16	*KL;TGFB1;HGF;FZD8;NRG1;DKK1;CNKSR2;FGF5;NEURL1B;FGF16;KITLG;MYC;MET*
Polo-like kinase mediated events	15	*CCNB2;CCNB1;CENPF;PLK1;MYBL2;LIN9;FOXM1;CDC25C;PKMYT1;CDC25A*
Cellular Senescence	15	*CCNA2;MAPKAPK3;CCNE2;H2AFZ;UBE2C;E2F1;HMGA1;HMGA2;E2F2;EZH2;MAP4K4;LMNB1*
Signaling by WNT	15	*TLE2;WNT5B;H2AFZ;CAV1;SOX13;FZD8;DKK1;SFRP1;GNG2;MYC;RAC2;RSPO2;RAC3*
MAPK1/MAPK3 signaling	14	*CNKSR2;FGF5;FGF16;DUSP5;KL;KITLG;DUSP2;HGF;CDK1;NRG1;MET;DUSP6*
Infectious disease	14	*NDC1;RPL39L;RPS28;TGFB1;SYT1;LIG1;HMGA1;RPL22L1;AP1S3;SLC25A5;MET;STX1A*
Nucleosome assembly	13	*CENPU;CENPW;H2AFZ;HJURP;KNL1;CENPA;CENPH;CENPI;CENPK;CENPM;OIP5;CENPN;CENPO*
Deposition of new CENPA-containing nucleosomes at the centromere	13	*CENPU;CENPW;H2AFZ;HJURP;KNL1;CENPA;CENPH;CENPI;CENPK;CENPM;OIP5;CENPN;CENPO*
PPARA activates gene expression	12	*SREBF1;GLIPR1;RAC3;G0S2;PPARG;ANGPTL4;AGT*
Degradation of the extracellular matrix	11	*ADAMTS4;FBN2;SCUBE3;LAMA5;MME;LAMB3;COL7A1;SPP1;COL4A6;COL6A3;NID1*
Removal of licensing factors from origins	11	*CCNA2;CDT1;ORC6;MCM7;ORC1;MCM8;MCM4;MCM5;MCM10;CDC6;MCM2*
Unwinding of DNA	10	*GINS1;GINS2;CDC45;MCM7;MCM8;GINS3;GINS4;MCM4;MCM5;MCM2*
Laminin interactions	10	*LAMA5;LAMB3;ITGA3;LAMA1;COL7A1;COL4A6;ITGA7;ITGA6;NID1;NID2*
Orc1 removal from chromatin	10	*CCNA2;CDT1;ORC6;MCM7;ORC1;MCM8;MCM4;MCM5;CDC6;MCM2*
Integrin cell surface interactions	10	*IBSP;ITGA3;COL7A1;SPP1;COL4A6;COL6A3;ITGA7;ITGA6;ITGA5;ITGA9*
Collagen formation	10	*COLGALT2;PCOLCE2;LAMB3;COL7A1;P4HA3;P3H2;COL4A6;COL6A3;PLOD2;ITGA6*

Table 9 Continued.

TCF dependent signaling in response to WNT	10	*SFRP1;TLE2;H2AFZ;CAV1;MYC;SOX13;RSPO2;FZD8;DKK1*
Organelle biogenesis and maintenance	10	*PLK4;TUBA1C;TUBA1B;HAUS8;TUBB;PLK1;CDK1;KIF24;NEK2*
AURKA Activation by TPX2	9	*PLK4;HAUS8;TUBB;PLK1;CDK1;NEK2;HMMR;AURKA*
Oxidative Stress Induced Senescence	9	*MAPKAPK3;H2AFZ;E2F1;E2F2;EZH2;MAP4K4*
SUMO E3 ligases SUMOylate target proteins	9	*NDC1;TOP2A;BLM;TFAP2C;AIM1;BIRC5;CDCA8;BRCA1;AURKB ;AURKA*
PI3K/AKT Signaling in Cancer	9	*FGF5;FGF16;KL;KITLG;HGF;NRG1;MET*
Collagen biosynthesis and modifying enzymes	8	*COLGALT2;PCOLCE2;COL7A1;P4HA3;P3H2;COL4A6;COL6A3;P LOD2*
ECM proteoglycans	8	*LAMA5;TGFB1;IBSP;LAMA1;COL4A6;COL6A3;ITGA7;ITGA9*
Transcriptional regulation of white adipocyte differentiation	8	*SREBF1;TGFB1;RAC3;ADIRF;PPARG;ANGPTL4*
Programmed Cell Death	8	*DAPK2;E2F1;HMGB2;PMAIP1;VIM;CLSPN;LMNB1*
Diseases of glycosylation	8	*ADAMTS4;ADAMTSL1;CHST6;OGN;SDC1;GPC5;THSD1;THSD4*
Non-integrin membrane-ECM interactions	7	*LAMA5;TGFB1;LAMB3;LAMA1;COL4A6;SDC1;ITGA6*
B-cat independent WNT signaling	7	*GNG2;WNT5B;MYC;RAC2;FZD8;RAC3*
Ub-specific processing proteases	7	*CDC20;CCNA2;AR;RNF128;MYC;CLSPN;CDC25A*
SUMOylation of DNA replication proteins	6	*NDC1;TOP2A;AIM1;BIRC5;CDCA8;AURKB;AURKA*
Condensation of Prophase Chromosomes	6	*CCNB1;H2AFZ;PLK1;NCAPG2;CDK1;SMC4*
Signaling by TGF-beta family members	6	*DRAP1;RBL1;TGFB1;MYC;BMPR1B*

Table 9 Continued.

Signaling by NOTCH	6	*NEURL1B;TLE2;MYC;E2F1*
Signaling by Hedgehog	6	*TUBA1C;TUBA1B;TUBB;HHIP;GPC5*
Assembly of collagen fibrils and other multimeric structures	5	*LAMB3;COL7A1;COL4A6;COL6A3;ITGA6*
Protein ubiquitination	5	*RNF144A;UBE2S;UBE2C;UBE2T;RNF152*
Transcriptional regulation by RUNX3	5	*TGFB1;MYC;SPP1*
Transcriptional regulation by RUNX2	5	*AR;CCNB1;CDK1;ITGA5*
Chromatin modifying enzymes	5	*SUV39H2;H2AFZ;SUV39H1;WHSC1;EZH2*
Chromatin organization	5	*SUV39H2;H2AFZ;SUV39H1;WHSC1;EZH2*
Neurodegenerative Diseases	4	*CDC25C;CDC25A;CDK5R1;LMNB1*
Diseases associated with glycosaminoglycan metabolism	4	*CHST6;OGN;SDC1;GPC5*
Collagen degradation	4	*MME;COL7A1;COL4A6;COL6A3*
Signaling by Type 1 Insulin-like Growth Factor 1 Receptor (IGF1R)	4	*FGF5;FGF16;KL*
Signaling by TGF-beta Receptor Complex	4	*RBL1;TGFB1;MYC*
XBP1(S) activates chaperone genes	4	*EXTL1;KDELR3*
Activation of HOX genes during differentiation	4	*H2AFZ;RARB;RAC3;EZH2*
Signaling by VEGF	4	*FLT1;MAPKAPK3;CAV1;PGF*
Epigenetic regulation of gene expression	4	*UHRF1;H2AFZ;SUV39H1;EZH2*
Unfolded Protein Response (UPR)	4	*EXTL1;KDELR3*

Table 9 Continued.

Transport of inorganic cations/anions and amino acids/oligopeptides	4	*SLC4A8;SLC20A1;SLC1A1;SLC25A22*
Signaling by NGF	4	*MAPKAPK3;MCF2L;RAC3;DUSP6*
Phase I - Functionalization of compounds	4	*CYP4B1;CYP3A5*
Repression of WNT target genes	3	*TLE2;MYC*
Senescence-Associated Secretory Phenotype (SASP)	3	*CCNA2;H2AFZ;UBE2C*
Degradation of B-cat by the destruction complex	3	*TLE2;MYC*
Hedgehog 'off' state	3	*TUBA1C;TUBA1B;TUBB*

FIGURES

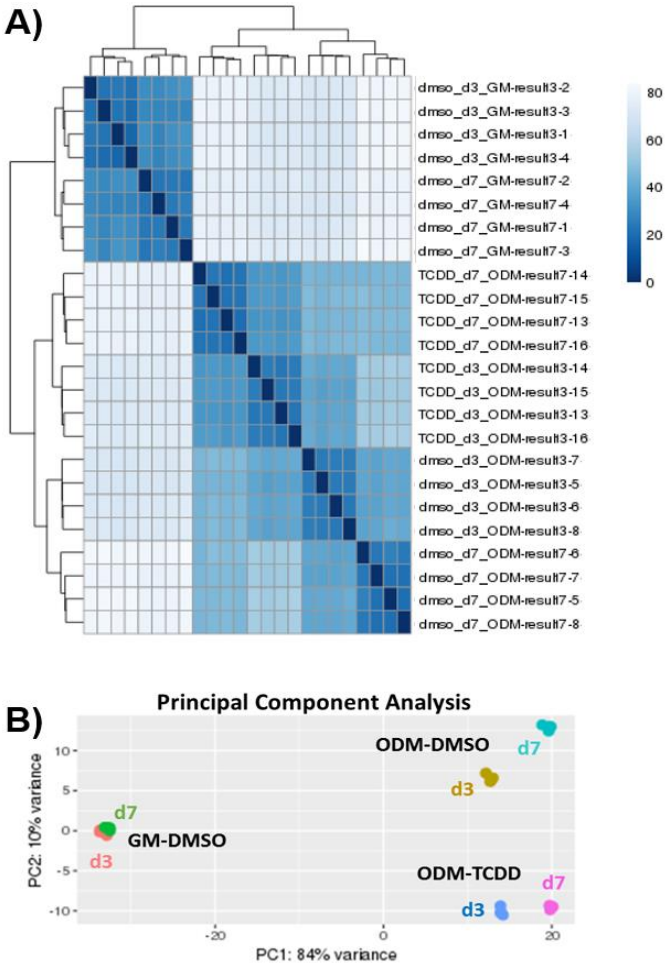

Figure 1. Cluster analysis of 3 dpi and 7 dpi RNA-Seq. Heat map in (A) demonstrates sample clustering by media type (GM vs ODM) and by treatment (DMSO vs. TCDD). Principal component analysis (PCA)) in (B) map illustrates the influence of media (X-axis) and treatment (Y-axis) on observed changes in gene expression. Abbreviations : d3= 3 days post induction (dpi), d7= 7 dpi, GM= growth media + 0.1% DMSO, ODM= osteogenic differentiation media + 0.1% DMSO, ODM-TCDD= osteogenic differentiation media + 10 nM TCDD.

Differential Gene Expression Under Osteogenic Conditions (ODM vs. GM)

A) Upregulated Genes (>1.5x)

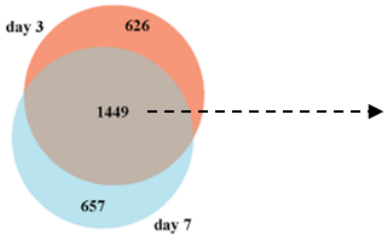

Pathway	# Genes
Extracellular matrix organization	41
Degradation of the extracellular matrix	21
Cellular Senescence	21
Organelle biogenesis and maintenance	20
Signaling by WNT	18
PIP3 activates AKT signaling	14
AURKA Activation by TPX2	13
Signaling by VEGF	12
Collagen degradation	11
ECM proteoglycans	11
Signaling by TGF-beta family members	11
Transcriptional regulation by RUNX2	10
Signaling by NOTCH	9
Signaling by Hedgehog	9
Collagen biosynth. and modifying enzymes	8
Chromatin modifying enzymes	8

B) Downregulated genes (<0.67x)

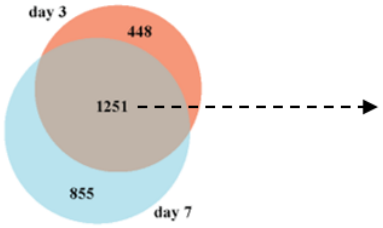

Pathway	# Genes
Extracellular matrix organization	32
Signaling by WNT	11
Organelle biogenesis and maintenance	10
Signaling by TGF-beta family members	10
Signaling by NOTCH	10
Collagen biosynth. and modifying enzymes	9
Degradation of the extracellular matrix	9
Transcriptional regulation by RUNX2	9
Signaling by FGFR	8
ECM proteoglycans	6
Chromatin modifying enzymes	5
Signaling by Hedgehog	5
AURKA Activation by TPX2	4
Collagen degradation	3

Figure 2. Comparative gene expression analysis at 3 dpi and 7 dpi under osteogenic conditions (ODM-DMSO). Genes were selected based on 1.5-fold increase (1.5x) in (A), or decrease (0.67x) in (B) relative to undifferentiated hBMSCs in GM-DMSO. BioVenn (Hulson *et al.*, 2008) was used to identify overlapping gene expression patterns between 3 dpi and 7 dpi. Genes with overlapping increased (A), or attenuated (B) expression were analyzed by Reactome to identify cellular, functional, and disease pathways associated alterations in gene expression (Joshi-Tope *et al.*, 2005). Mesenchymal- or osteoblast-specific pathways are highlighted here; however, a complete list with pathways and their corresponding genes can be found in Tables 1-4.

Differential Gene Expression Under Osteogenic Conditions ± TCDD (ODM-TCDD vs. ODM-DMSO)

A) Upregulated Genes (> 1.5x)

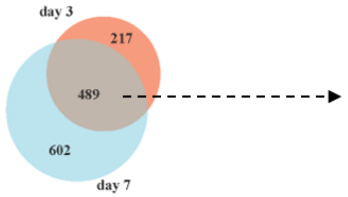

Pathways	# Genes
Extracellular matrix organization	19
Signaling by WNT	15
Diseases of signal transduction	15
TCF dependent signaling in response to WNT	12
Phase I - Functionalization of compounds	9
ECM proteoglycans	8
Transcriptional regulation by RUNX1	8
Assembly of collagen fibrils	6
Collagen degradation	6
Signaling by FGFR in disease	6
Collagen formation	6
Signaling by FGFR	6
Arachidonic acid metabolism	6
Cytochrome P450	6
Cellular Senescence	5
Ub-specific processing proteases	5
Collagen biosynthesis and modifying enzymes	4
Senescence-Associated Secretory Phenotype	4
Signaling by TGF-beta family members	4

B) Downregulated Genes < 0.67x)

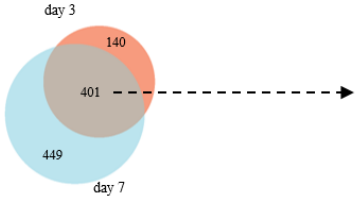

Pathways	# Genes
Signaling by Interleukins	17
Extracellular matrix organization	15
Chromosome Maintenance	10
Nucleosome assembly	8
Cellular Senescence	8
SUMOylation	7
AURKA Activation by TPX2	6
Collagen formation	6
Diseases of glycosylation	6
Unfolded Protein Response (UPR)	4
Signaling by Hedgehog	4
Signaling by WNT	4
Formation of Senescence-Associated Heterochromatin Foci (SAHF)	3

Figure 3. Comparative gene expression analysis at 3 dpi and 7 dpi under osteogenic conditions in the presence of absence of TCDD (ODM-TCDD vs. ODM-DMSO). Genes were selected based on 1.5-fold increase (1.5x) (A), or decrease (0.67x) (B) relative to undifferentiated hBMSCs in GM-DMSO. BioVenn (Hulson *et al.*, 2008) was used to identify overlapping gene expression patterns between 3 dpi and 7 dpi. Genes with overlapping increased (A) or attenuated (B) expression were analyzed by Reactome to identify cellular and functional pathways associated alterations in gene expression (Joshi-Tope *et al*., 2005). Mesenchymal- or osteoblast-specific pathways are highlighted here; however, a complete list with pathways and their corresponding genes can be found in Tables 5-8.

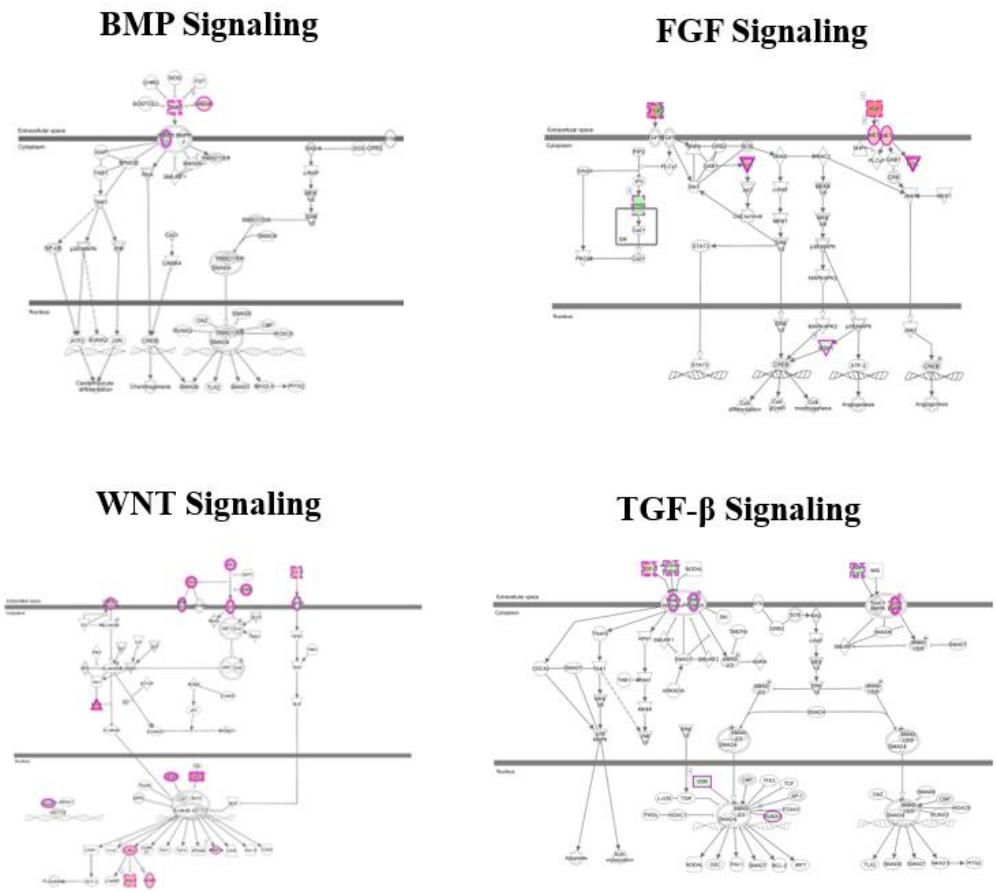

Figure 4. IPA assessment of ODM-TCDD vs ODM-DMSO cells at 7 dpi highlighted enrichment of genes within key developmental signaling pathways (Wnt, BMP, FGF, TGF-β) associated with osteogenesis. Genes highlighted in fuschia demonstrate either 1.5-fold induction (red) or attenuation (green) in expression following TCDD-exposure.

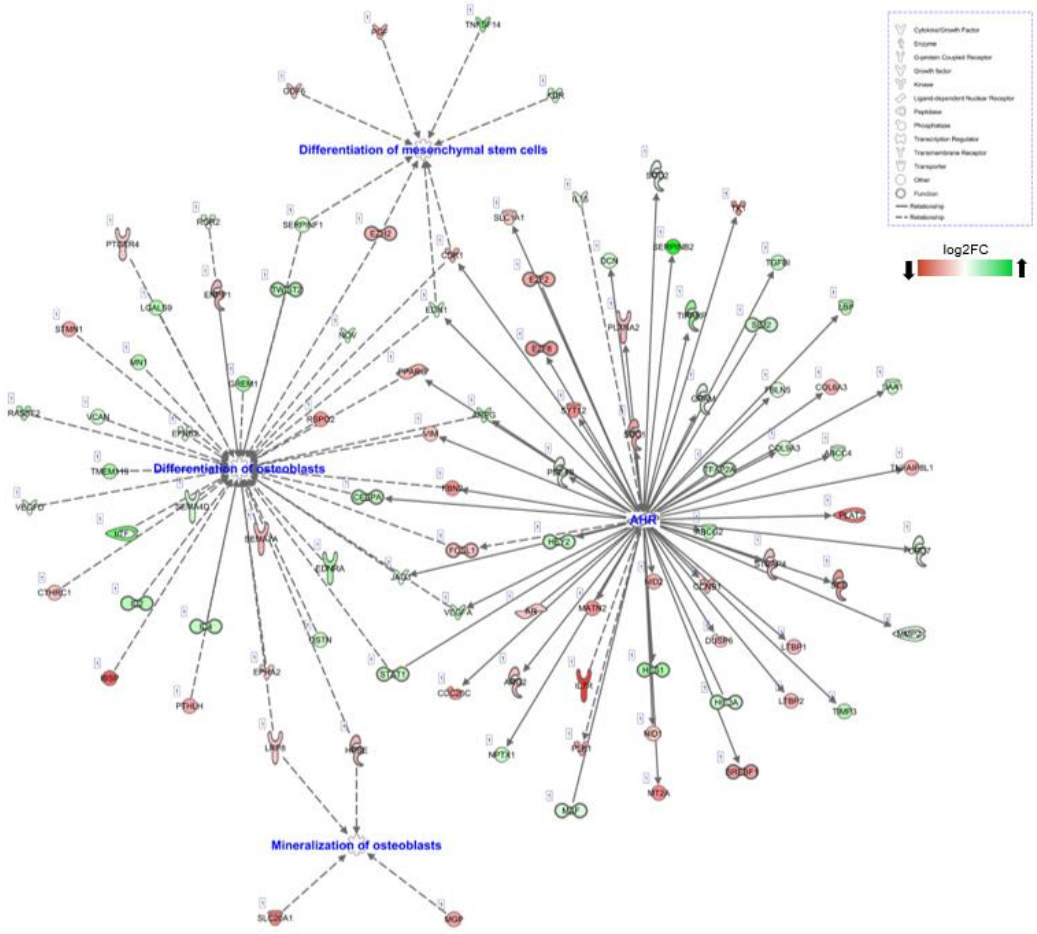

Figure 5. IPA functional analysis of DEGs from ODM-TCDD vs ODM-DMSO-treated samples at 7 dpi. Genes enriched in pathways associated with the aryl hydrocarbon receptor function, differentiation of mesenchymal stem cells, differentiation of osteoblasts, mineralization of osteoblasts are highlighted.

A) ↑ Osteogenic Conditions (ODM-DMSO vs GM-DMSO) **and** ↓ Osteogenic Conditions + TCDD (ODM-TCDD vs. ODM-DMSO)

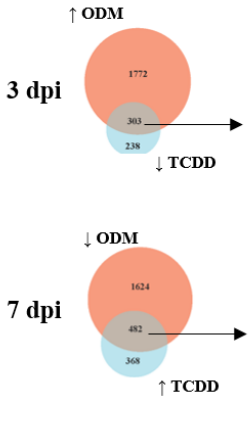

Osteogenic Signaling Mediators	ECM Formation/Composition	Epigenetic Modifiers
DKK1, *FGFR3*, ***LTBP2***, ***RSPO2***	***ALPL***, *ADAMTSL3*, ***COL7A1***, *COL9A2*, ***FBN2***, *ITGA3*, ***ITGA5***, ***ITGA9***, ***LMNB1***, ***MGP***, ***COLGALT2***, ***SEMA7A***, *SERPINB7*	*LINC01356, LINC01389, LINC01592,* ***LINC00707***, ***CENPF***, ***CENPH***, ***CENPI***, ***CENPK***, ***CENPM***, ***CENPU***, ***CENPW***, ***PRC1***, ***METTL7A***, ***METTL7B***, ***SUSD2***, *KNL1,* ***AURKA***, ***AURKB***
IGFBP2, IGFBP6, BMPR1B, ***DKK1****, WNT5B, ,* ***LTBP2***, ***RSPO2****, CAV1, FGF5, PPARG, PAX9*	***ALPL****, ENPP1, COL6A3,* ***COL7A1***, ***COLGALT2***, ***ITGA5***, ***ITGA9***, ***LMNB1****, LMNB2, ADAMTS4,* ***SEMA7A****, SERPINA5, IBSP,* ***FBN2***, ***MGP***	*LINC00704, LINC01415, LINC01423,* ***LINC00707***, ***AURKA***, ***AURKB****, EZH2,* ***PRC1****, SCUBE3,* ***METTL7A***, ***METTL7B****, SUV39H1, SUV39H2, WDR62, WDR76, WHSC1,* ***SUSD2****, SUSD3, CENPA, CENPE,* ***CENPF***, ***CENPH***, ***CENPI***, ***CENPK***, ***CENPM****, CENPN,* ***CENPO***, ***CENPU***, ***CENPW***

B) ↓ Osteogenic Conditions (ODM-DMSO vs GM-DMSO) **and** ↑ Osteogenic Conditions + TCDD (ODM-TCDD vs. ODM-DMSO)

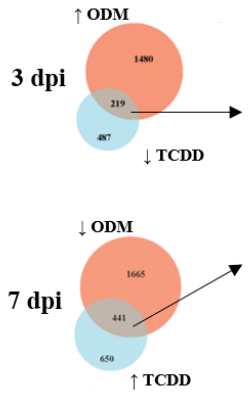

Osteogenic Signaling Mediators	ECM Formation/Composition	Epigenetic Modifiers
FGF16, THSD1, IL12A, IL13RA2, IL31RA, G0S2	*ADAMTSL1, ANXA10, LAMB3, OGN, PHEX, PLOD2*	*LINC00346, LINC00629, LINC01048, LINC01060, LINC01119, , LINC01182, LINC01605*
AHRR, FGF1, FGF9, FZD3, , FZD7, GDF5, SALL4, IGFBP3, TNFRSF11B, WNT9A, HEY2, CCL2, CXCL12, PRDM16, VEGFA,TGFBI, TGFBR1, IGF1, ACVR2A,INHBB,	*ADAMTS1, COL15A1, COL5A3, COLEC12, ITGA11, ITGB7, MMP2, OLFM2, OSTN, SEMA5A, SEMA5B, SERPINB2, ADAMTS14, ADAMTS15, ADAMTS5, TIMP3*	*LINC00284, LINC00304, LINC00623, LINC00640, LINC00670, LINC00869, LINC00900, LINC00982, LINC01018, LINC01021, LINC01268, LINC01296, LINC01515, LINC01616, MIR181A1HG, MIR181A2HG, TBX18, ADAMTS9-AS2,*

Figure 6. Comparative analysis of candidate genes sensitive to TCDD exposure at 3 dpi and 7 dpi. Genes in (A) exhibit 1.5-fold induction under osteogenic conditions (ODM-DMSO vs. GM-DMSO) and 1.5-fold attenuated expression when exposed to TCDD under osteogenic conditions (ODM-TCDD vs. ODM-DMSO), and vice versa in (B), 1.5-fold attenuated expression under osteogenic conditions and 1.5-fold induction with exposure to TCDD. BioVenn (Hulson *et al.*, 2008) was used to identify overlapping gene expression patterns, and selected genes with roles in osteogenic signaling, epigenetic regulation, and extracellular matrix synthesis, remodeling, and mineralization are highlighted for A) and B).

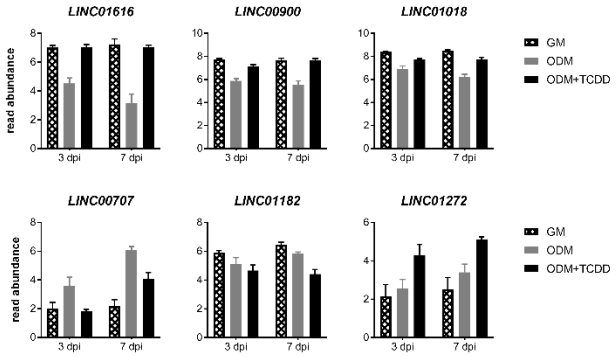

Figure 7. Identification of candidate lncRNAs exhibiting differential expression with ODM ± TCDD. Read abundance was measured for each condition (GM, ODM, ODM + TCDD) at 3 dpi and 7 dpi.

REFERENCES

Abdallah, B.M. and Kassem, M. (2008) Human mesenchymal stem cells: from basic biology to clinical applications. *Gene Ther.*, **15**, 109–116.

Abel, J. and Haarmann-Stemmann, T. (2010) An introduction to the molecular basics of aryl hydrocarbon receptor biology. *Biol. Chem.*, **391**, 1235–1248.

Adams, J.D. *et al.* (1987) Toxic and carcinogenic agents in undiluted mainstream smoke and sidestream smoke of different types of cigarettes. *Carcinogenesis*, **8**, 729–731.

Addison, W.N. *et al.* (2007) Pyrophosphate inhibits mineralization of osteoblast cultures by binding to mineral, up-regulating osteopontin, and inhibiting alkaline phosphatase activity. *J. Biol. Chem.*, **282**, 15872–15883.

Alexander, P.G. *et al.* (2016) Prenatal exposure to environmental factors and congenital limb defects. *Birth Defects Res. Part C - Embryo Today Rev.*, **108**, 243–273.

Apschner, A. *et al.* (2011) Not All Bones are Created Equal – Using Zebrafish and Other Teleost Species in Osteogenesis Research Third Edit. Elsevier Inc.

Avery, S. *et al.* (2017) Analysing the bioactive makeup of demineralised dentine matrix on bone marrow mesenchymal stem cells for enhanced bone repair. *Eur. Cells Mater.*, **34**, 1–14.

Baker, A.H. *et al.* (2015) Tributyltin Engages Multiple Nuclear Receptor Pathways and Suppresses Osteogenesis in Bone Marrow Multipotent Stromal Cells. *Chem. Res. Toxicol.*, **28**, 1156–1166.

Baker, T.R. *et al.* (2014) Adverse effects in adulthood resulting from low-level dioxin exposure in juvenile zebrafish. *Endocr. Disruptors*, **2**, 1–6.

Baker, T.R. *et al.* (2013) Early dioxin exposure causes toxic effects in adult zebrafish. *Toxicol. Sci.*, **135**, 241–250.

Baksh, D. *et al.* (2004) Adult mesenchymal stem cells: characterization, differentiation, and application in cell and gene therapy. *J. Cell. Mol. Med.*, **8**, 301–316.

Baldridge, D. *et al.* (2010) Signaling pathways in human skeletal dysplasias. *Annu Rev Genomics Hum Genet*, **11**, 189–217.

Barbour, K.E. *et al.* (2014) Inflammatory Markers and Risk of Hip Fracture in Older White Women: The Study of Osteoporotic Fractures. *J. Bone Miner. Res.*, **29**, 2057–2064.

Baron, R. and Kneissel, M. (2013) WNT signaling in bone homeostasis and disease: from

human mutations to treatments. *Nat. Med.*, **19**, 179–192.

Baroncelli, M. *et al.* (2017) Comparative proteomic profiling of human osteoblast-derived extracellular matrices identifies proteins involved in mesenchymal stromal cell osteogenic differentiation and mineralization. *J. Cell. Physiol.*, 1–9.

Baroncelli, M. *et al.* (2017) Comparative Proteomic Profiling of Human Osteoblast-Derived Extracellular Matrices Identifies Proteins Involved in Mesenchymal Stromal Cell Osteogenic Differentiation and Mineralization. *J Cell Physiol*.

Benjamini, Y. and Hochberg, Y. (1995) Controlling the False Discovery Rate: A Practical and Powerful Approach to Multiple Testing. *J. R. Stat. Soc. Ser. B*, **57**, 289–300.

Benvenuti, S. *et al.* (2007) Rosiglitazone stimulates adipogenesis and decreases osteoblastogenesis in human mesenchymal stem cells. *J. Endocrinol. Invest.*, **30**, 26–30.

Bialek, P. *et al.* (2004) A Twist Code Determines the Onset of Osteoblast Differentiation. *Dev. Cell*, **6**, 423–435.

Bishop, N. (2016) Bone Material Properties in Osteogenesis Imperfecta. *J. Bone Miner. Res.*, **31**, 699–708.

Bodle, J.C. *et al.* (2014) Age-related effects on the potency of human adipose derived stem cells: Creation and evaluation of superlots and implications for musculoskeletal tissue engineering applications. *Tissue Eng. Part C Methods*, **20**, 1–43.

Bone health and osteoporosis: a report of the Surgeon General (2004) Rockville, Maryland.

Bonventre, J.A. *et al.* (2012) Craniofacial abnormalities and altered wnt and mmp mRNA expression in zebrafish embryos exposed to gasoline oxygenates ETBE and TAME. *Aquat. Toxicol.*, **120**–**121**, 45–53.

Boyce, B.F. and Xing, L. (2007) Biology of RANK, RANKL, and osteoprotegerin. *Arthritis Res. Ther.*, **9 Suppl 1**, S1.

Briggs, A.M. *et al.* (2016) Musculoskeletal Health Conditions Represent a Global Threat to Healthy Aging: A Report for the 2015 World Health Organization World Report on Ageing and Health. *Gerontologist*, **56**, S243–S255.

Burns, F.R. *et al.* (2015) Dioxin disrupts cranial cartilage and dermal bone development in zebrafish larvae. *Aquat. Toxicol.*, **164**, 52–60.

Bustin, S.A. *et al.* (2009) The MIQE Guidelines: Minimum Information for Publication of Quantitative Real-Time PCR Experiments. *Clin. Chem.*, **622**, 611–622.

Carpi, D. *et al.* (2009) Dioxin-sensitive proteins in differentiating osteoblasts: Effects on bone formation in vitro. *Toxicol. Sci.*, **108**, 330–343.

Charoenpanich, A. *et al.* (2014) Cyclic tensile strain enhances osteogenesis and angiogenesis in mesenchymal stem cells from osteoporotic donors. *Tissue Eng. Part A*, **20**, 67–78.

Chen, G. *et al.* (2012) TGF-β and BMP Signaling in Osteoblast Differentiation and Bone Formation. *Int. J. Biol. Sci.*, **8**, 272–288.

Chopra, M. and Schrenk, D. (2011) Dioxin toxicity, aryl hydrocarbon receptor signaling, and apoptosis-persistent pollutants affect programmed cell death. *Crit. Rev. Toxicol.*, **41**, 292–320.

Chrisman, K. *et al.* (2004) Gestational Ethanol Exposure Disrupts the Expression of FGF8 and Sonic hedgehog during Limb Patterning. *Birth Defects Res. Part A - Clin. Mol. Teratol.*, **70**, 163–171.

Christiansen, H.E. *et al.* (2010) Homozygosity for a Missense Mutation in SERPINH1, which Encodes the Collagen Chaperone Protein HSP47, Results in Severe Recessive Osteogenesis Imperfecta. *Am. J. Hum. Genet.*, **86**, 389–398.

Clarke, B. (2008) Normal bone anatomy and physiology. *Clin. J. Am. Soc. Nephrol.*, **3 (Suppl 3**.

Derrien, T. *et al.* (2012) The GENCODE v7 catalogue of human long non-coding RNAs : Analysis of their structure , evolution and expression. *Genome Res.*, **22**, 1775–1789.

Ding, D. *et al.* (2012) Over-expression of Sox2 in C3H10T1/2 cells inhibits osteoblast differentiation through Wnt and MAPK signalling pathways. *Int. Orthop.*, **36**, 1087–1094.

Dobin, A. *et al.* (2013) STAR: Ultrafast universal RNA-seq aligner. *Bioinformatics*, **29**, 15–21.

Dolk, H. *et al.* (2010) The Prevalence of Congenital Anomalies in Europe. In, Paz,M.P. de la and Croft,S.C. (eds), *Rare Diseases Epidemiology*. Springer, New York, New York, pp. 305–334.

Dominici, M. *et al.* (2006) Minimal criteria for defining multipotent mesenchymal stromal cells. The International Society for Cellular Therapy position statement. *Cytotherapy*, **8**, 315–7.

Dong, B. and Matsumura, F. (2008) Roles of cytosolic phospholipase A2 and Src kinase in the early action of 2,3,7,8-tetrachlorodibenzo-p-dioxin through a nongenomic pathway in MCF10A cells. *Mol. Pharmacol.*, **74**, 255–263.

Dong, W. *et al.* (2012) TCDD disrupts hypural skeletogenesis during medaka embryonic development. *Toxicol. Sci.*, **125**, 91–104.

Dong, W. *et al.* (2010) TCDD Induced Pericardial Edema and Relative COX-2 Expression in Medaka (Oryzias Latipes) Embryos. *Toxicol. Sci.*, **118**, 213–223.

Dudakovic, A. *et al.* (2015) Epigenetic Control of Skeletal Development by the Histone Demethylase Ezh2. *J. Biol. Chem.*, **290**, 27604–27617.

Ekanayake, S. and Hall, B.K. (1987) The development of acellularity of the vertebral bone of the Japanese medaka, *Oryzias latipes* (Teleostei; Cyprinidontidae). *J. Morphol.*, **193**, 253–261.

Ekanayake, S. and Hall, B.K. (1988) Ultrastructure of the osteogenesis of acellular vertebral bone in the Japanese medaka, Oryzias latipes (Teleostei, Cyprinidontidae). *Am. J. Anat.*, **182**, 241–249.

Ellis, L.D. *et al.* (2014) Use of the zebrafish larvae as a model to study cigarette smoke condensate toxicity. *PLoS One*, **9**, e115305.

Etemad, L. *et al.* (2012) Epilepsy drugs and effects on fetal development: Potential mechanisms. *J. Res. Med. Sci.*, **17**.

Fakhry, A. *et al.* (2005) Effects of FGF-2/-9 in calvarial bone cell cultures: Differentiation stage-dependent mitogenic effect, inverse regulation of BMP-2 and noggin, and enhancement of osteogenic potential. *Bone*, **36**, 254–266.

Felson, D.T. *et al.* (2000) Osteoarthritis: new insights. Part 1: the disease and its risk factors. *Ann. Intern. Med.*, **133**, 635–646.

Fernández-González, R. *et al.* (2015) A Critical Review about Human Exposure to Polychlorinated Dibenzo-p-Dioxins (PCDDs), Polychlorinated Dibenzofurans (PCDFs) and Polychlorinated Biphenyls (PCBs) through Foods. *Crit. Rev. Food Sci. Nutr.*, **55**, 1590–1617.

Finnilä, M.A.J. *et al.* (2010) Effects of 2,3,7,8-tetrachlorodibenzo-p-dioxin exposure on bone material properties. *J. Biomech.*, **43**, 1097–1103.

Fleming, A. *et al.* (2015) Building the backbone: the development and evolution of vertebral patterning. *Development*, **142**, 1733–44.

Flynn, R.A. and Chang, H.Y. (2014) Long noncoding RNAs in cell-fate programming and reprogramming. *Cell Stem Cell*, **14**, 752–761.

Forlino, A. *et al.* (2011) New perspectives on osteogenesis imperfecta. *Nat. Rev. Endocrinol.*,

7, 540–557.

Forlino, A. and Marini, J.C. (2016) Osteogenesis imperfecta. *Lancet*, **387**, 1657–1671.

Franz-Odendaal, T.A. *et al.* (2006) Buried alive: How osteoblasts become osteocytes. *Dev. Dyn.*, **235**, 176–190.

Gadupudi, G. *et al.* (2015) PCB126 inhibits adipogenesis of human preadipocytes. *Toxicol. Vitr.*, **29**, 132–141.

Gallagher, J.C. and Sai, a. J. (2010) Molecular biology of bone remodeling: Implications for new therapeutic targets for osteoporosis. *Maturitas*, **65**, 301–307.

Gennari, L. *et al.* (2016) MicroRNAs in bone diseases. *Osteoporos. Int.*, 1–23.

Golub, E.E. and Boesze-Battaglia, K. (2007) The role of alkaline phosphatase in mineralization. *Curr. Opin. Orthop.*, **18**, 444–448.

Gordon, J.A.R. *et al.* (2015) Chromatin modifiers and histone modifications in bone formation, regeneration, and therapeutic intervention for bone-related disease. *Bone*, **81**, 739–745.

Gordon, J.A.R. *et al.* (2014) Epigenetic pathways regulating bone homeostasis: Potential targeting for intervention of skeletal disorders. *Curr. Osteoporos. Rep.*, **12**, 496–506.

Greco, S.J. *et al.* (2007) Functional Similarities Among Genes Regulated by Oct4 in Human Mesenchymal and Embryonic Stem Cells. *Stem Cells*, **25**, 3143–3154.

Grotmol, S. *et al.* (2005) A segmental pattern of alkaline phosphatase activity within the notochord coincides with the initial formation of the vertebral bodies. *J. Anat.*, **206**, 427–436.

Håkelien, A.M. *et al.* (2014) The regulatory landscape of osteogenic differentiation. *Stem Cells*, **32**, 2780–2793.

Hardy, R. and Cooper, M.S. (2009) Bone loss in inflammatory disorders. *J. Endocrinol.*, **201**, 309–320.

Heo, J. *et al.* (2015) Comparison of molecular profiles of human mesenchymal stem cells derived from bone marrow, umbilical cord blood, placenta and adipose tissue. *Int. J. Mol. Med.*, 115–125.

Herlin, M. *et al.* (2015) Inhibitory effects on osteoblast differentiation in vitro by the polychlorinated biphenyl mixture Aroclor 1254 are mainly associated with the dioxin-like constituents. *Toxicol. Vitr.*, **29**, 876–883.

Herlin, M. *et al.* (2013) New insights to the role of aryl hydrocarbon receptor in bone phenotype and in dioxin-induced modulation of bone microarchitecture and material properties. *Toxicol. Appl. Pharmacol.*, **273**, 219–26.

Herlin, M. *et al.* (2010) Quantitative characterization of changes in bone geometry, mineral density and biomechanical properties in two rat strains with different Ah-receptor structures after long-term exposure to 2,3,7,8-tetrachlorodibenzo-p-dioxin. *Toxicology*, **273**, 1–11.

Hermanns, P. and Lee, B. (2002) Transcriptional dysregulation in skeletal malformation syndromes. *Am. J. Med. Genet.*, **106**, 258–271.

Hernandez, C.J. *et al.* (2003) A theoretical analysis of the relative influences of peak BMD, age-related bone loss and menopause on the development of osteoporosis. *Osteoporos. Int.*, **14**, 843–847.

Holz, J.D. *et al.* (2007) Environmental agents affect skeletal growth and development. *Birth Defects Res. Part C - Embryo Today Rev.*, **81**, 41–50.

Huang, J. *et al.* (2010) MicroRNA-204 regulates Runx2 protein expression and mesenchymal progenitor cell differentiation. *Stem Cells*, **28**, 357–364.

Hulsen, T. *et al.* (2008) BioVenn – a web application for the comparison and visualization of biological lists using area-proportional Venn diagrams. *BMC Genomics*, **9**, 488.

Imai, Y. *et al.* (2013) Nuclear Receptors in Bone Physiology and Diseases. *Physiol. Rev.*, **93**, 481–523.

Inose, H. *et al.* (2009) A microRNA regulatory mechanism of osteoblast differentiation. *Proc. Natl. Acad. Sci. U. S. A.*, **106**, 20794–20799.

Ito, T. *et al.* (2010) Identification of a Primary Target of Thalidomide Teratogenicity. *Science (80-.).*, **327**, 1345–1351.

Ito, T. *et al.* (2011) Teratogenic effects of thalidomide: Molecular mechanisms. *Cell. Mol. Life Sci.*, **68**, 1569–1579.

Itoh, T. *et al.* (2009) MicroRNA-141 and -200a Are Involved in Bone Morphogenetic Protein-2-induced Mouse Pre-osteoblast Differentiation by Targeting Distal-less Homeobox 5. *J. Biol. Chem.*, **284**, 19272–19279.

Jämsä, T. *et al.* (2001) Effects of 2,3,7,8-Tetrachlorodibenzo-p-Dioxin on Bone in Two Rat Strains with Different Aryl Hydrocarbon Receptor Structures. *J. Bone Miner. Res.*, **16**, 1812–1820.

Jensen, E.D. *et al.* (2010) Regulation of gene expression in osteoblasts. *Biofactors*, **36**, 25–32.

Jenuwein, T. *et al.* (2001) Translating the Histone Code. *Science (80-.).*, **293**, 1074–1080.

Johnell, O. and Kanis, J.A. (2006) An estimate of the worldwide prevalence and disability associated with osteoporotic fractures. *Osteoporos. Int.*, **17**, 1726–1733.

Joshi-Tope, G. *et al.* (2005) Reactome: A knowledgebase of biological pathways. *Nucleic Acids Res.*, **33**, 428–432.

Kang, H. *et al.* (2017) Osteogenesis imperfecta: new genes reveal novel mechanisms in bone dysplasia. *Transl. Res.*, **181**, 27–48.

Kanis, J. (2007) Assessment of osteoporosis at the primary health care level.

Kanis, J. *et al.* (2005) Smoking and fracture risk: A meta-analysis. *Osteoporos. Int.*, **16**, 155–162.

Karsenty, G. *et al.* (2009) Genetic Control of Bone Formation. *Annu. Rev. Cell Dev. Biol.*, **25**, 629–648.

Karsenty, G. (2008) Transcriptional Control of Skeletogenesis. *Annu. Rev. Genomics Hum. Genet.*, **9**, 183–196.

Kawai, M. *et al.* (2010) The many facets of PPARgamma: novel insights for the skeleton. *Am. J. Physiol. Endocrinol. Metab.*, **299**, E3–E9.

Kimura, H. (2013) Histone modifications for human epigenome analysis. *J. Hum. Genet.*, **58**, 439–445.

King-Heiden, T.C. *et al.* (2012) Reproductive and developmental toxicity of dioxin in fish. *Mol. Cell. Endocrinol.*, **354**, 121–138.

Klareskog, L. *et al.* (2007) Smoking as a trigger for inflammatory rheumatic diseases. *Curr. Opin. Rheumatol.*, **19**, 49–54.

Ko, C.I. *et al.* (2016) Repression of the Aryl Hydrocarbon Receptor Is Required to Maintain Mitotic Progression and Prevent Loss of Pluripotency of Embryonic Stem Cells. *Stem Cells*, **34**, 2825–2839.

Komori, T. (2010) Regulation of bone development and extracellular matrix protein genes by RUNX2. *Cell Tissue Res.*, **339**, 189–195.

Komori, T. *et al.* (1997) Targeted disruption of Cbfa1 results in a complete lack of bone

formation owing to maturational arrest of osteoblasts. *Cell*, **89**, 755–64.

Korkalainen, M. *et al.* (2009) Dioxins interfere with differentiation of osteoblasts and osteoclasts. *Bone*, **44**, 1134–1142.

Kornak, U. and Mundlos, S. (2003) Genetic disorders of the skeleton: a developmental approach. *Am. J. Hum. Genet.*, **73**, 447–74.

Kotake, S. *et al.* (1996) Interleukin-6 and Soluble Interleukin-6 Receptors in the Synovial Fluids from Rheumatoid Arthritis Patients Are Responsible for Osteoclast-like Cell Formation. *J. Bone Miner. Res.*, **11**, 88–95.

Krakow, D. and Rimoin, D.L. (2010) The skeletal dysplasias. *Genet. Med.*, **12**, 327–41.

Kung, M.H. *et al.* (2011) Aryl hydrocarbon receptor-mediated impairment of chondrogenesis and fracture healing by cigarette smoke and benzo(α)pyrene. *J. Cell. Physiol.*, **227**, 1062–1070.

Lacey, D.C. *et al.* (2009) Proinflammatory cytokines inhibit osteogenic differentiation from stem cells: implications for bone repair during inflammation. *Osteoarthr. Cartil.*, **17**, 735–742.

Laize, V. *et al.* (2014) Fish : a suitable system to model human bone disorders and discover drugs with osteogenic or osteotoxic activities. *Drug Discov. Today Dis. Model.*, **13**, 29–37.

Lam, J. *et al.* (2000) TNF-α induces osteoclastogenesis by direct stimulation of macrophages exposed to permissive levels of RANK ligand. *J. Clin. Invest.*, **106**, 1481–1488.

Law, M.R. and Hackshaw, a K. (1997) A meta-analysis of cigarette smoking, bone mineral density and risk of hip fracture: recognition of a major effect. *BMJ*, **315**, 841–846.

Lee, J.J. *et al.* (2013) The musculoskeletal effects of cigarette smoking. *J. Bone Jt. Surg.*, **95**, 850–9.

Lee, M.H. *et al.* (2003) BMP-2-induced Osterix expression is mediated by Dlx5 but is independent of Runx2. *Biochem. Biophys. Res. Commun.*, **309**, 689–694.

Lee, M.H. *et al.* (2005) Dlx5 specifically regulates Runx2 type II expression by binding to homeodomain-response elements in the Runx2 distal promoter. *J. Biol. Chem.*, **280**, 35579–35587.

Lefebvre, V. and Bhattaram, P. (2010) Vertebrate Skeletogenesis. In, Koopman,P. (ed), *Current Topics in Developmental Biology: Organogenesis in Development*. Elsevier Inc., San Diego, pp. 291–317.

Li, L. *et al.* (2013) Targeted Disruption of Hotair Leads to Homeotic Transformation and Gene Derepression. *Cell Rep.*, **5**, 3–12.

Li, W. *et al.* (2008) Development of a human adipocyte model derived from human mesenchymal stem cells (hMSC) as a tool for toxicological studies on the action of TCDD. *Biol. Chem.*, **389**, 169–177.

Lian, J.B. *et al.* (2006) Networks and hubs for the transcriptional control of osteoblastogenesis. *Rev. Endocr. Metab. Disord.*, **7**, 1–16.

Lindner, U. *et al.* (2010) Mesenchymal stem or stromal cells: Toward a better understanding of their biology? *Transfus. Med. Hemotherapy*, **37**, 75–83.

Liu, B. *et al.* (2013) Depleting the methyltransferase Suv39h1 improves DNA repair and extends lifespan in a progeria mouse model. *Nat. Commun.*, **4**, 1868.

Liu, P. *et al.* (1996) Alteration by 2,3,7,8-Tetrachlordibenzo-p-dioxin of CCAAT/Enhancer Binding Protein Correlates with Suppression of Adipocyte Differentiation in 3T3-L1 Cells. *Mol. Pharmacol.*, **49**, 989–997.

Livak, K.J. and Schmittgen, T.D. (2001) Analysis of relative gene expression data using real-time quantitative PCR and the 2(-Delta Delta C(T)) Method. *Methods*, **25**, 402–8.

Long, F. (2011) Building strong bones: molecular regulation of the osteoblast lineage. *Nat. Rev. Mol. Cell Biol.*, **13**, 27–38.

Lorentzon, M. *et al.* (2007) Smoking is associated with lower bone mineral density and reduced cortical thickness in young men. *J. Clin. Endocrinol. Metab.*, **92**, 497–503.

Love, M.I. *et al.* (2014) Moderated estimation of fold change and dispersion for RNA-seq data with DESeq2. *Genome Biol.*, **15**, 550.

Lu, J. *et al.* (2015) Effect of fibroblast growth factor 9 on the osteogenic differentiation of bone marrow stromal stem cells and dental pulp stem cells. *Mol. Med. Rep.*, **11**, 1661–1668.

Lu, J. *et al.* (2014) The Effect of Fibroblast Growth Factor 9 on the Osteogenic Differentiation of Calvaria-Derived Mesenchymal Cells. *J. Craniofac. Surg.*, **25**, 502–505.

Manolagas, S.C. (2000) Birth and death of bone cells: basic regulatory mechanisms and implications for the pathogenesis and treatment of osteoporosis. *Endocr. Rev.*, **21**, 115–137.

Mansukhani, A. *et al.* (2005) Sox2 induction by FGF and FGFR2 activating mutations

inhibits Wnt signaling and osteoblast differentiation. *J. Cell Biol.*, **168**, 1065–1076.

Marcellini, S. *et al.* (2012) Control of osteogenesis by the canonical Wnt and BMP pathways in vivo: cooperation and antagonism between the canonical Wnt and BMP pathways as cells differentiate from osteochondroprogenitors to osteoblasts and osteocytes. *BioEssays News Rev. Mol. Cell. Dev. Biol.*, **34**, 953–62.

Marotti, G. (1996) The structure of bone tissues and the cellular control of their deposition. *Ital. J. Anat. Embryol.*, **101**, 25–79.

McCormack, S.E. *et al.* (2017) Association Between Linear Growth and Bone Accrual in a Diverse Cohort of Children and Adolescents. *JAMA Pediatr.*, **19104**, 1–9.

Miettinen, H.M. *et al.* (2005) Effects of in utero and lactational TCDD exposure on bone development in differentially sensitive rat lines. *Toxicol. Sci.*, **85**, 1003–1012.

Mizuno, Y. *et al.* (2008) miR-125b inhibits osteoblastic differentiation by down-regulation of cell proliferation. *Biochem. Biophys. Res. Commun.*, **368**, 267–272.

Montecino, M. *et al.* (2015) Multiple levels of epigenetic control for bone biology and pathology. *Bone*, **81**, 733–738.

Mundy, G.R. (2007) Osteoporosis and Inflammation. *Nutr. Rev.*, **65**.

Murante, F.G. and Gasiewicz, T.A. (2000) Hemopoietic Progenitor Cells Are Sensitive Targets of 2,3,7,8-Tetrachlorodibenzo-p-dioxin in C57BL/6J Mice. *Toxicol. Sci.*, **54**, 374–383.

Nakase, T. *et al.* (1997) Interleukin-1 beta enhances and tumor necrosis factor-alpha inhibits bone morphogenetic protein-2-induced alkaline phosphatase activity in MC3T3-E1 osteoblastic cells. *Bone*, **21**, 17–21.

Nakashima, K. *et al.* (2002) The novel zinc finger-containing transcription factor osterix is required for osteoblast differentiation and bone formation. *Cell*, **108**, 17–29.

Nakashima, T. *et al.* (2012) New insights into osteoclastogenic signaling mechanisms. *Trends Endocrinol. Metab.*, **23**, 582–90.

Narkowicza, S. *et al.* (2013) Environmental Tobacco Smoke: Exposure, Health Effects, and Analysis. *Biocontrol Sci. Technol.*, **43**, 121–161.

Naruse, M. *et al.* (2002) 3-Methylcholanthrene, which binds to the arylhydrocarbon receptor, inhibits proliferation and differentiation of osteoblasts in vitro and ossification in vivo. *Endocrinology*, **143**, 3575–81.

Nishio, Y. *et al.* (2006) Runx2-mediated regulation of the zinc finger Osterix/Sp7 gene. *Gene*, **372**, 62–70.

Nordvik, K. *et al.* (2005) The salmon vertebral body develops through mineralization of two preformed tissues that are encompassed by two layers of bone. *J. Anat.*, **206**, 103–114.

Ohtake, F. *et al.* (2009) AhR acts as an E3 ubiquitin ligase to modulate steroid receptor functions. *Biochem. Pharmacol.*, **77**, 474–84.

Orioli, I.M. *et al.* (1986) The birth prevalence rates for the skeletal dysplasias. *J. Med. Genet.*, **23**, 328–32.

Ornitz, D.M. and Marie, P.J. (2015) Fibroblast growth factor signaling in skeletal development and disease. *Genes Dev.*, **29**, 1463–1486.

Padilla, S. *et al.* (2012) Zebrafish developmental screening of the ToxCast^{TM} Phase I chemical library. *Reprod. Toxicol.*, **33**, 174–187.

van de Peppel, J. *et al.* (2017) Identification of Three Early Phases of Cell-Fate Determination during Osteogenic and Adipogenic Differentiation by Transcription Factor Dynamics. *Stem Cell Reports*, **172**, 5457–5476.

Pillai, H.K. *et al.* (2014) Ligand Binding and Activation of PPARγ by Firemaster 550: Effects on Adipogenesis and Osteogenesis in Vitro. *Environ. Health Perspect.*, **122**, 1225–1232.

Podechard, N. *et al.* (2009) Inhibition of human mesenchymal stem cell-derived adipogenesis by the environmental contaminant benzo(a)pyrene. *Toxicol. In Vitro*, **23**, 1139–44.

Pohl, H. *et al.* (1998) Toxicological profile for chlorinated dibenzo-p-dioxins.

Puga, A. *et al.* (2000) Aromatic Hydrocarbon Receptor Interaction with the Retinoblastoma Protein Potentiates Repression of E2F-dependent Transcription and Cell Cycle Arrest. *J. Biol. Chem.*, **275**, 2943–2950.

Puga, A. *et al.* (2009) The aryl hydrocarbon receptor cross-talks with multiple signal transduction pathways. *Biochem. Pharmacol.*, **77**, 713–722.

Quiroz, F.G. *et al.* (2010) Housekeeping gene stability influences the quantification of osteogenic markers during stem cell differentiation to the osteogenic lineage. *Cytotechnology*, **62**, 109–120.

Rahman, M.S. *et al.* (2015) TGF-β/BMP signaling and other molecular events: regulation of osteoblastogenesis and bone formation. *Bone Res.*, **3**, 15005.

Redlich, K. and Smolen, J.S. (2012) Inflammatory bone loss: pathogenesis and therapeutic intervention. *Nat. Rev. Drug Discov.*, **11**, 234–250.

Riekstina, U. *et al.* (2009) Embryonic stem cell marker expression pattern in human mesenchymal stem cells derived from bone marrow, adipose tissue, heart and dermis. *Stem Cell Rev. Reports*, **5**, 378–386.

Riss, T.L. *et al.* (2004) Cell Viability Assays Assay Guidance Manual. *Assay Guid. Man.*, 1–23.

Rizzoli, R. *et al.* (2010) Maximizing bone mineral mass gain during growth for the prevention of fractures in the adolescents and the elderly. *Bone*, **46**, 294–305.

Rosano, A. *et al.* (2000) Limb defects associated with major congenital anomalies: Clinical and epidemiological study from the international clearinghouse for birth defects monitoring systems. *Am. J. Med. Genet.*, **93**, 110–116.

Rosen, E.D. and MacDougald, O.A. (2006) Adipocyte differentiation from the inside out. *Nat. Rev. Mol. Cell Biol.*, **7**, 885–896.

Rosset, E.M. and Bradshaw, A.D. (2016) SPARC/osteonectin in mineralized tissue. *Matrix Biol.*, **52**–**54**, 78–87.

Ryan, E.P. *et al.* (2007) Environmental toxicants may modulate osteoblast differentiation by a mechanism involving the aryl hydrocarbon receptor. *J. Bone Miner. Res.*, **22**, 1571–80.

Safe, S. *et al.* (1998) Ah receptor agonists as endocrine disruptors: antiestrogenic activity and mechanisms. *Toxicol. Lett.*, **102**–**103**, 343–7.

Safe, S. (1995) Cellular and molecular biology of aryl hydrocarbon (Ah) receptor-mediated gene expression. *Arch. Toxicol.*, **17**, 99–115.

Sakaguchi, Y. *et al.* (2009) Suspended cells from trabecular bone by collagenase digestion become virtually identical to mesenchymal stem cells obtained from marrow. *Stem Cells*, **104**, 2728–2735.

Sargis, R.M. *et al.* (2009) Environmental Endocrine Disruptors Promote Adipogenesis in the 3T3-L1 Cell Line through Glucocorticoid Receptor Activation. *Obesity*, **18**, 1283–1288.

Schönitzer, V. *et al.* (2014) Sox2 is a potent inhibitor of osteogenic and adipogenic differentiation in human mesenchymal stem cells. *Cell. Reprogram.*, **16**, 355–65.

Schroeder, T.M. *et al.* (2005) Runx2: A master organizer of gene transcription in developing and maturing osteoblasts. *Birth Defects Res. Part C - Embryo Today Rev.*, **75**, 213–225.

Sciullo, E.M. *et al.* (2009) Characterization of the pattern of the nongenomic signaling pathway through which TCDD-induces early inflammatory responses in U937 human macrophages. *Chemosphere*, **74**, 1531–1537.

Scolaro, J.A. *et al.* (2014) Cigarette Smoking Increases Complications Following Fracture. *J. Bone Jt. Surg.*, 674–681.

Seo, E. *et al.* (2011) Distinct Functions of Sox2 Control Self-Renewal and Differentiation in the Osteoblast Lineage. *Mol. Cell. Biol.*, **31**, 4593–4608.

Sheng, G. (2015) The developmental basis of mesenchymal stem/stromal cells (MSCs). *BMC Dev. Biol.*, **15**, 44.

Shimba, S. *et al.* (2001) Aryl hydrocarbon receptor (AhR) is involved in negative regulation of adipose differentiation in 3T3- L1 cells : AhR inhibits adipose differentiation independently of dioxin. *J. Cell Sci.*, **114**, 2809–2817.

Siegel, G. *et al.* (2013) Phenotype, donor age and gender affect function of human bone marrow-derived mesenchymal stromal cells. *BMC Med.*, **11**, 146.

Simonet, W.S. *et al.* (1997) Osteoprotegerin: a novel secreted protein involved in the regulation of bone density. *Cell*, **89**, 309–19.

Singh, K.P. *et al.* (2009) Treatment of mice with the Ah receptor agonist and human carcinogen dioxin results in altered numbers and function of hematopoietic stem cells. *Carcinogenesis*, **30**, 11–19.

Sinha, K.M. and Zhou, X. (2013) Genetic and molecular control of osterix in skeletal formation. *J. Cell. Biochem.*, **114**, 975–84.

Sipes, N.S. *et al.* (2011) Zebrafish-as an integrative model for twenty-first century toxicity testing. *Birth Defects Res. Part C, Embryo Today Rev.*, **93**, 256–267.

Sloan, A. *et al.* (2010) The effects of smoking on fracture healing. *Surg. J. R. Coll. Surg. Edinburgh Irel.*, **8**, 111–6.

Smith, K.J. *et al.* (2011) Identification of a high-affinity ligand that exhibits complete aryl hydrocarbon receptor antagonism. *J. Pharmacol. Exp. Ther.*, **338**, 318–327.

Sozen, T. *et al.* (2017) An overview and management of osteoporosis. *Eur. J. Rheumatol.*, **4**, 46–56.

Spandidos, A. *et al.* (2010) PrimerBank : a resource of human and mouse PCR primer pairs for gene expression detection and quantification. **38**, 792–799.

Staines, K.A. *et al.* (2012) The importance of the SIBLING family of proteins on skeletal mineralisation and bone remodelling. *J. Endocrinol.*, **214**, 241–255.

Su, N. *et al.* (2008) FGF signaling: its role in bone development and human skeletal diseases. *Front. Biosci.*, **13**, 2842–2865.

Teraoka, H. *et al.* (2006) Impairment of lower jaw growth in developing zebrafish exposed to 2,3,7,8-tetrachlorodibenzo-p-dioxin and reduced hedgehog expression. *Aquat. Toxicol.*, **78**, 103–113.

Teraoka, H. *et al.* (2006) Muscular contractions in the zebrafish embryo are necessary to reveal thiuram-induced notochord distortions. *Toxicol. Appl. Pharmacol.*, **212**, 24–34.

The Health Consequences of Smoking - — 50 Years of Progress A Report of the Surgeon General (2014) Rockville, Maryland.

Tian, L. *et al.* (2017) miR-148a-3p regulates adipocyte and osteoblast differentiation by targeting lysine-specific demethylase 6b. *Gene*, **627**, 32–39.

Tian, Y. *et al.* (2002) Ah receptor and NF-kB interactions: Mechanisms and physiological implications. *Chem. Biol. Interact.*, **141**, 97–115.

Tilton, F. *et al.* (2006) Dithiocarbamates have a common toxic effect on zebrafish body axis formation. *Toxicol. Appl. Pharmacol.*, **216**, 55–68.

Tox21: Chemical testing in the 21st century (2017) Research Triangle Park, NC.

Truong, L. *et al.* (2014) Multidimensional in vivo hazard assessment using zebrafish. *Toxicol. Sci.*, **137**, 212–233.

Tye, C.E. *et al.* (2015) Could lncRNAs be the Missing Links in Control of Mesenchymal Stem Cell Differentiation? *J. Cell. Physiol.*, **230**, 526–534.

Tyl, R.W. *et al.* (2007) Altered Axial Skeletal Development. *Birth Defects Res. Part B-Developmental Reprod. Toxicol.*, **472**, 451–472.

Voss, A. *et al.* (2016) Extracellular Matrix of Current Biological Scaffolds Promotes the Differentiation Potential of Mesenchymal Stem Cells. *Arthrosc. - J. Arthrosc. Relat. Surg.*, **32**, 2381–2392.e1.

van de Vyver, M. *et al.* (2014) Thiazolidinedione-induced lipid droplet formation during osteogenic differentiation. *J. Endocrinol.*, **223**, 119–132.

Wade, S.W. *et al.* (2014) Estimating prevalence of osteoporosis: examples from industrialized countries. *Arch. Osteoporos.*, **9**, 182.

Wang, C.-K. *et al.* (2009) Aryl hydrocarbon receptor activation and overexpression upregulated fibroblast growth factor-9 in human lung adenocarcinomas. *Int. J. Cancer*, **125**, 807–815.

Wang, Y. *et al.* (2010) Dioxin Exposure Disrupts the Differentiation of Mouse Embryonic Stem Cells into Cardiomyocytes. **115**, 225–237.

Wang, Z. *et al.* (2012) Distinct lineage specification roles for NANOG, OCT4, and SOX2 in human embryonic stem cells. *Cell Stem Cell*, **10**, 440–454.

Ward, K.D. and Klesges, R.C. (2001) A Meta-Analysis of the Effects of Cigarette Smoking on Bone Mineral Density. *Calcif. Tissue Int.*, **68**, 259–270.

Watson, A.T.D. *et al.* (2017) Embryonic Exposure to TCDD Impacts Osteogenesis of the Axial Skeleton in Japanese medaka, Oryzias latipes. *Toxicol. Sci.*, **155**, 485–496.

Watt, J. and Schlezinger, J.J. (2015) Structurally-diverse, PPARγ-activating environmental toxicants induce adipogenesis and suppress osteogenesis in bone marrow mesenchymal stromal cells. *Toxicology*, **331**, 66–77.

Wilffert, B. *et al.* (2011) Pharmacogenetics of drug-induced birth defects: what is known so far? *Pharmacogenomics*, **12**, 547–558.

Wilson, C.L. and Safe, S. (1998) Mechanisms of ligand-induced aryl hydrocarbon receptor-mediated biochemical and toxic responses. *Toxicol. Pathol.*, **26**, 657–671.

Witten, P.E. *et al.* (2016) Small teleost fish provide new insights into human skeletal diseases Elsevier Ltd.

Witten, P.E. and Huysseune, A. (2009) A comparative view on mechanisms and functions of skeletal remodelling in teleost fish, with special emphasis on osteoclasts and their function. *Biol. Rev.*, **84**, 315–346.

Wong, P.K.K. *et al.* (2007) The effects of smoking on bone health. *Clin. Sci.*, **113**, 233–41.

Wu, H. *et al.* (2017) Chromatin Dynamics Regulate Mesenchymal Stem Cell Lineage Specification and Differentiation to Osteogenesis. *Biochim. Biophys. Acta - Gene Regul. Mech.*, **1860**, 438–449.

Wu, M. *et al.* (2016) TGF-β and BMP signaling in osteoblast, skeletal development, and bone formation, homeostasis and disease. *Bone Res.*, **4**, 16009.

Yamashita, T. *et al.* (2012) New roles of osteoblasts involved in osteoclast differentiation. *World J. Orthop.*, **3**, 175–81.

Yanbaeva, D.G. *et al.* (2007) Systemic effects of smoking. *Chest*, **131**, 1557–66.

Yang, J.-H. and Lee, H.-G. (2010) 2,3,7,8-Tetrachlorodibenzo-p-dioxin induces apoptosis of articular chondrocytes in culture. *Chemosphere*, **79**, 278–284.

Yoon, V. *et al.* (2012) The effects of smoking on bone metabolism. *Osteoporos. Int.*, **23**, 2081–92.

Zhang, G. (2009) An evo-devo view on the origin of the backbone: evolutionary development of the vertebrae. *Integr. Comp. Biol.*, **49**, 178–186.

Zhang, Y.H. *et al.* (1990) Interleukin-6 induction by tumor necrosis factor and interleukin-1 in human fibroblasts involves activation of a nuclear factor binding to a kappa B-like sequence. *Mol. Cell. Biol.*, **10**, 3818–23.

CONCLUSIONS AND FUTURE DIRECTIONS

CONCLUSION

The skeletal system is uniquely sensitive to toxicological insult given its rapid morphogenesis during early developmental windows and its continual remodeling throughout adult life. Skeletal dysplasias comprise approximate 20% of all birth defects (Dolk *et al.*, 2010; Rosano *et al.*, 2000), and of those cases, 10-12% can be attributed to *in utero* exposure to environmental chemicals acting through diverse mechanisms (Wilffert *et al.*, 2011). Meanwhile, degenerative bone diseases (e.g. osteoporosis/osteopenia) are prevalent in the elderly and represent a significant cost burden to health care systems. These costs are sure to rise as life expectancy increases globally, and as industrialized countries experience a rapid rise in their aging demographics (Wade *et al.*, 2014; The Health Consequences of Smoking - — 50 Years of Progress A Report of the Surgeon General, 2014; Kanis, 2007). While several factors influence the etiology of osteoporosis, one critical determinant is peak bone mass accrued during childhood and adolescence (McCormack *et al.*, 2017). Therefore, in addition to impacting developmental patterning and growth of skeletal tissues, chemical exposure resulting in attenuated ossification may predispose individuals to developing osteoporosis or other degenerative bone diseases.

AhR ligands remain among the most potent and ubiquitous contaminants in the environment. Among the common sources of exposure are direct and secondhand cigarette smoke, which contains numerous AhR ligands (e.g. benzo[a]pyrene, 3-methylcholanthrene). While smoking is certainly a contributing risk factor for several diseases, this practicehas a strong association with the pathogenesis of rheumatoid arthritis and osteoporosis (Yanbaeva

et al., 2007; Yoon *et al.*, 2012), and delayed fracture repair (Sloan *et al.*, 2010; Scolaro *et al.*, 2014). Given these observations, we hypothesized that TCDD impacts bone development and homeostasis through dysregulation of osteogenic differentiation from mesenchymal stem cells. The research presented here demonstrates the role of 2,3,7,8-tetrachlorodibenzo-*p*-dioxin (TCDD) in dysregulating osteogenic signaling networks following developmental exposure in Japanese medaka (*Oryzias latipes*), and *in vitro* using human bone-derived mesenchymal stem cells.

We approached our primary set of experiments (Chapter 2) with the overall goal of establishing a teleost *in vivo* model to illustrate how embryonic exposure to TCDD altered vertebral bone morphology. In medaka and zebrafish, the vertebral bone is formed through intramembranous ossification (i.e. in the absence of a cartilaginous template) in which mesenchymal stem cells migrate, undergo osteoblast differentiation, and secrete osteoid bone matrix in segmental fashion to form individual vertebrae. Thus, to interrogate the inhibitory role of TCDD in intramembranous bone formation, wildtype and transgenic medaka [tg:(*twist*:EGFP), tg:(*osx*:mCherry), tg:(*col10a1*:nlGFP)] were exposed to 0.3 nM TCDD for one hour during early embryonic development (4 hours post fertilization) and individuals were reared to the larval stage at 20 days post fertilization when a full osteogenic assessment was conducted. Confocal microscopy of Alizarin complexone- or Calcein-stained transgenic medaka offered a high-resolution assessment of ossified vertebral body morphology in conjunction with altered osteoblast and osteoblast-progenitor cell populations. A morphological assessment revealed TCDD-mediated attenuation of centrum, neural arch, and hemal arch ossification. Qualitatively, we observed a reduction in *col10a1*:nlGFP-positive and

osx:mCherry-positive osteoblasts in areas undergoing ossification, which suggested that osteogenic differentiation was indeed impacted by TCDD exposure. We confirmed this observation through both targeted and global gene expression analyses demonstrating reduced expression of osteogenic regulators *osx* and *runx2*, and their downstream ECM gene targets following TCDD exposure. An interesting observation from TCDD-exposed individuals, however, revealed undifferentiated *twist*:EGFP-positive mesenchymal cells localized on top of the centrum. Given prior studies indicating these cells give rise to osteoblasts, it is possible that these cells were in the process of migrating and/or differentiating to become osteoblasts. This finding aided in the refinement of our overall hypothesis, which is that AhR transactivation can inhibit multipotent mesenchymal stem cell (MSC) populations capable of chondrogenic, adipogenic, and osteogenic differentiation.

In Chapter 3 we transitioned to human bone-derived mesenchymal stem cells (hBMSCs) *in vitro* to directly assess how osteogenic differentiation was impacted with TCDD exposure. In this model, hBMSCs cultured in osteogenic differentiation medium can be assessed for markers corresponding to early (mRNA expression of osteogenic regulators), intermediate (alkaline phosphatase activity), and apical stages (matrix mineralization) of differentiation. Cells from three individual donors of varying age, genetic, and osteoporotic backgrounds were tested and revealed consistent responses when exposed to TCDD. Consistent responses included reduced *DLX5* expression (early and intermediate), alkaline phosphatase activity (intermediate), and ECM mineralization and *OPN* and *IBSP* expression (apical). Co-exposure to the AhR antagonist, GNF351, partially rescued these responses suggesting an inhibitory role of ligand-activated AhR in osteogenesis. Across donors,

expression profiles of stemness markers *OCT4*, *SOX2*, and *NANOG* in TCDD-exposed cells more closely resembled profiles of undifferentiated cells. Contrary to our hypothesis and results in Chapter 2, we observed no change in *OSX* expression and an actual increase in *RUNX2* expression. This may suggest a greater role for DLX5 in promoting mesenchymal-to-osteoblast differentiation *in vitro*, and/or reflect distinctions between medaka bone development *in vivo* and human MSC differentiation *in vitro*. qPCR analysis from Chapter 3 also revealed FGF signaling, which plays a critical role in bone and cartilage development, as a particularly sensitive target of TCDD exposure. Although AhR toxicity may not be a novel topic, we argue that these hBMSCs are an excellent model for screening compounds suspected of causing skeletal toxicity through dysregulation of osteogenic, chondrogenic, and adipogenic differentiation.

While our targeted gene expression analysis in Chapter 3 revealed several candidate genes, a more complete transcriptomic analysis was needed to identify additional signaling mediators (e.g. FGF, WNT, BMP/TGF-β), ECM components, and epigenetic modifiers impacted upon exposure to TCDD. Thus, a temporal transcriptomic RNA-Seq assessment was conducted with GM-DMSO, ODM-DMSO, and ODM-TCDD treated samples at 3 hours post induction (hpi), 24 hpi, 3 dpi, 7 dpi, and 17 dpi. Although data from 3 dpi and 7 dpi are the only two timepoints currently available, we observed several long intergenic non-coding RNAs (LINCRNAs), and mediators of developmental signaling pathways whose expression is significantly impacted with TCDD expression. The fact that TCDD alters the expression of several inhibitors and promoters of the WNT, BMP/TGF-β, and FGF pathways suggests that multiple pathways are targets of ligand-activated AhR (Figure 1). At these same timepoints we

observe significant alterations in genes enriched in pathways involved in ECM matrix formation, ECM remodeling, and vesicle-mediated transport, which demonstrates that TCDD alters the extracellular environment as early as 3 dpi. This is especially noteworthy given a recent study suggesting the importance of the ECM composition in promoting osteogenic differentiation of MSCs (M Baroncelli *et al.*, 2017), and we expect data from the apical timepoint at 17 dpi to provide additional insight into how TCDD exposure can alter the extracellular landscape during osteogenesis. Gene expression analyses from the remaining timepoints at 3 hpi, and 24 hpi may provide critical insight into osteogenic lineage specification events governing osteoblast differentiation. We are especially interested in whether TCDD exposure results in differential regulation of epigenetic "readers", "writers", and "erasers" that inhibit the expression of genes that promote osteogenesis and/or induce the expression of genes that serve to inhibit osteogenesis. When this data analysis is complete it will be among the only studies with a transcriptomic analysis of undifferentiated (GM-DMSO), differentiated (ODM-DMSO), and TCDD-exposed hBMSCs

In conclusion, the data presented in Chapters 2-4 support results from other studies that demonstrate AhR-mediated alterations on bone formation. Using a combination of *in vivo* and *in vitro* models, we demonstrate attenuated expression of early regulators of osteogenic differentiation (*DLX5* in hBMSCs; *osx* and *runx2* in medaka), downstream genes encoding extracellular matrix proteins, and that matrix mineralization is significantly reduced following TCDD exposure. While it is important to acknowledge the limitations of each model, the overall mechanisms underlying bone formation are remarkably well-conserved across vertebrate species (Witten *et al.*, 2016; Apschner *et al.*, 2011). TCDD exposure resulted in an

overall consistent phenotypic and genotypic response whereby osteoblasts and osteoblast progenitors were inhibited from reaching terminal maturation. Given these results, both models should be used to complement traditional rodent models used in toxicity testing. Teleost bone development occurs rapidly and can be used to quickly screen libraries of chemicals suspecting of causing skeletal teratogenicity. For chemicals that do induce skeletal deficits, subsequent hBMSCs experiments can aid in defining the precise mechanisms underlying osteogenic disruption. The experiments conducted in Chapters 2-4 addressed several questions regarding the role of ligand-activated AhR and osteogenic inhibition; however, several questions were raised in the process. Below, I offer a handful of research avenues worth pursuing for future undergraduate, graduate, or postdoctoral trainees.

FUTURE DIRECTIONS:

- FACS sort and isolate GFP+ mesenchymal cells from tg(*twist*:EGFP) medaka, and attempt/optimize culture conditions to establish a teleost MSC in vitro model to compare with hBMSCs.
- Screen candidate organophosphate (OP) flame retardants (e.g. triphenyl phosphate) for their ability to promote/inhibit osteogenic and adipogenic differentiation in hBMSCs.
- Interrogate the role of AhR transactivation in FGF/FGFR signaling during osteogenesis.
- Optimize the osteoclastogenic medaka model *rankl*:HSE:CFP/*cathespinK*:mCherry. In addition to its potential as a translational model to detect chemicals that may induce/skew osteoclastogenesis, it would also be amenable to screening anabolic drug therapies. Through a simple heat-shock incubation (38-39^0 C, 30-90 minutes) one can

induce expression of *rankl*, an osteoclast regulator, and image mCherry 2-3 days later in mature osteoclasts expressing *cathepsin k* (*cstk*). With calcein as a marker for mineralized bone one can image cell-mediated bone resorption along the vertebrae over the course of 24-72 hours using light-sheet or confocal microscopy.

FIGURES

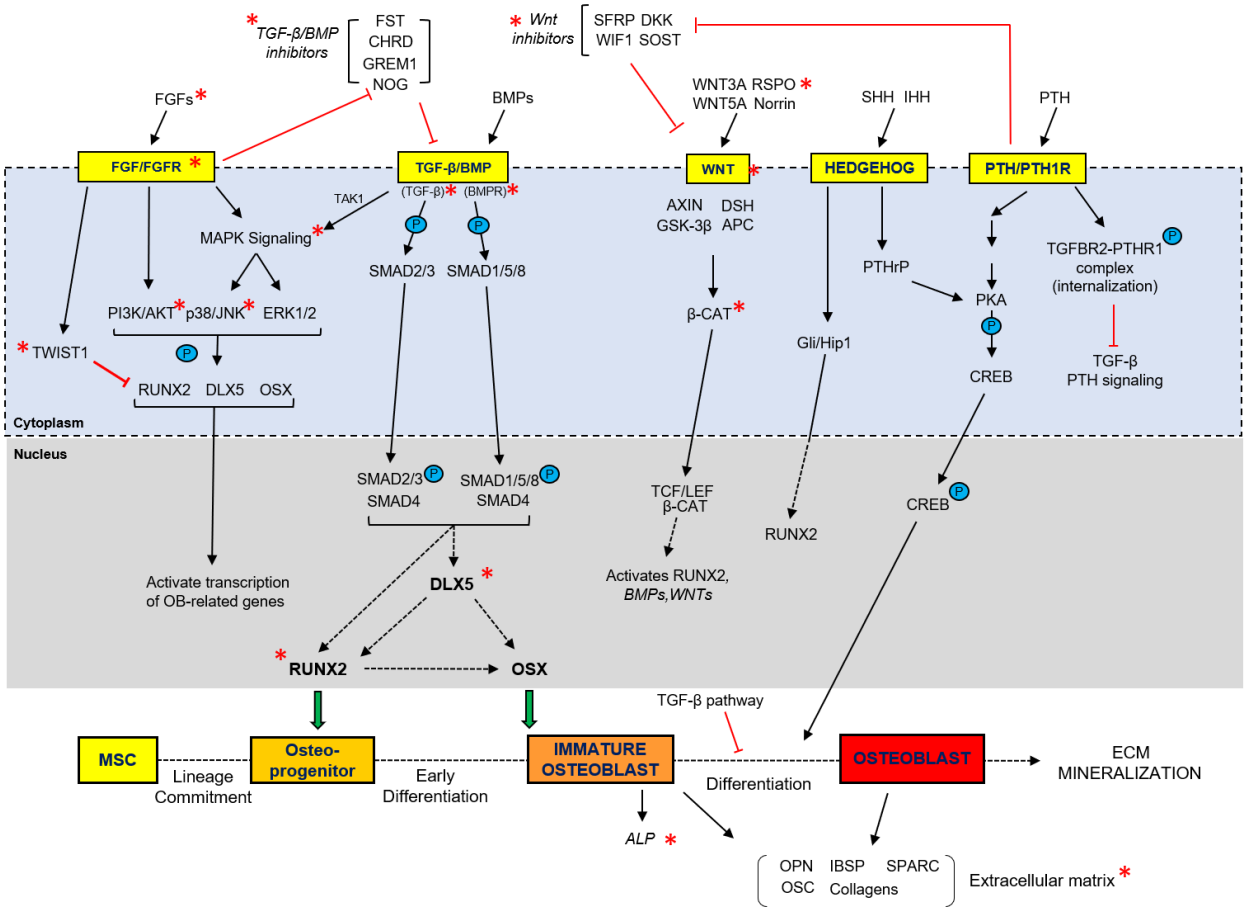

Figure 1. Overview of multiple signaling pathways influencing osteogenic differentiation from a mesenchymal stem cells (adapted from Baron and Kneissel, 2013; Chen et al., 2012; Karsenty, 2008; Ornitz and Marie, 2015; Rahman et al., 2015; Wu et al., 2016). Red asterisks (*) indicate genes and/or pathways whose expression is impacted following TCDD exposure.

REFERENCES

Apschner, A. *et al.* (2011) Not All Bones are Created Equal – Using Zebrafish and Other Teleost Species in Osteogenesis Research Third Edit. Elsevier Inc.

Baroncelli, M. *et al.* (2017) Comparative Proteomic Profiling of Human Osteoblast-Derived Extracellular Matrices Identifies Proteins Involved in Mesenchymal Stromal Cell Osteogenic Differentiation and Mineralization. *J Cell Physiol*.

Dolk, H. *et al.* (2010) The Prevalence of Congenital Anomalies in Europe. In, Paz,M.P. de la and Croft,S.C. (eds), *Rare Diseases Epidemiology*. Springer, New York, New York, pp. 305–334.

Kanis, J. (2007) Assessment of osteoporosis at the primary health care level.

McCormack, S.E. *et al.* (2017) Association Between Linear Growth and Bone Accrual in a Diverse Cohort of Children and Adolescents. *JAMA Pediatr.*, **19104**, 1–9.

Rosano, A. *et al.* (2000) Limb defects associated with major congenital anomalies: Clinical and epidemiological study from the international clearinghouse for birth defects monitoring systems. *Am. J. Med. Genet.*, **93**, 110–116.

Scolaro, J.A. *et al.* (2014) Cigarette Smoking Increases Complications Following Fracture. *J. Bone Jt. Surg.*, 674–681.

Sloan, A. *et al.* (2010) The effects of smoking on fracture healing. *Surg. J. R. Coll. Surg. Edinburgh Irel.*, **8**, 111–6.

The Health Consequences of Smoking - — 50 Years of Progress A Report of the Surgeon General (2014) Rockville, Maryland.

Wade, S.W. *et al.* (2014) Estimating prevalence of osteoporosis: examples from industrialized countries. *Arch. Osteoporos.*, **9**, 182.

Wilffert, B. *et al.* (2011) Pharmacogenetics of drug-induced birth defects: what is known so far? *Pharmacogenomics*, **12**, 547–558.

Witten, P.E. *et al.* (2016) Small teleost fish provide new insights into human skeletal diseases Elsevier Ltd.

Yanbaeva, D.G. *et al.* (2007) Systemic effects of smoking. *Chest*, **131**, 1557–66.

Yoon, V. *et al.* (2012) The effects of smoking on bone metabolism. *Osteoporos. Int.*, **23**, 2081–92.